TURUN
YLIOPISTO
UNIVERSITY
OF TURKU

B CELL-MEDIATED IMMUNITY AND SIGNAL REGULATION

The roles of MIM/MTSS1 and IRF4

Alexey Sarapulov

TURUN YLIOPISTON JULKAISUJA – ANNALES UNIVERSITATIS TURKUENSIS
SARJA – SER. D OSA – TOM. 1615 | MEDICA – ODONTOLOGICA | TURKU 2022

TURUN
YLIOPISTO
UNIVERSITY
OF TURKU

B CELL-MEDIATED IMMUNITY AND SIGNAL REGULATION

The roles of MIM/MTSS1 and IRF4

Alexey Sarapulov

TURUN YLIOPISTON JULKAISUJA – ANNALES UNIVERSITATIS TURKUENSIS
SARJA – SER. D OSA – TOM. 1615 | MEDICA – ODONTOLOGICA | TURKU 2022

University of Turku

Faculty of Medicine
Institute of Biomedicine
Pathology
Turku Doctoral Programme of Molecular Medicine

Supervised by

Docent, Pieta Mattila
Institute of Biomedicine
Faculty of Medicine
University of Turku
Turku, Finland

Reviewed by

Associate Professor, Susanna Fagerholm
Department of Biosciences
Faculty of Biological and Environmental Sciences
University of Helsinki
Helsinki, Finland

Professor, Tuure Kinnunen
Clinical Microbiology and Immunology
Institute of Clinical Medicine
University of Eastern Finland
Kuopio, Finland

Opponent

Professor, Lars Nitschke
Division of Genetics
Friedrich-Alexander University Erlangen-Nürnberg
Erlangen, Germany

The originality of this publication has been checked in accordance with the University of Turku quality assurance system using the Turnitin OriginalityCheck service.

ISBN 978-951-29-8789-4 (PRINT)
ISBN 978-951-29-8790-0 (PDF)
ISSN 0355-9483 (PRINT)
ISSN 2343-3213 (ONLINE)
Painosalama, Turku, Finland, 2022

Science here might be theoretical,
but the person is real

UNIVERSITY OF TURKU
Faculty of Medicine
Institute of Biomedicine
Pathology
SARAPULOV, ALEXEY: B cell-mediated immunity and signal regulation
Doctoral dissertation, 194 pp.
Turku Doctoral Programme of Molecular Medicine
February 2022

ABSTRACT

B cells constitute an important part of the adaptive immune system and produce antibodies, which protect organism against infectious agents. Recognition of the antigen by the B cell receptor and the following B cell activation are key steps toward production of protective antibodies. In recent years it has been shown that the actin cytoskeleton is actively involved in the regulation of early events of B cell activation. Therefore, understanding the factors that influence actin cytoskeleton remodeling in B cells is essential for the understanding of B cell-mediated immunity.

The focus of this work is on the membrane and actin cytoskeleton regulatory protein, MIM/MTSS1, and on the B cell-specific transcription factor, IRF4. In order to reveal unexplored MIM functions, the gene and protein sequences of MIM were analyzed by using computational tools, bioinformatic resources and online databases. The analysis demonstrates a high overall degree of MIM conservation in vertebrates and we also report on the presence of various short functional motifs. We also show that expression of MIM is downregulated in samples from patients with poor prognosis chronic lymphocytic leukemia (CLL). The role of MIM in B cells was studied by analysis of MIM knock-out (KO) mice. MIM-deficiency results in impaired BCR signaling upon stimulation with surface-bound but not soluble antigen, and elevated reprogramming toward higher oxidative metabolic state upon TLR4/9 stimulation. MIM KO animals also exhibit lower antibody responses against T cell-independent antigen immunization. Finally, the impact of IRF4-deficiency on BCR signaling was examined in an IRF4-KO DT40 cell line. We show that IRF4 deficiency results in disturbed BCR signaling, characterized by impaired Syk, BLNK, MAPK1/2 activation and F-actin engagement, low SHIP phosphatase levels and upregulation of PI3K, PLCγ and Ca^{2+} signaling.

This work is the first comprehensive study of the actin-regulatory protein MIM in B cell-mediated immunity and provides an evolutionary standpoint on the functional significance of MIM protein regions. This study also highlights the fact that IRF4 is not only a downstream effector of BCR signaling but by itself can influence B cell activation via developmental stage-specific expression in B cells.

KEYWORDS: MIM, MTSS1, IRF4, B cell, actin cytoskeleton, BCR signaling, B cell activation, immune response, antibody production, metabolism, evolutionary analysis

TURUN YLIOPISTO
Lääketieteellinen tiedekunta
Biolääketieteen laitos
Patologia
SARAPULOV, ALEXEY: B cell-mediated immunity and signal regulation
Väitöskirja, 194 s.
Molekyylilääketieteen tohtoriohjelma
Kuukausi 2022

TIIVISTELMÄ

B-solut muodostavat tärkeän osan opittua immuunijärjestelmää tuottaen infektioilta suojaavia vasta-aineita. Antigeenin tunnistus B-solureseptorin välityksellä ja sitä seuraava B-soluaktivaatio ovat kriittiset ensivaiheet kohti vasta-ainetuotannon käynnistymistä. Viime vuosina on osoitettu, että solun aktiinitukiranka on aktiivisesti mukana B-soluaktivaation alkuvaiheiden säätelyssä. Tästä syystä aktiinitukirangan säätelyyn vaikuttavien tekijöiden ymmärtäminen on erittäin tärkeää myös B-soluvälitteisen immuniteetin ymmärtämisessä.

Tässä työssä keskityttiin solukalvoa ja aktiinitukirankaa säätelevään MIM/MTSS1-proteiiniin sekä B-soluspesifiseen IRF4-transkriptiofaktoriin. Aiemmin selvittämättömiä MIM-proteiinin funktioita pyrittiin tunnistamaan MIM:n geeni- ja proteiinisekvenssiä tietokonepohjaisilla menetelmillä tutkien sekä bioinformatiikan työkaluja sekä datapankkeja käyttäen. Tämä analyysi osoitti MIM:n voimakkaan konservoitumisen selkärankaisissa eläimissä sekä raportoi useita lyhyitä toiminnallisia sekvenssijaksoja. Työssä näytämme myös, että MIM-proteiinin määrä on alentunut huonon ennusteen kroonisessa lymfosyyttisessä leukemiassa (CLL). MIM-proteiinin roolia B-soluissa tutkittiin MIM-poistogeenistä hiirimallia käyttäen. Havaitsimme alentuneen B-solureseptorisignaloinnin pinnalla esiteltyä antigeenia vastaan, mutta ei liukoista antigeenia vastaan, sekä lisääntyneen uudelleenohjelmoinnin kohti kohonnutta oksidatiivista energia-aineenvaihtoa TLR4/9 stimulaatiossa. MIM-poistogeenisissä hiirissä vasta-ainereaktio T-soluista riippumattomassa immunisaatiossa oli madaltunut. Tutkimme myös B-solureseptorisignalointia IRF4-poistogeenisessä DT40 B-solulinjassa. Havaitsimme, että IRF4:n puute johtaa häiriintyneeseen B-solureseptorisignalointiin, mikä oli nähtävissä madaltuneina Syk, BLNK ja MAPK1/2 signaaliproteiinien aktivaationa, puutteellisena aktiinitukirangan toimintana, alentuneena SHIP-proteiinin tasona, sekä lisääntyneenä PI3K, PLCγ ja Ca^{2+} signalointina.

Tämä työ on ensimmäinen kattava tutkimus aktiinia säätelevän MIM-proteiinin roolista B-soluvälitteisessä immuniteetissa ja tarjoaa evolutiivisen näkökulman proteiinin eri osien merkitykseen ja toimintaan. Työ myös tuo esiin, että IRF4 ei ole pelkkä B-solureseptorisignaloinnin alavirran toimija, vaan voi myös itse vaikuttaa B-solujen aktivoitumiseen solun erilaistumisasteesta riippuvan ilmentymisensä kautta.

ASIASANAT: MIM, MTSS1, IRF4, B-solu, aktiinitukiranka, BCR-signalointi, B-solujen aktivaatio, immuunivaste, vasta-ainetuotanto, metabolia, evoluutioanalyysi.

Table of Contents

Abbreviations

Ab	Antibody
ABP	Actin binding protein
Ag	Antigen
AICD	Activation-induced cell death
APC	Antigen-presenting cell
BAR	Bin-Amphiphysin-Rvs (domain, protein family)
BCR	B cell receptor
BM	Bone marrow
CCD	Coiled-coil domain
CLL	Chronic lymphocytic leukemia
CLP	Common lymphoid progenitors
CRAC	Calcium release-activated channel
CRISPR	Clustered regularly interspaced short palindromic repeats
cSMAC	Central supramolecular activation cluster
CSR	Class-switch recombination
CTV	Cell trace violet
CytoD	Cytochalasin D
DAG	Diacylglycerol
DBR	Disordered binding region
DC	Dentritic cell
DLBCL	Diffuse large B cell lymphoma
DZ	Dark zone
ECAR	Extracellular acidification rate
ER	Endoplasmic reticulum
ERM	Ezrin-Radixin-Moesin (family of proteins)
F-actin	Filamentous actin
Fab	Fragment antigen binding
FDC	Follicular dendritic cell
G-actin	Globular actin
GAP	GTPase activation factor
GBD	GTPase binding domain
GC	Germinal center
GDI	GDP dissociation factor
GEF	Guanine nucleotide exchange factor
Ig	Immunoglobulin
IHC	Immunohistochemistry

IS	Immunological synapse
IRF4	Interferon regulatory factor 4
IRM	Interference reflection microscopy
ITAM	Immunoreceptor tyrosine-based activation motif
ITIM	Immunoreceptor tyrosine-based inhibitory motif
Jasp	Jasplakinolide
LatA	Latrunculin A
LLPC	Long-lived plasma cell
LN	Lymph node
LPS	Lipopolysaccharide
LRR	Leucine-rich region
LZ	Light zone
mAb	Monoclonal antibody
MHC	Major histocompatibility complex
MIM	Missing-In-Metastasis
MSA	Multiple sequence alignment
MTdR	Mitotracker dRed
MTG	Mitotracker green
MTOC	Microtubule organizing center
MTSS1	Metastasis suppressor 1
MZ	Marginal zone
NPF	Nucleation promoting factor
OCR	Oxygen consumption rate
OxPhos	Oxidative phosphorylation
PAA	Polyacrylamide
PALS	Periarteriolar lymphoid sheath
PB	Plasmablast
PCR	Polymerase chain reaction
PDMS	Polydimethylsiloxane
PerC	Peritoneal cavity
$PI(3,4,5)P_3$, PIP3	Phosphatidylinositol-(3,4,5)-triphosphate
$PI(4,5)P_2$, PIP2	Phosphatidylinositol-(4,5)-diphosphate
PMS	Plasma membrane sheet
PRD, PRR	Proline-rich domain, Proline-rich region
pSMAC	Peripheral supramolecular activation cluster
PFM, PWM	Position frequency matrix, Position weight matrix
ROS	Reactive oxygen species
SEM	Scanning electronic microscopy
SHM	Somatic hypermutation
SLB	Supported lipid bilayer
SLC	Surrogate light chain
SLPC	Short-lived plasma cell
SNP	Single nucleotide polymorphism
SOCE	Store-operated calcium entry
SRD, SRR	Serine-rich domain, Serine-rich region
TCA	Tricarboxylic acid (cycle)
TCR	T cell receptor

TD	T cell-dependent (antigen, immune response)
TF	Transcription factor
TFBS	Transcription factor binding site
Tfh	T follicular helper cell
TI-1	T cell-independent type 1 (antigen, immune response)
TI-2	T cell-independent type 2 (antigen, immune response)
TIRF	Total internal reflection fluorescence (microscopy)
TLR	Toll-like receptor
TMRE	Teramethylrhodamine ester
TSS	Transcription start site
Ub	Ubiquitin
WB	Western blotting
WH2	WASp-homology 2 (domain)

List of Original Publications

This dissertation is based on the following original publications, which are referred to in the text by their Roman numerals:

I Petrov, P., Sarapulov, A.V., Eöry, L., Scielzo, C., Scarfò, L., Smith, J., Burt, D.W. and Mattila, P.K. Computational analysis of the evolutionarily conserved Missing In Metastasis/Metastasis Suppressor 1 gene predicts novel interactions, regulatory regions and transcriptional control. *Sci. Rep.*, 2019; 9:4155.

II Sarapulov, A.V., Petrov, P., Hernández-Pérez, S., Šuštar, V., Kuokkanen, E., Cords, L., Samuel, R.V.M., Vainio, M., Fritzsche, M., Carrasco, Y.R. and Mattila, P.K. Missing-in-metastasis/metastasis suppressor 1 regulates B cell receptor signaling, B cell metabolic potential, and T cell-independent immune responses. *Front. Immunol.*, 2020; 11:1–20.

III Budzyńska, P.M., Niemelä, M., Sarapulov, A.V., Kyläniemi, M.K., Nera, K.-P., Junttila, S., Laiho, A., Mattila, P.K., Alinikula, J. and Lassila, O. IRF4 deficiency leads to altered BCR signalling revealed by enhanced PI3K pathway, decreased SHIP expression and defected cytoskeletal responses. *Scand. J. Immunol.*, 2015; 82: 418–28.

1 Introduction

Defense mechanisms of our immune system confer protection of the organism against invading pathogens and rely on the coordinated action of various specialized cells and tissues. All defense reactions start with the recognition of the threat by cellular receptors and triggering of a functional response, specific to the type of the responding immune cell. B cells, or B lymphocytes, contribute to the immune defense via production of antibodies, which bind and neutralize infectious agents, lowering their infectious potential and preventing the disease. B cell identity and function is governed by the presence of B cell receptors (BCR), surface antigen-recognition immunoglobulin molecules, with unique specificity toward cognate antigen. Recognition of the antigen triggers intracellular signaling cascades important for B cell differentiation into plasma cells, which secrete soluble version of the B cell receptor – antibodies. Expression of the signaling-competent BCR is also crucial during the development of B cells in the bone marrow, assuring that functional B cells are produced. As cells of the adaptive immune system, the identity of their BCRs is not permanently fixed and can be changed by the introduction of somatic mutations during ongoing immune reactions in the secondary lymphoid organs, such as lymph nodes or spleen. This process is termed somatic hypermutation and occurs in the anatomical structures, called germinal centers. The germinal center reaction is crucial for the development of antibodies with high affinity to the antigen and a prerequisite for the efficient pathogen neutralization by antibodies. Selection of these high affinity B cell clones is believed to depend on stronger BCR signaling conferred by strong antigen-BCR interactions compared to weak interactions. At the molecular level, how recognition of the antigen triggers BCR signaling is still unclear. In recent years, studies have highlighted a critical role of the actin cytoskeleton in the initiation and regulation of BCR signaling and activation. The actin cytoskeleton consists of protein filaments made of actin. Its function is governed by actin regulatory proteins, which are often cell-type specific, modulate actin polymerization and filament disassembly to remodel cellular membranes. Actin reorganization is induced downstream of B cell receptors. At the same time, actin cytoskeleton inhibitors can trigger activation of BCR signaling modules in the absence of antigen binding and deficiency in many of the actin regulatory proteins manifests in immunodeficiencies and autoimmunity, suggesting a tight interplay between BCR signaling and actin dynamics. Besides this, the actin cytoskeleton plays a crucial role in the reorganization of cellular membranes assisting uptake and secretion of molecules, cell division and

migration.

The goal of this thesis is to understand the role of Missing-In-Metastasis / Metastasis Suppressor 1 protein, or MIM/MTSS1, and Interferon Regulatory Factor 4 transcription factor, or IRF4, in BCR signaling and B cell functions. Previous studies established MIM as an actin-binding protein with membrane deforming activities. Multiple other interacting partners of MIM were identified, pointing on its diverse roles in cellular physiology, including regulation of actin and plasma membrane dynamics and cilia function. In several solid tumors lack of MIM expression was associated with cancer metastatic potential. MIM expression is enriched in B cells and MIM knockout mice were found to have aberrant B cell numbers. Moreover, MIM knockout mice were reported to develop lymphomas upon reaching 8 months of age. The reason and mechanisms behind this phenotype manifestation are unclear. We hypothesized that the regulatory role of MIM toward organization of the plasma membrane and the actin cytoskeleton can modulate BCR signaling and in this way result in disturbed B cell development and B cell function, ultimately affecting the generation of the antibody response in MIM-deficient animals. Chronically active BCR signaling is also a hallmark of several types of lymphoma, and thus studying BCR signaling in B cells from MIM knockout animals could provide a clue on how deficiency in MIM may support lymphomagenesis. To study BCR signaling in MIM-deficient cells, as well as to characterize in detail B cell development and antibody responses in MIM-deficient animals, we took advantage of MIM knockout mice generated previously. Contrary to the previous report we found largely undisturbed development of B cells in MIM knockout animals. We showed, however, that MIM-deficient B cells exhibit impaired BCR signaling in response to surface-bound antigen, which we believe is in line with the lowered IgM antibody response to T cell-independent antigen immunization. Finally, we observed that in response to LPS and CpG, pathogen-associated stimuli, MIM-deficient B cells undergo metabolic reprogramming characterized by enhanced mitochondrial functional capacity. Our results suggest that MIM may be involved in the discrimination of properties and form of the encountered antigen by B cell receptors.

To better understand the function and generate new hypotheses about the mechanisms of its action in various cellular settings, we also performed analysis of MIM sequence in the context of its changes during evolution, explored presence of annotated short functional motifs and association with cancer using computational tools and online databases. Our analysis revealed the highly conserved nature of the MIM protein, suggesting importance of the preserved sequence composition. In addition, we report on the presence of several functional motifs, implicating MIM in actin regulation, clathrin-mediated endocytosis, and centrosome homeostasis and propose these motifs for experimental validation. Finally, among B cell cancers, MIM expression levels were shown to be highest in the mantle cell lymphoma, hairy cell leukemia and CLL. In samples from patients in CLL, a B cell cancer with chronically activated BCR signaling, we found, however, that MIM downregulation is associated with poor

disease prognosis.

IRF4 is an important transcription factor, which controls early B cell development and is critical for the GC reaction and plasma cell differentiation. IRF4 expression is induced downstream of BCR. Given the crucial role of BCR signaling in B cell development and plasma cell differentiation, it is important to understand how developmental stage-specific changes in the BCR signaling are driven by implementation of the B cell transcriptional programs. To study the role of IRF4 in BCR signaling, IRF4 knockout DT40 B cells were generated. Our findings suggest that IRF4 deficiency results in changes in the expression levels of BCR signaling components and their abnormal activation upon antigenic challenge. IRF4-deficient cells showed impaired activation of Syk, BLNK and MAPK1/2 proteins and a defected cytoskeletal response. At the same time, BCR signaling in IRF4-deficient cells was characterized by upregulation of PI3K, PLCγ and Ca^{2+} signaling, potentially due to low expression levels of SHIP.

This work is the first comprehensive study on the role of of the actin-regulatory protein MIM in B cell-mediated immunity and provides an evolutionary standpoint on the functional significance of the protein regions of MIM. This study also highlights the fact that IRF4 not only is a downstream effector of BCR signaling but also potently changes expression pattern of the BCR signaling components to support further developmental fate decisions.

As considerable amount of the thesis work and my personal contribution have been largely dedicated to studying the role of MIM/MTSS1 in B cells, the Literature review chapter aims at providing the information to the reader that helps to understand how regulatory activities of MIM toward actin cytoskeleton may influence B cell-mediated immunity.

In particular, the role of different forms of the antigen in B cell activation is discussed as well as the current knowledge on the interplay between actin cytoskeleton and B cell receptor activation. The actin cytoskeleton may play an important role in sensing and transmitting the physical properties of the antigen through dynamic association with B cell receptors on the membrane and thus affecting B cell receptor signaling. Accordingly, B cell-specific actin- and membrane-regulatory proteins, such as MIM, will be an essential players in B cell receptor signaling transduction and beyond. In addition, overview of the known functional connections between B cell activation, differentiation and metabolic reprogramming are introduced in connection with our results suggesting that MIM deficiency in B cells disturbs normal mitochondrial function in response to Toll-like receptor activation.

The Materials and Methods, Results and Discussion chapters are written on publication-to-publication basis, followed by a Conclusions chapter.

2 Literature review

2.1 B cells and the adaptive immunity

2.1.1 Introduction

In our world of nucleic acid-based life, all living organisms are under constant threat of being exploited for energy sources by other forms of life to sustain their functioning and propagation. During the evolutionary history of life, various forms of defense mechanisms to protect the host from foreign nucleic acids have been acquired, as exemplified by CRISPR systems and restriction-modification systems of prokaryotes or RNA interference systems of both pro- and eukaryotes (Koonin and Makarova, 2019; Shabalina and Koonin, 2008; Vasu and Nagaraja, 2013). With the appearance of complex multicellular organization, specialized sets of genes, their products as well as new types of cells and tissues, dedicated to the host defense have evolved, which we can collectively refer to as the **immune system**. Based to a large extent on the array of cell surface receptors, the immune system responds to signs of foreign genetic information, imprinted in the composition and structural features of pathogen molecules. Bearing collection of ancient and more advanced defense mechanisms, the immune system of higher organisms is subdivided into innate and adaptive arms (Table 1) (Goldsby et al., 2003; Delves et al., 2017; Paul, 2008).

Table 1. Overview of the immune system

Innate immunity	Adaptive immunity
evolutionary ancient	evolutionary more recent
limited repertoire of recognition receptors	large set of antigen-recognition receptor specificities
e.g. recognition receptors for pathogen-associated molecular patterns	e.g. T cell and B cell receptors
rapid response but fairly unspecific	delayed response but highly specific
no classical memory	generation of cells of the immunological memory

In simple terms, **innate immunity** responds to molecular patterns, which are usually shared between closely related pathogens. The repertoire of innate immune system receptors is limited and any given receptor may not recognize strain-specific modifications of the pathogen molecules with enough specificity. Typical examples of innate immune receptors of vertebrates are Leucine-rich repeats (LRR) receptors, such as Toll-like receptors (TLR), which respond to pathogen-associated molecules such as bacterial lipopolysaccharides (LPS), or unmethylated CpG-rich nucleic acids.

The genes encoding receptors of the **adaptive immune system** are also limited and encoded in the germ-line DNA. However, through mechanisms of combinatorial and mutational diversification, their gene segments can potentially encode receptors for every possible pathogen structure that an organism may encounter. These receptors are expressed on T and B lymphocytes, and termed T cell (TCR) and B cell receptors (BCR), respectively. Development of T and B cells from hematopoietic stem cells takes place in primary lymphoid organs - B cells develop in the bone marrow and T cell development starts in the bone marrow and continues in the thymus. During development, rearrangements of multiple gene segments encoding TCR and BCR occurs, which are brought together to code for functional receptor polypeptides. Within the scope of this introduction, I focus only on B cell receptors, however, it should be noted that the structure of the genomic loci for T cell receptors is highly similar.

The B cell receptors recognize cognate molecular structures of a pathogen, called **antigens**. The antigen-binding part of the B cell receptor consists of two plasma membrane-anchored polypeptides, or heavy chains (HC), and two smaller polypeptides, or light chains (LC), associated with them (Figure 1). Antigen-binding surfaces are formed by N-terminal parts of each pair of the heavy and light chains, and thus each BCR has two antigen-binding sites. Diversity of the BCRs in respect to antigen is provided by variability of their antigen-binding sites, and hence each BCR polypeptide consists of constant and variable regions, encoded by corresponding constant and variable gene segments of the immunoglobulin loci.

There are three immunoglobulin loci in both the mouse and human genomes. IgH locus encodes heavy chains and two IgL loci can be used to make light chain polypeptides, namely Igκ and Igλ. Each locus has gene segments encoding constant and variable regions of heavy (C_H/V_H) and light chains (C_L/V_L). The gene segments for variable regions of the BCR, which determine diversity and specificity of the antigen-binding sites are further subdivided into V, D (only for heavy chains) and J segments. Each mature B cell has uniquely rearranged V-(D)-J segments and in this way the whole B cell population of an organism possesses a broad repertoire of antigen specificities (Figure 2).

Mechanisms contributing to the generation of the diverse BCR repertoire include: 1) multiple germ-line gene segments encoding variable regions, 2) combinatorial diversity of V-(D)-J segments, 3) imprecise joining of the V-(D)-J segments, 5) addition of P-nucleotides during recombination, 6) addition of N-nucleotides by terminal

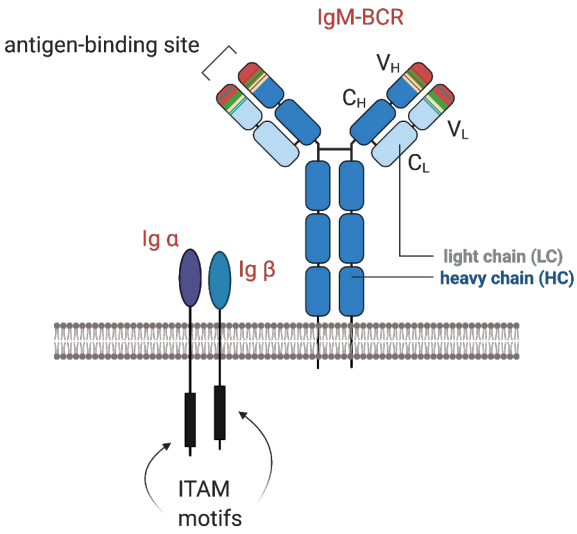

Figure 1. Structure of the B cell receptor.
B cell receptor (BCR) consists of antigen-recognition part, which is represented by plasma membrane-tethered immunoglobulin molecule, and signal-transduction module, which is represented by associated Igα/Igβ polypeptides. Each immunoglobulin molecule comprised of two heavy chains (HC) and two light chains (LC) bridged by disulphide bonds. Both heavy and light chains have constant (C) and variable (V) domains. Antigen-binding site is formed by V domains of each HC-LC pairs, resulting in two antigen-binding sites per immunoglobulin molecule. Upon recognition of cognate antigen the immunoreceptor tyrosine-based activation motifs (ITAM) on Igα/Igβ are phosphorylated leading to B cell receptor activation.

deoxynucleotidyl transferase (TdT) in heavy chain sequences, 7) pairing of heavy and light chains. In addition, during immune responses, the strength of the binding between the antigen-binding site and the antigen, called **affinity**, can be further increased by introduction of mutations into variable-region coding sequences by the process of **somatic hypermutation** (SHM), providing enhanced level of BCR specificity for the antigen.

A unique feature of B cells is their ability to express their antigen-recognition receptors in both membrane-bound and secreted form, called immunoglobulins, or **antibodies**. There are 5 major antibody classes, including IgM, IgD, IgG, IgA and IgE, determined by constant gene segments of the heavy chains. Mature B cells express IgM- and IgD-BCR receptors, and unlike for other classes, IgM/IgD switch and expression of secreted forms are regulated at the level of RNA splicing. Upon antigen binding, initiation of biochemical cascades downstream of the BCR leading to B cell activation is provided by the BCR signaling module, Igα and Igβ polypeptides. The strength of the interaction between antigen and B cell receptor, called affinity, determines the signaling strength. Appropriate level of BCR signaling together with co-stimulatory signals provided by other cells, ensues expansion of B cell clones with

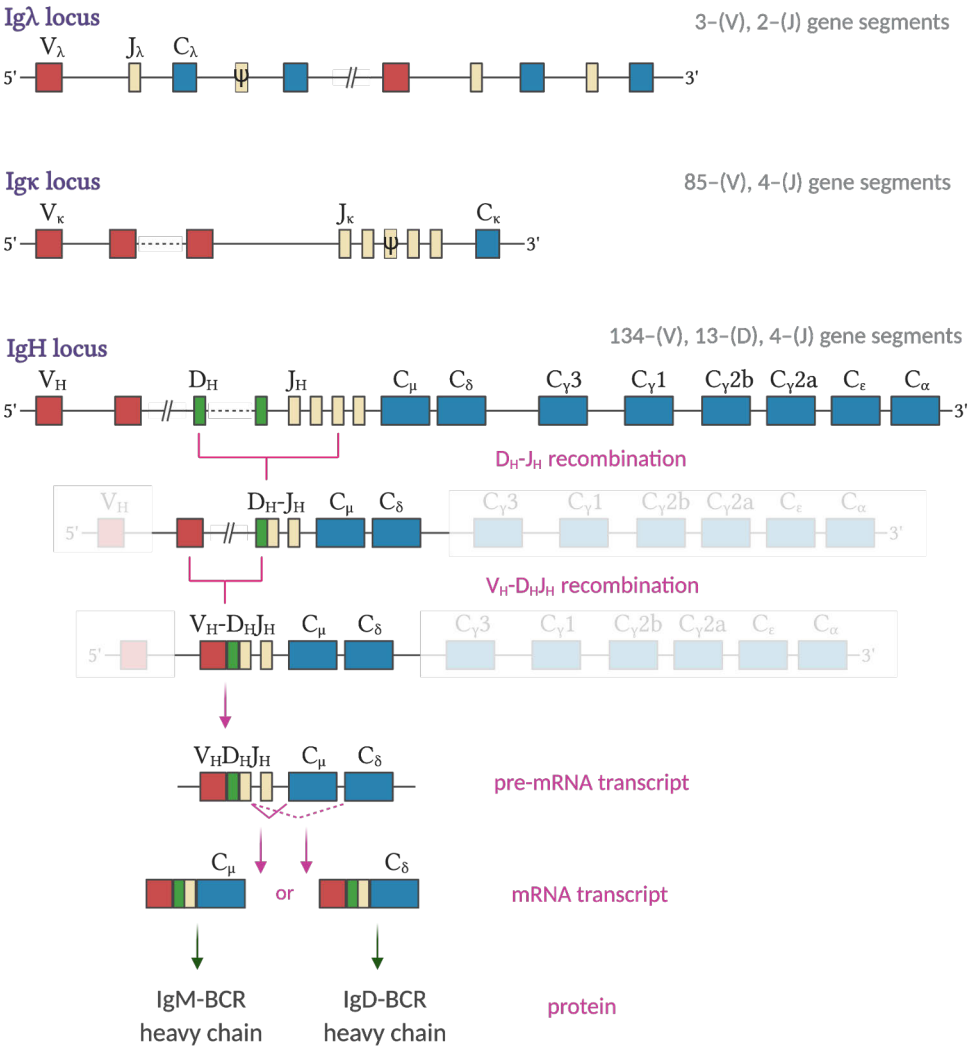

Figure 2. Immunoglobulin loci of mice and schematics of heavy chain locus gene rearrangements. See also: Goldsby et al. (2003).
The heavy and light chain polypeptides of the BCR are encoded by immunoglobulin genes. During the development of B cells gene segments corresponding to variable and constant regions of the BCR are brought together to encode for unique polypeptides. Random joining of V, (D) and J gene segments encoding variable regions accounts for the combinatorial diversity of the resulting antigen-binding sites in the expressed B cell receptor. The gene segments encoding constant regions are responsible for the isotype of the expressed BCR.

BCR specific for the antigen and differentiation into antibody-secreting, or plasma cells. The type of the antibody that plasma cell will produce may also change from IgM/IgD to IgG, IgA or IgE class in the process of **class-switch recombination** (CSR), depending on the nature of the pathogen and cytokine milieu. Another important feature of adaptive immunity is generation of memory B (and T) cells, which upon secondary exposure to the antigen are able to elicit immune responses that are stronger and faster than the initial response (Figure 3).

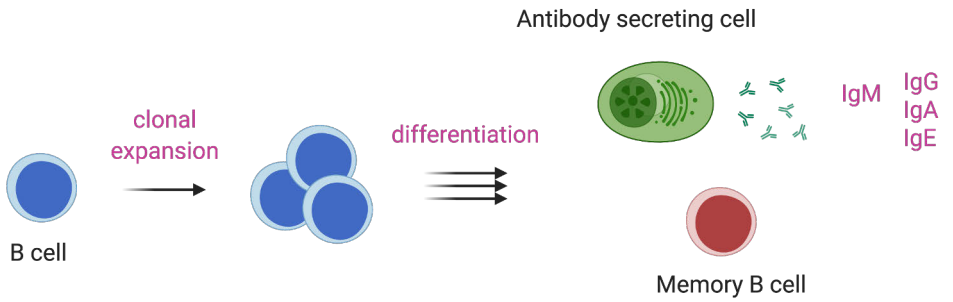

Figure 3. Clonal expansion and differentiation of the B cell during an immune response. Recognition of the cognate antigen and co-stimulatory signals from accessory cells can lead to B cell proliferation and differentiation into antibody-secreting (ASC), or plasma cells. Important feature of the adaptive immune response is the generation of memory B cells, which may persist for long periods of time and differentiate into antibody-secreting cells with a faster kinetics upon secondary antigen exposure.

The function of the B cell-mediated immunity is in large part determined by the ability of B cells to secrete high-specificity antibodies, which neutralize pathogens or target them to degradation and which is the main mechanism of protection by many vaccines. On the other hand, disturbed function of B cells, can lead to hypo- or hyper-responsive immunity, which may contribute to increased susceptibility to infections or autoimmune diseases.

Other important functions of B cells in immunity in addition to antibody production include antigen presentation, which supports antibody responses, but also secretion of various cytokines, crucial for host defense and homeostasis (Kalampokis et al., 2013). Significance of B cell-derived cytokines was reported, for instance, in lymphoid tissue organization for LTα/β (Tumanov et al., 2003), monocyte mobilization in tissue injury for Ccl-7 (Zouggari et al., 2013; Inaba et al., 2020) and control of bacterial infections and sepsis for GM-CSF (Rauch et al., 2012; Weber et al., 2014). Numerous reports describe the role of B cell-derived IL-10 in both promoting B cell responses, for instance, by supporting generation of germinal centers (GC) in malaria model (Guthmiller et al., 2017) and immunosuppression, as shown in the model of experimental autoimmune encephalomyelitis (EAE) and resolution of severe autoimmunity (Fillatreau et al., 2002).

2.1.2 B cell development

Following yolk sac and fetal liver hematopoiesis, the bone marrow is the major site of blood cell development in adult mice and humans throughout life (Yoder, 2002). As a primary lymphoid organ, the bone marrow supports the development of immature B cells, and thus leads to the generation of the primary immune repertoire of B cell antigen receptors. The developmental path from the common lymphoid progenitor (CLP) to the immature B cell is governed by the realization of a complex transcriptional program, rearrangements of the genes of the immunoglobulin loci and is marked by expression of key transcription factors and cell surface determinants (González et al., 2007; Nutt and Kee, 2007; Hardy et al., 2007) (Figure 4).

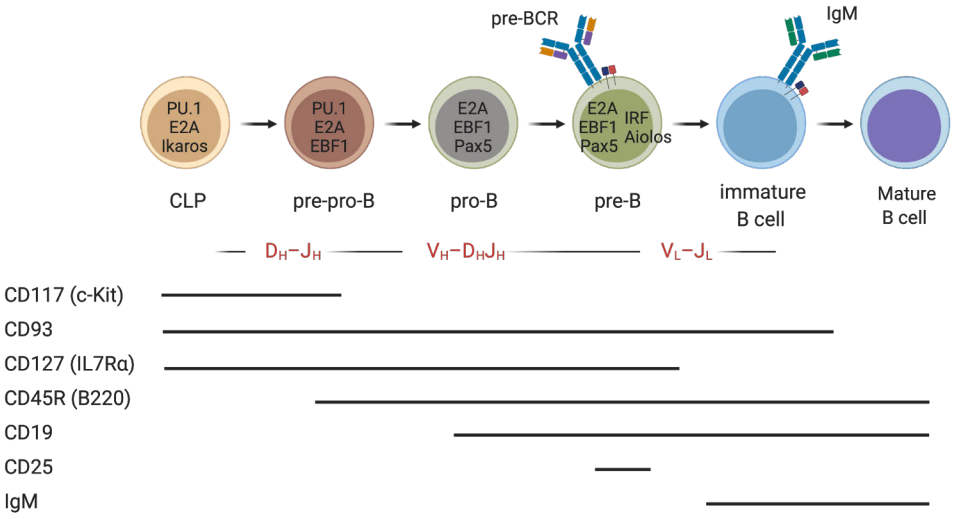

Figure 4. B cell development in the bone marrow.
Consequent developmental stages from CLP toward mature B cell, major transcriptional regulators, and V(D)J recombination events are shown. The expression timeline of corresponding cell surface receptors is indicated by black horizontal lines below. See also: Hardy et al. (2007); Nutt and Kee (2007).

During development, a sequential rearrangements of immunoglobulin genes occurs, first at the heavy chain (IgH) locus and later at the Igκ and/or Igλ loci. Important developmental checkpoints include the pre-B cell stage, where successful rearrangements of the IgH locus manifest in surface expression of the pre-B cell receptor (pre-BCR) and the immature B cell stage after successful rearrangement of the light chain (IgL) loci, which results in surface expression of the IgM-BCR (Hendriks and Middendorp, 2004). Developmental decisions are made based on the ability of these molecules to initiate appropriate level of signaling via Igα/Igβ to support survival and maturation. Before rearrangement of the IgL loci commences, the role of light chains is taken by surrogate light chains (SLC) consisting of VpreB and λ5 polypep-

tides. Unproductive gene rearrangements or pairing of IgH with VpreB-λ5 SLC in pre-BCR result in inability to signal and lead to apoptosis of the developing B cell. Likewise, unsuccessful pairing of the IgH with Igκ or Igλ light chains also results in clonal deletion (Kline et al., 1998). Random Ig gene rearrangements can lead to expression of self-reactive BCRs. To ensure that the developing B cell will commit no damage to the organism, tolerance mechanisms have evolved to eliminate these potentially harmful B cell clones from the mature B cell pool. Central tolerance for signaling-competent receptors in the bone marrow can be achieved through receptor editing by additional rounds of light chain rearrangements (Casellas et al., 2001). If this fails, autoreactive B cell clones are either deleted or a state of unresponsiveness, or anergy, ensues, which, however, seem to take place in the periphery (Goodnow et al., 1988; Erikson et al., 1991; Hartley et al., 1991; Nemazee, 2017).

To highlight the importance of BCR-mediated signaling in B cell differentiation, it was noted that severe maturation defects beyond pre-B cell stage are observed in mice deficient in several BCR signaling components: Syk/Zap-70 (Schweighoffer et al., 2003), SLP–65/LAT (Su and Jumaa, 2003) or SLP-65/Btk (Jumaa et al., 2001).

2.1.3 Peripheral B cell subsets

Transitional B cells

It is believed that after bone marrow egress, immature B cells in the periphery are represented by populations of $CD93^+$ $CD19^+$ $B220^+$ transitional (T) B cells. Progression from T1 to T3 stages are marked by reductions in surface IgM expression, upregulation of IgD and acquisition of CD23 and CD21 on the cell surface (Monroe and Dorshkind, 2007). Functionally, there are conflicting results on the proliferation outcome. However, T1 cells appear to more readily undergo apoptosis than more mature populations after BCR crosslinking (Allman et al., 2001; Chung et al., 2002; Petro et al., 2002; Su et al., 2002). Immature B cells are able to present MHCII-peptide complexes, however, they do not upregulate the T cell co-stimulatory molecule, CD86, and are likely to be purged from the B cell repertoire if activated (Chung et al., 2003; Marshall-Clarke et al., 2000). Transitional B cells are also highly dependent on BAFF cytokine for survival, and B cell development is stalled in BAFF- or BAFF-R-deficient animals at around the T1 stage (MacKay and Schneider, 2009).

Follicular and marginal zone B cells

Splenic mature B cell subsets (B2 cells) largely contain IgM^{lo} IgD^{hi} follicular (Fo) B cells, which represent the principal B cell population of the host, and IgM^{hi} IgD^{lo} marginal zone (MZ) B cells, located in the marginal zones of the spleen at the periphery of periarteriolar lymphoid sheaths (PALS) and B cell follicules (Martin and Kearney, 2002). Follicular B cells is the major population of B cells and it is this subset that respond to T cell-dependent (TD) proteinaceous antigens, form germinal centers (GC) and implicated in generation of memory B cells. MZ B cells are $CD21^{hi}$ $CD23^{lo}$

and their strategic anatomical placement allows for immediate access to blood-borne antigens. MZ B cells are responsible for early wave of extrafollicular plasmablast differentiation as shown in the response to T cell-independent (TI) lipid antigen (Martin et al., 2001; Martin and Kearney, 2000). At the same time, high CD21 levels allow for efficient transfer of complement-bound TD antigens into the follicles, where Fo B cells can be activated (Pillai and Cariappa, 2009). Developmental mechanisms of MZ B cells are not very clear but several important factors that affect their development and function have been reported, including, Notch2 (Saito et al., 2003; Case et al., 2015), Taok3-ADAM10 (Hammad et al., 2017) and Pyk2 (Guinamard et al., 2000). It is important to note that the splenic marginal zone is not formed until 2–3 weeks of age in mice and 1–2 years in humans, which coincides with immaturity of the immune system and unresponsiveness to certain T-independent antigens (Martin and Kearney, 2002; Scher, 1982; Smith et al., 1973).

B1 cells

Separate populations of B cells predominantly residing in coelomic cavities are called B1 cells. Mostly studied in the peritoneal cavity of the mice, these cells are further divided into B1a ($CD5^+$) and B1b ($CD5^-$) cells. CD11b and CD43 are also used, however, both populations can differentially express CD11b and CD43, whereas $CD43^+$ B1 cells are mostly found outside the body cavities (Baumgarth, 2010). Developmentally, B1 cells are thought to be distinct from other peripheral B cells. B1 cells are efficiently reconstituted by cells from splanchnopleura and fetal liver, however, the adult bone marrow have also been shown to provide some supply of B1 progenitors (Hayakawa et al., 1985; Esplin et al., 2009; Ghosn et al., 2008; Godin et al., 1993). B1 cells are characterized by biased usage of V-D-J gene segments, high proportion of IgH sequences without N-insertions (Tornberg and Holmberg, 1995; Kantor et al., 1997; Yang et al., 2015; Prohaska et al., 2018) and they secrete antibodies with specificity to self- and pathogen-associated antigens (see also: Baumgarth (2010); Racine and Winslow (2009)). B1 cells are thought to be responsible for the large amount of natural serum IgM, which they generate outside body cavities after activation and migration to secondary lymphoid organs, bone marrow or local tissue (Baumgarth et al., 1999; Thurnheer et al., 2014; Choi et al., 2012; Ha et al., 2006; Yang, 2007; Weber et al., 2014). There are conflicting results on the effect of BCR stimulation on B1 cell proliferation (Baumgarth, 2010; Holodick and Rothstein, 2013). However, it seems that B1 (and especially B1a) cells can exhibit a restricted capacity to enter cell cycle in response to anti-IgM stimulation (Bikah et al., 1996; Morris and Rothstein, 1993). BrdU labeling experiments suggested that similar to B2 cells, B1 cells are long-lived with a slow turnover rate. However, their ability to expand is believed to be achieved through self-renewal (Deenen and Kroese, 1993; Förster and Rajewsky, 1987). Functions of B1 cells include immunity to infections via production of neutralizing pathogen-specific natural antibodies by B1a cells (Choi and Baumgarth, 2008; Martin et al., 2001; Haas et al., 2005), specific immune antibody production by B1b cells (Haas et al., 2005) and elimination of apoptotic

cells or tissue damage via self-reactive IgM (Chen et al., 2009; Zhang et al., 2006).

2.1.4 BCR signaling pathways

B cell activation can be loosely described as a process that is triggered by external stimuli to initiate intracellular biochemical reactions that have a potential to drive B cell differentiation into an antibody-secreting cell, or plasma cell. The differentiation path toward antigen-specific antibody production requires engagement of the B cell receptor with the cognate antigen and triggers several signaling cascades that are crucial for priming of plasma cell development, including PI3K-, Ca^{2+}-, Ras-MAPK- and NF-κB-pathways (Tanaka and Baba, 2020) (Figure 5).

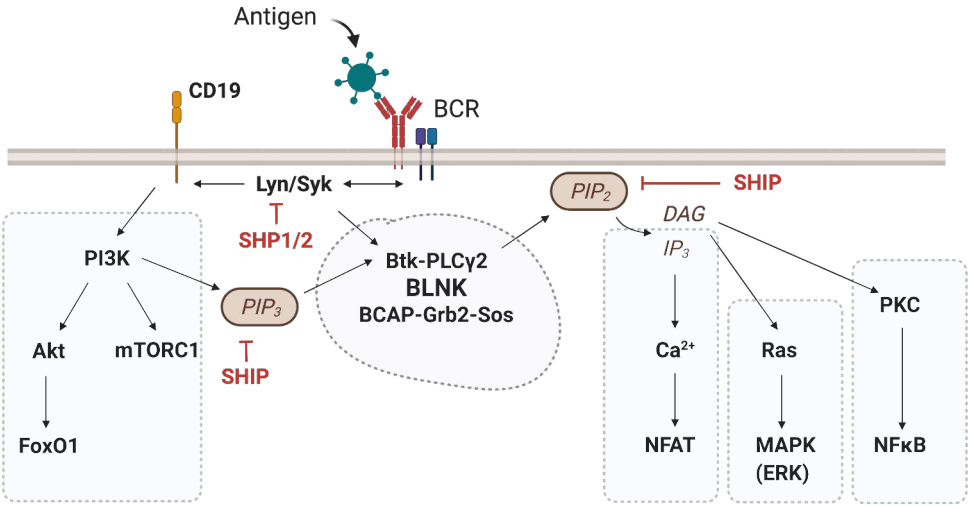

Figure 5. BCR signaling pathways.
Major components of the conventional signaling pathways (dashed outlines) activated downstream of the BCR complex are shown. Lipid species ($PI(4,5)P_2$, $PI(3,4,5)P_3$) and their metabolites (DAG, IP_3) are indicated in brown. Negative regulators of the selected signaling modules are shown in red (SHP1/2, SHIP).

Proximal signaling

Src family kinases, and most notably Lyn, are the first to become activated upon BCR engagement by antigen (Gauld and Cambier, 2004). The role of CD45 and CD148 receptor phosphatases are also important at this stage. These phosphatases regulate the activity of Src kinases by dephosphorylation of negative regulatory tyrosines (Zhu et al., 2008). This is followed by phosphorylation of Igα/Igβ ITAM (immunoreceptor tyrosine-based activation motifs) sequences of B cell receptor complex by Src and recruitment and activation of Syk kinase (Hagman, 2009; Sanchez et al., 1993; Cornall et al., 2000). Syk-mediated phosphorylation of its targets initiate recruitment and assembly of the so-called signalosome, a complex of adaptor and ef-

fector proteins, including BLNK (SLP-65), CIN85, CD2AP, Dok3, Grb2, Vav, Nck2, which leads to recruitment and activation of Btk and phospholipase C-γ2 (PLCγ2), two crucial enzymes in the BCR signaling pathway (Fu et al., 1998; Pal Singh et al., 2018; Oellerich et al., 2011; Kim et al., 2004).

PI3K pathway

The PI3K-Akt pathway, important for development, survival and proliferation of B cells and activated downstream of BCR, requires the CD19 co-receptor and BCAP adaptor protein (Donahue and Fruman, 2004; Aiba et al., 2008). Tyrosine-phosphorylated cytoplasmic tail of CD19 recruits phosphatidylinositol-3 kinase (PI3K) directly as well as Src kinases (Lyn, Fyn), Grb2-Sos, Vav and PLCγ2. CD19 can operate as an adaptor molecule but also may be directly ligated with BCR via complement-bound antigens through the complement receptor, CD21, with which it constitutes the CD19 co-receptor complex (together with CD81 and CD225) (Sato et al., 1997; Carter et al., 2002). Bridging of CD19-PI3K to BCR may also be mediated through direct Nck binding to BCAP and Igα (Castello et al., 2013). Phosphatidylinositol-3 kinase involved in the generation of 3'-phosphorylated inositol lipids, provides membrane PI(3,4,5)P_3 (or PIP_3) for PH (pleckstrin homology) domain-containing Akt (protein kinase B, PKB), which is activated via phosphorylation by PDK1 and mTOR protein complex 2 and translocates to the nucleus to target its substrates, such as FoxO1 (Szydłowski et al., 2014). Of note, PI(3,4,5)P_3 is also required for membrane recruitment of Btk (Pal Singh et al., 2018), which links PI3K to other pathways. Another important signaling cascade that is initiated downstream of PI3K is the activation of mTOR complex 1 (mTORC1), implicated in metabolic regulation of cell physiology (Limon and Fruman, 2012; Donahue and Fruman, 2007).

Ca^{2+} signaling

Recruitment of PLCγ2 and its activation by Btk and other kinases results in hydrolysis of PI(4,5)P_2 (or PIP_2) into diacylglycerol (DAG) and inositol-1,4,5-triphosphate (IP_3). Ca^{2+} release is initiated by IP_3 binding to its receptors on the ER membranes, and once ER stores are depleted, extracellular influx is sustained by opening of the CRAC channels through store-operated calcium entry (SOCE) process. Ca^{2+} regulates activity of Ca^{2+}-binding effectors and their targets, exemplified by the activity of NFAT transcription factor in promoting survival and proliferation (Kim et al., 2004; Scharenberg et al., 2007).

MAPK signaling

Generation of DAG links the BCR to the activation of Ras-MAPK and NF-κB signaling. Ras activation is associated with interaction of DAG and RasGRP; the latter exerts its guanyl-nucleotide exchange factor (GEF) activity toward Ras triggering activation of mitogen-activated protein kinases (MAPK), which translocate into the nucleus to phosphorylate its targets (Oh-Hora et al., 2003; Coughlin et al., 2005; Tordai et al., 1994; Morrison, 2012). In human B cells, Grb2-Sos rather than RasGRP activity was associated with MAPK activation (Vanshylla et al., 2018).

NF-κB signaling

DAG also activates protein kinase C-β (PKCβ). PKCβ-mediated activation of the CARMA1-TAK1-MALT1-BCL10 complex in turn leads to phosphorylation and activation of the IκB kinase complex, IKK, which by action on IκB, targets it to Ubiquitin (Ub)-mediated degradation thus releasing NF-κB transcription factor for nuclear import (Thome et al., 2010; Shinohara et al., 2005; Saijo et al., 2002; Su et al., 2002). It is important to note that members of classical (DAG- and Ca^{2+}-regulated), novel (DAG-regulated) and atypical PKC family members all seem to be important regulators of NF-κB and more broadly of B cell activation and functioning (Guo et al., 2004).

Negative regulation

To avoid uncontrolled activation and autoimmunity, BCR signaling is balanced by feedback loops and inhibitory activity of multiple regulatory proteins. Protein tyrosine phosphatases SHP-1/2 are known regulators of Src downmodulation, acting downstream of ITIM (immunoreceptor tyrosine-based inhibitory motif)-containing co-receptors. A number of them have been reported to negatively regulate BCR signaling and functions. In mice these include FcγRIIb, CD22, Siglec-10 (Siglec-G), CD72, CD5, PECAM-1 (CD31), CEACAM-1 (CD66a), LIR-3 (PIR-B), PD-1 and LAIR-1 (CD305) (Tsubata, 2018; Pritchard and Smith, 2003; Pao et al., 2007). Importantly, ITIM phosphorylation for association with SHP1/2 or Csk is mediated by Lyn, which thus plays a dual role in BCR signaling (Xu et al., 2005). There are also known negative regulators specific to each activation pathway. For instance, PTEN counteracts the activity of PI3K, whereas SHIP-1 removes 5'-phosphate from phosphoinositides, antagonizing PI(4,5)P_2- and PI(3,4,5)P_3-mediated cascades. The NF-κB pathway can be downmodulated by A20 and CYLD deubiquitinases. Dok-1 adaptor (via RasGAP) and PTP-PEST phosphatase can downmodulate MAPK signaling (Tanaka and Baba, 2020).

2.1.5 Antibody responses against T cell-dependent and T cell-independent antigens

Efficient and controlled BCR signaling is one of the prerequisite steps toward generation of productive antigen-specific antibody responses. The nature of the antigen itself influences the path through which generation of plasma cells occurs and which cell subsets will participate in the immune response. Participation of T cells to provide cell-mediated co-stimulatory signals to responding B cells marks an important distinction between protein-based and non-proteinaceous antigens, where the former are thought to provide more specific and long-lasting immunity against infectious agents through a process of clonal selection of best-fit-to-antigen B cell clones and generation of persistent memory cells.

T-dependent antibody responses

Immunization experiments in neonatally thymectomized mice revealed T cell-dependence of antibody responses to protein-based antigens (Miller and Mitchell, 1968; Mitchell and Miller, 1968; Crotty, 2015). In order to support B cell antibody responses, T cells need to be activated, or primed, by cognate antigen. Unlike BCRs, T cell receptors (TCR) can only recognize peptide fragments of the protein antigens bound to major histocompatibility complex (MHC) molecules. The peptide-MHC (pMHC) complexes are formed in the process termed antigen presentation (Ag presentation) and cells capable of performing this task are called antigen-presenting cells (APC). In the process of the antigen presentation, parts of the captured and hydrolyzed protein antigens are complexed with MHC molecules in the endocytic compartments and displayed to T cells on the surface of APC. Typically, antigens are delivered to the draining lymph nodes by dendritic cells, monocytes or neutrophils, or can access spleen via blood circulation (Italiani and Boraschi, 2014; Hampton and Chtanova, 2019; Siegrist, 2018). The delivery of both intact protein as well as non-proteinaceous antigens to B cell follicules in the secondary lymphoid organs can occur via conduit systems for small antigen molecules (Nolte et al., 2003) and via cell-mediated transfer, for instance, by supcapsular sinus (SCS) macrophages in lymph nodes (Carrasco and Batista, 2007; Junt et al., 2007), and marginal zone macrophages and B cells in spleen (Ferguson et al., 2004; You et al., 2011). Priming of naive helper T cells (pMHC recognition and T cell activation), typically performed by macrophages or dendritic cells, results in the differentiation programs, such as differentiation to T follicular helper cells (Tfh). B cells are also professional APCs, however, Ag presentation by B cells also serves an important role in engaging cognate T cells to support development of antigen-specific B cells into antibody-secreting or memory B cells (Crotty, 2015, 2019; Nurieva et al., 2009; Johnston et al., 2009; Liu et al., 2012c). The amount of T cell help received by B cell in the form of co-stimulatory signals is directly proportional to the efficiency of antigen presentation and T cell activation during T cell-B cell interactions (Gitlin et al., 2014; Shulman et al., 2014). Tfh cells can support either an extrafollicular B cell response, characterized by the development of short-lived plasmablasts secreting low-affinity antibodies, or a germinal center (GC) responses in the B cell follicular areas, where long-lived antibody-secreting cells are generated producing high-affinity antibodies (Figure 6). The germinal center reaction in essence constitutes an iterative process where B cells that improve their BCR specificity through somatic hypermutation of immunoglobulin genes (affinity maturation) are selected to develop into long-lived antibody secreting cells (Victora and Nussenzweig, 2012). Structurally, the GC light zone (LZ) is an area where antigen presentation and interaction with Tfh cells occurs, while the GC dark zone (DZ) is enriched in proliferating B cells. Key factors that determine T cell help include CD40L-, IL-21-, IL-4-, CXCL13-, SAP- and ICOS-delivered signals (Crotty, 2015). Class-switching (change of the Ig isotype) per se as well as plasmablast differentiation are not dependent on the germinal center reaction and

may occur outside B cell follicles. At the same time both processes depend on cell proliferation (Stavnezer et al., 2008; Vinuesa and Chang, 2013). Transcriptional programs of T and B cells that govern GC reaction are mostly BCL-6-mediated, whereas generation of both short- and long-lived antibody-secreting cells is under IRF4 and BLIMP-1 transcriptional control (Nutt et al., 2015).

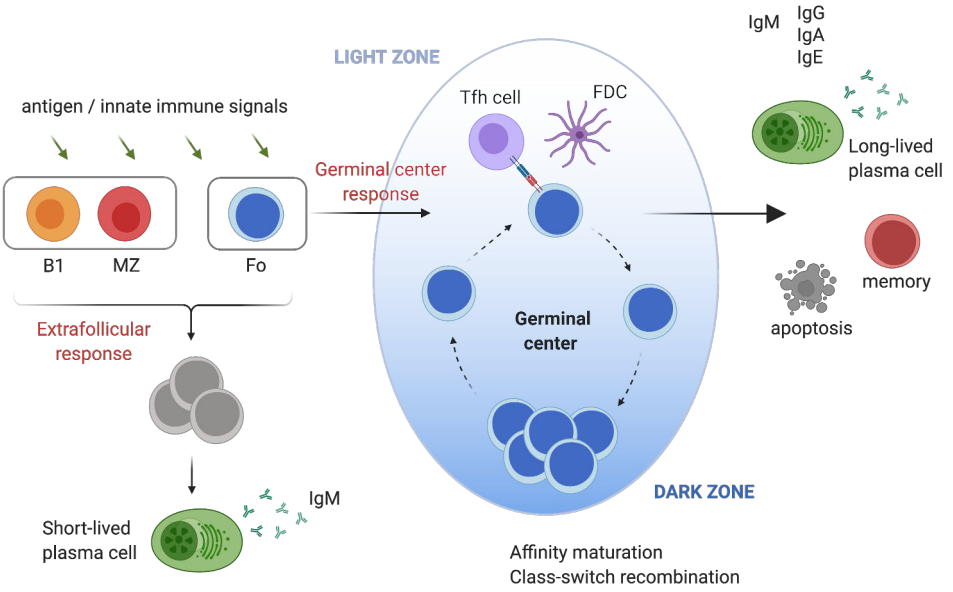

Figure 6. B cell antibody responses.
Antigen recognition or innate immune signals can drive proliferation and differentiation of B cells into antibody-secreting plasma cells outside of the B cell follicles. These signals are typically delivered by T cell-independent antigens and result in generation of short-lived plasma cells that secrete antibodies of mainly IgM isotype. T cell-dependent protein antigens are delivered to follicular dendritic cells (FDC) in the secondary lymphoid organs, captured and processed by follicular B cells to be ultimately presented as peptide-MHCII complexes to cognate T follicular helper (Tfh) cells. Activation of B cells through cognate interactions with Tfh cells drives the so-called germinal center (GC) response, where proliferating B cell clones in the dark zone of the GC compete for T cell-derived co-stimulatory signals in the light zone of the GC. Germinal center reaction outputs B cell clones with the BCR that can recognize antigen with high-specificity (high-affinity). Upon recognition of the antigen such B cells can efficiently differentiate into long-lived antibody-secreting cells producing antibodies of various isotypes. Memory B cells are also believed to be produced in the germinal center reaction. Non-productive interaction within GC result in B cell apoptosis. See also: Roghanian and Newman, immunology.org.

T-independent antibody responses

Antigens that can elicit antibody responses in athymic mice were termed T-independent (TI) (Mond et al., 1980; Mosier and Subbarao, 1982). Further studies categorized TI antigens into type 1 and type 2 based on the ability of these antigens to induce antibody responses in CBA/N strain and neonatal mice (Scher, 1982) (Table 2). TI-1 antigens are represented by molecules that typically can induce polyclonal activation of B cells independently of BCR recognition. For instance, pathogen-associated molecules, LPS and CpG, exert their action through toll-like receptors and induce proliferation and plasmablast differentiation without the need of T cell help in vitro and in vivo (Vinuesa and Chang, 2013). On the other hand, TI-2 antigens are unable to elicit antibody responses in CBA/N (Xid) mice, which is explained by compromised B cell compartment and BCR signaling due to mutation in *btk* gene, although T cell-dependent (TD) responses are present in these mice (Thomas et al., 1993; Rawlings et al., 1993; Maas and Hendriks, 2001). TI-2 antigens are typically represented by polyvalent molecules, such as bacterial polysaccharides, able to potently engage multiple surface B cell receptors (BCR crosslinking) and therefore these responses are highly dependent on the intact BCR signaling. In fact, TI-1 responses are also compromised in BCR-impaired settings, which can be explained by shared signaling molecules used by BCR and TLRs (Scher et al., 1975; Scher, 1982; Otipoby et al., 2015; Morbach et al., 2016; Nyhoff et al., 2018). However, unlike stimulation with TLR agonists, BCR crosslinking will ultimately result in cell death, and thus in vivo responses to TI-2 antigens, although T cell-independent, are likely promoted by co-stimulatory signals from other sources (Parker, 1980).

Table 2. Characteristics of T cell-independent antigens

	TI type 1	**TI type 2**
Antibody responses in neonatal or CBA/N (Btk-deficient) mice	+	−
Antibody responses in adult mice	+	+
Requirement for accessory cells for antibody responses	−	+

FICOLL polysaccharide conjugates are typical TI-2 model antigens used in immunological studies. Both marginal zone B cells and peritoneal cavity B1b cells are thought to be responsible for hapten-specific antibody production to FICOLL conjugates (Girkontaite et al., 2001; Guinamard et al., 2000; Haas, 2011). Responses to TNP-FICOLL in reconstituted BM chimeras can be restored by transfer of splenic (SPL), lymph node (LN) or peritoneal cavity (PerC) cells and that PerC cells are more potent than SPL cells in their ability to induce anti-TNP antibody levels (Prior et al., 1994), which also happens in the absence of MZ B cell population in the spleen (Hsu et al., 2006). Contrary to this, TNP-FICOLL responses after spleen autotransplantation in mice and with related TI-2 antigen, DNP-HES (hydroxyethylstarch), in rats show that induction of hapten-specific antibodies closely correlates with reappearance of marginal zone B cells (Claassen et al., 1989; Lane et al., 1986). It is plausible to assume that both PerC and spleen compartments contain recirculating B cells with the ability to confer responses to TI-2 antigens. An interesting observation on the requirement for IgM-BCR-dependent surface display of TNP-FICOLL by TNP-specific B cells for responses in vitro may explain requirement for MZ B cells in responses to large TI-2 antigens in vivo, which may bind and display antigen to responding follicular B cells (Kirkland et al., 1980). Nonetheless, additional requirements in the form of cytokines or adherent cell populations are essential for differentiation into antibody secreting cells (Mosier and Subbarao, 1982).

2.2 Regulation of B cell responses

2.2.1 B cell activation in response to different forms of antigen

B cells can respond to a variety of antigens. While T cell receptors recognize membrane-bound peptide-MHC complexes, after protein has been hydrolyzed and coupled with major histocompatibility molecules (MHC) in the endosomes of an antigen-presenting cell, B cell receptors can interact with unprocessed antigens in their native form. Thus, B cell can be triggered by antigens of various chemical composition and physical properties, which include not only proteins, but also other molecules such as carbohydrates, lipids and nucleic acids. These antigens can be encountered by B cells in either free circulating or cell-bound form. It is, however, believed that B cells recognize majority of the antigens as bound and displayed to them on the surface of other cells (Heesters et al., 2016). The capture, transfer and cell surface display of the antigen in the secondary lymphoid organs can be mediated through direct antigen binding by scavenger receptors (You et al., 2011; Junt et al., 2007) or through binding of the antigen in immunocomplexes by receptors to antibodies and complement receptors (Guinamard et al., 2000; Youd et al., 2002; Ferguson et al., 2004; Phan et al., 2007). Several immune cell types were shown to display captured antigen to antigen-specific B cells, including SCS macrophages (Carrasco and Batista, 2007), MZ macrophages (You et al., 2011), MZ B cells (Cinamon et al.,

2008), and follicular dendritic cells (FDC) (Heesters et al., 2013; Suzuki et al., 2009).

Acknowledging this physiological way of antigen "presentation" to B cells in lymphoid organs, in the following section I will summarize different types of antigens that a B cell can encounter. Although, we gained a lot of understanding about B cell physiology from studies that involve antigen-stimulation of B cells, it appears that the nature of the antigen and mode of its presentation to B cell may have a considerable impact on B cell activation and thus may profoundly influence in vivo antibody responses and therefore important factors to consider.

Monovalent vs. polyvalent antigens

One of the first properties that was immediately acknowledged by researchers was valency of the stimulatory agent. This property characterizes the number of similar structures, or epitopes, that can be recognized by B cell receptor on one antigenic molecule. An antigen molecule that possesses more than one epitope can be recognized by two or more BCR molecules on the same B cell. This was found to be determinative for the ability of an antigen to activate B cells. One universal antigen that can trigger B cell activation regardless of the B cell antigen specifity is antibodies that are raised against B cell receptor molecules themselves and that are bivalent by nature. From earlier days and until today anti-immunoglobulin (anti-Ig, or anti-BCR) antibodies and their fragments are commonly used as surrogate antigens in B cell research (Figure 7).

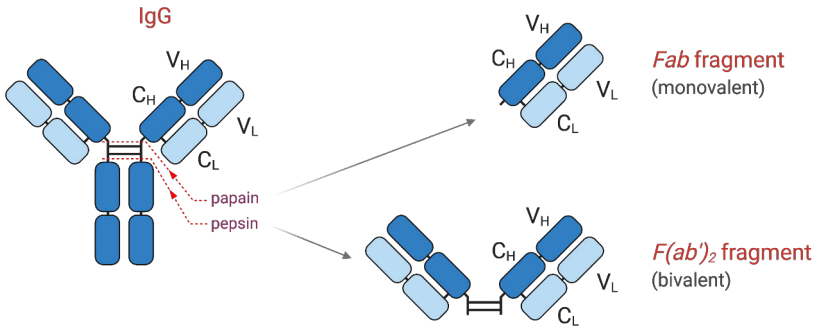

Figure 7. IgG antibody and its fragments generated by papain and pepsin enzymatic digestion.

Experiments with mixed lymphocyte cultures showed that anti-lymphocyte serum, its IgG or F(ab')$_2$ fragments induced cell proliferation, whereas Fab' did not (Woodruff et al., 1967). Ultimately, when it was proven that anti-Ig proliferative responses were attributed to B cells (Sieckmann et al., 1978), similar findings were observed where Fab' fragments were unable to induce Ca^{2+} signaling or plasma membrane depolarization, the early events of B cell activation (Pozzan et al., 1982; Monroe and Cambier, 1983). Ability of specific antibodies to activate various surface cell receptors led to a hypothesis of monomer receptor dimerization in activation (Heldin, 1995). Recent research, however, shows that high proportion of B cell and T cell receptors

on the cell surface of resting cells already reside within formed nanoclusters (Lillemeier et al., 2010; Mattila et al., 2013). Nonetheless, specific antibodies do activate receptors upon binding and this is commonly referred to as receptor cross-linking.

Inability of monovalent Fab' fragments to induce BCR signaling, however, cannot be generalized to all monomeric antigens. Indeed, there are reports where monovalent ligation of HEL-, OVA-, or NIP-specific BCRs leads to receptor activation (Kim et al., 2006; Avalos and Ploegh, 2014; Volkmann et al., 2016). Antibodies against BCR commonly used for in vitro B cell activation bind outside of the antigen-binding site and so do their monovalent Fab' fragments. Although it was reported that only Fab' fragments that recognize antigen-binding site (idiotype) of the BCR may induce receptor signaling (Volkmann et al., 2016), in yet another study the same anti-idiotypic antibodies have failed to induce Ca^{2+} response in B cells with the cognate B cell receptor (Minguet et al., 2010). The reason for this is unknown and results may be influenced by differences in experimental conditions. In summary, it can be concluded that certain monovalent antigens can trigger BCR signaling and B cell activation, although the strength of such stimulation is usually lower than for polyvalent antigens. In some studies monovalent Fab fragments, although inefficient in BCR triggering, can still be presented by B cells and lead to proliferation and antibody secretion determined by the amount of T cell help (Tony et al., 1985), where in others, monovalent HEL has failed to promote antigen presentation efficiently (Kim et al., 2006).

Polyvalent antigens or aggregated monomeric antigens, on the other hand, have long been known to elicit efficient immune responses in vivo and proliferative responses in vitro (Feldmann and Basten, 1971; CRUMPTON, 1974; Sieckmann et al., 1978). One category of these substances displaying highly repetitive antigenic determinants was termed TI-2 antigens (T cell-independent antigens) (Scher, 1982) and discussed earlier in the section 2.1.5. Antibody responses to TI-2 antigens are clearly dependent on intact BCR signaling as Btk-deficient animals are defective in such responses, and also requires a certain level of maturity of the immune system in vivo (Scher, 1982; Martin and Kearney, 2002). Mature splenic B cell pool consists of a large fraction of anergic B cells, characterized by downmodulation of surface IgM and high IgD expression. Although these cells are called anergic, they assumed to constitute a mature B cell state unresponsive to low-valency antigens (Goodnow et al., 1988; Merrell et al., 2006; Zikherman et al., 2012; Quách et al., 2011; Setz et al., 2019). These mature B cells may, however, respond to high-valency antigen. It has been shown that oligo- and polyvalent HEL antigens trigger signaling from both IgM and IgD, whereas IgD-BCR were unresponsive to monovalent HEL ligation and this was dependent on the IgD hinge region (Übelhart et al., 2015; Setz et al., 2019). Although the responsiveness of IgD-BCR to monovalent antigen has been challenged in another study (Sabouri et al., 2016), breaking the tolerance by BCR engagement with multivalent antigens fits well with the notion of B cell responses to VSV viral particles in transgenic mice expressing membrane VSV-G (Bachmann et al., 1993).

Soluble vs. surface

Both monovalent and polyvalent antigens can be encountered by B cells in the form of free circulating molecules, as part of larger structures, such as microorganisms, or cell-bound form.. Antigenic determinants on the surface of viruses and bacteria, foreign and autologous antigens of the cell plasma membranes, or molecules bound to cell surface receptors directly (e.g. lectins) or captured as immunocomplexes by complement (CD21/35) or antibody receptors (Fc receptors) can be viewed as ”surface” forms of an antigen. In vitro, this form of antigenic display is usually mimicked by antigen-coated beads, plastic and glass surfaces, or antigen-bearing supported lipid bilayers.

Similarly to polymeric antigens with repetitive antigenic determinants (Brunswick et al., 1988; Rehe et al., 1990; CRUMPTON, 1974), it was noted that beads conjugated with anti-BCR antibodies are more efficient in driving mitogenic responses than antibodies in solution (Puré and Vitetta, 1980; Henriksen et al., 1980). To a certain extent, anti-Ig coating indeed represents a way to create a polyvalent particulate antigen. Although, B cell responses to anti-Ig ”crosslinking” manifest in DNA synthesis and cell cycle progression, it is well known that this signal alone is insufficient to support long-term proliferation, differentiation into antibody-producing cells and eventually results in activation-induced cell death (AICD) (Parker, 1980). Extensive ”crosslinking” of BCR with soluble anti-Ig leads to enhanced apoptosis (Parry et al., 1994a; Kozono et al., 1995), suggesting a role for BCR signaling strength in the response (Rehe et al., 1990). Consistent with this, BCR ”crosslinking” by anti-Ig-coated cell culture plastic or anti-Ig-bearing membranes of accessory cells progressively lead to apoptosis as well (Parry et al., 1994b; Watanabe et al., 1998).

The relationship of soluble and surface-bound anti-Ig with secondary signals were also found to be qualitatively different. For instance, it was shown that IFNγ inhibits B cell proliferation induced by soluble but not sepharose-bound anti-Ig (Mond et al., 1985) and soluble but not surface anti-IgM inhibits in vitro antibody secretion from B cells co-cultured with anti-CD3-activated T cells (Zamorano et al., 1995). Thus, by the 2000s it was apparent that different types of antigens elicit different B cell responses. It is important to note that the outcome of the BCR-induced responses is also clearly dependent on the developmental stage and phenotype of the B cells as large (immature) B cells are rather unresponsive to anti-IgM stimulation (Maruyama et al., 1985). In contrast, MZ B cells, although exhibit markedly impaired proliferative responses to anti-μ (anti-IgM) or anti-δ (anti-IgD) BCR-stimulation delivered together with IL-5 or combination of IL-5 and IL-4, secrete more antibodies in these culture conditions (Snapper et al., 1993). More recent studies also agree on the induction of apoptosis in activated B cells (Akkaya et al., 2018), while some rather point on increased B cell viability and proliferation with increasing concentrations of stimulatory anti-IgM antibodies (Berry et al., 2020). These results are interesting and may reflect the fact that pure populations of $CD23^{+}$ splenic B cells were studied in Berry et al. (2020).

It is reasonable to assume that discrimination of antigenic properties occurs at the time of BCR engagement. Therefore, studying events that happen immediately after the B cell encounters its cognate antigen and finding correlates of productive B cell activation is crucial for understanding of the B cell immune responses. Much of the information on early events of B cell activation we received from microscopy studies, the method best suited to capture these events. It has been noted that soluble antigen engagement results in aggregation of BCRs in patches, which often concentrate at one pole of the cell in a process that is commonly referred to as BCR "capping" (Taylor et al., 1971; Schreiner and Unanue, 1977; de Groot et al., 1981; Liu et al., 2012a). In its turn, B cell activation by surface-displayed antigens is characterized by rapid cell spreading over the flat surface and also results in appearance of BCR-antigen aggregates called BCR microclusters, especially prominent when the antigen is mobile (Depoil et al., 2008; Weber et al., 2008). B cell interaction with antigen-surfaces characterized by a relatively small radius of curvature, such as antigen-coated beads, typically results in BCR accumulation at the site of the contact (Batista et al., 2001). BCR microclusters are more distinct when the B cell encounters antigen on artificially-made supported lipid bilayers (SLB), which may be a more physiological representation of the in vivo situation where B cell would typically recognize antigens bound and displayed on the surface of other cells (Nossal et al., 1968; Carrasco and Batista, 2007; Phan et al., 2009; Heesters et al., 2013).

Mobile antigens and substrate stiffness

Although surface-presented antigens can be considered polyvalent, they possess at least two characteristics that are not pertinent to soluble antigens. The first is the rigidity of the underlying substrate, and the second is the mobility of the antigen tethered to this substrate. Genuine or artificial membranes allows for tethered antigen to be laterally mobile. Spreading of B cells on such membranes is characterized by consequent movement of the forming BCR microclusters into the center of the contact and contraction of the contact area (Fleire et al., 2006). The process is analogous to the one observed in situation where T cell interacts with membrane-bound antigens (Grakoui et al., 1999). Similarly, the contact zone between the B cell and antigen-presenting cell or surface is called the immunological synapse (IS). After a contraction phase, the mature IS consists of at least two distinct concentric areas, called supramolecular activation clusters (SMAC). The central (cSMAC) area, contains accumulated antigen-bound BCRs, and peripheral (pSMAC) area is characterized by the presence of CD45 and adhesion molecules (Dustin and Choudhuri, 2016; Batista et al., 2001; Fleire et al., 2006) (Figure 11).

As was discussed earlier, BCR signaling strength determines progression in the cell cycle and rate of B cell apoptosis. BCR signaling is also intimately interconnected with cell spreading, formation of BCR microclusters, the contraction response and BCR-Ag centralization, Ag internalization and efficiency of antigen presentation. (Liu et al., 2010b; Harwood and Batista, 2011; Kuokkanen et al., 2015). In turn, defects in BCR signaling pathway components (Niiro and Clark, 2002), manifest in ab-

normal area of spreading, size and number of formed microclusters, antigen-BCR accumulation, suggesting direct involvement of the cell cytoskeleleton – moving force of membrane rearrangements (Weber et al., 2008). Indeed, defects in actin and microtubule cytoskeleton result in crippled B cell responses (discussed in section 2.2.3)

However, B cell activation upon soluble, membrane-bound or surface-adsorbed antigens may demonstrate distinct requirements for intact function of proteins involved in the regulation of BCR signaling and cytoskeletal rearrangements. For instance, inhibition of actin polymerization via Arp2/3 actin nucleator resulted in lower CD79 (Ig alpha) phosphorylation in response to membrane-bound but not soluble antigen, suggesting a regulatory role for actin in B cell activation on surface-presented antigens (Bolger-Munro et al., 2019). Distinct effects have been observed, when B cells were deficient in BCR receptor complex proteins, CD19 or CD81. The lack of CD19 results in reduced B cell spreading, ability to form microclusters as well as lower Ca^{2+} signaling in $CD19^{-/-}$ B cells in response to membrane-bound antigens (Depoil et al., 2008; Mattila et al., 2013). In contrast, Ca^{2+} mobilization in response to soluble antigen was shown to be normal in $CD19^{-/-}$ B cells (Sato et al., 1997; Fujimoto et al., 1999; Depoil et al., 2008), except one report (Buhl et al., 1997). A Ca^{2+} response, however, cannot be used as the only estimate of BCR signaling efficiency, and $CD19^{-/-}$ B cells still exhibit severely reduced pTyr accumulation and defective proliferative responses to soluble antigen stimulation (Sato et al., 1997; Fujimoto et al., 1999). To complicate the picture, proliferative responses to sepharose bead-immobilized anti-IgM were also normal in the absence of CD19 (although IL-4 was present in the culture) (Rickert et al., 1995).

Comparison of B cell responses on supported lipid bilayers and substrates with immobilized antigen shows that the accumulation of BCR microclusters and their pTyr signal are higher on substrates with mobile antigen (Ketchum et al., 2014). The maximum area of cell spreading is reportedly higher on immobilized ligands, noted for B and T cells, probably reflecting the inability of cells to contract soon after the contact (Ketchum et al., 2014; Dillard et al., 2014; Bolger-Munro et al., 2019). However, due to the lack of other comparative studies, the situation is likely to vary depending on experimental conditions. It has been reported that in T cells both immobilized and mobile antigen support TCR signaling (Luxembourg et al., 1998; Hsu et al., 2012).

Another important characteristic of antigen-presenting surfaces is their rigidity, or stiffness (defined as how well the object resists deformation in response to an applied force). Stiffness of an entire object depends on the physical characteristics of both the object and the applied force. To characterize stiffness, elastic (or Young's) modulus of the material is commonly used. Elastic modulus can vary from Pa–kPa range for cells and tissues to MPa–GPa for bone tissues, viruses and common cell culture plastic (Baumgart and Cordey, 2001; Gasiorowski et al., 2013; Mateu, 2012). It is well established that the physical properties of the cell microenvironment have a direct impact on their physiology (Discher et al., 2005). Although cell responses

require time for adaptation, activation of immune cells is a rapid process and studies suggest that lymphocytes are sensitive to biomechanical cues provided by antigen-presenting substrates. Glass supported polymeric gels of polyacrylamide (PAA) or polydimethylsiloxane (PDMS) are typically used and variability in substrate stiffness is achieved by changing the degree of crosslinking. B cell stimulation on antigen-coated PAA substrates suggest that higher stiffness (22.1 kPa vs. 2.6 kPa) results in more prominent BCR microclusters, stronger pTyr and pSyk staining intensities and enhanced ability to discriminate BCR affinity in transgenic B cell lines and enhanced induction of CD69 in splenic B cells (Wan et al., 2013). This was later confirmed on stiffer PDMS substrates (1100 kPa vs. 20 kPa) with more articulate responses for primary B cells and also when antigen-carrying lipid bilayers were introduced on top of the matrices. Interestingly, softer substrates induced stronger activation of PI3K-Akt-FoxO1 pathway and mildly elevated class-switch responses with no apparent effect on Ag-induced proliferation (Zeng et al., 2015). Experiments in DT40 knock-out cell lines demonstrated the importance of Lyn, Syk, Btk, PLCγ2, BLNK signaling molecules for stiffness discrimination, the dependence on PKCβ-mediated focal adhesion kinase (FAK) activation and a possible involvement of signaling to integrins (Shaheen et al., 2017).

Antigen extraction and presentation

Whether soluble, particulate or surface-bound, antigen engagement by BCR leads to its internalization, and in the case of protein-based molecules, this event initiates the process of antigen presentation, which is crucial for T cell-dependent immune responses (Taylor et al., 1971; Lanzavecchia, 1985; Batista and Neuberger, 2000; Batista et al., 2001). Soluble antigens are internalized by B cells mostly via clathrin-mediated endocytosis (Stoddart et al., 2005; Roberts et al., 2020). Affinity of BCR was shown to be important for antigen presentation, whereas BCR signaling appeared to be dispensable for T cell activation in long term co-cultures (24 hrs) (Batista and Neuberger, 2000). In contrast, presentation of particulate antigens, required signaling-competent BCR, which above a certain affinity threshold can efficiently induce antigen phagocytosis. The amount of bead-bound antigen positively correlated with efficiency of the antigen presentation (Batista and Neuberger, 2000). Surface-bound antigens in a form that cannot be internalized by B cells require force-mediated extraction, which strongly depend on BCR affinity (Batista and Neuberger, 2000; Natkanski et al., 2013) and, if unsuccessful, is followed by enzymatic extraction through secretion of lysosomal content into the immune synapse structure (Spillane and Tolar, 2017; Yuseff et al., 2011). These studies also suggest that higher stiffness of the antigen-presenting surface leads to more stringent affinity discrimination as shown on artificial supported lipid bilayers (SLB) and PEGylated glass (stiff substrates) versus antigen on more flexible plasma membrane sheets (PMS). This was supported by experiments on antigen extraction from stiff follicular dendritic cells (FDC) versus extraction from softer dendritic cells (DC) that appear to have more flexible membranes. Force-mediated extraction and affinity discrimination in

these studies were strongly linked to myosin IIa activity (Spillane and Tolar, 2017; Natkanski et al., 2013). In contrast to the inability of B cells to extract antigen from stiff SLBs, acquisition and presentation of plastic-adsorbed but not covalently-linked antigen was shown earlier to stimulate T cells in long term co-cultures and was less dependent on signaling-competent BCR (Batista and Neuberger, 2000). Although, differences in the tethering strength and timing may influence results of these studies, a similar ability of stiff substrates to support affinity discrimination were reported on PAA matrices (Wan et al., 2013).

The role of the type of the BCR molecule itself in differential responses to antigens sensitive to force-mediated extraction has also been reported. Thus, antigens that require stronger forces for extraction from glass substrate led to enhanced BCR signaling downstream of IgM, IgD or IgA. In contrast. IgG- or IgE-BCR responded equally well to antigens that required extraction forces in the range of 12–56 nN (Wan et al., 2015). For IgG, this was found to be dependent on the ability to recruit $PI(4,5)P_2$ via positively charged aminoacids in the IgG cytoplasmic tail (Wan et al., 2018).

2.2.2 The actin cytoskeleton

Among cytoskeletal systems of eukaryotes, including microfilaments of actin, intermediate filaments, microtubules and, recently, septins, the actin cytoskeleton is best suited to provide force and support for rearrangements of cellular membranes (Alberts et al., 2015). Actin is a highly conserved, 42 kDa protein and, unlike proteins of other cytoskeletal systems, in mammals comprises a group of only 6 isoforms of which 4 are muscle-specific and 2 are ubiquitously expressed as non-muscle, cytoplasmic β- and γ-actin isoforms (Figure 8) (Dugina et al., 2019).

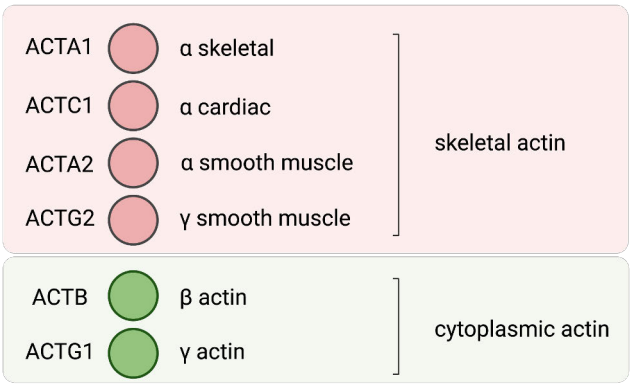

Figure 8. Human actin isoforms.

Monomeric, globular G-actin molecules polymerize into polar actin filaments, or F-actin, which are single left-handed helices of ∼5–9 nm thickness and with 13 actin molecules per 6 turns repeating every 36 nm (Grazi, 1997; Dominguez and Holmes, 2011). Actin molecules possess ATPase activity and, once incorporated into a filament, hydrolyze bound ATP, which changes protomer conformation and reduces filament stability. Thus, ATP-bound actin is found at the growing, or (+) end of the filament, and ADP-actin marks aging filament toward (−) end (Dominguez and Holmes, 2011). Historically, based on electron microscopy appearance of myosin-decorated actin filaments due to specific orientation of myosin molecules, (+) ends were called ”barbed” ends, and the opposite, (−) ends, are referred to as ”pointed” ends (Moore et al., 1970) (Figure 9).

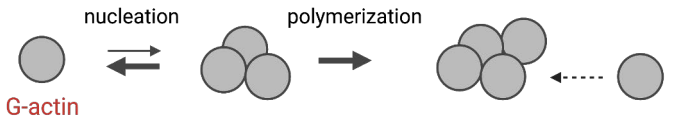

(a) Actin nucleation

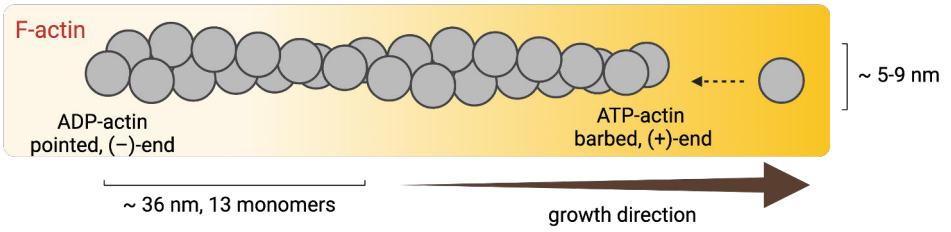

(b) Actin polymerization

Figure 9. Actin polymerization and structure of the actin filament. See also: Goode and Eck (2007).
(a) Formation of di- and trimers of G-actin, or nucleation of actin, is a rate-limiting step in actin polymerization. Actin polymerization is more efficient in the presence of proteins that promote actin nucleation.
(b) Polymerization into filamentous actin, or F-actin, occurs by incorporation of ATP-actin monomers at the growing (+), or barbed-end of the filament. Actin monomers in the aged filament hydrolyze ATP, which eventually leads to dissociation of ADP-actin from (−), or pointed end, and F-actin disassembly. Structurally, actin filament is a single left-handed helix of ∼5–9 nm in diameter, in which 13 actin subunits per 6 turns repeat every 36 nm.

The existence of a universal polymerizable pool of actin to assist diverse biological functions in different types of cells imposes requirement for precise and complex level of regulation (Gunning et al., 2015). This is achieved by a multitude of actin regulatory proteins. The formation of the nucleation seed is a rate limiting step in the filament assembly and is facilitated by actin nucleators. (Pollard, 2007). Linear filament formation is catalyzed by 4 types of nucleators, including ubiquitously expressed Formin family. Branched actin polymerization at 70° from mother filament is

initiated by a 7-subunit Arp2/3 complex, which itself becomes a part of the filament (Wickramarachchi et al., 2010) (Table 3). Arp2/3 nucleation is assisted by nucleation promoting factors (NPFs). Class I NPFs include WCA (or VCA; WASP homology 2, or Verprolin (WH2, W, or V), central (C) and acidic (A)) domain-containing proteins and class II NPFs are proteins which stabilize F-actin:Arp2/3 interaction (Campellone and Welch, 2010; Firat-Karalar and Welch, 2011) (Table 3). In turn, activation of Arp2/3 NPFs and formins is orchestrated by the Rho family of small GTPases. Typically, Rho GTPase binding to GTPase-binding domain (GBD) of autoinhibited formin homodimers releases dimeric FH2 actin-binding domains to perform nucleation and elongation of linear filaments. Binding of Rho GTPase to the GBD domains of autoinhibited class I NPFs releases WCA domains, which bridge Arp2/3 complex with actin monomer being incorporated (Lee and Dominguez, 2010; Campellone and Welch, 2010; Tyler et al., 2016). In turn, the functioning of the RhoGTPases is under control of guanine nucleotide exchange factors (GEFs), GTPase activation factors (GAPs) and GDP dissociation inhibitors (GDIs) that regulate GTP-GDP exchange and membrane localization of Rho GTPases and thus their activity (Cherfils and Zeghouf, 2013) (Figure 10).

Table 3. Actin nucleators and nucleation promoting factors

Function	Proteins		Description
Linear filament nucleation and elongation	Formins		Diverse tissue expression, 15 members
	Cobl (Cordon-Bleu)		Brain-specific
	Lmod1–3 (Leiomodins)		Cardiac and skeletal muscle
	Spire1/2		Nervous and digestive tract, liver, testes
Branched actin nucleation	Arp2/3 complex		Complex of 7 proteins, the only nucleator for branched actin network
Nucleation promoting factors (NPFs)	class I NPFs	WASP, N-WASP, WAVE, WASH, WHAMM, JMY	WCA, or VCA domain-containing proteins
	class II NPFs	Cortactin, HS1	Filament stabilization

See also: Wickramarachchi et al. (2010); Campellone and Welch (2010).

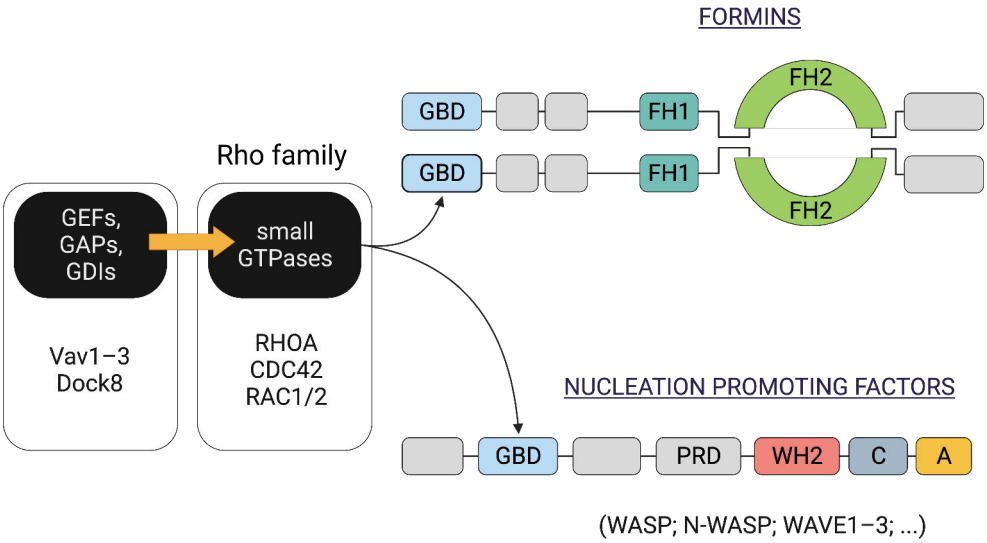

(a) Rho family of small GTPases orchestrate actin polymerization via activation of formins and nucleation promoting factors (NPFs)

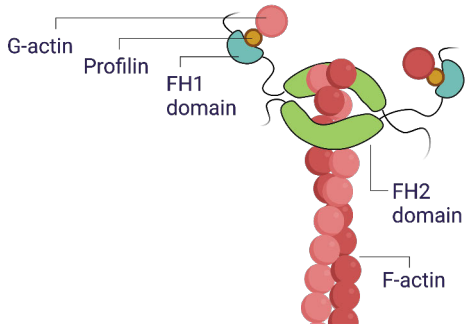

(b) Linear actin polymerization performed by formins

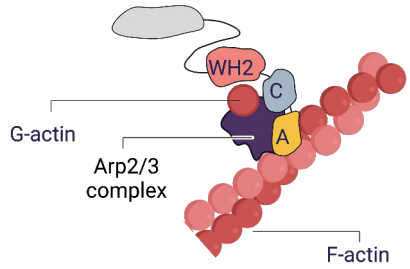

(c) Formation of branched actin network is mediated by Arp2/3 complex and nucleation promoting factors (NPFs)

Figure 10. Formin family of proteins and Arp2/3 complex are main actin nucleators in the cell. See also: Campellone and Welch (2010).
(a) The binding of small GTPases, RhoA, Cdc42 or Rac1/2, to the GBD (GTPase binding domain) of formins and nucleation promoting factors leads to their activation and promotes actin nucleation and polymerization. The activity of small GTPases is under regulatory control of GEFs, GAPs and GDIs. Vav1–3 and Dock8 are important guanine nucleotide exchange factors (GEFs) in hematopoietic cells, including B cells.
(b) Homodimers of formin homology 2 (FH2) domains bind to the $(+)$ end of the nascent actin filament stabilizing actin seeds. Formin homology 1 (FH1) domains bind G-actin-binding protein, profilin, to assist addition of ATP-G-actin to the growing actin filament.
(c) WH2-Central-Acidic (WCA) domain-containing nucleation promoting factors (NPFs) promote Arp2/3 complex-dependent actin nucleation. The C-A domains bridge Arp2/3 complex with actin monomer delivered by WH2 (W) domain.

Apart from nucleation and filament assembly, a multitude of other regulatory proteins participate in the actin structure dynamics in the living cells. Many of such proteins interact with G- or F-actin directly and are collectively called actin binding proteins (ABP). Profilin is the major protein contributing to the maintenance of polymerizable pool of actin. Capping (e.g. F-actin capping protein, gelsolin) and anti-capping proteins (e.g. Ena, VASP) regulate addition of monomers at the barbed ends. Sequestering proteins (e.g. thymosin β4, twinfilin) inhibit polymerization by binding to actin monomers. Actin depolymerization and severing is regulated by proteins of the ADF/cofilin family (Lee and Dominguez, 2010; Wickramarachchi et al., 2010). Actin crosslinking and bundling proteins (e.g. α-actinin, fascin) connect and reinforce formed filaments (Tseng et al., 2005). Generation of forces and rearrangements of cellular membranes are achieved by actin-based motors, myosins, and connection to cellular membranes and transmembrane proteins is mediated by, for instance, BAR domain and Merlin-ERM (Ezrin-Radixin-Moesin) proteins (Lee and Dominguez, 2010; Maravillas-Montero and Santos-Argumedo, 2012; Michie et al., 2019).

2.2.3 The role of the actin cytoskeleton in B cell activation

The association of the actomyosin network with cap formation, which in essence is accumulation of antigen-BCR complexes at one pole of the cell upon surface Ig crosslinking, was noted as early as 1970s by microscopy and in biochemical assays (Taylor et al., 1971; GABBIANI et al., 1977; Schreiner et al., 1977; Flanagan and Koch, 1978). Treatment of B cells with actin depolymerizing drugs, cytochalasins, inhibited cap formation in mouse lymphocytes (Taylor et al., 1971; Teti et al., 1981), disrupted formed caps (Schreiner and Unanue, 1976), but dependence of cap formation on microfilament network may be species-specific and appears different in rabbit B cells (de Groot et al., 1981; Bourguignon and Bourguignon, 1984). The latest studies, which also employed actin inhibitors, suggest a tight interplay between the actin cytoskeleton and BCR signaling (Tolar, 2017; Mattila et al., 2016; Li et al., 2019).

It was noted that disruption of the actin cytoskeleton with actin depolymerizing drugs (Table 4), latrunculins (Lat A/B) or cytochalasin D (Cyto D), in B cells induced an increase in intracellular Ca^{2+} and induction of pERK and pAkt in the absence of antigen-induced stimulation (Baeker et al., 1987; Hao and August, 2005; Treanor et al., 2010). An actin stabilizing drug, Jasplakinolide (Jasp), on the other hand, failed to induce pERK or pTyr upregulation (Hao and August, 2005; Liu et al., 2012a), but still induced Ca^{2+} flux (Treanor et al., 2010).

Table 4. Commonly used actin cytoskeleton inhibitors*

Inhibitor	Activity	K_d
Actin stabilizing / filament binding		
Jasplakinolide	F-actin binding and stbilization	100 nM
Actin depolymerizing / monomer binding		
Latrunculin A	monomer sequestering	200 nM
Latrunculin B	monomer sequestering	200 nM
Actin depolymerizing / filament binding		
Cytochalasin D	barbed ends binding (capping), interferes with actin assembly	2 nM
Cytochalasin B	actin binding (not capping), interferes with actin assembly	

*(Eitzen, 2003)

Actin reorganization during B cell activation

Inability of actin depolymerizing drugs to induce signaling in B cells devoid of B cell receptors or CD19 co-receptor molecules suggests a strong regulatory role for actin reorganization in BCR-mediated signaling (Mattila et al., 2013). Both antigen binding and disruption of F-actin lead to a transient increase in the diffusion of BCR, which was found to be higher in actin- and ezrin-poor membrane regions. Such behavior would be consistent with the model where induced cytoskeletal changes in the cortical actin cytoskeleton remove diffusion barriers for BCR and facilitate receptor clustering and interaction with co-receptors to assist in signaling initiation (Treanor et al., 2010, 2011; Mattila et al., 2013). In line with the increase in BCR diffusion following antigen binding is the global reorganization of the actin cytoskeleton, which undergoes rapid depolymerization seconds after BCR engagement followed by repolymerization in localized areas (Hao and August, 2005; Liu et al., 2012a). Mechanistically, changes in BCR diffusion and actin depolymerization can be attributed to a localized activity of the actin severing protein, cofilin, and transient uncoupling of the actin network from transmembrane proteins and plasma membrane via ERM proteins, such as ezrin (Freeman et al., 2011; Treanor et al., 2011). Although actin reorganization is evident in B cells stimulated by both soluble and surface-bound antigens (Liu et al., 2012a,b), a substantial amount of work has been focused on describing B cells interacting with membrane-bound or glass-tethered antigens, where total internal reflection (TIRF) microscopy, best suited for imaging of the cell membrane-coverslip interface, can be applied to full advantage. Following initiation of BCR signaling and formation of the first BCR-Ag microclusters, B cell undergoes spreading over the Ag surface, via polymerization of the cortical actin at the edges of the cell, or lamellipodial region (Fleire et al., 2006). Spreading allows for searching and engaging new antigen molecules by BCRs and their coalescence to form new microclusters. At the same time, formed F-actin filaments appear to bundle and bend behind the lamellipodial region, forming thick F-actin arcs, enriched in

myosin IIa molecules, similar to those of T cells, which move centripetally toward the actin-poor central region of the cell (Wang and Hammer, 2020; Bolger-Munro et al., 2019; Murugesan et al., 2016) (Figure 11). This flow of actin and actomyosin contraction is believed to be responsible for the initial stages of the microcluster motion. The spreading phase may take 10-15 min on antigen-coated glass and 1-5 min on antigen-presenting surfaces carrying mobile ligands (Fleire et al., 2006; Roman-Garcia et al., 2018; Ketchum et al., 2014). On mobile antigens, after B cells are fully spread, the contraction phase takes place, the mechanisms of which are not entirely clear, but are likely to also involve actomyosin activity (Wang and Hammer, 2020). This process is concomitant with the ongoing movement of BCR-Ag microclusters toward the center of the synapse to form the cSMAC area. At this stage, the movement of the microclusters appear to also be supported by dynein-dependent activity and the microtubule network. This network forms underneath the synapse contact zone along with the repositioning of the microtubule organizing center (MTOC) to the same area (Wang et al., 2017; Schnyder et al., 2011). The same myosin- and dynein-mediated pulling forces seem to be responsible for affinity discrimination and antigen acquisition by cytoskeleton-associated BCRs in the synapse, which are also seen as traction forces exerted towards the substrates bearing antigens with restricted mobility (Batista et al., 2001; Natkanski et al., 2013; Wang et al., 2018).

Upon successful antigen acquisition, the actin cytoskeleton also participates in the largely clathrin- and dynamin-dependent internalization of BCR-Ag complexes, demonstrated for soluble antigens (Stoddart et al., 2005; Roberts et al., 2020; Brown and Song, 2001; Onabajo et al., 2008; Malhotra et al., 2009), and likely involving similar mechanisms when antigen is acquired from an antigen-presenting surface in the synapse. When force-mediated antigen extraction is unsuccessful, enzymatic degradation of the antigen occurs. This is achieved by enzymes secreted from the lysosomes polarized to the immunological synapse (Yuseff et al., 2011; Spillane and Tolar, 2017). This process, in accordance with general involvement of actin filaments and microtubules in endocytosis, exocytosis and vesicle trafficking (Porat-Shliom et al., 2013; Smythe and Ayscough, 2006), requires concerted action of these two cytoskeletal systems. It needs to be noted, however, that this fairly universal model of immune synapse formation for B and T cells on artificial surfaces appears to be distinct for a particular differentiation stage of B cells. Thus, it was shown that GC B cells do not form conventional IS, but rather engage antigen in podosome-like structures and then traffic Ag-BCR microclusters to the periphery of the synapse, suggesting specialized actin cytoskeleton engagement in these cells (Nowosad et al., 2016; Kwak et al., 2018).

BCR signaling to the actin cytoskeleton

The general mechanisms of how actin reorganization is regulated by BCR signaling are relatively easy to envision, although spatio-temporal details and specific protein interactions continue to be revealed. Major events that occur downstream of the BCR include sequential upregulation of activity of various kinases and phos-

phatases, which directly participate in the activation or downmodulation of actin cytoskeleton regulatory proteins. Another important aspect is the alteration of the lipid microenvironment at the plasma membrane and generation of different phosphoinositide species, which recruit and modulate the activity of multiple actin regulatory proteins (Saarikangas et al., 2010).

Upon initiation of BCR signaling, transient dephosphorylation of ezrin and cofilin occurs, concomitant with the disassembly and clearance of cortical actin (Treanor et al., 2011; Hao and August, 2005). The exact mechanisms are not well defined and likely to involve complex regulation. In T cells, the release of ezrin and moesin was shown to be dependent on PLC activation and PI(4,5)P_2 depletion (Hao et al., 2009). Cofilin dephosphorylation, likely by slingshot phosphatase (SSH), and its actin severing activity is thought to be under control of Rap activation and high [Ca^{2+}] (Freeman et al., 2011; Maus et al., 2013; Wang et al., 2005) (Figure 12a). As PLCγ converts PIP_2 lipids into DAG and IP_3 and in this way regulates Ca^{2+} signaling, the PLCγ pathway is particularly important in the regulation of F-actin levels. In T cells high Ca^{2+} levels were also noted to promote actin depolymerization (Hartzell et al., 2016). In other organisms and cell types, Ca^{2+} at high concentrations is known to promote actin fragmentation and depolymerization via villin/gelsolin, G-actin sequestering by profilin or direct G-actin binding, which inhibits polymerization (Hepler, 2016) (Figure 12b). Lymphocytes express rather low levels of gelsolin and most of the severing activity is likely mediated by ADF/cofilin proteins.

The phosphorylation of ezrin T567 and interaction with PI(4,5)P_2 releases its autoinhibition state to allow for actin binding (Gupta et al., 2006; Michie et al., 2019; Treanor et al., 2011; Pore and Gupta, 2015). Cofilin S3 rephosphorylation by LIM kinase also downstream of Rap GTPases after the dephosphorylation phase promotes B cell spreading and formation of BCR microsclusters (Freeman et al., 2011; Bolger-Munro et al., 2019). In turn, Rap activation may proceed through RapGEF1 via Crk/Cas/Cbl adaptor proteins linked with the BCR signalosome or via PLCγ and DAG-dependent pathways (Ingham et al., 1996; McLeod et al., 1998) (Figure 12a).

As was mentioned in the section 2.2.2, polymerization of actin filaments is orchestrated by the Rho family GTPases. Similar to many Ras superfamily proteins, the active GTP- or inactive GDP-bound state of Rho proteins is regulated by guanine nucleotide exchange factors (GEFs), GTPase activation factors (GAPs) and GDP dissociation inhibitors (GDIs) (Wennerberg et al., 2005; Cherfils and Zeghouf, 2013). Although there are dozens of Rho GTPase GEFs and GAPs with sometimes shared activity toward other proteins of Ras superfamily, they often show cell-type specific expression profiles (Tybulewicz and Henderson, 2009). In B cells, Vav proteins were identified as critical Rho GEFs involved in regulation of B cell development and many aspects of B cell activation (Fujikawa et al., 2003; Tybulewicz and Henderson, 2009; Weber et al., 2008). Vav proteins are shown to be a part of the BLNK-Btk-PLCγ2-Vav signaling complex (signalosome) module, associate with CD19 and promote Btk- and PI(4,5)P_2-dependent activation of WASP and Ca^{2+} signaling (Fu et al.,

1998; Wienands et al., 1998; Brooks et al., 2000; Sharma et al., 2009; Fujikawa et al., 2003). The GEF activity of Vav proteins is also known to be regulated by tyrosine phosphorylation and in B cells likely lies downstream of Src, Syk and Btk kinases (Sharma et al., 2009; López-Lago et al., 2000). Adaptor proteins, such as Nck, can link BCR-signaling to the actin cytoskeleton through WIP, WASP/N-WASP and profilin (Okrut et al., 2015; Castello et al., 2013; Antón et al., 1998; Ramesh et al., 1997) and Grb2 via Vav recruitment (Johmura et al., 2003). Actomyosin contractility downstream of BCR may proceed through RhoA activation of ROCK, Ca^{2+}-calmodulin activation of myosin light chain kinase (MLCK) or can be inhibited by PKC activity, which all converge at the level of the regulatory light chain (RLC) of non-muscle myosin II (Figure 13a) (Vicente-Manzanares et al., 2009).

Conversion of the plasma membrane phosphoinositides downstream of BCR is another mechanism that can have a profound effect on global actin reorganization (Donahue and Fruman, 2004). Thus, many actin binding proteins, including ADF/cofilin, profilin, twinfillin, gelsolin, villin, α-actinin, vinculin, talin, spectrin and ERM proteins, are able to bind PI(4,5)P_2 or PI(3,4,5)P_3 species, which recruit or sequester them at the plasma membrane thereby modulating their activity (Saarikangas et al., 2010) (Figure 13b).

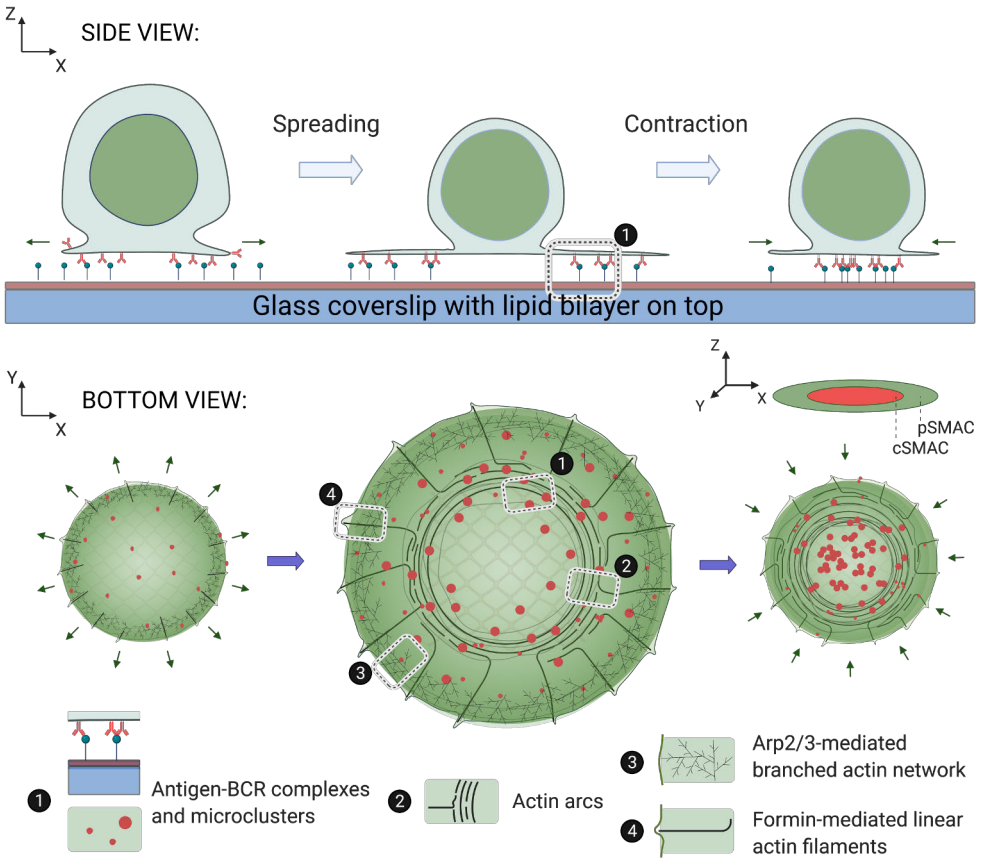

Figure 11. B cell spreading and contraction response. Immunological synapse.
See also: Wang and Hammer (2020).
SIDE VIEW: Schematic stages of B cell spreading and contraction response on glass-supported lipid bilayers carrying antigens.
BOTTOM VIEW: The same stages are shown as visualized by microscopy from the coverslip-bilayer side. Upon the contact with antigen-bearing lipid bilayer formin- and Arp2/3-mediated actin polymerization at the lamellipodial region extends the plasma membrane leading to B cell spreading. During this phase antigen-BCR complexes are formed and coalesce into larger BCR microclusters. The actin cytoskeleton directly participates in the formation of BCR microclusters and their gathering in the center of the structure called immunological synapse (IS) after a contraction phase. In the mature immunological synapse at least two zones are recognized: central supramolecular activation cluster (cSMAC) region, where antigen-BCR complexes are accumulated, and peripheral SMAC (pSMAC) outer region,where adhesion molecules are commonly encountered.

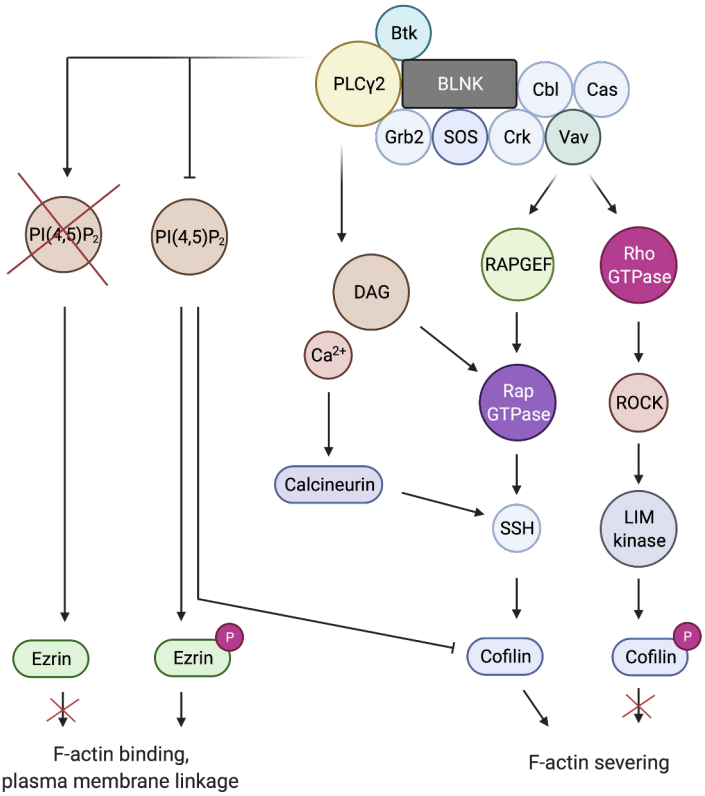

(a) Regulation of actin by ezrin and cofilin

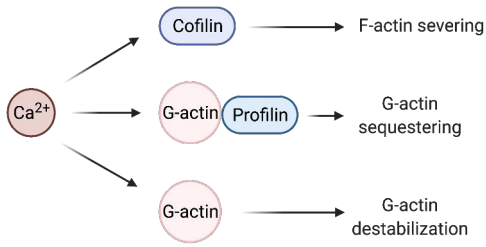

(b) Negative regulation of F-actin by calcium

Figure 12. BCR signaling to actin. Part 1.
(a) Assembly of BCR signalosome complex of proteins leads to activation of phospholipase Cγ2 (PLCγ2). PLCγ2 depletes plasma membrane phosphatidylinositol-(4,5)-diphosphate (PI(4,5)P_2) and blocks ezrin recruitment to the plasma membrane and F-actin binding. Conversion of PI(4,5)P_2 also leads to increase in cytoplasmic Ca^{2+} concentration and activation of Rap GTPases, which in turn leads to dephosphorylation of cofilin and promotes its F-actin severing activity. At the same time inhibition of cofilin activity may proceed through cofilin phosphorylation downstream of Vav activity and activation of Rho family of small GTPases.
(b) Increased Ca^{2+} levels may disrupt actin polymerization via several mechanisms. Calcium-dependent dephosphorylation and activation of cofilin downstream of calcineurin and SSH promotes F-actin severing. Sequestering of G-actin:profilin complex at high Ca^{2+} levels. Direct binding of Ca^{2+} by G-actin leads to inhibition of actin polymerization.

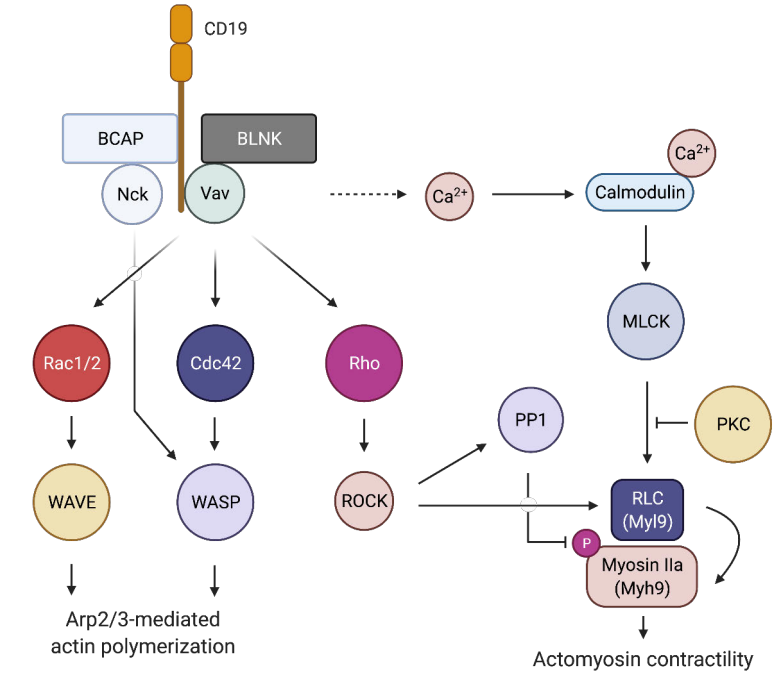

(a) Regulation of actin polymerization and myosin contractility by Rho GTPases

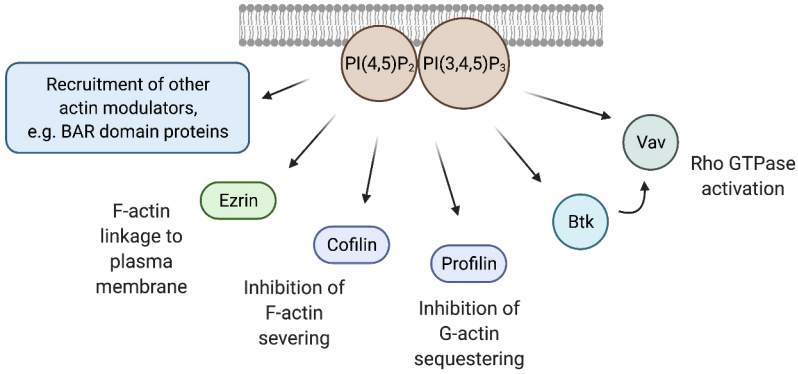

(b) Regulation of actin by phosphoinositides

Figure 13. BCR signaling to actin. Part 2.
(a) Signaling downstream of BCR and CD19 co-receptor leads to activation of Vav. Vav proteins are guanine nucleotide exchange factors (GEFs) for Rho family of small GTPases, Rac, Cdc42 and Rho. Activation of nucleation promoting factors (NPFs), WAVE and WASP downstream of Rho GTPases promotes Arp2/3-mediated actin polymerization. Adaptor protein Nck can also activate WASP via direct binding. Actomyosin contractility is modulated via regulatory light chain (RLC) of the Myosin IIa downstream of Rho-dependent activation of Rho-associated protein kinase (ROCK) or by Ca^{2+} via myosin light chain kinase (MLCK). Negative regulation of myosin IIa activity can proceed via direct dephosphorylation by PP1 phosphatase or by inhibition of MLCK activity by protein kinase C (PKC).
(b) Accumulation or conversion of different phosphoinositide lipids in the plasma membrane leads to recruitment and activation or sequestration of various actin cytoskeleton regulatory proteins, which modulate actin dynamics at the plasma membrane.

Table 5. Actin regulatory proteins in B cells

Protein	Role in actin cytoskeleton regulation	Method	B cell phenotype	References
Arp2/3 complex	actin nucleation	CK666 inhibitor, Arpc3 siRNAs, ARPC2 CRISPR targeting	Reduced cSMAC formation, impaired BCR signaling, increased tonic signaling (membrane-bound antigen on COS-7 but not soluble antigen) Impaired proliferation and CD69/CD86 upregulation (membrane-bound antigen on COS-7) Internalization of soluble antigen is less affected	(Bolger-Munro et al., 2019)
			Abnormal IS formation, actin architecture and dynamics, impaired antigen extraction/uptake (membrane-bound antigen on PMS) Internalization of soluble antigen is less affected	(Roper et al., 2019)
Formins	actin nucleaton and elongation	SMIFH2 inhibitor	Abnormal IS formation, actin architecture and dynamics, impaired antigen extraction/uptake (membrane-bound antigen on PMS) Internalization of soluble antigen is less affected	(Roper et al., 2019)

Table 5. Actin regulatory proteins in B cells

Protein	Role in actin cytoskeleton regulation	Method	B cell phenotype	References
WASP, N-WASP	Nucleation promoting factors, type I	BM chimeras, conditional B cell and whole knock-out mice	B cell-specific WASP deficiency leads to B cell developmental defects, impaired immune responses but elevated serum IgM and autoantibody production and autoimmunity Interplay of WASP and N-WASP in BCR signaling and IS formation Enhanced BCR signaling in N-WASP KO B cells Double KO of WASP and N-WASP in B cells results in defective B cell proliferation impaired TD responses, decreased autoantibody production Autoimmunity in the absence of WASP is N-WASP-mediated	(Becker-Herman et al., 2011) (Recher et al., 2012) (Westerberg et al., 2012) (Liu et al., 2013) (Dahlberg et al., 2015) (Volpi et al., 2016)
HCLS1 (HS1, cortactin homolog)	Nucleation promoting factor, type II	HS1 knockout mice, WEHI-231-derived B cells	Possible role in BCR-mediated apoptosis Impaired BCR-mediated proliferation, reduced TI-2 antibody response	(Taniuchi et al., 1995) (Fukuda et al., 1995) (Yamanashi et al., 1997)
RhoA	Rho family small GTPase	N19RhoA DN (dominant negative), V14RhoA CA (constitutively active), C3 exoenzyme *C. Botulinum* toxin (inhibitor)	Inhibits BCR-mediated Ca^{2+} flux, IP_3 and phosphoinositide synthesis, impaired proliferation	(Saci and Carpenter, 2005)

Table 5. Actin regulatory proteins in B cells

Protein	Role in actin cytoskeleton regulation	Method	B cell phenotype	References
Cdc42	Rho family small GTPase	Conditional B cell knock-out mice	Defects in B cell development, impaired or abnormal BCR signaling, impaired antigen presentation, plasma cell generation and antibody responses	(Guo et al., 2009) (Burbage et al., 2015)
Rac1, Rac2	Rho family small GTPases	conditional B cell or whole Rac1, Rac2 knock-out mice or double knock-out (DKO) animals, Rac1 DN peptide (inhibits Rac1 membrane localization), Rac2V12 and Rac1Q61L CA constructs	Defects in late B cell development and BCR-mediated proliferation, upregulation of BAFFR and survival (Rac1/2-dependent) Defects in CD40L- and LPS-mediated proliferation (Rac2-dependent) Impaired BCR-mediated membrane ruffling and spreading in transitional B cells, reversed by cholesterol supplementation Specific role of Rac2 in ICAM-1-mediated adhesion, actin polarization to and formation of pSMAC, antigen accumulation at low densities	(Walmsley et al., 2003) (Brezski and Monroe, 2007) (Arana et al., 2018)

2.2.4 B cell activation and metabolic reprogramming

The normal physiology of the B cell is supported by reactions of cellular metabolism. Anabolic reactions result in biosynthesis of new molecules from nutrients, whereas catabolic reactions provide energetic needs for anabolism and cellular activity. Glycolysis is the central metabolic pathway that provides an ATP energy source from conversion of glucose molecules. The net reaction is not energy efficient and aerobic organisms use the citric acid cycle (tricarboxylic acid, TCA cycle) and oxidative phosphorylation (OxPhos) as higher efficiency reactions to produce ATP and regenerate NAD^+ in the mitochondria. Access to novel tools now allow for relatively easy metabolic profiling of cultured cells, such as estimating the level of glycolysis via extracellular acidification rate (ECAR) measurements or OxPhos via oxygen consumption rate (OCR) monitoring. In combination with the fluorescent probes and inhibitors of metabolic activity as well as transgenic mouse models, these tools help to uncover the metabolic regulation of B cell functions and cross-talk with signaling pathways.

B cell subsets

Metabolic requirements of different B cell subsets are not extensively covered in the literature. Reports suggest that both B1 and MZ B cells exhibit increased levels of glycolysis and lipid uptake at the steady state (Muri et al., 2019; Clarke et al., 2018). In particular, peritoneal B1a cells, show increased levels of both glycolysis and OxPhos, higher cellular ROS (reactive oxygen species), lipid peroxidation and depend on glycolysis, fatty acid synthesis and autophagy for their homeostasis (Muri et al., 2019; Clarke et al., 2018).

BCR activation

Metabolic activity is significantly altered upon B cell activation to support the GC reaction, and later plasma cell development. Metabolic reprogramming is also distinct depending on the stimulus involved and associated differentiation stage. In response to commonly used stimuli, B cell activation in general results in upregulation of Glut1 glucose transporter, glucose uptake, increased glycolysis, OxPhos, mitochondrial mass and mitochondrial membrane potential and is usually assessed at 12–24 hrs post-activation (Doughty et al., 2006; Dufort et al., 2007; Caro-Maldonado et al., 2014; Price et al., 2018; Waters et al., 2018; Akkaya et al., 2018). Differences, however, exist in metabolic processes and reprogramming in response to different types of stimuli. Thus, upon BCR stimulation the uptake of glucose and increased glycolysis are PI3K- and PKCβ-dependent (Doughty et al., 2006; Blair et al., 2012; Dufort et al., 2007). Glucose flux is more substantial through glycolysis compared to TCA cycle (Doughty et al., 2006). Increase in OCR is also mediated by the BCR signaling components, Syk, Btk, PI3K and JNK, but not p38 or MEK (Akkaya et al., 2018; Akkaya and Pierce, 2019). Treatment of B cells with oligomycin, which is used to inhibit ATP synthase, suggested importance of OxPhos in B cell spreading,

Ag internalization and Ag presentation (Akkaya et al., 2018; Bonifaz et al., 2015; Van Dyke, 1993). Suppression of Ag presentation by oligomycin may, however, work via increase in lysosomal acidification (Van Dyke, 1993).

It was proposed that BCR stimulation leads to mitochondrial damage through elevated Ca^{2+} entry and thus activation-induced cell death (AICD) (Akkaya et al., 2018). In contrast, increased Ca^{2+} entry upon BCR stimulation via SOCE channels was proposed to mediate survival and proliferation of B cells (see section 2.2.1). It is unclear whether the experimental differences or the use of purified $CD23^{+}$ cells were responsible for these opposite conclusions (Berry et al., 2020). It is also unclear whether mitotracker green (MTG) staining of mitochondria can adequately indicate mitochondrial damage, but nevertheless Ca^{2+} chelators but not antioxidants were able to revert the increased MTG staining, which was found to negatively correlate with B cell viability in different culture conditions (Akkaya et al., 2018).

TLR activation

Exposure to LPS or CpG not only leads to activation of B cells but also triggers plasmablast differentiation. There are, however, conflicting results on the metabolic state and relative level of OCR and reactive oxygen species (ROS) in naive B cells, activated B cells and plasmablast stages of LPS-stimulated differentiation (Price et al., 2018; Jang et al., 2015). LPS-induced increase in ECAR and OCR is cMyc-dependent, and glycolytic rate was shown to be higher in activated B cells compared to plasmablasts (Price et al., 2018; Caro-Maldonado et al., 2014). Conflicting results are reported when OxPhos was promoted in LPS-activated B cells, ranging from increased plasmablast generation in one study (Price et al., 2018) to suppression of proliferation and antibody production upon LPS and CpG stimulation in another study (Caro-Maldonado et al., 2014). Inhibition of OxPhos in plasmablasts has been shown to reduce antibody secretion for most of the used inhibitors (Price et al., 2018). ROS manipulation in plasmablasts did not impact antibody secretion in one study (Price et al., 2018), but use of antioxidant in LPS-stimulated cells promoted plasmablast differentiation in another study (Jang et al., 2015). It was suggested, that markers of mitochondrial mass (mitotracker green, MTG) and mitochondrial membrane potential (mitotracker dRed, MTdR) can be used to distinguish between MTG^{hi} $MTdR^{hi}$ class-switched (”CSR”) and MTG^{lo} $MTdR^{lo}$ plasmablast (”PB”) fates of LPS- and anti-CD40-stimulated B cells (Jang et al., 2015). Inhibition of glucose utilization or mTORC1 increased generation of ”CSR” and suppressed generation of ”PB” cells (Jang et al., 2015). Inhibition of mTORC1 signaling by rapamycin also led to concomitant increase in ROS production in LPS-activated cells, which would be consistent with the promotion of plasmablast differentiation by antioxidants (Jang et al., 2015; Tsui et al., 2018). Interestingly, it was found that upregulation of heme biosynthesis supports plasmablast differentiation in LPS-activated B cells even in the presence of high ROS (Jang et al., 2015; Tsui et al., 2018). Effect of heme on plasma cell differentiation is mediated by direct suppression of BACH2 activity in B cells ultimately promoting upregulation of Blimp1 (Watanabe-Matsui et al., 2011). Compared

to anti-IgM stimulation, LPS or CpG stimulation result in higher metabolic profiles of OCR and ECAR as well as mitochondrial biogenesis. However, it is the anti-IgM that was found to promote high ROS accumulation, high cytoplasmic Ca^{2+} levels and activation-induced cell death (AICD). Second signals provided by Toll-like receptors or CD40L have been suggested to rescue BCR-induced mitochondrial damage and AICD through regulation of Ca^{2+} levels (Akkaya et al., 2018).

CD40 activation

CD40-mediated B cell activation results in extensive B cell proliferation and is a crucial signal for class-switched antibody responses in vivo (Pone et al., 2012; Xu et al., 1994). Metabolic changes upon CD40 stimulation (in combination with IL-4) have some unique features. Although glucose is fluxing through the glycolytic pathway, its flux through the TCA cycle is minimal, suggesting that glucose carbons are diverted to biomass synthesis. Depletion of glucose, resulted only in class-switching defects, but spared differentiation and proliferation. In contrast, glutamine uptake was shown to fuel TCA cycle and was found critical for differentiation, class switching, and proliferation. Suppression of OxPhos by oligomycin treatment at later stages of activation (day 3) suppressed CSR and differentiation. Mitochondrial remodeling resulted in an average increase of 5 mitochondria per cell compared to 2.6 in naive B cells without an increase in mitochondrial DNA suggesting a fission process (Waters et al., 2018).

GC and plasma cells

Metabolic signatures of GC B cells, are likely an integration of BCR- and Tfh cell-supported B cell activation signals. Similar to CD40-stimulated cells, only minimal amount of glucose is metabolized into TCA intermediates and in general GC B cells are only minimally glycolytic. GC B cells were shown to rely on fatty acid oxidation as their energy source (Weisel et al., 2020). It was suggested that GC B cells experience hypoxia, especially in the light zone (Cho et al., 2016). Hypoxia is believed to be an important factor for development and function of both, germinal center B cells and plasma cells. Low oxygen tension in GC areas results in HIF stabilization, reduction in mTORC1 and cMyc activity in LZ B cells, and induction of glycolytic program (Boothby and Rickert, 2017). Opposite to this, another group reported significantly downregulated expression of hypoxia-related and glycolytic genes in GC B cells (Weisel et al., 2020). Dual BCR and CD40 signaling in LZ GC B cells was proposed to induce mTORC1 and cMyc that regulate metabolic fueling and division potential of proliferating DZ GC B cells, respectively (Choi and Morel, 2020; Ersching et al., 2017; Finkin et al., 2019). The upregulation of mTORC1 and cMyc, however, in conflict with the predominant view of induction of glycolytic program by hypoxia (Taylor and Colgan, 2017).

Development of plasma cells appears to be supported by hypoxic conditions as well, which was shown for human plasma cells (anti-CD40 + TLR9 + cytokines at 5% ptO_2). In these cells hypoxia upregulated glycolysis, HIF2A and VEGFA, but also

cMYC expression. Further shortage of oxygen (1–3%), however, led to increase in cell death (Schoenhals et al., 2017). mTORC1 inhibition reduces antibody secretion, whereas enhancement of mTORC1 signaling leads to increased antibody secretion, but also reduces plasma cell lifespan (Choi and Morel, 2020). Comparison of mouse and human long-lived plasma cells (LLPC), residing in the bone marrow, and splenic short-lived plasma cells (SLPC) showed elevated OCR profiles for LLPC, which was explained by shortage of substrates for mitochondrial oxidation in SLPC, rather than functional mitochondrial remodeling. Although LLPC glucose uptake is high, most of it is used for protein glycosylation (Lam et al., 2016). Inhibition of glucose utilization impairs plasma cell differentiation and survival (Lam et al., 2016). Defects in autophagy and mitochondrial pyruvate import also lead to loss of LLPC (Pengo et al., 2013; Lam et al., 2016). Metabolomics studies reveal that carbon sources other than glucose are primarily used for biomass generation in antibody-secreting B cell lines (Garcia-Manteiga et al., 2011), whereas synthesis of fatty acids from glucose was found to be essential at the stages preceding plasma cell differentiation (Dufort et al., 2014).

2.2.5 Role of the transcription factor IRF4 in B cells

Interferon regulatory factor 4, or IRF4, is a multidomain, DNA binding protein that belongs to an IRF family of transcription factors (Antonczyk et al., 2019). Along with homologous IRF8, IRF4 expression is restricted to lymphoid and myeloid lineages. IRF4 is particularly important for development and functioning of B and T cells (Shukla and Lu, 2014; Huber and Lohoff, 2014; Mittrücker et al., 1997). Beyond early B cell development, IRF4 is critical for BCR-induced proliferation (Mittrücker et al., 1997), GC formation (Ochiai et al., 2013; Willis et al., 2014), class switch recombination and plasma cell differentiation (Sciammas et al., 2006; Klein et al., 2006). Expression of IRF4 in GC B cells is low if present, which is interesting in the light of the fact that IRF4 seems to be important for the germinal center reaction and is induced downstream of B cell receptor and c-Rel (NF-kB) (Cattoretti et al., 2006; De Silva et al., 2012; Grumont and Gerondakis, 2000). This contrasts with plasmablasts, in which expression of IRF4 is high (Sciammas et al., 2006). IRF4 is known to regulate the expression of activation-induced cytidine deaminase (AID), crucial for somatic hypermutation and class-switch recombination in the immunoglobulin loci, and genes involved in plasma cell differentiation program including Prdm-1, coding for BLIMP1 plasma cell transcription factor, and XBP-1 and its targets (Sciammas et al., 2006). However, it is not known if IRF4-dependent transcriptional changes influence differentiation of B cells at the level of BCR signaling.

2.3 Missing-In-Metastasis / Metastasis Suppressor 1

Missing-in-Metastasis (MIM), or Metastasis suppressor 1 (MTSS1) is an enigmatic protein with biochemically proven membrane-deforming and actin-binding activities. Moreover, a large set of interacting partners of MIM has been identified implicating MIM in a variety of functions ranging from cancer invasion and ciliagenesis to bone marrow cell migration and development of cerebellar neurons. Although in vitro data is often compelling, there are conflicting results and available MIM knockout mouse models show rather mild phenotypes, leaving a question of the real significance of MIM and redundancy in its proposed functions.

Missing-in-Metastasis (MIM), or Metastasis suppressor 1 (MTSS1) was identified as a 316 bp cDNA corresponding to the KIAA0429 gene (NM_014751 transcript), which was expressed in benign but absent or minimally present in metastatic breast, bladder and prostate cancer cell lines. At the time of discovery, the transcript NM_014751 coded WH2-containing 356 aa protein, named MIM-A (Lee et al., 2002). Later, two splice variants were described, encoding the 759 aa MIM-B protein and 755 aa MIM(12delta), which lacks 4 amino acids from the N-terminal sequence (Loberg et al., 2005).

With respect to the longest 759 aa isoforms in the RefSeq database, human and mouse sequences are 100% identical for the first 346 aa, with the exception of the

154–157 aa exon sequence and an additional Ser280, and almost identical for the rest of the polypeptides, with the exception of deletions/different sequences in the 350–431 aa portion and insertion in the mouse isoform at positions 527–541 aa.

In published reports, expression of Mim RNA was detected in mouse embryo developing heart, skeletal muscle and CNS, liver, limb bud, kidneys (branching collecting ducts, tubules and glomeruli), whereas adult animals showed high expression in liver and moderate to low in kidneys (renal cortex), heart, spleen, brain, lung and testes (Mattila et al., 2003; Xia et al., 2010). In contrast, antibody reactivity towards MIM showed specificity for mouse brain, bladder and spleen (Bompard, 2005). Large human proteomics screens reveal high expression levels of MIM in liver, spleen, lymph nodes, ovaries, adipose tissue and brain. Specific cell types with high MIM expression include B cells, NK cells and platelets (access via https://www.ebi.ac.uk/gxa/home) (Pinto et al., 2014; Wang et al., 2019).

2.3.1 MIM in the regulation of actin cytoskeleton and membrane dynamics

MIM is an I-BAR (IMD, IRSp53/MIM homology domain) domain protein (Yamagishi et al., 2004; Millard et al., 2005), which places it into a superfamily of BAR domain-containing proteins (Table 6). In addition to N-terminal I-BAR domain (1–241 aa), MIM contains a C-terminal WH2 domain (728–754 aa) as well as regions rich in serine (SRR, 242–363 aa) and proline (PRR, 612–727 aa) (Mattila et al., 2003; Machesky and Johnston, 2007) (Figure 15).

Table 6. BAR domain families*

Domain	Current and alternative names	Membrane deformation
BAR/N-BAR	Bin-Amphiphysin-Rvs, or normal BAR domain	negative curvature
EFC/F-BAR	extended Fer-Cip4 homology or FCH and BAR domain; Pombe Cdc15 homology (PCH) domain	negative curvature
I-BAR	inverse BAR, or IMD (IRSp53/MIM homology domain)	positive curvature

*(Rao and Haucke, 2011; Safari and Suetsugu, 2012)

MIM I-BAR domains form homodimers, presented as a bundle of six helices (3 from each I-BAR domain) and despite extensive contacts cannot be classified as having a classical coiled-coil structure (Lee et al., 2007). MIM I-BAR dimers interact with membrane $PI(4,5)P_2$ and, to a much lesser degree, with $PI(3,4)P_2$ lipids via

electrostatic interactions of their positively charged amino acids mapped to the tips of the dimers (Mattila et al., 2007; Quinones et al., 2010). Unlike N-BAR or F-BAR domains, which form concave (crescent or banana-shaped) lipid-binding surfaces, I-BAR domains dimerize into a convex surface, exerting negative curvature toward the lipid interface (i.e. directed from the protein) (Rao and Haucke, 2011). Consequently, I-BAR domains generate inward tubulation of artificial vesicles in vitro, with an effective diameter of 61–78 nm (Mattila et al., 2007; Saarikangas et al., 2009), which likely result from oligomerization of the dimers into a lattice structure, which is a model for membrane tubulation by other BAR domains (Shimada et al., 2007; Simunovic et al., 2015).

Apart from its lipid binding and membrane deforming activities, MIM is an actin-binding protein. Specifically, the I-BAR domain, but not the C-terminal MIM portion, binds F-actin in high-speed co-sedimentation experiments (Mattila et al., 2003; Yamagishi et al., 2004). This binding was shown to depend on the same positively charged amino acids at the tips of the I-BAR dimers responsible for PI(4,5)P_2 binding (Mattila et al., 2007; Bompard, 2005). Dissociation constants for F-actin were estimated from $\sim$0.15 (full-length, low salt) to $\sim$17 μM (I-BAR, normal salt) (Gonzalez-Quevedo et al., 2005; Lee et al., 2007).

There are also reports indicating that the MIM I-BAR domain may bundle F-actin in low-speed co-sedimentation experiments (Yamagishi et al., 2004; Bompard, 2005; Gonzalez-Quevedo et al., 2005). However, only one study used physiological (100 mM KCl) salt concentration in the bundling assay (Yamagishi et al., 2004) and all subsequent studies failed to detect this activity (Lee et al., 2007; Mattila et al., 2007).

Monomeric G-actin binding of MIM is attributed to a conserved WH2 domain (728–754 aa) and is not seen when this domain is deleted (Mattila et al., 2003; Gonzalez-Quevedo et al., 2005; Lin et al., 2005). In addition, MIM (404–759) shows higher affinity for ATP-G-actin ($K_{\mathrm{d}} \sim 0.06$ μM) vs ADP-G-actin (~ 0.30 μM) and inhibits nucleotide exchange rate on actin monomers (Mattila et al., 2003). Dissociation constants for G-actin in other studies were estimated to range from ~ 0.094 (full-length) to ~ 0.4 μM (full-length, low salt) (Lin et al., 2005; Gonzalez-Quevedo et al., 2005). Crystal structure of G-actin with the WH2 peptide suggests importance of the amino acids 728–749 aa, as well as the canonical ^{741}LKKT sequence found in other actin-binding proteins, for the interaction with actin (Lee et al., 2007). At the same time, there is an indication that the sequence adjacent to the WH2 domain may also be important for G-actin binding as C-terminal MIM (565–759 aa) but not MIM (664–759 aa) was the minimal MIM fragment that bound monomeric actin in pull-down experiments (Woodings et al., 2003).

In vitro, actin-binding abilities of MIM have been shown to inhibit actin polymerization through monomer sequestering by WH2 domain (Mattila et al., 2003; Woodings et al., 2003; Lin et al., 2005). Actin assembly on F-actin seeds showed that MIM efficiently inhibits pointed-end polymerization of gelsolin-capped actin and reduces

but doesn't block barbed-end polymerization on phalloidin-stabilized actin (Mattila et al., 2003) (Figure 14).

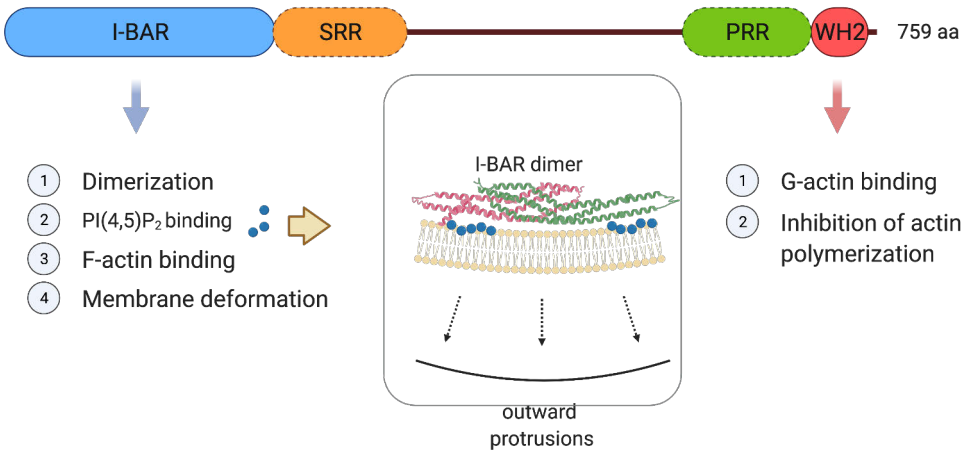

Figure 14. MIM in the regulation of actin cytoskeleton and membrane dynamics. See the text for additional details.

MIM is also reported to interact with the NPF activator Rac1 and class II NPF, cortactin (Lin et al., 2005; Bompard, 2005; Mattila et al., 2007) (Table 8). In vitro actin polymerization experiments show that MIM inhibits Arp2/3 + cortactin-mediated actin assembly and promotes it only at low MIM protein concentrations. The effect of MIM on Arp2/3 + N-WASP-VCA-mediated actin assembly is inhibitory (Lin et al., 2005).

Structural and biochemical studies of MIM strongly suggest a function as a membrane and cytoskeletal regulatory protein in the cellular context. Indeed, overexpression of full-length MIM or its truncated versions in various adherent cell lines shows that the most consistent phenotype is a ragged appearance of the cell fringe, also described as generation of filopodia-like protrusions (Woodings et al., 2003; Yamagishi et al., 2004; Bompard, 2005; Gonzalez-Quevedo et al., 2005; Mattila et al., 2007; Cao et al., 2012) and loss of stress fibers (Woodings et al., 2003; Bompard, 2005; Gonzalez-Quevedo et al., 2005). Although, cytoskeletal phenotypes vary between cell lines and construct used, localization to plasma membrane is primarily mediated by the I-BAR domain as deletion or mutations in this region result in reduction or loss of such association (Woodings et al., 2003; Bompard, 2005; Mattila et al., 2007; Bershteyn et al., 2010). Additionally, tyrosine phosphorylation by Src kinases has been shown to regulate membrane localization of MIM (Wang et al., 2007).

2.3.2 MIM in cancer

Initial identification as a gene the expression of which is lost in metastatic cancer cells and a given name assured interest in this protein for many cancer researchers. Since then, MIM expression was reported to be down- or upregulated in a variety of primary tumors and cancer cell lines. These studies are summarized in the Table 7. It is important to note, however, that availability of good validated antibodies, which would unambiguously identify the endogenous MIM protein by immunolabeling in paraffin-embedded tissue sections or in fixed cells by fluorescence microscopy, presents an obstacle to this date. Therefore, interpretations of protein expression in tissue sections must be considered cautiously.

Table 7. MIM in cancer

Cancer	Phenotype	Evidence	Samples	References
Bladder cancer (but also breast and prostate cancer)	downregulated	RNA (PCR) – MIM-A isoform	cancer cell lines (human)	(Lee et al., 2002)
Bladder cancer	downregulated	RNA (PCR); protein (IHC). Antibodies info – NA*	cancer samples; cancer cell lines (human)	(Du et al., 2011)
Bladder uroepithelium cell carcinoma	downregulated (also in poor prognosis)	RNA (PCR); protein (WB). Antibodies: Santa Cruz Biotechnology, Cat. # – NA	cancer samples (human)	(Du et al., 2017)
Prostate cancer	downregulated	RNA (PCR) – MIM-A, MIM-B, MIM-(12del)	tumor samples; cancer cell lines (human)	(Loberg et al., 2005)
Breast cancer	downregulated (poor prognosis)	RNA (PCR); protein (IHC). Antibodies: Abnova, Cat. # – NA	tumor samples; cancer cell lines (human)	(Parr and Jiang, 2009)
Gastric cancer	downregulated (in poor prognosis)	RNA (PCR); Protein (IHC, WB). Antibodies: Abcam ab56780, discontinued	tumor samples (human)	(Liu et al., 2010a)
Kidney cancer	downregulated	RNA (PCR); Protein (IHC). Antibodies info and article file – NA	cancer cell lines (human)	(Du et al., 2012)
B-ALL acute lymphoblastic leukemia; B cell cancer lines	downregulated	RNA (microarray); protein (WB). Antibodies info – NA	tumor samples (human); cancer cell lines (human, mouse)	(Yu et al., 2012)
Acute myeloid leukemia	downregulated (in poor prognosis)	RNA (PCR); protein (WB). Antibodies: Cell signaling Technology #4386, discontinued	tumor samples; leukemia cell lines (human)	(Schemionek et al., 2015)
Pancreatic ductal adeno-carcinoma	downregulated (in metastatic cell lines)	Protein (WB). Antibodies: Cell signaling Technology #4386, discontinued	cancer cell lines (human)	(Zeleniak et al., 2017)
Lung adenocar-cinoma	downregulated (also in metastasis and poor prognosis)	RNA; protein (WB). Antibodies: Thermo, Cat. # – NA	cancer cell lines (human); orthotopic xenograft model; TCGA database	(Taylor et al., 2018)

Table 7. MIM in cancer

Cancer	Phenotype	Evidence	Samples	References
Hepatocellular carcinoma	upregulated	RNA (PCR) – MIM-B; protein (WB). Antibodies: A.Oro lab	tumor samples (human)	(Ma et al., 2007)
Head and neck squamos cell carcinoma	upregulated	RNA (microarray)	primary tumor samples (human)	(Dawson et al., 2012)

*NA - not available

2.3.3 MIM as multifunctional protein

In addition to, and sometimes complementary to its functions as actin cytoskeletal regulatory and membrane remodeling protein, MIM has been reported to interact with a number of other proteins (Table 8, Figure 15). These and other studies implicate MIM in the regulation of actin cytoskeleton and membrane dynamics (Section 2.3.1), cancer migration and survival (Table 7), cilia maintenance (Bershteyn et al., 2010; Atwood et al., 2013; Drummond et al., 2018), renal epithelium function (Saarikangas et al., 2011; Xia et al., 2010), Purkinje cell function (Minkeviciene et al., 2019; Saarikangas et al., 2015; Sistig et al., 2017; Brown et al., 2020), CXCR4 downmodulation (Zhan et al., 2016; Li et al., 2017), and even point on genetic association with cardiac function (Wild et al., 2017; Morley et al., 2019; Andersson et al., 2019; Aung et al., 2019).

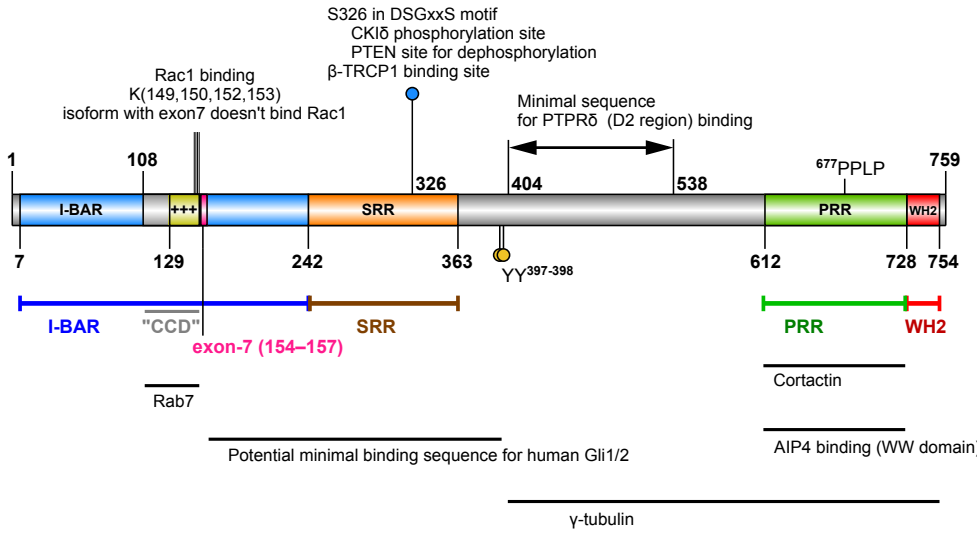

Figure 15. MIM domain structure and interactions.
See the text for additional details.

Table 8. MIM interacting partners

Interacting partner	Evidence	Proposed function	System	References
Rac1	MIMΔ(I-BAR) or K$\rightarrow$D mutations at 149, 150, 152, 153 – prevent Rac binding. I-BAR domain from long MIM isoform with exon 7 [154–157] – does not precipitate Rac.	Rac1 activation, lamellipodia formation.	COS-7 (monkey kidney), Swiss 3T3 (mouse embryonic fibroblasts) U2OS cells (human osteosarcoma)	(Bompard, 2005) (Mattila et al., 2007)
RPTPδ	MIM (404–759), (404–705), (400–538) – precipitate PTPRδ. RPTPδ D2 region is responsible for the interaction.	MIM links receptor tyrosine phosphatase with actin cytoskeleton reorganization and responsible for RPTPδ localization at the plasma membrane. However, RPTPδ catalytic activity is dispensible for MIM overexpression phenotype.	human MIM (bait), Y2H screen (human brain library); COS-7 cell line lysates	(Woodings et al., 2003) (Gonzalez-Quevedo et al., 2005)
Cortactin	MIM precipitates cortactin. MIM PRD is responsible for binding to SH3 domain of cortactin. MIM (403–759) poorly binds cortactin. dMIMΔPRD (drosophila) doesn't bind dCortactin. MIM PRD is likely responsible for binding to SH3 domain of cortactin.	MIM promotes cortactin-Arp2/3-mediated actin polymerization. But inhibits Arp2/3-VCA actin polymerization.	in vitro actin polymerization	(Lin et al., 2005) (Quinones et al., 2010) (Bershteyn et al., 2010)
Src kinase	MIM is phosphorylated at Y397, Y398 by recombinant Src in vitro.	PDGF-induced translocation of MIM to plasma membrane; induction of dorsal ruffles.	NIH3T3 (mouse embryonic fibroblasts)	(Wang et al., 2007)

Table 8. MIM interacting partners

Interacting partner	Evidence	Proposed function	System	References
Daam1 formin	Daam1 precipitates MIM in Xenopus embryos and p8 mouse cerebellar lysates. CC2 fragment of Daam1 precipitate SRD or PRD domains of MIM.	Actin cytoskeleton organization in neuroepithelial cells of Xenopus laevis embryos. Neural tube closure. MTSS1 opposes Daam1 activity in Purkinje cells, determining neural morphology.	human C-Daam1 (bait), rat brain cDNA library (identification) xenopus MIM - human Daam1	(Liu et al., 2011) (Kawabata Galbraith et al., 2018)
Gli1/2, Sufu	Full-length human MIM and MIM (1–399) bind Gli1/2 and Sufu. As MIM (1–538) and MIM (160–755) potentiate Gli-mediated transcription activity, perhaps MIM (160–399) is the minimal required sequence. In contrast, Saarikangas et al., showed that mouse MIM doesn't bind Gli1/2 or potentiate Gli-mediated transcription.	MIM is a Sonic hedgehog-responsive gene in regenerated human epidermis. MIM is able to potentiate Gli1/2-dependent transcription in cells with active Shh signaling such as human basal carcinomas.	Regenerated human skin graft keratinocytes, MEFs, HEK293 (IP)	(Callahan et al., 2004) (Saarikangas et al., 2011)
γ-tubulin	γ-tubulin precipitates with full-length MIM (dermal cells). MIM (277–755) and MIM (400–755) are able to localize at basal body. PRD (400–755) is most likely responsible for the interaction.	MIM plays role in the assembly of primary cilia in dermal cells (possibly via p60 Src and cortactin regulation) and hair follicle morhogenesis.	C3H10T1/2 (mouse embryo sarcoma), MEFs, primary dermal cells	(Bershteyn et al., 2010)
atypical PKC-ι/λ and PARD3	Reciprocal precipitation of MIM and aPKC, PARD3 in mouse dermal cells.	MIM may serve as a scaffolding protein that regulates primary cilia and Gli-mediated Shh signaling possibly via interactions with aPKC-ι/λ.	Mouse basal cell carcinoma cells, mouse fibroblasts, keratinocytes, dermal cells	(Atwood et al., 2013)

Table 8. MIM interacting partners

Interacting partner	Evidence	Proposed function	System	References
CKIδ, β-TRCP1	S322 (S326 in the long isoform) is phosphorylated by CKIδ (casein kinase) for β-TRCP-mediated ubiquitination and degradation. β-TRCP1 (both isoforms 1A/2B) bind DSGxxS motif when phosphorylated by CKIδ. β-TRCP1 (R474A) mutant fails to bind MIM.	Loss of MIM through proteosomal degradation increases growth and migratory potential of breast and prostate cancer cells.	PC3 and MDA-MB-321 cell lines	(Zhong et al., 2013)
PTEN	Reciprocal immunoprecipitation of MIM and PTEN PTEN is likely dephosphorylates S322 (S326) within DSGxxS motif.	Loss of MIM leads to increased invasion, migration and increased survival of PDAC (pancreatic cancer) cell line. PTEN blocks proteosomal degradation of MIM. Decreased MIM expression in PTEN-deficient cells promotes migration and invasion of pancreatic cancer cell line.	PANC-1, MIA PaCa-2, and BxPC-3 from primary pancreatic cancer sites. L3.6pl, Hs 766T, and AsPC-1 from pancreatic cancer metastatic sites. HEK293T (IP), S63 and NIH3T3 fibroblasts	(Zeleniak et al., 2017) (Zeleniak et al., 2018)
AIP4 (CXCR4), Rab5, Rab7 upon SDF-1 (CXCL12) stimula-tion	MIM (612–730) PRD binds AIP4 (possibly via WW-domain). MIM (612–730) PRD also binds CXCR4 in AIP4-dependent manner. MIM also precipitates: Rab5 (within 5 min) Rab7 (within 30 min). Rab7 binding is independent of AIP4/CXCR4 and depend on CCD (coiled-coil domain) [108–153]	MIM promotes CXCR4 ubiquitination and internalization through AIP4 and targeting to endocytic compartments via transient interactions with Rab5 and Rab7	Hela, Raw264 cell lines, bone marrow mononuclear cells	(Li et al., 2017)

Table 8. MIM interacting partners

Interacting partner	Evidence	Proposed function	System	References
CLC (Clathrin light chain), Rab5, Rab7 upon magnetic nanoparticle treatment	MIM precipitates: CLC (5–10 min) Rab5 (0–3 min and 60–240 min) Rab7 (5–60 min)	Role in endocytosis of magnetic nanoparticles	Raw264.7 cell line	(Zhao et al., 2019)
SCAMP1	MIM and SCAMP1 interaction by IP and PLA	MIM and SCAMP1 inhibit migration and invasiveness of breast cancer cells (SkBr3, MDA-MB-453 and BT-474 breast cancer cell lines)	SkBr3, MDA-MB-453 and BT-474 breast cancer cell lines	(Vadakekolathu et al., 2018)

2.3.4 MIM in B cells

According to several gene and protein expression databases, MIM is present at high levels in mouse and human B cells, suggesting functional importance in this cell subset. Study of Yu et al., 2012 reported disturbed B cell compartment in MIM knockout mice and generation of lymphomas in aged animals (Yu et al., 2012). Specifically, they reported a 50% reduction in $CD19^+$ cells in the spleen, and increased fraction (by 20% or more) of $CD19^+$ cells in the bone marrow and blood. Immature $CD19^+/CD117^-/CD25^+$ B cells were increased by 35% in the bone marrow, whereas IgM^+ cells were reduced by 22%. In the spleen, IgM^+ B cells were reduced by 73% and IgD^+ by 50%. This was accompanied by 5-fold reduction in CXCR5-mediated directional migration in vitro. The majority of MIM knockout animals died between 14 to 24 month of age, 81% had enlarged spleens and 56% had enlarged livers. Morphologically, infiltrated lymphocytes were characterized as murine diffuse large B cell lymphoma. These tumors were rather monoclonal and positive for $CD19^+$, $B220^+$, $CD20^+$, and $CD5^+$. In the later study, however, the same group reported comparable B cell numbers in the bone marrow and periphery of MIM knockout animals, leaving open the question of the real consequences of MIM deletion for B cell development and function (Zhan et al., 2016).

2.4 Computational tools and resources for interrogation of gene and protein function

In order to infer biological function of a gene or a protein, researchers would usually resort to experimental examination of their hypotheses. There are, however, non-wet-lab approaches that allow for interrogation of nucleotide and amino acid sequences and generation of biological knowledge, which may help, if not to fully uncover the function, in refining research hypotheses for experimental verification. With the increasing complexity and amount of biological knowledge, bioinformatics methods and tools constitute an essential part of biological research at all levels. Development of bioinformatics methods, but also their application require a fair amount of special knowledge and training, and may not be a straightforward procedure to implement. At the same time, increasingly more high-quality web-based tools have become available for researchers without in-depth bioinformatics background to perform various computational analyses and explore publicly available databases and should not be ignored.

Analysis of amino acid sequence alone can bring a wealth of useful information about the protein. Databases of annotated protein sequences contain information on often validated structured regions, or protein domains, and unstructured, intrinsically disordered regions (IDR) of the proteins. Quite frequently IDRs are enriched in short linear functional motifs, found in protein interaction interfaces (Kumar et al., 2020). Analysis of evolutionary conservation of protein orthologs can also highlight functional significance of the protein regions. Sequence evolution is constrained by essential molecular interactions and therefore contacting positions in proteins exhibit correlated patterns of sequence evolution (Avila-Herrera and Pollard, 2015). Analysis of single nucleotide polymorphisms (SNP), can also give information about functionally important protein regions. Although, neutral SNPs constitute the majority of genetic variation, non-synonymous SNPs in the coding gene regions are predicted to negatively affect protein function in 25–30% cases (Ramensky et al., 2002; Ng and Henikoff, 2006). It can be expected that regions with a low level of polymorphisms are under pressure of negative selection and thus functionally important. Tissue distribution profiles directly point toward functional importance of a particular gene or protein in a given cell type. Similarly, cancer gene expression databases can be helpful in determining important molecular players in certain tumors. In addition to functional correspondence of protein-coding regions in orthologs, conservation of gene regulatory elements, such as promoters, enhancers and transcription factor binding sites (TFBS), across taxa may point on similar regulatory control and, thus, function between proteins from different species.

3 Aims of the study

The goal of the study was to understand the contribution of MIM and IRF4 to B cell-mediated immunity with the focus on their regulatory role in B cell activation and modulation of the actin cytoskeleton.

1. To perform analysis of MIM/MTSS1 sequence to get a better understanding of its functions by using available computational tools, bioinformatics resources and public online databases.

2. To characterize the immunological phenotype of MIM/MTSS1 knock-out mice with the focus on B cell-mediated immunity and antibody responses.

3. To reveal the molecular targets of IRF4 transcriptional regulation in B cells that are immediate components of the BCR signaling pathway.

4 Materials and methods

The "Materials and Methods" chapter of the thesis is a compilation of the "Materials and Methods" sections from the corresponding original publications reproduced in their entirety with only minor changes.

4.1 *Publication I*

A graphical overview of the computational workflow is presented in Supplementary Fig. S1 (Publication I), following the order of the sections below.

Identification of orthologs

MTSS1 transcript variant 1 from human (RefSeq: NM_001282971.1) and mouse (RefSeq: NM_144800.2) were used to identify orthologous transcripts in G. gallus (chicken), A. carolinensis (green anole lizard) and L. oculatus (spotted gar) from the NCBI database (National Center for Biotechnology Information, https://www.ncbi.nlm.nih.gov/). Translated MIM sequences from human, chicken
(RefSeq: XM_015283097.1), lizard (RefSeq: XM_016992753.1) and spotted gar (RefSeq: XM_015357664.1) were then used in TBLASTN searches at NCBI against mammalian, avian, reptilian and fish databases, respectively. To assess that the identified orthologs (***I***, Supplementary Table S2) correspond to isoform 1 from human (and mouse), we considered the BLAST similarity scores and the exon/intron organization. For example, exon 7 is alternatively spliced in the human MTSS1 transcript variant 2 (RefSeq: NM_014751.5, UniProt: O43312, see next section) so we expected the real orthologs to have the exon 7 like in the human transcript variant 1. In case a detailed comparison between orthologues was required, we used SIM (alignment tool for protein sequences, https://web.expasy.org/sim/) and inspected the results in LalnView (Duret et al., 1996). As a final verification, we performed reciprocal BLAST hit searches for each sequence against human and obtained a match to MTSS1 isoform 1.

Protein sequence characterization

MIM domains were predicted by SMART (Letunic and Bork, 2018) (Simple Modular Architecture Research Tool, http://smart.embl-heidelberg.de/) in "normal mode" with the option to consider Pfam domains. Short functional motifs were searched at ELM (Dinkel et al., 2016) (Eukaryotic Linear Motif, http://elm.eu.org/), by MIM UniProt Identifier (such as "MTSS1_HUMAN O43312") to retrieve the conservation scores (cs) (Chica et al., 2008) of the motifs. Motif coordinates following

isoform 1 of MIM, with cs >0.6 (motif is present in over 60% of all homologous sequences at UniRef (Letunic and Bork, 2018)) are listed in (***I***, Supplementary Table S1). We assume that our chosen cut-off values are biologically reasonable, as for example the experimentally validated DSG(XX)S degron motif is identified by ELM as DEG_SCF_TRCP1_1 with a p-value = 1.264E-04 and cs = 0.710. For regions where positively selected sites were identified (see "Molecular Evolution Study" below), we used the NetPhos (Blom et al., 2004) tool (http://www.cbs.dtu.dk/services/NetPhos/) at CBS (Center for Biological Sequences analyses) to conduct a more broad search for potential phosphorylation regions. Like ELM, NetPhos was also able to spot sites that are experimentally validated for MIM, such as Y397 and Y398 (Wang et al., 2007), which were detected even slightly below the threshold. Disordered binding regions (DBR) were predicted at IUPred2A (Mészáros et al., 2018) (https://iupred2a.elte.hu/) and regions with IUPred and ANCHOR scores greater than 0.8 were indicated onto MIM. Primary and secondary structure features were observed by SA (Sequence Analysis v1.7.2, http://informagen.com/SA/) and tools from EMBOSS93 (European Molecular Biology Open Software Suite, v6.6.0). Coordinates defining protein topology were listed in JSON syntax and submitted to the Pfam custom domain generator (http://pfam.xfam.org/generate_graphic/).

Sequence alignment

We created multiple sequence alignments (MSA) separately for mammalian orthologues, as well as a combined alignment for all species (***I***, Supplementary Datasets S1 and S2). Amino acid sequences were aligned by PRANK (Löytynoja, 2014) (v150803), using guide trees obtained from TimeTree (Kumar et al., 2017) (http://www.timetree.org/) and using a total of 10 iterations (option '-iterate = 10'). Coding DNA sequences (CDS) of orthologs were codon aligned by PAL2NAL (Suyama et al., 2006) (v14.0), following their protein MSA.

Molecular evolution study

The codon alignments and phylogenetic trees from above were subjected to a series of evolutionary selection tests by PAML (Yang, 2007) (Phylogenetic Analysis using Maximum Likelihood) and HyPhy (Pond et al., 2005) (Hypothesis testing using Phylogenies). CodeML from PAML (v4.9 h) was used with ModelFree (free ratios: independent ω for each branch) for all species. Omega values for branches, estimated by CodeML were rendered in color-code onto the tree by PhyTools95 package for R (https://www.r-project.org/). Branches with omega >0.15 are listed in (***I***, Supplementary Table S3) and node labels are found in (***I***, Supplementary Fig. S2). For mammals, CodeML nested models M7 versus M8, and M8A versus M8, were used. Model pairs were compared (2ΔL) in Gnumeric (http://www.gnumeric.org/) and the chidist formula (survival function of the χ^2 distribution) was used to calculate the likelihood estimate (p-value) for rejecting the null hypothesis (Supplementary Table S4). Both neutral models (M7 and M8A) were rejected in favor of the model for positive selection (M8). Sites determined to be under positive selection by Bayes Empirical Bayes (BEB) with posterior probability (PP) higher than 0.9 were consid-

ered (BEB PP $>$ 0.9). In HyPhy (v2.3.14) we used the methods SLAC [1] (Kosakovsky Pond and Frost, 2005) (Single-Likelihood Ancestor Counting), FUBAR [2] (Murrell et al., 2013) (Fast Unconstrained Bayesian AppRoximation) and MEME [3] (Murrell et al., 2012) (Mixed Effects Model of Evolution). For SLAC, sites determined to be under negative or positive selection with $p < 0.05$ were considered. For FUBAR, we considered sites determined to be under negative or positive selection with Bayesian PP $>$ 0.9. For MEME, sites determined to be under episodic (diversifying) selection with $p < 0.05$ were considered. More information on the positively selected sites (including SLAC and MEME results with the default $p < 0.1$) can be found in (***I***, Supplementary Tables S5–S8). In our ModelFree run, we encountered a technical problem: the data acquired by CodeML reported abnormally high omega values for three branches: 97..100 (ancestral to S. salar and E. lucius) with ω = 551.9418, 118..119 (ancestral to P. humilis, P. major, S. vulgaris and F. albicollis) with ω = 203.0243 and 178..11 (M. nemestrina) with ω = 999.0000 (species tree with node labels is shown in (***I***, Supplementary Fig. S2). The branches had dS = 0.0000, which resulted in the abnormal estimation of ω, therefore, we excluded these ω values from (***I***, Fig. 2), and these branches were coloured in black.

Co-evolutionary analyses

Intra-molecular co-dependence between amino acids was determined by MISTIC (Simonetti et al., 2013) (Mutual Information Server to Infer Coevolution, (http://mistic.leloir.org.ar/, accessed August 2017). We used MSA of all mammalian species (***I***, Supplementary Dataset S2), as described at the "Sequence alignment" step. Circular representation of MIM protein topology was rendered in GIMP (https://www.gimp.org/).

Structural analyses

Conservation of the 3D structure of the I-BAR domain was estimated at the ConSurf (Ashkenazy et al., 2016) server (http://consurf.tau.ac.il/), using an MSA of MIM from all species (***I***, Supplementary Dataset S1). Crystal structure of the I-BAR domain (PDB: 2D1L) (Lee et al., 2007) from M. musculus was visualised and exported by UCSF Chimera 96 (Pettersen et al., 2004).

Distribution of SNPs and mutations in cancer

The 1000 Genomes project (Consortium et al., 2015) data at Ensembl (GRCh38.p12, Ensembl (Rice et al., 2000): Jul 2018) was searched for missense SNPs of MTSS1 isoform 1 (ENST00000325064.9). In our searches, PolyPhen-2 (Adzhubei et al., 2010) (HumVar) automatically classified SNPs with low to medium scores (0–0.444) as "benign", those with medium to high scores (0.453–0.906) as "possibly damaging", and those with the highest scores (0.909–1) as "probably damaging". The cBioPortal (Gao et al., 2013; Cerami et al., 2012) for Cancer Genomics

[1] SLAC – approximate method, good for large datasets

[2] FUBAR – medium to large datasets, recommended for analysis of pervasive selection

[3] MEME – preferred method for analysis of positive selection at individual sites

(http://www.cbioportal.org/, accessed August 2018) was used to search for mutations in MIM identified in different cancers. To obtain PolyPhen-2 (HumVar) scores for these mutations, we submitted their genomic coordinates (GRCh37) to Ensembl Variant Effect Predictor (https://www.ensembl.org/Tools/VEP). Similarly to the scores for SNPs, PolyPhen-2 classified the mutations as "benign" (0–0.445), "possibly damaging" (0.485–0.905) and "probably damaging" (0.91–1). The PolyPhen-2 scores were plotted in Gnumeric onto the protein topology of MIM, where we chose 0.45 as the borderline value to distinguish between benign and possibly/probably damaging SNPs or mutations found in cancer.

Cancer expression databases and web tools

Expression data and plots for solid cancers were retrieved from TCGA (https://cancergenome.nih.gov, cancer studies, matched control samples) and GTEx (https://gtex-portal.org/home, normal control samples data) databases using GEPIA (Tang et al., 2017) web tool (http://gepia.cancer-pku.cn) with the following cut-off values: Log2FC (fold change) = 1, *p $<$ 0.001, accessed in August of 2018. Expression data in lymphomas/leukaemias and corresponding plots were retrieved using the Oncomine (Rhodes et al., 2004) portal (https://www.oncomine.org/, Thermo Fisher Scientific), accessed in August of 2018. Oncomine platform filters corresponding to (***I***, Fig. 5), Gene: MTSS1, Analysis Type: Cancer vs Normal Analysis, Cancer Type: Chronic Lymphocytic Leukemia. Dataset tab: Basso lymphoma (Basso et al., 2005) (Fig. 5c) or Haferlach leukaemia (Haferlach et al., 2010) (***I***, Fig. 5d) with default dataset threshold values. Dataset visualization tab: grouped by: Cancer and Normal Type, Show: All Samples in Dataset. Differential analysis in GEPIA is done by one-way ANOVA, using disease state (Tumor or Normal) as variable for calculating differential expression. Oncomine returns fold change as the difference in the means of the two groups being compared and t-test is applied.

Human ethics statement

CLL patients were diagnosed according to the updated National Cancer Institute Working Group (NCIWG) guidelines (Hallek et al., 2018). Peripheral blood samples were obtained after patients' informed consent (written), as approved by the institutional ethics committee of San Raffaele University Hospital (Milano, Italy). The study has been specifically approved by the OSR ethics committee in the protocol VIVI-CLL titled: "In vivo and in vitro characterization on CLL". All methods were performed in accordance with the relevant guidelines and regulations.

Human primary sample purification

Leukemic lymphocytes were obtained from peripheral blood of CLL patients, diagnosed according to the updated National Cancer Institute Working Group (NCIWG) guidelines (Hallek et al., 2018). All patients were either untreated or off therapy for at least 6 months before the beginning of the study. Leukemic CD19 cells were negatively selected from fresh peripheral blood using RosetteSep B-lymphocyte enrichment kit (STEMCELL Technologies). Purity of all preparations was always more than 99%, and the cells co-expressed CD19 and CD5 on their cell surfaces as checked

by flow cytometry (FC500; Beckman Coulter); preparations were virtually devoid of natural killer (NK) cells, T lymphocytes, and monocytes. Patients have been divided into GOOD prognosis and POOR prognosis based on clinical (RAI, Binet staging and prognosis) and biological parameters (IgHV mutational status, CD38 and ZAP70 expression).

RT-qPCR

RNA was isolated from both cell lines and primary samples with ReliaPrep RNA Cell mini Prep System (Promega) according to the manufacturer's instructions. cDNA was synthesized according to the manufacturer's protocol using Maxima RevertAid H minus First Strand cDNA Synthesis Kit reagents (Thermo Fisher scientific). qRT-PCR analysis was performed using an ABI7900 Thermal Cycler instrument (Applied Biosystem) for human MTSS1 (NM_001282974.1, NM_014751.5, NM_001282971.1) with the SYBR GREEN system using following primers: CATCATCAGCGACATGAAGG (forward) and CACATCCTGGTGAGAGCAGA (reverse). GAPDH was used as a reference gene and delta Ct values were analyzed by two-tailed t-test with Welch correction. Data are presented as $2^{-\Delta Ct}$.

Transcription factor binding

A 20 kb region (chr8:124717884–124737884, GRCh38/hg38), defined as ±10 kb from the transcription start site of MTSS1 gene (relative to transcript variant 1, RefSeq `NM_001282971.1` or Gencode ENST00000325064.9) was searched for evidence of TFBSs. The coordinates of the short genomic regions, where transcription factors are reported at ENCODE (Davis et al., 2018) (v3, GRCh37/hg19, https://www.encodeproject.org/) were obtained (http://hgdownload.soe.ucsc.edu/goldenPath/hg19/encodeDCC/wgEncodeRegTfbsClustered/ from file "wgEncodeRegTfbsClusteredV3.bed") and used at the UCSC Genome Browser. Genomic coordinates corresponding to the GRCh38/hg38 human genome assembly were identified (***I***, Supplementary Table S9) by the LiftOver tool (http://genome.ucsc.edu/cgi-bin/hgLiftOver). Similarly, their coordinates in the genomes (***I***, Supplementary Table S11) of other species were extracted again by LiftOver. Sequences were retrieved by "fastaFromBed" within the BedTools package (http://bedtools.readthedocs.io/) and sorted by region. The TFBS reported for human were searched across species by MAST (Motif Alignment and Search Tool), part of the MEME suite (Bailey et al., 2009) (v4.12.0) with relaxed cutoff values (-mev 10, -ev 10). We obtained position frequency matrices (PFMs) from JASPAR core 2018 (redundant and non-redundant) and HOCOMOCO v11 (core and full) databases (Khan et al., 2018; Kulakovskiy et al., 2018). To search for novel TFBS, we selected a genomic region (chr8:124736177–124736777, GRCh38/hg38, named "SEARCH" in ***I***, Fig. 6) based on its enrichment for H3K4Me3, H3K27Ac, H3K4Me1 histone marks for seven ENCODE cell lines and PhyloP conservation scores for 100 vertebrates at the UCSC Genome Browser (***I***, Fig. 6). Sequences were collected from different species as described above and processed by a custom shell script in a three step MEME suite analysis (see "Software and data"). First, screens for novel motifs were done by MEME

(Multiple Em for Motif Elicitation), utilizing all three distribution options (-oops, -zoops, -anr) in series, as well as, allowing the size of the discovered motif to increase by a single nucleotide in the range of 6–24. To avoid false-positives, sequences were masked by RepeatMasker (http://www.repeatmasker.org/) and a Markov model background profile was generated by "fasta-get-markov" (part of MEME suite). Then, TomTom was used to match all identified motifs from all distribution/size combinations against JASPAR core 2018 (non-reduncant) database, considering the 9 available function distributions in individual runs. In the third step, PFMs of identified transcription factors were collected and used in a MAST run against the original DNA sequences, with strict settings (-mev 0.0001 -ev 0.0001) filtering the best matches. Graphical representation of the MTSS1 gene, genomic regulatory elements and TFBS coordinates was rendered by the UCSC Genome Browser.

Software and data

All bioinformatics software used for this work was installed on a Slackware (http://www.slackware.com/) GNU/Linux system, almost exclusively from the scripts available at the SlackBuilds.org project (http://slackbuilds.org/). Materials such as custom shell scripts, bed files, sequences, phylogenetic trees and raw data are accessible at our GitHub repository (https://github.com/mattilalab/), a link to which is provided on our web-site (http://mattilalab.utu.fi/).

4.2 *Publication II*

Antibodies and Chemicals

List of antibodies and reagents used in the study can be found in Table 9 (or Table 1 of the original publication).

Mice

MIM knockout mouse strain was a kind gift from Prof. Pekka Lappalainen and Dr. Pirta Hotulainen from the University of Helsinki and Minerva Foundation Institute for Medical Research (Saarikangas et al., 2011). The strain, in C57Bl/6 background, had no apparent health problems until the age of 8 months when mice were last sacrificed; however, we observed that from all genotyped animals that were kept alive, 18 pups developed hydrocephaly over the study period. Among them, 17 were knockout, 1 heterozygote, and 0 wild type. To generate this strain, Saarikangas et al. (Saarikangas et al., 2011) introduced a Neo-cassette, containing several stop codons, by homologous recombination into Exon 1 of *MIM/Mtss1* gene in 129/Sv ES-cells. Chimeric mice were backcrossed to C57Bl/6J background for several generations and the colony in Turku was established by breedings of heterozygote founder animals. All experiments were done with age- and sex-matched animals and WT littermate controls were used whenever possible.

Immunizations

At the age of 3–4 months, groups of WT and $MIM^{-/-}$ females were immunized with NP_{40}-FICOLL (F-1420, Biosearch Technologies) for T-independent (TI) im-

munization or NP_{31}-KLH (N-5060, Biosearch Technologies) for T-dependent (TD) immunization. Each mouse received 50 µg of antigen in 150 µL of PBS (NP_{40}-FICOLL) or PBS/Alum (77161, Thermo Fisher) adjuvant (2:1 ratio) (NP_{31}-KLH) solution by intraperitoneal injection. Blood ($\sim$100 µL) was sampled from lateral saphenous veins on day -1 (preimmunization) and every week after immunization on days +7, +14, +21, and +28 for both FICOLL and KLH cohorts. Secondary immunization of KLH cohort was performed on day +135 (0) and blood was sampled on days +134 (-1), +139 (+4), +143 (+8), and +150 (+15). Coagulated blood was spun at +4°C/2000 rpm for 10 min and serum was collected and stored at -20°C. All animal experiments were approved by the Ethical Committee for Animal Experimentation in Finland. They were done in adherence with the rules and regulations of the Finnish Act on Animal Experimentation (62/2006) and were performed according to the 3R-principle (animal license numbers: 7574/04.10.07/2014, KEK/2014-1407-Mattila, 10727/2018).

ELISA

Total and NP-specific antibody levels were measured by ELISA on half-area 96-well plates (Greiner Bio-One, 675061). Wells were coated overnight at +4°C with capture antibodies (2 µg/mL) or NP-conjugated carrier proteins, $NP_{(1\text{-}9)}$-BSA or $NP_{(>20)}$-BSA (N-5050L, N-5050H, Biosearch Technologies) at 50 µg/mL in 25 µL. Non-specific binding sites were blocked for 2 h in 150 µL of blocking buffer (PBS, 1% BSA, 0.05% NaN_3). Appropriate, experimentally determined dilutions (see below) of 50 µL serum samples in blocking buffer were added for overnight incubation at +4°C. Biotin-conjugated detection antibodies (2 µg/mL) in 50 µL of blocking buffer were added for 1 h followed by 50 µL ExtrAvidin-Alkaline phosphatase (E2636, Sigma-Aldrich, 1:5000 dilution) in blocking buffer for 1 h at room temperature (RT). In between all incubation steps, plates were washed with 150 µL washing buffer (PBS, 0.05% Tween-20) either three times for the steps before sample addition or six times after addition of the mouse sera. The final wash was completed by washing two times with 150 µL of water. Finally, 50 µL of alkaline phosphatase-substrate, SIGMAFAST p-nitrophenyl phosphate (N2770, Sigma-Aldrich) solution was added and OD was measured at 405 nm. Serum dilutions were determined experimentally to fall into the linear part of the dose-response curve of the absorbance measurements for any given isotype and typical values are as follows: IgM levels (1:3000–1:4000), IgG levels (1:20000–1:80000). Different dilutions of AP-streptavidin were used where necessary. Typical time for AP-substrate incubation before measurement was about 30 min at RT. All ELISA samples were run in duplicates, OD values were averaged and blank background was subtracted. Absolute concentrations of total antibody levels were extrapolated from calibration curves prepared by serial dilution of mouse IgM or subclasses of IgG from C57Bl/6 immunoglobulin panel. Relative NP-specific antibody levels were extrapolated from reference curves prepared by serial dilution of pooled serum, in which the highest dilution step received an arbitrary unit of 0.5.

Immunophenotyping

All cells were isolated in B cell isolation buffer (PBS, 2% FCS, 1 mM EDTA). Bone marrow cells were isolated by flushing the buffer through mouse femoral and tibial bones. Splenocytes were isolated by mashing the spleen in small buffer volumes with syringe plunger in 48-well plates. Peritoneal cavity cells were isolated by filling the cavity with ∼10 ml buffer volume through puncture and collecting the fluid back. Cell suspensions were filtered through 70- µM nylon cell strainers. As a general flow cytometry protocol, all subsequent steps were done in flow cytometry buffer I (PBS, 1% BSA). Fc-block was done with 0.5 µL of anti-mouse CD16/32 antibodies in 70 µL of flow cytometry buffer I for 10 min and cells were stained for 30 min Washings were done three times in 150 µL of flow cytometry buffer I. All steps were carried out on ice in U-bottom 96-well plates at a cell density of $0.25–0.5\times10^6$/well. Before acquisition, cells were resuspended in 130 µL of flow cytometry buffer II (PBS, 2.5% FCS). Samples were acquired on BD LSR Fortessa, equipped with four laser lines (405, 488, 561, and 640 nm). Compensation matrix was calculated and applied to samples either in BD FACSDiva® software (BD Biosciences) or in FlowJo (Tree Star, Inc) based on fluorescence of conjugated antibodies using compensation beads (01-1111-41, Thermo Fisher Scientific). FMO (fluorescence minus one) controls were used to assist gating. Data were analyzed with FlowJo software.

B Cell Isolation

Splenic B cells were isolated with EasySep® Mouse B Cell Isolation Kit (19854, STEMCELLS Technologies) according to the manufacturer's instructions and let to recover in RPMI (10% FCS, 20 mM HEPES, 50 µM β-mercaptoethanol, 1:200 Pen/Strep) in an incubator at +37°C and 5% CO_2 for 1–2 h.

Class-Switch Recombination and Proliferation

Isolated splenic B cells ($\sim10–20\times10^6$ cells) were stained first with 5 µL (5 mM) of Cell Trace Violet (C34557, Thermo Fisher Scientific) in 10 ml of PBS for 10 min at RT and let to recover in complete RPMI (+37°C, 5% CO_2) for 1–2 h. To induce class-switching, B cells were cultured in 24-well plates at 0.5×10^6 /mL density in complete RPMI supplemented with indicated doses of LPS (4 µg/mL), CD40L (150 ng/mL), IL-4 (5 ng/mL), IFN-γ (100 ng/mL), and TGF-β (3 ng/mL) for 3 days. Cells were blocked with anti-mouse anti-CD16/32 and stained for 30 min with antibodies against IgG subclasses. Additionally, cells were stained with 4 µg/mL 7-AAD (ABD-17501, Biomol) for live/dead cell discrimination and samples were acquired on BD LSR II equipped with three laser lines (405, 488, and 640 nm) and analyzed with FlowJo software.

BCR Signaling and Immunoblotting

For analysis of BCR signaling, isolated splenic B cells were starved for 10 min in plain RPMI and 0.5×10^6 cells in 100 µL of plain RPMI were stimulated in duplicates with anti-mouse IgM µ-chain-specific (anti-IgM) antibodies, or their $F(ab')_2$ fragments, either in solution or bound to the culture dish surface, for 3, 7, and 15 min For soluble stimulation, 5 µg/mL of anti-IgM was used, in 96-well plates. For surface-bound mode, 48-well plates were coated with 5 µg/mL of anti-IgM antibodies in

120 µL of PBS at +4°C, overnight, and washed three times with 500 µL of ice-cold PBS before experiment. Equimolar concentrations of $F(ab')_2$ fragments were used for soluble stimulations and coating for surface-bound stimulations. After activation, B cells were instantly lysed with 25 µL of 5× SDS lysis buffer (final: 62.5 mM Tris–HCl, pH ∼6.8, 2% SDS, 10% glycerol, 100 mM β-mercaptoethanol, and bromophenol blue) and sonicated for 7.5 min (1.5 ml tubes, high power, 30 s on/off cycle, Bioruptor plus, Diagenode). Lysates (20–30 µL) were run on 8–10% polyacrylamide gels and transferred to PVDF membranes (Trans-Blot Turbo Transfer System, Bio-Rad). Membranes were blocked with 5% BSA in TBS (TBS, pH ∼7.4) for 1 h and incubated with primary antibodies (typically ∼1:1000) in 5% BSA in TBST (TBS, 0.05% Tween-20) at +4°C, overnight. Secondary antibody incubations (1:20000) were done for 2 h at RT in 5% milk in TBST for HRP-conjugated antibodies and with addition of 0.01% SDS for fluorescently conjugated antibodies. Washing steps were done in 10 ml of TBST for 5 × 5 min Membranes were scanned with Odyssey CLx (LI-COR) or visualized with Immobilon Western Chemiluminescent HRP Substrate (WBKLS0500, Millipore) and ChemiDoc MP Imaging System (Bio-Rad). Phospho-antibodies were stripped in 25 mM glycine-HCl buffer, pH ∼2.5, for 10 min, and membranes were blocked and probed again for evaluation of total protein levels. Images were background-subtracted and the raw integrated densities for each band were measured in ImageJ. Ratios of phosphorylated-vs-total protein levels were analyzed with ratio paired t-test. For data presentation, these ratios were normalized to WT value at 0 min

Intracellular Ca^{2+} Flux

Splenic B cells were resuspended at a concentration of $2.5–5\times10^6$ cell/mL in RPMI supplemented with 20 mM HEPES and 2.5% FCS and loaded with 1 µM Fluo-4 (F14201, Thermo Fisher Scientific) and 3 µM Fura Red (F3021, Thermo Fisher Scientific) for 45 min (+37°C, 5% CO_2). Cell suspension was diluted in 10 volumes of complete RPMI and incubated for 10–15 min at RT. Cells were centrifuged at 200 g, RT for 5 min and resuspended at 2.5×10^6 cells/mL in PBS supplemented with 20 mM HEPES, 5 mM glucose, 0.025% BSA, 1 mM $CaCl_2$, 0.25 mM sulfinpyrazone (S9509, Sigma-Aldrich), and 2.5% FCS. Cells were allowed to rest at RT for 20 min and were kept on ice before acquisition. Anti-IgM antibodies were added into pre-warmed (+37°C, 5 min) B cell suspension aliquots to final concentrations of 10, 5, 2.5, and 1 µg/mL and samples were acquired on BD LSR Fortessa. Alternatively, equimolar concentrations of anti-IgM $F(ab')_2$ fragment were used. Fluorescence of Fluo-4 and Fura Red were recorded by a continuous flow for 5 min Data were analyzed in FlowJo and presented as ratiometric measurement of Fluo-4/Fura Red median intensity levels. Peritoneal cavity B cells were washed with L-15 medium, resuspended in 75 µL acquisition buffer [HBS (HEPES buffered saline):L-15 (1:1 ratio), 2.5 µM probenecid (P8761, Sigma-Aldrich)] and labeled by addition of 75 µL of acquisition buffer with 10 µM Fluo-4 for 5 min at +37°C. Cells were washed in 1 ml, resuspended in 200 µL and divided into two wells. B cells were prestained for

10 min on ice with anti-CD23-Alexa Fluor (AF)-594 antibodies, washed and resuspended in 100 µL of acquisition buffer on ice. Samples were prewarmed (+37°C) in a total volume of 300 µL of acquisition buffer and 50 µL of anti-IgM F(ab')$_2$-AF633 were added. Cells were acquired on a BD LSR Fortessa for 3–5 min and analyzed in FlowJo.

Scanning Electron Microscopy

For the analysis of resting B cells, wells of the microscope slides (10028210, Thermo Fisher Scientific) were coated with CellTak (354240, Corning) in PBS (3.5 µg/cm^2 of surface area, according to manufacturer's recommendations) for 20 min (RT), washed once with water and allowed to dry. For the analysis of activated B cells, wells were coated with 5 µg/mL of anti-IgM in PBS for 1 h (RT) and washed in PBS. 10^5 B cells in 20 µL of complete RPMI were placed on coated wells for 10 min (+37°C, 5% CO_2) and fixed by adding 20 µL PFA in PBS (4% PFA final, pH 7.0–7.5) for 15 min Samples were further fixed in 4% PFA/2.5% gluteraldehyde in PBS for 30 min, washed in PBS and post-fixed in 1% OsO_4 containing 1.5% potassium ferrocyanide, and dehydrated with a series of increasing ethanol concentrations (30, 50, 70, 80, 90, 96, and twice 100%). Specimens were immersed in hexamethyldisilazane and left to dry by solvent evaporation. The cells were coated with carbon using Emscope TB 500 Temcarb carbon evaporator and imaged with Leo 1530 Gemini scanning electron microscope.

Immunofluorescence Microscopy and Cell Spreading

TIRF Microscopy

MatTek microscopy dishes were coated with 7.5 µg/mL of anti-IgM antibodies in PBS at +37°C for 30 min and washed once with PBS. Isolated splenic B cells (10^6) were left unstained or labeled with 0.17 µL of anti-B220-AF647 antibodies in 400 µL PBS for 10 min in 1.5 ml tubes on ice, spun (2500 rpm, 5 min), washed twice in 900 µL of ice-cold PBS and resuspended in 200 µL of Imaging buffer (PBS, 10% FBS, 5.5 mM D-glucose, 0.5 mM $CaCl_2$, and 0.2 mM $MgCl_2$). Equal amounts of unstained and labeled cells of different genotypes were mixed and loaded onto coated MatTek dishes at 35 µL/well. Cells were incubated for 10 min (+37°C, 5% CO_2), fixed in prewarmed (+37°C) 4% formaldehyde/PBS for 10 min (RT), permeabilized in 0.1% Triton X-100/PBS for 5 min (RT), washed once with PBS, and blocked in blocking buffer (PBS, 1% BSA) at +4°C (overnight). Cells were stained with 1:50 Phalloidin-AF555 and 1:500 anti-pTyr primary antibody (4G10) in blocking buffer for 1 h (RT), washed four times with PBS, and stained with 1:500 secondary anti-mouse IgG2b-AF488 in blocking buffer for 1 h (RT), washed four times in PBS, and imaged in PBS with total internal reflection fluorescence (TIRF) mode in DeltaVision OMX Imaging System (GE Healthcare). TIRF images of cortical actin and pTyr were processed with ImageJ macro using B220 and bright-field channels to discriminate between attached WT or MIM-KO cells. Spreading area (determined on pTyr channel), mean fluorescence intensity, and total fluorescence intensity (integrated density) of phalloidin and pTyr stainings of each cell were analyzed (∼50–340 cells per sam-

ple). For cumulative scatter plots, equal numbers (here 92 cells) were randomly selected from each experiment.

Spinning Disk Confocal Microscopy

Twelve-well PTFE diagnostic slides (Thermo Fisher Scientific, #10028210) were coated with 5 µg/mL anti-mouse IgM (µ-chain-specific antibodies) in PBS at +4°C O/N and washed with PBS. As a non-activated control, wells were coated with 4 µg/mL fibronectin. Isolated splenic B cells (10^6/mL) were labeled with 1 µM CFSE (21888, Sigma-Aldrich) or left unlabeled. Equal amounts of unstained and labeled cells of different genotypes were mixed (1:1 ratio) and seeded at a density of 100000 cells/well. Dye-switched experiments were performed systematically. Cells were incubated for 3, 5, 7, 10, or 15 min (+37°C, 5% CO_2), fixed in 4% formaldehyde/PBS for 10 min (RT), and permeabilized/blocked in 0.3% Triton X-100/5% donkey serum/ PBS for 20 min (RT). Staining was performed in 0.3% Triton X-100/1%BSA/ PBS at +4°C O/N, followed by washes with PBS and incubation with the secondary antibodies for 30 min at room temperature in PBS. Samples were mounted in FluoroMount-G (Thermo Fisher Scientific). Images were acquired on 3i CSU-W1 (Intelligent Imaging Innovations) Marianas spinning disk confocal microscope equipped with 63× Zeiss Plan-Apochromat objective and a Photometrics Prime BSI sCMOS camera. Cells were visualized at the plane of contact and 5–10 fields of view per sample were acquired. Images of F-actin, pBtk, and pSyk were processed with ImageJ using CTV channel to discriminate between WT or MIM-KO cells. Spreading area (determined on the phalloidin channel) and mean fluorescence intensity of pBtk or pSyk staining per cell were analyzed (∼25–150 cells per condition per experiment).

Supported Lipid Bilayers

Artificial planar lipid bilayers containing GPI-linked mouse ICAM-1 (200 molecules/ μM^2) were formed as previously described (Grakoui et al., 1999; Carrasco et al., 2004). Briefly, unlabeled GPI-linked ICAM-1 liposomes and liposomes containing biotinylated lipids were mixed with 1,2-dioleoyl-PC (DOPC) (850375P, Avanti lipids, Inc) at various ratios to obtain the specified molecular densities. Planar membranes were assembled on FCS2 dosed chambers (Bioptechs) and blocked with PBS/2% FCS for 1 h at RT. Antigen was tethered by incubating membranes with AF647-streptavidin, followed by monobiotinylated anti-kappa light chain antibodies (20 molecules/ μM^2). The isolated B cells from WT and $MIM^{-/-}$ mice were labeled with 1 µM CFSE (21888, Sigma-Aldrich) or left unlabeled, mixed at 1:1 ratio, and injected into prewarmed chambers (4×10^6 cells/chamber, +37°C) with 100 nM recombinant murine CXCL13. Fluorescence, differential interference contrast (DIC), and interference reflection microscopy (IRM) images were acquired at the plane of the cell contact in one position once every 30 s immediately after injecting the cells into the chamber for 10 min After the 10-min movie was recorded, several snapshots were acquired for quantification of the mature synapses in different locations of the chamber at 10–15 min after cell injection. All assays were performed in PBS, supplemented with 0.5% FCS, 0.5 g/L D-glucose, 2 mM $MgCl_2$, and 0.5 mM

$CaCl_2$. Images were acquired on a Zeiss Axiovert LSM 510-META inverted microscope, equipped with 40× oil-immersion objective (Madrid), or a Zeiss LSM 780 inverted microscope, equipped with 40× water-immersion objective (Turku), and analyzed in ImageJ. The spreading area (determined on IRM channel), area of collected antigen, and mean fluorescence intensity of antigen were quantified from each experiment (∼100 cells per experiment).

Intracellular Ca^{2+} Flux on Supported Lipid Bilayers

Splenic WT or $MIM^{-/-}$ B cells (3.2×10^6) were resuspended in 75 µL of L-15 medium and labeled by addition of 75 µL of HBS (HEPES buffered saline), supplemented with 2.5 µM probenecid and 20 µM Fluo4 for 5 min at +37°C. Cells were washed in 1 ml of HBS-probenecid and resuspended in 500 µL of HBS-probenecid for immediate injection into FCS2 chambers. Acquired movies were preprocessed in ImageJ and analyzed with a MATLAB-implemented high-throughput software *CalQuo*^{2} (Lee et al., 2017). Cells were categorized as single peak, oscillatory, or not triggering. Cells showing more than two intensity peaks are classified as oscillatory. Data presented as mean percentages of three independent experiments with at least 1000 cells analyzed per experiment.

Metabolic Assay

Splenic B cells were seeded at a density of 10^6 cells/mL in complete RPMI and treated with the indicated combinations of IL-4 (10 ng/mL), anti-mouse IgM (10 µg/mL), LPS (4 µg/mL), and CpG (10 µg/mL) for 24 h at +37°C, 5% CO_2 in a humidified incubator. Cells were then spun and resuspended in Seahorse XF RPMI (103576-100, Agilent), supplemented with 1 mM pyruvate, 2 mM L-glutamine, and 10 mM D-glucose. Cell number was adjusted and 0.15×10^6 cells were seeded per well on a 96-well XF plate, pre-coated with CellTak (354240, Corning). Plate coating was done with 22.4 µg/mL CellTak in $NaHCO_3$, pH 8.0, at +4°C overnight, followed by two washings with water. Seeded cells were spun at 200 g for 1 min with no brake and left for 1 h at 37°C to attach to coated wells in a humidified incubator without CO_2 to avoid medium acidification. Seahorse XF96 plate (101085-004, Agilent) was used following the manufacturer's instructions for XF Cell Mito Stress Test Kit (103015-100, Agilent). In this test, sequentially, 1 µM oligomycin, 2 µM FCCP, and 0.5 µM rotenone/antimycin A were added to the media. Oxygen consumption rate (OCR) and extracellular acidification rate (ECAR) data were recorded by WAVE software (Agilent). OCR and ECAR data were normalized to cell count and first baseline measurement of WT cells. Basal, maximum, and spare respiratory capacities were extracted with area under curve analysis in GraphPad Prism.

Analysis of Mitochondria

For TMRE staining, B cells were washed in 150 µL PBS, stained with 1:500 Zombie Violet for dead cell discrimination in PBS on ice, washed 2 × 100 µL with complete RPMI, and stained with 5 nM TMRE (T669, Thermo Fisher Scientific) in 200 µL of complete RPMI at RT for 20 min Resuspended in 150 µL of complete RPMI, cells were immediately analyzed by flow cytometry, on BD LSR Fortessa. For

Tom20 staining, B cells were stained with Zombie Violet as described above, fixed with 1.6% formaldehyde in PBS for 10 min, washed 2 × 150 µL PBS, permeabilized with 0.1% Triton X-100 in PBS for 5 min at RT, and blocked for 1 h at RT. Incubation with primary Tom20 antibodies was done at 1:500 dilution for 30 min, followed by 3 × 150 µL washes, staining with 1:1000 dilution of anti-rabbit-AF488 secondary antibodies, and 3 × 150 µL washes. Cells were then resuspended in 130 µL and analyzed by flow cytometry, on BD LSR Fortessa. Antibody incubations, blocking, and washings were done in flow cytometry buffer I on ice. Geometric mean fluorescence intensities were extracted with FlowJo software.

Statistics and Data Presentation

Statistical analysis was performed in GraphPad Prism. Student's t-test was applied to the data comparing WT and MIM-KO groups. Antibody titers and microscopy data were analyzed with unpaired two-tailed t-test unless otherwise stated. Additionally, for TIRF microscopy datasets, geometric means were extracted for each biological replicate and means were analyzed by ratio paired t-test. In all other experiments, where pairing of WT and MIM-KO data was based on the day of the experiment, ratio paired t-test was also applied. Multiple-measures two-way ANOVA was additionally used to compare the antibody responses upon immunization. Data are presented as mean ± SEM, unless stated otherwise. Significance is denoted as *p < 0.05, **p < 0.01, ***p < 0.001, ****p < 0.0001. Inkscape and Adobe Illustrator were used for figure assembly, and Biorender was used to generate schematic figures.

Table 9. MIM reagents

Name	Catalog	Company	Application
AffiniPure Donkey Anti-Mouse IgM, μ Chain Specific	715-005-020	Jackson ImmunoResearch	Stimulatory antibodiies, ELISA, capture antibody
AF647 AffiniPure F(ab')2 Fragment Donkey Anti-mouse IgM	715-606-020	Jackson ImmunoResearch	Stimulatory antibodies
Monobiotinylated Purified Rat anti-mouse Ig κ light chain	559749 or 21343	BD Biosciences or Thermo Fisher Scientific	Stimulatory antibodies
Purified Rat Anti-Mouse IgM - Clone II/41 (RUO)	553435	BD Biosciences	ELISA, capture antibody
AffiniPure Goat Anti-Mouse IgG, Fcγ Fragment Specific	115-005-071	Jackson ImmunoResearch	ELISA, capture antibody
Goat Anti-Mouse IgG1-BIOT	1071-08	SouthernBiotech	ELISA, detection antibody
Goat Anti-Mouse IgG2b-BIOT	1091-08	SouthernBiotech	ELISA, detection antibody
Goat Anti-Mouse IgG2c-BIOT	1078-08	SouthernBiotech	ELISA, detection antibody
Goat Anti-Mouse IgG3, Human/Bovine/Horse SP ads-BIOT	1103-08	SouthernBiotech	ELISA, detection antibody
Goat Anti-Mouse IgG Fc-BIOT	1033-08	SouthernBiotech	ELISA, detection antibody

Table 9. MIM reagents

Name	Catalog	Company	Application
Biotin Rat Anti-Mouse IgM, Clone R6-60.2 (RUO)	553406	BD Biosciences	ELISA, detection antibody
C57BL/6 Mouse Immunoglobulin Panel	5300-01B	SouthernBiotech	ELISA, standard
Purified Rat Anti-Mouse CD16/CD32	553142	BD Biosciences	Flow cytometry, Fc-block
FITC Rat Anti-Mouse IgG1	553443	BD Biosciences	Flow cytometry, CSR
FITC Rat Anti-Mouse IgG2b	553395	BD Biosciences	Flow cytometry, CSR
FITC Rat Anti-Mouse IgG3	553403	BD Biosciences	Flow cytometry, CSR
AffiniPure Goat anti-Mouse IgG2c, FITC-conjugated	115-095-208	Jackson ImmunoResearch	Flow cytometry, CSR
LPS, Lipopolysaccharides from Escherichia coli	L2887-5MG	Sigma-Aldrich	CSR, Metabolism
CpG ODN 1826	tlrl-1826	Invivogen	Metabolism
CD40L, Recombinant Mouse CD40 Ligand/TNFSF5 (HA-tag)	8230-CL-050	RD Systems	CSR
IL-4, Recombinant Mouse IL-4	404-ML-010	RD Systems	CSR, Metabolism
IFNγ, Recombinant Mouse IFNγ	575304	BioLegend	CSR
TGF-β, Recombinant Mouse TGF-beta 1	7666-MB-005	RD Systems	CSR
BD Horizon™ V450 Rat Anti-Mouse IgM Clone R6-60.2	560575	BD Biosciences	Flow cytometry
AF488 anti-mouse IgD [11-26c.2a]	405718	Biolegend	Flow cytometry
AF700 anti-mouse CD19 [6D5]	115528	Biolegend	Flow cytometry
APC anti-mouse CD19 [6D5]	115512	Biolegend	Flow cytometry
APC/Cy7 anti-mouse/human CD45R/B220 [RA3-6B2]	103224	Biolegend	Flow cytometry
APC anti-mouse CD21/CD35 (CR2/CR1) [7E9]	123412	Biolegend	Flow cytometry
Alexa Fluor™ 594 anti-mouse CD23 [B3B4]	101628	Biolegend	Flow cytometry
PE anti-mouse CD93 (AA4.1, early B lineage) [AA4.1]	136503	Biolegend	Flow cytometry
PE anti-mouse CD3e [145-2C11]	100308	Biolegend	Flow cytometry
FITC anti-mouse CD4 [GK1.5]	100406	Biolegend	Flow cytometry
APC anti-mouse CD5 [53-7.3]	100626	Biolegend	Flow cytometry
Tom20 (FL-145)	sc-11415	Santa Cruz Biotechnology	Flow cytometry, metabolism
Goat anti-Rabbit IgG (H+L), AF488	A-11008	Thermo Fisher Scientific	Flow cytometry, metabolism
MTSS1 (P549) Ab	4385S	Cell Signaling Technologies	Immunoblotting
MTSS1 (N747) Ab	4386S	Cell Signaling Technologies	Immunoblotting

Table 9. MIM reagents

Name	Catalog	Company	Application
Phospho-Zap-70 (Tyr319)/Syk (Tyr352) Ab	2701P	Cell Signaling Technologies	Immunoblotting
Syk (D3Z1E) XP™ Rabbit mAb	13198S	Cell Signaling Technologies	Immunoblotting
Phospho-Lyn (Tyr507) Ab	2731P	Cell Signaling Technologies	Immunoblotting
Lyn (C13F9) rabbit mAb	2796S	Cell Signaling Technologies	Immunoblotting
Phospho-CD19 (Tyr531) Ab	3571S	Cell Signaling Technologies	Immunoblotting
CD19 Ab	3574S	Cell Signaling Technologies	Immunoblotting
Phospho-PI3 Kinase p85 (Tyr458)/p55 (Tyr199) Ab	4228S	Cell Signaling Technologies	Immunoblotting
Phospho-CD19 (Tyr531) Ab	3571S	Cell Signaling Technologies	Immunoblotting
Phospho-Akt (Ser473) (193H12) Rabbit mAb	4058S	Cell Signaling Technologies	Immunoblotting
Akt1 (C73H10) Rabbit mAb	2938S	Cell Signaling Technologies	Immunoblotting
Phospho-NF-kappa-B p65 (Ser536) (93H1) Rabbit mAb	3033S	Cell Signaling Technologies	Immunoblotting
NF-κB p65 (D14E12) XP™ Rabbit mAb	8242S	Cell Signaling Technologies	Immunoblotting
p44/42 MAPK (Erk1/2) Ab	9102S	Cell Signaling Technologies	Immunoblotting
Phospho-p44/42 MAPK (Erk1/2) (Thr202/Tyr204) Ab	9101S	Cell Signaling Technologies	Immunoblotting
Phospho-Btk (Tyr223) (D1D2Z) Rabbit mAb	87457	Cell Signaling Technologies	Immunoblotting
Peroxidase AffiniPure Goat Anti-Rabbit IgG (H+L)	111-035-144	Jackson ImmunoResearch	Immunoblotting
Peroxidase AffiniPure Goat Anti-Mouse IgG, Fcγ-Specific Ab	115-035-071	Jackson ImmunoResearch	Immunoblotting
Donkey Anti-Rabbit IgG Ab, IRDye 800CW Conjugated	926-32213	LI-COR Biosciences	Immunoblotting
AF555 Phalloidin	A34055	Thermo Fisher Scientific	Microscopy
AF647 anti-mouse/human CD45R/B220 Ab	103229	BioLegend	Microscopy
Anti-Phosphotyrosine Ab, clone 4G10™	05-321	Merck Miilipore	Microscopy
Goat anti-Mouse IgG2b, AF488 conjugate	A-21141	Thermo Fisher Scientific	Microscopy
CXCL13	250-24-5ug	PeproTech	Microscopy, SLB

4.3 *Publication III*

Generation of IRF4KO B cells

The IRF4 gene was inactivated by targeting constructs, which removed the second and third exon in IRF4KO1 and IRF4KO2. In IRF4KO2 exon 4 and part of exon 5 were additionally deleted in one of three IRF4 alleles. Start codon in the second exon was changed to stop codon in all of the targeting constructs. The 1 kb left arm was amplified from the WT DT40 cell line by PCR using primers: C-LF (GGGCGCGGCCGCCTCCATCATATAAAGAAACT) and C-LR (ACTCACCCGGATCCAAGTTCTAGCCACTCTTA). The PCR product was digested with NotI and BamHI. The 1.2-kb right arm was amplified with C-RF (AGTGTACAGAATAGTGCCAGAAGGAGCTCAAAAAG) and C-RR (CTCATGGGGCACCATGTAGTTGGGTACCTATT) and digested with EcoRI and Acc65I. The alternative 1.8-kb right arm used in IRF4KO2 was amplified with C-RF2 (CGGATCCTGATATCCCCTACCAGTGTG) and C-RR2 (CTCAGGAGGGGCTCGAGCATAAAAGGTTC) and digested with BamHI and XhoI. The digested arms were cloned into pBluescript vector. The floxed bsr and neo selection cassettes from pLoxBSR and pLoxNeo vectors (Arakawa et al., 2001) and HisD selection were transferred as BamHI fragments to the targeting vectors between homologous arms. Targeting vectors were linearized with NotI and introduced into DT40 B cells by electroporation using 710 V and 25 µF. The clones were selected in the presence of 30 µg/mL blasticidin, 2 mg/mL G418 or 1 mg/mL L-histidinol dihydrochloride. The deletion of IRF4 exon 2 and 3 was verified by genomic PCR (***III***, Fig. 1C) with primers p1 (CTGGTGTGGGAGAATGACGAGAAGAGCATC) and p2 (CTCTTGTTCAAAGCACACCTCAATCTGGTC). The loss of IRF4 expression was confirmed by western blotting with anti-IRF4 Ab (***III***, Fig. 1D).

Re-expression of IRF4 in IRF4KO cells

Chicken IRF4 was amplified from WT DT40 cDNA using primers IRF4-f (TATAAGCTTATGAACTTGGAGCCGGGTGA) and IRF4-r (TTAGCTAGCGGATCTTATTCTTGAATAGAGGAATGG), which created HindIII and NheI sites in PCR product, respectively. After digestion, PCR product was cloned between HindIII and NheI sites of the pExpress vector (Arakawa et al., 2001), and then, the Puro selection cassette was inserted into XhoI site. The resulting plasmid was sequenced and linearized with NotI and transfected to IRF4KO cells with electroporation (710 V and 25 µF). Transfectant clones were selected in the presence of 0.5 µg/mL puromycin, and IRF4 expression within selected clones was verified by western blotting with anti-IRF4 Ab (***III***, Fig. 1D).

Cells and antibodies

The chicken DT40 cell line was described previously (Buerstedde and Takeda, 1991). WT and mutant chicken DT40 B cells were maintained in RPMI 1640 (Sigma-Aldrich, St. Louis, MO, USA) supplemented with 10% fetal calf serum (GE, Logan, UT, USA), 1% chicken serum (BioWest, Nuaillé, France), 50 µM β-mercaptoethanol, 2 mM L-glutamine, penicillin and streptomycin in a humidified atmosphere with 5% CO_2 at +40°C. Anti-BCAP Ab (Okada et al., 2000), anti-PLCγ2 Ab, anti-BLNK Ab (Ishiai et al., 1999) and anti-Syk Ab (Takata et al., 1994) were described pre-

viously. The anti-pSYK Y525/526 Ab (#2711), anti-pERK 1/2 mAb (#4370), anti-ERK1/2 (137F5) mAb (#4695), anti-pPI3K p85 (Tyr458)/p55 (Tyr199) Ab (#4228), anti-pAkt S473 Ab (#9271) and anti-Akt Ab (#9272) were purchased from Cell Signaling Technology, Danvers, MA, USA. Anti-IRF4 (M-17) Ab (sc-6059) and anti-pY mAb (PY99) (sc-7020) were from Santa Cruz Biotechnology, Dallas, TX, USA. Anti-chicken IgM-RPE (clone M-1) and anti-chicken IgM (clone M-4) were from Southern Biotechnology Associates Inc., Birmingham, AL, USA. Phalloidin-Alexa 568 (A12380) and anti-mouse IgG2b-Alexa-633 (A21146) were from Life Technologies, Carlsbad, CA, USA.

Gene expression array

Total RNA was prepared from 5×10^6 cells of three independent cultures of WT and IRF4KO cells with RNeasy Mini Kit (Qiagen, Valencia, CA, USA) with RNase-free DNase (Qiagen, Valencia, CA, USA) treatment according to manufacturer's instructions. Two hundred nanograms of total RNA was amplified and Cy3-labeled with Agilent's Low Input Quick Amp Labeling kit (one-color) and hybridized onto Agilent's 4×44K Chicken V2 chip according to manufacturer's instructions. Arrays were scanned with Agilent Technologies Scanner and numerical results extracted with Feature Extraction version 10.7.1. The data were analysed using R/Bioconductor tool (Bioconductor version 2.7, R version 2.12.0). The data were quantile normalized and a comprehensive quality analysis was performed to ensure the validity of the data. Minimum Pearson correlation value between replicate samples was 0.982 indicating good reproducibility within the experiment. Statistical testing was carried out using limma package and false-discovery rate below 0.05 and an absolute fold change above 2 was required for filtering the differentially expressed genes. Further functional analysis was performed with Ingenuity Pathway Analysis (Ingenuity Systems, www.ingenuity.com). The microarray data have been deposited in the NCBI Gene Expression Omnibus and are accessible through GEO accession number GSE56165.

Immunoprecipitation and western blotting

For immunoprecipitations and western blot analysis, unstimulated and stimulated cells were starved in PBS for 10 min at +40°C and then stimulated with 4 μg/mL mAb M4 for indicated times (1, 3, 10 or 15 min). The samples for immunoprecipitations with anti-BLNK and anti-PLCγ2 antibodies, and whole-cell lysates for western blot analysis were prepared as previously described (Alinikula et al., 2010, 2011). Western blots probed with anti-Syk or anti-pSyk were analyzed with the Odyssey FC system (Li-Cor Biosciences, Lincoln, NE, USA).

Calcium measurements and flow cytometry

The calcium measurements in DT40 cells were performed as described in (Stork et al., 2004). Cells were loaded with 1 μM Fluo4 AM (Life Technologies, Carlsbad, CA, USA) with 0.015% pluronic F-127 and stimulated with 1 μg/mL M4 Ab. Changes in the fluorescence intensity were monitored using a FACS Calibur cytometer (BD, Franklin Lakes, NJ, USA). The equal loading of samples was controlled by treatment with 100 nM ionomycin (Sigma-Aldrich, St. Louis, MO, USA). The

kinetics overlay was performed with FlowJo software (version 9.7.1; FlowJo LLC, Ashland, OR, USA). The sIgM staining was performed with anti-chicken IgM-RPE mAb (clone M-1).

Microscopy

For confocal and TIRF microscopy multiwell microscope slides or chambered coverslips, respectively, were coated with 5 µg/mL anti-chicken IgM (M4) in PBS. Cells in imaging buffer (PBS, 0.5 mM $CaCl_2$, 2 mM $MgCl_2$, 1 g/L D-glucose, 0.5% FCS) were let to settle on slides for 20 min at 37°C in CO_2 incubator and fixed in 4% formaldehyde. Fixed cells were permeabilized with 0.1% Triton X-100 in PBS for 5 min and stained with Phalloidin-Alexa-568. Samples were mounted in Fluoromount-G for confocal or PBS for TIRF microscopy. Confocal images were acquired using Zeiss LSM510, equipped with Plan-Apochromat
63×/1.40 Oil DIC M27 objective, or Zeiss TIRF microscope, equipped with alpha Plan-Apochromat 100×/1.46 Oil DIC (UV) objective and ORCA-Flash 4.0 CMOS digital camera (Hamamatsu, Hamamatsu City, Japan) (Cell Imaging Core, Turku Centre for Biotechnology). Data processing and analysis were performed in FIJI (http://fiji.sc/Fiji). For quantification of F-actin intensity, binary images were generated with blind manual thresholding to create regions of interest (ROI) corresponding to F-actin staining area of the cells. The intensity within ROIs was measured from 17 to 21 cells per condition. Statistical analysis was performed with two-tailed Student's t-test.

RT-PCR analysis

Total RNA was extracted from the cell lines with RNeasy Mini Kit (Qiagen, Valencia, USA) with RNase-free DNase treatment. Poly-A RNA was reverse transcribed from total RNA using First-strand cDNA Synthesis Kit for RT-PCR (Roche, Basel, Switzerland). Quantitative real-time PCR analysis was performed using Light Cycler FastStart DNA Master SYBR Green I Kit with Light Cycler equipment (Roche, Basel, Switzerland). The magnesium concentration and annealing temperature were optimized for each primer pair. The data are from two technical replicates. WT expression level was used as an average (±SD) of at least three biological replicates with standard giving the value of 1. The expression levels of individual genes were normalized to GAPDH expression for each cDNA sample. The obtained results were analyzed with Biogazelle qbase PLUS 2.4 software (Biogazelle, Zwijnaarde, Belgium) and for statistical analysis was used Student's t-test was used. The following primers were used: GAPDH (forward GAGGTGCTGCCCAGAACATCATC, reverse CCCGCATCAAAGGTGGAGGAAT) and SHIP (forward GGAGTCAGGACCACCTGCCACCTG, reverse TCTTTCCGTGAGGCCTTGGGGTAGT).

Chromatin immunoprecipitation (ChIP)

ChIP assay was performed as described in (Alinikula et al., 2010). Chromatin was immunoprecipitated with polyclonal goat Ab against IRF4 (M-17, Santa Cruz Biotechnology, Dallas, TX, USA) and irrelevant polyclonal goat Ab as a control (IgG). The promoter region of INNP5D was amplified with primers SHIP-f (GTGT-

CATGCTCGCTCTCTGAGCTG) and SHIP-r (ATCCATGGCTGCAGCTGGAGGA-AAC). The PCR products were quantified from agarose gel with Image Studio Lite program (Li-Cor Biosciences, Lincoln, NE, USA), and binding of IRF4 and non-specific antibody to INNP5D promoter region was calculated as % of input DNA. The result was calculated from three biological replicates.

5 Results and discussion

5.1 Computational analysis of MIM/MTSS1 (*Publication I*)

5.1.1 Novel short functional motifs and features in MIM protein sequence

To collect the data that can provide new insights into biological function of MIM we started by reviewing MIM amino acid sequence structure and current state of the MIM protein annotation in the public online databases. In addition to previously described protein domains and regions (Machesky and Johnston, 2007), we observed a short ∼13 aa, highly hydrophilic sequence in the center of the protein (431–444 aa) as well as a relatively short Ser/Thr-rich (443–453 and 462–476 aa) and a Leu-rich region (480–503 aa) residing C-terminal from it (***I***, Fig. 1a). The score values for disordered protein structures predicted by the IUPred2A (Erdős and Dosztányi, 2020) server are increasing from N- to the C-terminal part of the protein. The high-score regions cover most of the proline-rich region (PRR) (630–730 aa) and sequence following the serine-rich region (SRR) (420–480 aa). In addition, two smaller regions with a moderate score occupy the center of the protein (285–300 and 330–360 aa) (***I***, Fig. 1a and data not shown).

The search for possible functional sites in the Eukaryotic Linear Motif (ELM) resource revealed multiple short functional motifs inside MIM sequence. Although, many of them have been reported previously (Glassmann et al., 2007), we turned our attention to functional sequences, which would be in line with the described role of MIM in regulation of actin and membrane remodeling. We found that MIM contains several sites for clathrin-adaptor proteins, AP2α and APμ, key regulators of endocytosis (Heilker et al., 1999). In the I-BAR domain, these also overlap with a LC3-interacting motif (LIR) to bind ATG8 involved in autophagy (Johansen and Lamark, 2011). I-BAR domain analysis of surface hydrophobicity and electrostatic potential suggest that unlike AP2α, APμ is better suited to serve as a site for protein-protein interaction (***I***, Fig. 1a, d, e). Another interesting finding was detection of a "C-helix" motif (483–491 aa) in the leucine-rich region (***I***, Fig. 1b). This motif is found in actin nucleation promoting factors, such as WASP and N-WASP, and is in these proteins responsible for their autoinhibition due to interaction with GTPase-binding domains (GBD) (Okrut et al., 2015). A full list of identified motifs is provided in the ***I***, Table 1.

Analysis of MIM sequences from chicken (*Gallus gallus*), lizard (*Anolis carolinensis*) and black-spotted gar (*Lepisosteus oculatus*) revealed that the overall protein topology of MIM in birds, reptiles and fish, respectively, is very similar to that of human and mouse, underlining a high degree of conservation (***I***, Fig. 1c).

Based on all of the collected orthologous sequences (***I***, Table S2, Fig. 2), we generated a structure conservation plot mapped onto the crystal structure of the mouse I-BAR domain, which is 98.9% identical to the human MIM I-BAR (Lee et al., 2007; Ashkenazy et al., 2016). This analysis has also confirmed a high degree of sequence conservation (***I***, Fig. 1d). Despite the highly conserved sequence, a small 4 amino acid-long variable part (154–157 aa) clearly stood out from the rest of the I-BAR domain, corresponding to the exon 7 found in the long transcript of the human MIM. Several other variable amino acid positions were found in the central part and in the NES motif of the I-BAR domain.

5.1.2 Evolutionary analysis of MIM

To evaluate the overall evolutionary conservation of MIM and evolutionary relations of its orthologues, we performed homology searches for MIM against publicly available databases at NCBI and identified orthologs in mammals (52), birds (24), reptiles (10) and fish (8) (***I***, Table S2). Phylogenetic analysis revealed that overall ω values were distinctly low (typically $\omega < 0.1$, with the highest $\omega \sim 0.6$), suggesting that negative (purifying) selection has operated across branches (***I***, Fig. 2).

Analysis of evolutionary selection in mammals, confirmed that MIM has been subjected to a broad negative selection with positively selected sites (**pervasive** or *episodic* selection) identified in the Ser-rich region (**Y357**, *T368*, *A395*), small Ser/Thr regions (**T447**, **A449**, **T471**) and in the Pro-rich region (*Q715* and **I716**) (***I***, Fig. 3).

5.1.3 Intra-molecular co-evolution and polymorphisms

Molecular interactions are functionally important and contacting positions in interacting proteins or inside one protein can have correlated patterns of sequence evolution (Avila-Herrera and Pollard, 2015).

Intra-molecular co-evolution was detected between amino acids in the Pro-rich region (631–728 aa), the middle of the Ser-rich region (333–412 aa), and its adjacent small hydrophilic patch and the small Ser/Thr region (430–454 aa). Only four residues in the I-BAR domain showed high co-dependence and co-evolved with several sites at various MIM locations. These 4 residues mostly correspond to the exon 7 mentioned above. Whereas the majority of the co-evolving amino acids was detected between different parts of MIM, co-dependence within the same domain have been detected only in the proline-rich region (***I***, Fig. 4a).

Single nucleotide polymorphisms also provide insights into the possible functional significance of the protein sequence. We examined the distribution of SNPs in

the protein-coding regions of *MTSS1*. According to the PolyPhen scores, which classify SNPs as "benign" and "possibly/probably damaging" (Adzhubei et al., 2010), MIM sequence contains fewer annotations with amino acid changes classified as non-pathogenic ("benign" by PolyPhen) (∼38%) than the pathogenic ("possibly/probably damaging") ones (∼62%) (***I***, Fig. 4b). However, distribution of the pathogenic polymorphisms across the MIM sequence was nonuniform and a low frequency of them was observed in the second part of the Ser-rich region, small hydrophilic and Ser/Thr-rech regions and for the most part of the Pro-rich region (***I***, Fig. 4b). These regions were found to overlap with those marked by strong intra-molecular co-evolution (***I***, Fig. 4a, d).

Although, MIM expression was suggested to modify cancer behavior, no cancer-specific mutations in MIM have been identified to date. Our analysis of MIM mutations across TCGA cancer samples in cBioPortal (Gao et al., 2013; Cerami et al., 2012) showed that annotated mutations were largely scattered across MIM sequence and according to PolyPhen scores were predominantly pathogenic (***I***, Fig. 4c). Again, a reduced frequency of pathogenic amino acid changes was detected in the regions previously characterized by high functional co-dependence (***I***, Fig. 4c, d).

5.1.4 MIM expression in cancer

Our searches on cBioPortal also showed that MIM is altered in 6% of the cancers and majority of these alterations were amplifications. In the literature, however, MIM is mainly considered as a metastatic suppressor, and therefore we next revisited its expression by looking at TCGA cancers using the GEPIA web tool (Tang et al., 2017). The data showed that the expression of *MTSS1* is differentially regulated in various solid tumors, consistent with the fact that MIM can also be found upregulated in some cancers (Ma et al., 2007; Dawson et al., 2012). In TCGA cancer samples, MIM is downregulated in melanoma, testicular, lung and ovarian cancers, whereas its levels are higher than matched GTEx controls in tumors of the brain and kidney (***I***, Fig. 5a, b).

In normal tissues, MIM expression is one of the highest in spleen, rich in B and T lymphocytes. For this reason, we investigated the expression levels of *MTSS1* in lymphomas and leukaemias using the Oncomine portal (Rhodes et al., 2004). MIM expression was the highest in hairy cell and mantle cell lymphomas (***I***, Fig. 5c). Among various types of leukemia, MIM expression was highest in CLL (***I***, Fig. 5c, d) but at the same time the range of expression levels was wide across the samples.

To analyze whether the expression of MIM in CLL correlates with cancer prognostic factors, we used lymphocytes from 17 CLL patients, which were stratified into poor and good prognosis cases (see methods). We measured the levels of MTSS1 transcript by real-time PCR and found that MTSS1 levels were significantly lower in poor prognosis samples as compared to good prognosis samples ($p = 0.0416$) (***I***, Fig. 5e).

5.1.5 Identification of transcription factor binding sites in the *MTSS1* locus

Mechanisms underlying variation of MIM expression levels in cancer and different tissue types are not well understood. We examined the transcriptional regulation of MTSS1 by looking at the region surrounding its transcriptional start site (TSS) (±10 kb) to obtain information on its conservation across species.

The ENCODE database contained information about 84 transcription factor binding sites (TFBS) for 38 unique transcription factors within the 20 kb region of interest (***I***, Fig. 6a, Table S9 and S10) (Davis et al., 2018; Heintzman et al., 2007). We used position frequency matrices (PFMs) obtained from the JASPAR and HOCOMOCO databases (Khan et al., 2018; Kulakovskiy et al., 2018) in order to scan for the presence of TFBS reported at ENCODE in the selected mammalian species. Many of these TFBS were identified in the analyzed MIM orthologs, suggesting a high level of conservation (***I***, Fig. 6b). In addition, we identified four unreported conserved TFBS for EWSR1-FLI1, NEUROG2, SRF and Sox17 within the putative enhancer region marked by H3K4Me1.

5.1.6 Discussion (I)

Differential expression of MIM has been observed in several cancers and associated with their metastatic potential. This has attracted a fair amount of attention among researches in order to understand its function. In addition to its described role in the regulation of actin cytoskeleton and membrane remodeling, MIM has been reported to possess other physiological functions, for instance, in hedgehog signaling and primary cilia biogenesis (Machesky and Johnston, 2007; Mattila et al., 2007; Atwood et al., 2013). We undertook an in silico approach in an attempt to explore the MIM sequence, generate new hypotheses and propose unexplored functionalities for experimental investigation of this enigmatic protein.

Multiple short functional motifs can be found in the MIM sequence. In line with the proposed function of MIM in actin cytoskeleton and membrane dynamics regulation, we focused our attention on the binding motifs for the α- and μ-subunits of the adaptor protein complex (AP2α-int and APμ-int) as well as the amphipathic C-helix motif (483–491 aa). The C-helix is known for its ability to interact with the GTPase-binding (GBD) domain of class I nucleation promoting factors (e.g. WASP, N-WASP), Arp2/3 complex and monomeric actin (Kelly et al., 2006; Okrut et al., 2015) and thus in various ways can modulate actin polymerization. Existing literature shows that in vitro truncated versions of MIM protein that lack WH2 domain but still contain the C-helix are unable to bind monomeric actin with any detectable affinity (Mattila et al., 2003; Woodings et al., 2003). At the same time, the [404–759 aa] portion of MIM much less efficiently inhibits actin polymerization than MIM[664–759 aa], which lacks the C-helix, whereas addition of MIM[404–705 aa] results in a slight

increase in actin polymerization in vitro (Woodings et al., 2003), suggesting that MIM C-helix can promote actin polymerization. Future studies may show whether MIM C-helix has any functional role toward class I NPFs and Arp2/3-mediated actin polymerization and whether human vs mouse differences exist.

Although the majority of the detected motifs are not yet supported by experimental evidence, there are examples of validated interactions, which reinforce the likelihood of these motifs to be functional. For instance, the ^{321}DSG(XX)S^{326} degron motif, which coincides with the site for casein kinase I (CKI) delta and PTEN activity (Zhong et al., 2013; Zeleniak et al., 2018) as well as various SH3-interacting sites, which in the PRR can mediate interaction with the SH3 domain of cortactin (Lin et al., 2005). Selected candidate motifs that we propose for future validation studies are listed in the ***I***, Table 1. Among them are, for instance, phosphorylation sites for centrosome-associated Polo-like kinases 1 and 4 as well as NEK2 kinase, involved in cilia biogenesis (Barr et al., 2004; Kim et al., 2015; Wang et al., 2013; White and Quarmby, 2008) in line with the proposed regulatory role for MIM in cilia maintenance (Atwood et al., 2013; Bershteyn et al., 2010; Callahan et al., 2004; Drummond et al., 2018).

In addition, we noted a highly hydrophilic region in the center of MIM, mostly consisting of basic residues, which can promote association with negatively charged targets. Intrinsically disordered regions (IDR, or disordered binding regions, DBR) have been found predominantly in the latter half of the protein. The DBRs typically convey interactions by folding upon binding to the partner protein (Mészáros et al., 2012) and can be a place for most of the peptides implicated in binding (Stein et al., 2009). These would cover most of the PRR and WH2 domain, for instance. Indeed, folding upon binding may operate in the case of actin-binding WH2 domain, which for the large part is unstructured (Paunola et al., 2002; Safer et al., 1997)

Our analysis of the vertebrate sequences showed that MIM is a highly conserved protein, which suggests that preservation of the domain structure is crucial for its functions in fish, reptiles, birds and mammals. Only few selected sites were found to be under positive selection in mammals. Among them, for instance, V368 and A447 ancestral residues have been changed to phosphorylation-amenable threonine in primates, thus affecting MIM in *H.sapiens*. Analysis of non-coding regions in the *MIM* locus showed predominant conservation of the TFBS and suggests a similar transcriptional regulation for the *MTSS1* gene across species. The prediction of new TFBSs (EWSR1-FLI1, NEUROG2, SRF and Sox17) points toward a role in cancer as well as embryonic and neuronal development.

Intramolecular co-evolution analysis showed high co-dependence between amino acids in the Pro-rich region (631–728 aa), the middle of the Ser-rich region (333–412 aa) and its adjacent small hydrophilic patch and small Ser/Thr region (430–454 aa). Interestingly, these were largely coinciding with the regions bearing the lowest number of possibly damaging polymorphisms, implying high selective pressure against potentially deleterious non-synonymous substitutions and physiological importance

of these potential regulatory regions. Inability to detect interactions between residues in the I-BAR domain, which is known to be important for MIM dimerization, may suggest that this functionality has been established and locked long before the evolution of vertebrates. Indeed, it has been suggested that the BAR domain origin is approximately coincident with the appearance of the first eukaryotic common ancestor, FECA (Field et al., 2011). Notably, regions characterized by high intramolecular co-dependence also possessed a low concentration of potentially pathogenic SNPs, which may point toward a potentially important functional or regulatory role of these regions.

Differential expression in various malignancies rather suggests a complex role for MIM in cancer instead of simple downmodulation of metastasis. Microarray data points toward high levels of *MTSS1* among different leukemia types. Our analysis of MIM expression levels in CLL from a cohort of patients showed that poor prognosis and increased organ infiltration was associated with significantly lower levels of MTSS1 expression. In blood cancers, MIM expression seems to be highest in mantle cell lymphoma and hairy cell leukemia. It remains to be seen whether high MIM expression can have a biomarker value for these cancers or have a functional role in their development.

5.2 Immunological phenotype of MIM knockout mice (*Publication II*)

5.2.1 B cell development and composition of peripheral B cell subsets in MIM$^{-/-}$ mice are largely undisturbed

In a previously reported MIM knock-out strain, aberrant B cell numbers and development of B cell lymphomas was observed, suggesting importance of MIM for B cells (Yu et al., 2012). We sought to address the immunological phenotype of MIM knock-out mice with the focus on B cell function in more detail.

We used a different MIM KO strain, generated previously (Saarikangas et al., 2011). The lack of protein expression in splenocytes was confirmed by western blot (***II***, Figure 1A).

Analysis of B cell development in the bone marrow of MIM KO mice showed slightly increased numbers of CD117$^+$ CD19$^-$ cells, corresponding to hematopoietic progenitors. However, this left overall numbers of CD19$^+$ and CD19$^+$ IgM$^+$ B cells undisturbed (***II***, Figures 1B–D and Supplementary Figure S1B).

Analysis of B cell maturation in the periphery showed similar percentages of splenic transitional (T1–3) and mature B cells, with only slightly increased numbers of marginal zone (MZ) B cells (***II***, Figure 1F). Splenic CD4$^+$ and CD8$^+$ T cell populations were also comparable to WT numbers (***II***, Figure 1E, Supplementary Figure S2A, B).

In the peritoneal cavity, no significant differences in the numbers of CD5$^+$ (B1a),

$CD5^-$ (B1b) and mature $CD23^+$ B cells (B2) were observed (***II***, Figure 1G). These results indicate that B cell development and maturation is not critically disturbed in the absence of MIM.

5.2.2 BCR signaling in response to surface-bound antigen is impaired in $MIM^{-/-}$ B cells

Organization of the plasma membrane and its regulation by the underlying actin cytoskeleton have been shown to regulate signaling downstream of B cell receptors (Mattila et al., 2016; Treanor et al., 2010; Mattila et al., 2013). To understand whether MIM regulatory activity toward actin and cellular membranes can modulate BCR signaling, the activation status of established BCR signaling molecules as well as Ca^{2+} signaling were examined.

Mobilization of intracellular calcium in response to stimulation with various concentrations of anti-IgM, or their $F(ab')_2$ fragments showed similar patterns in WT and $MIM^{-/-}$ splenic B cells (***II***, Figure 2A and Supplementary Figure S3F). Analysis of anti-CD23 Alexa Fluor (AF)-594 prestained peritoneal cavity B cells stimulated with AF633-labeled anti-IgM antibodies also showed comparable Ca^{2+} flux in B1 (IgM^+ $CD23^-$) and B2 (IgM^+ $CD23^+$) cells (***II***, Supplementary Figure S3A).

Next we examined the activation of individual BCR signaling components by looking at their phosphorylation status. Soluble and plate-bound anti-IgM were used to stimulate splenic B cells for 3–15 minutes and their lysates were analyzed by immunoblotting (***II***, Figure 2B, C; Supplementary Figure S3C, D). It was readily seen that $MIM^{-/-}$ B cells were deficient in signaling in response to surface-bound anti-IgM (***II***, Figure 2B, C). We found that most of the analyzed molecules, including Syk, CD19, Btk, p65 NF-κB, and MAPK1/2 were moderately but significantly impaired in their phosphorylation status. However, defects in proximal signaling variably affected phosphorylation of downstream components. Thus, reduced activation of CD19 and PI3K did not result in reduction of Akt phosphorylation levels, whereas pp65 NF-κB and pMAPK1/2 were invariably downmodulated upon surface stimulation. In response to soluble anti-IgM only Syk phosphorylation levels were minimally but significantly downmodulated in $MIM^{-/-}$ B cells, whereas other components exhibited comparable activation status (***II***, Supplementary Figure S3B, C). These results suggest that MIM contributes to the regulation of BCR signaling in response to surface-presented antigens, which represents a situation where the function of the actin cytoskeleton is important (Bolger-Munro et al., 2019).

5.2.3 The formation of the immunological synapse in MIM$^{-/-}$ B cells is defected upon activation on the surface with immobilized ligands

The cortical actin network supporting plasma membrane morphology in resting B cells also undergoes dynamic changes when the B cell interacts with antigen-presenting surface, characterized by spreading over that surface forming an immunological synapse (IS) structure.

Scanning electron microscopy revealed that the general morphology of MIM$^{-/-}$ B cells in resting state and after 10 min activation on anti-IgM-coated glass coverslips appeared similar to WT, with well-formed round-shaped lamellipodia in spread cells (***II***, Figure 3A).

TIRF microscopy and quantitative analysis of the contact interface between the cell and coverslip revealed a diminished area of spreading for MIM$^{-/-}$ B cells at 10 min upon activation and reduced total and mean fluorescence intensity of the phospho-Tyr staining, confirming impaired BCR signaling. The mean fluorescence intensity of the phalloidin staining, however, indicated a similar density of F-actin in the synapse, whereas reduced total phalloidin fluorescence was consistent with a diminished spreading area (***II***, Figure 3B). Kinetics of the BCR signaling analyzed by microscopy showed reduced pSyk, pBtk and spreading area at different time points upon activation, again consistent with the impaired BCR signaling shown earlier (***II***, Figure 3C).

In vivo, the recognition of antigen on the surface of other cells can present a situation where antigen remains laterally mobile. We used glass-supported lipid bilayers (SLB), functionalized with anti-kappa antibodies to study BCR signaling and the formation of the immunological synapse in MIM$^{-/-}$ B cells upon interaction with a laterally mobile antigen. First, Ca^{2+} signaling on SLBs was analyzed with spinning disk confocal microscopy in a high-throughput manner. Both WT and MIM$^{-/-}$ B cells mobilized Ca^{2+} equally well and no major differences were found in proportions of B cells corresponding to ”single peak” or ”oscillatory” behavior, indicating productive response and weak stimulation, respectively (***II***, Figure 3D) (Lee et al., 2017). Similarly, no overt differences were found in the spreading area and contraction response detected by IRM channel or in the amount of antigen accumulation in the mature synapse, suggesting that MIM might be dispensable for BCR signaling in response to antigen structures with mobile ligands (***II***, Figure 3E).

5.2.4 Impaired antibody responses in MIM$^{-/-}$ animals upon immunization with T cell-independent antigen

To test whether the impaired signaling in MIM$^{-/-}$ B cells leads to defects in development of immune responses in vivo, WT and MIM$^{-/-}$ mice were immunized with model T cell-independent (TI) or T cell-dependent (TD) antigens and serum antibody

levels were followed by ELISA.

Basal IgM and IgG antibody levels in unimmunized animals were comparable (***II***, Figures 4A). Immunization of mice with the model TI antigen, NP-FICOLL, revealed impaired production of NP-specific and total IgM in MIM$^{-/-}$ animals (***II***, Figures 4B–C). Class-switched NP-specific IgG levels were comparable, but at the same time accompanied by reduction in total IgG concentrations, most notably for the IgG2b isotype (***II***, Figure 4D).

Immunization with a TD antigen, NP-KLH in alum, showed that MIM$^{-/-}$ mice can mount an efficient antibody response to this antigen, similar to WT animals (***II***, Supplementary Figure S4A–C). Secondary immunization 4 weeks later also revealed a robust generation of memory NP-specific IgG of all subclasses (***II***, Supplementary Figure S4D). Affinity maturation of the NP-antibodies also appeared normal, as indicated by signal ratios of NP-IgG antibodies bound to low- and high-density conjugated NP-carrier protein in ELISA (***II***, Supplementary Figure S4E).

Furthermore, no significant differences between WT and MIM$^{-/-}$ mice were found when development of high-affinity antibodies was analyzed by comparing binding to low and high densities of NP-epitopes in ELISA (***II***, Supplementary Figure S4E).

Defects in BCR signaling and TI IgM immune responses in MIM$^{-/-}$ mice, but normal responses to TD antigen may point to compensatory mechanisms in the system, such as T cell help. To investigate the intrinsic ability of B cells to generate IgG-producing cells, an in vitro class-switch recombination (CSR) assay was employed, where B cells were provoked to change their surface IgM-BCR into IgG-BCR of different isotypes.

For this, splenic B cells were stimulated for 3 days with LPS or CD40L, to mimick the encounter with pathogen or T cell help, respectively, in combination with cytokines to induce switching of surface BCR, and analyzed by flow cytometry.

As expected, the predominant IgG isotypes of the class-switched cells were determined by the cytokines present in the culture. We noted similar percentages of generated IgG^{+} B cells in response to LPS and CD40L between WT and MIM$^{-/-}$ B cells. Percentages of switched cells in response to the TLR4 ligand, LPS, were however, slightly elevated, considering the maximum switching rates in these experiments (***II***, Supplementary Figures S5A–D).

CSR experiments also allowed us to monitor proliferation of B cells. By looking at reduction in fluorescence of Cell Trace Violet (CTV) dye-loaded B cells, we found no major differences in the proliferation of the cells responding to LPS, CD40L or anti-IgM + CD40L, measured as proliferation index (PI) in all tested conditions. We found moderately increased division index (DI) for MIM$^{-/-}$ B cells in CD40L + IFNγ cultures, reflecting a higher numbers of cells that have undergone at least one division ((***II***, Supplementary Figure S5E).

5.2.5 MIM-deficiency results in higher oxidative metabolic reprogramming of B cells upon LPS and CpG stimulation

Cellular metabolism provides energy and structural building blocks supporting cellular physiology and functions. In B cells metabolic reprogramming driven by various stimuli modulates B cell responses to antigens and differentiation into plasma cells (Boothby and Rickert, 2017). We showed that MIM-deficency results in the impaired IgM antibody response to the TI-2 antigen, NP-FICOLL. In vivo, TI antigens usually come in conjunction with pathogenic determinants recognized by Toll-like receptors (TLR). To understand whether MIM is required for modulation of the B cell responses to TLR ligands, we performed metabolic profiling of mitochondrial function on a Seahorse platform.

To do this, splenic B cells were stimulated with TLR4 and TLR9 ligands, LPS and CpG, respectively, soluble anti-IgM + IL-4, or IL-4 alone for 24 hrs and oxygen consumption rates (OCR) were measured, while mitochondrial function was perturbed by consecutive addition of drugs to inhibit ATP production, mitochondrial membrane potential and respiration.

Our results showed that maximum respiration of MIM$^{-/-}$ B cells was to some extent elevated already after IL-4 culture and not significantly affected after anti-IgM + IL-4 stimulation. The response profiles were more pronounced when LPS and CpG-stimulated cells were analyzed. Baseline OCR rates, maximum and spare respiration were increased in both culture conditions. However, in the case of LPS only maximum respiration was significantly upregulated (***II***, Figure 5A). Ratio of OCR to ECAR (extracellular acidification rate) at the baseline was not different from WT, with some tendency to be higher for CpG stimulation (***II***, Figure 5A). Simultaneous anti-IgM + LPS/CpG stimulation mostly negated TLR-driven metabolic reprogramming, suggesting opposite metabolic effects for BCR and TLR signaling in MIM$^{-/-}$ B cells. To address this interplay more faithfully, IL-4 was also added to the anti-IgM + LPS/CpG cultures. Consistent with the effect of IL-4 alone, OCR of MIM$^{-/-}$ B cells were elevated in comparison with cultures without IL-4 addition (***II***, Supplementary Figure S6A).

To understand whether the observed OCR rates seen in MIM$^{-/-}$ after TLR stimulation are a result of higher functional activity or reflects an enhanced mitochondrial biogenesis, we analyzed mitochondrial mass and membrane potential by analysis of total Tom20 protein levels and TMRE mitochondrial sequestering, respectively, by flow cytometry. Interestingly, we found that in freshly isolated splenic B cells, mitochondrial content was elevated in MIM$^{-/-}$ B cells (***II***, Figure 5B). However, 24 hrs stimulation with LPS or CpG resulted in comparable levels of mitochondria and membrane potential in WT and MIM$^{-/-}$ B cells (***II***, Figure 5C). Forward scatter analysis of B cells showed that CpG-stimulated MIM$^{-/-}$ cells appeared somewhat larger than their WT counterparts. No difference in cell size was noted for cells cultured in anti-IgM + IL-4 or LPS (***II***, Supplementary Figure S6B).

These results suggest a negative role for MIM in metabolic reprogramming toward increased mitochondrial functional capacity in response to TLR ligands.

5.2.6 Discussion (II)

So far, there are three full (Yu et al., 2011; Saarikangas et al., 2011; Xia et al., 2010) and one conditional (Kawabata Galbraith et al., 2018) MIM knockout mouse strains reported in the literature. These studies suggest that MIM is dispensable for the mouse development, but mice acquire notable health issues later in life after the age of ∼5–8 months (Saarikangas et al., 2011; Yu et al., 2012; Xia et al., 2010), described as defects in the integrity of the kidney epithelia, renal cysts and development of lymphomas. At the time of initiation of this study, reported lymphomagenesis was accompanied by disturbed B cell development in young mice (Yu et al., 2012). This finding suggested that MIM may play a role in BCR signaling and thus, affect B cell development and B cell-mediated immunity, which we sought to address in the current study. In 2016, however, a study was published where the same MIM KO mice had no major B cell developmental defects leaving more questions on the role of MIM in B cells (Yu et al., 2012; Zhan et al., 2016).

Our results show that B cell development in the bone marrow and in the periphery of MIM KO mice is largely undisturbed with only a slightly elevated MZ B cell compartment observed. To rule out the possible effect of the gating strategy on the discrepancies in the results reported in (Yu et al., 2012) and our study, we analyzed the bone marrow populations in the same way and found no abnormalities in the numbers of pre-B cells (***II***, Supplementary Figures S1B, C).

The in vitro B cell activation experiments showed impaired BCR signaling in response to surface-bound antigen but not to soluble stimulation. This defect was also in line with the microscopy results, where smaller area of spreading and diminished tyrosine phosphorylation was observed for MIM$^{-/-}$ B cells activated on glass coverslips. These results suggest that MIM may participate in the sensing of antigen properties such as stiffness or antigen mobility during the BCR-mediated response. Consistent decrease in the amount of NF-κB and MAPK1/2 phosphorylation, suggests that the defect lies at the level of the DAG-PKC module (Mérida et al., 2010; Su et al., 2002; Coughlin et al., 2005). Recently, PKCβ-dependent activation of FAK was proposed to regulate substrate stiffness discrimination by B cells (Shaheen et al., 2017) and we speculate that defected activation of the same module in MIM-deficient B cells may also be responsible for the impaired BCR signaling on the anti-IgM-coated plastic surfaces and glass coverslips. In contrast, B cell activation on SLBs indicate that MIM$^{-/-}$ B cells are not defective in their capacity to engage the actin and microtubule cytoskeletal network to form an immunological synapse when laterally mobile ligands are presented (Schnyder et al., 2011; Liu et al., 2012a). SLBs cannot be fully compared to the situation where the cytoskeleton of the antigen-bearing cells can restrict the mobility of the antigen, counteracting the forces generated by

the B cell during activation (Ketchum et al., 2014; Luxembourg et al., 1998; Dillard et al., 2014). Moreover, ICAM-1-functionalized SLBs in our settings could deliver signaling that can lower the threshold for activation of B cells (Carrasco et al., 2004).

The immunization results showed that MIM KO mice have impaired antibody responses toward T cell-independent type 2 antigen, NP-FICOLL, whereas T cell-dependent response against NP-KLH was unaffected. Responses to NP-haptenated FICOLL polysaccharide, a typical TI-2 antigen, are often attributed to the marginal zone B cells and B1b cells (Guinamard et al., 2000; Girkontaite et al., 2001; Hsu et al., 2006; Haas, 2011). As MIM KO mice have normal B1 and rather elevated MZ B cell populations, it is unlikely that inadequate numbers of these subsets are responsible for the inefficient IgM antibody response. We propose that the cell surface-presentation of NP-FICOLL molecules in the secondary lymphoid organs leads to impaired BCR signaling, and hence impaired IgM antibody responses in the MIM KO mice. This we believe is consistent with stronger requirement for intact BCR signaling for TI type 2 antigens and recognition of antigen by antigen-specific B cells on the surface of other cells (Carrasco and Batista, 2007). Intact TD antibody responses as well as efficient production of NP-specific IgG upon NP-FICOLL immunization and normal class-switching suggest that the function of the T cells in MIM KO animals is not defective. This is also consistent with the low expression of MIM in T cells (Yu et al., 2012) and normal $CD4^+$ T cell numbers in the MIM KO strain.

Upon activation B cells upregulate their metabolic activity, which leads to an increase in the oxygen consumption and glycolysis (Caro-Maldonado et al., 2014; Akkaya et al., 2018; Jellusova, 2018; Price et al., 2018). Metabolic reprogramming plays an important role in adaptation to increased energetic needs and functional demands of proliferating B cells and their conversion into antibody-secreting cells (Jellusova, 2018; Boothby and Rickert, 2017).

Our results propose a negative role for MIM in metabolic reprogramming of B cells toward increased mitochondrial functional capacity upon TLR4, and especially TLR9 engagement, as higher OCR profiles were seen for $MIM^{-/-}$ cells stimulated with LPS and CpG.

In order to explain how the reduced BCR signaling and metabolic changes in response to TLR-stimulation may manifest in the same B cells, we propose two possible options. The first one is in line with the notion that many signaling molecules typically associated with the BCR signaling are known to be required for efficient activation of Toll-like receptors in B cells, including the BCR itself (Minguet et al., 2008; Jabara et al., 2012; Otipoby et al., 2015; Morbach et al., 2016; Schweighoffer et al., 2017; Suthers and Sarantopoulos, 2017; Bone and Williams, 2001). In particular, TLR4/9 signaling is crippled when defects in Dock8-Src-Syk-STAT3 (Jabara et al., 2012) and PI3K/Akt-GSK3β-Foxo1 (Otipoby et al., 2015) exist and these cells showed defective proliferation. When inhibited, defects in these modules as well as inhibition in MyD88-Pyk2-Lyn and CD19-PI3K-Akt (Morbach et al., 2016) in CpG-activated cells spares activation of NF-κB and MAPK1/2.

We found that MIM$^{-/-}$ B cells proliferate well in response to LPS and CpG (***II***, Supplementary Figure S5E and data not shown) and thus we speculate that the intrinsically impaired activation of particularly NF-κB and MAPK1/2 due to the MIM-deficiency results in the observed metabolic changes. In support of this hypothesis, NF-κB has been shown to reduce mitochondrial oxidative metabolism in cancer cells and MAPK1/2 has been reported to promote glycolysis in cancer and in rapidly proliferating cells (Londhe et al., 2018; Papa et al., 2019) (Figure 16).

Alternatively, we cannot rule out that even mildly elevated fraction of MZ B cells in splenic B cell preparations used in this study, may contribute to the observed in vitro BCR signaling and metabolic reprogramming phenotypes (Snapper et al., 1993; Oliver et al., 1997).

Although we observed that the metabolic profiles of WT and MIM$^{-/-}$ B cells are similar after 3 days in culture with LPS and CpG (data not shown), our results suggest that MIM deficiency has the potential to influence kinetics of the immune responses against antigens delivered together with TLR ligands as adjuvants, which can be tested in future studies.

We have not performed aging experiments and cannot rule out that our MIM KO strain could develop lymphoproliferative disease. Many B cell lymphomas are dependent on intact BCR signaling for their survival (Young and Staudt, 2013), whereas in our mice BCR signaling was impaired in the absence of MIM. There is, however, evidence that a subtype of diffuse large B cell lymphoma (DLBCL), called OxPhos DLBCL exists, which lacks functional BCR and has a gene expression signature suggestive of an elevated oxidative phosphorylation phenotype (Caro et al., 2012; Ricci and Chiche, 2018). It remains to be determined whether lymphomas noted in aged MIM KO animals (Yu et al., 2012) correspond to OxPhos type of DLBCL and whether any connection exists between the MIM expression and the metabolic activity of the tumor it is associated with.

MIM has also been connected to the hedgehog signaling and cilia biogenesis (Bershteyn et al., 2010; Drummond et al., 2018). We noted that among all the pups that have developed hydrocephalus during this study, all were of MIM knockout or heterozygote genotype. Hydrocephalus formation is associated with defects in primary cilia (Fliegauf et al., 2007), and there is a large body of evidence that MIM is important for primary cilia formation and maintenance. Supporting this are reports that point toward a role of MIM in the integrity of kidney epithelia and polycystic kidney disease (Saarikangas et al., 2011; Xia et al., 2010). It is clear that MIM deficiency alone may not be sufficient for manifestation of the disease and it remains to be seen what are the factors that influence the penetrance of the observed phenotypes, and especially the effects of aging.

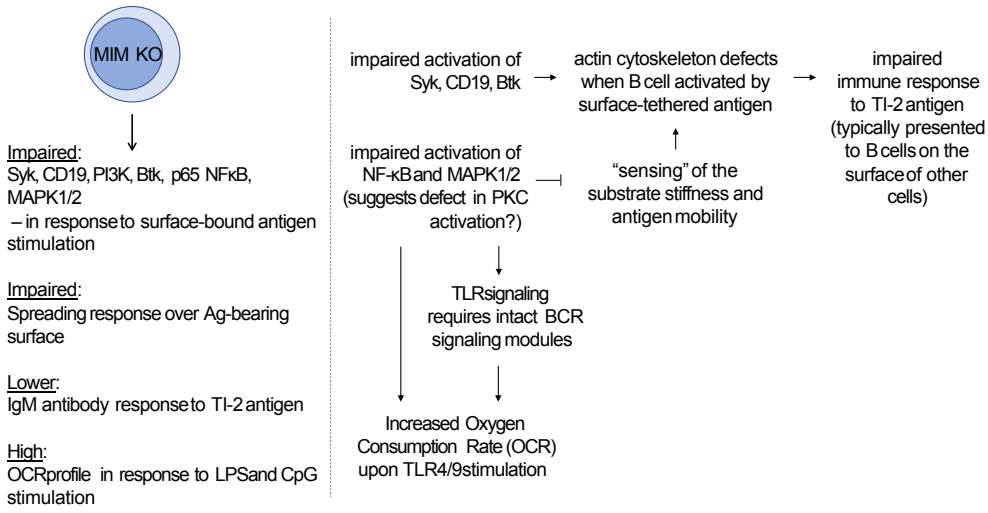

Figure 16. Overview of the major immunological defects associated with MIM-deficiency in B cells (on the left). A proposed model, which explains how MIM-deficiency may lead to observed phenotype (on the right).

5.3 Effect of IRF4 deletion on BCR signaling (*Publication III*)

5.3.1 Inactivation of IRF4 in B cells alters expression of the BCR signaling molecules and leads to diminished pSyk/pBLNK/pMAPK1/2 and enhanced Ca^{2+} signaling in response to BCR stimulation

To investigate the impact of IRF4-mediated transcriptional activity on BCR signaling, the *IRF4* gene was inactivated in the DT40 chicken B cell line by homologous recombination and 2 clones were generated (***III***, Fig. 1A–C). Additionally, IRF4-rescue clones (IRF4KO/IRF4) were established by stable expression of IRF4 in IRF4KO clones, which, however, restored IRF4 expression only up to 50% of WT levels (***III***, Fig. 1D).

Transcriptional profiling of WT and IRF4KO clones on an Agilent 4 × 44K Chicken V2 chip revealed changes in 2793 genes (1209 up- and 1584 downregulated genes; fold change $\geqslant 2$ and $P \leqslant 0.05$). Among them, genes for the products of the BCR signaling pathway: Syk, Blnk, Pik3ap1 (BCAP), Ptpn6 (SHP-1) and Akt were upregulated two-fold (***III***, Fig. S1 and Table S1). While surface IgM expression was unchanged, the peak of Ca^{2+} mobilization in response to anti-IgM stimulation was enhanced by 40% in the absence of IRF4 and IRF4KO/IRF4 restored lower Ca^{2+} flux proportionally to the IRF4 expression (***III***, Fig. 2A, B). Surprisingly, however, further investigation of BCR signaling revealed diminished phosphorylation of Syk

and BLNK, even though their total protein levels were increased in IRF4KO cells (***III***, Fig. 3A, B and Fig. S2). Diminished activation of the immediate BCR targets, Syk and BLNK, also led to delayed and attenuated MAPK1/2 (ERK1/2) phosphorylation (***III***, Fig. 3C). In contrast, and consistent with the enhanced Ca^{2+} flux, the levels of phosphorylated PLCγ2 in response to BCR stimulation were increased in IRF4KO cells (***III***, Fig. 3B and Fig. S2). Interestingly, hypomorhic IRF4 expression in IRF4KO/IRF4 cells only moderately elevated phosphorylation of Syk, but was almost inefficient in restoring the WT phenotype of BLNK, MAPK1/2 and lowering enhanced activation of PLCγ2 upon BCR stimulation (***III***, Fig. 3A–C).

5.3.2 IRF4KO cells exhibit impaired actin polymerization on antigen-presenting surface

BCR signaling activates a multitude of actin-regulating proteins, which coordinate the cell spreading and synapse formation. To study whether defects in activation of BCR signaling molecules result in an abnormal cytoskeletal phenotype, WT and IRF4KO B cells were allowed to spread onto anti-IgM-coated coverslips for 20 min, the actin cytoskeleton was stained with fluorescent phalloidin and the cell contacts with the antigen-presenting surface were visualized with confocal microscopy. A strong (50%) reduction in the amount of filamentous actin (F-actin) was observed (***III***, Fig. 4A, B). Corresponding experiments, where cell-glass coverslip contact zone was captured by TIRF microscopy, demonstrated an abnormal morphology of IRF4KO B cells. Unlike the uniform spreading of WT cells, the majority of IRF4KO cells had lost their radial symmetry and showed a spiky appearance under TIRF illumination (***III***, Fig. 4C). IRF4 supplementation was unable to restore the cytoskeletal defects seen in IRF4KO B cells, consistent with incomplete restoration of Syk, BLNK, PLCγ2 and MAPK1/2 activation (***III***, Fig. 4A–C).

5.3.3 Enhanced PI3K/Akt signaling and downmodulation of SHIP in IRF4-deficient cells

Another important signaling cascade that is activated downstream of BCR is the PI3K pathway. The short isoform of the PI3K adapter protein, BCAP, was upregulated two-fold in IRF4KO B cells. Phosphorylation of BCAP in response to BCR stimulation was also increased, especially for the short isoform (***III***, Fig. 5A). Consistently, phosphorylation of the regulatory subunit of the PI3K p55, as well as the S473 site of the Akt was dramatically increased during activation (***III***, Fig. 5B, C). It is important to note that Akt hyperphosphorylation was evident already in resting IRF4KO B cells. At the same time, hypomorhic IRF4 expression was efficient in restoring low WT levels of BCAP (even below WT levels) and Akt activation and reduced levels of PI3K phosphorylation proportionally to the level of IRF4 complementation (***III***, Fig. 5A–C).

To investigate the elevated Ca^{2+} signaling in IRF4-deficient cells, we turned our attention to the SHIP family of phosphatases in the microarray dataset as they are known to regulate the conversion of phosphoinositides species at the plasma membrane, which in turn modulates the output of IP_3 levels to open Ca^{2+} IP_3 channels (Scharenberg et al., 2007). We found downregulation of *Inpp5B* (Type II inositol 1,4,5-trisphosphate 5-phosphatase), *Inpp5F* (Phosphatidylinositide phosphatase SAC2, Inositol 4-phosphatase) and also showed 2-fold lower expression of *Inpp5d* (Phosphatidylinositol-3,4,5-trisphosphate 5-phosphatase, also known as SHIP) by RT-PCR (***III***, Fig. 6A). Finally, chromatin immunoprecipitation (ChIP) by anti-IRF4 antibodies from nuclear extracts of WT DT40 cells and subsequent PCR showed that IRF4 binds the promoter region of the *Inpp5d* in vivo directly (***III***, Fig. 6B).

5.3.4 Discussion (III)

Microarray analysis revealed alterations in the expression of genes associated with BCR signaling pathway in IRF4 deficient cells. Surprisingly, however, these changes were not directly correlated with the in vitro phosphorylation levels of the corresponding proteins upon B cell receptor stimulation. It is known that mRNA levels are often poor estimators of protein abundance (Liu et al., 2016). Our results suggest that even when gene expression and protein levels correspond, functional consequences may show the opposite.

While phosphorylation of Syk and BLNK was diminished and downstream activation of MAPK1/2 and cytoskeletal responses were consistently attenuated (***III***, Fig. 3C; Fig.4) (Imamura et al., 2009; Weber et al., 2008), the BCAP-PI3K-Akt pathway as well as Ca^{2+} mobilization were shown to be hyperactivated in IRF4-deficient cells (***III***, Fig. 5A–C). BLNK can regulate Ca^{2+} signaling via PLCγ2 recruitment and activation (Kurosaki, 2011; Gerlach et al., 2003). BCAP has also been implicated in BCR-induced Ca^{2+} release (Yamazaki et al., 2002). While BCAP hyperactivation will upregulate Ca^{2+} in IRF4KO cells, lower levels of BLNK phosphorylation would supposedly downmodulate PLCγ2 activity. It has been reported that measurements of BLNK phosphorylation, whereby proteins immunprecipitated by BLNK-specific antibodies are detected by phospho-Tyr-specific antibodies, may be inaccurate as pTyr antibodies only weakly recognize BLNK $pY^{1}19$ site, which mediates PLCγ2 docking and activation (Engelke et al., 2013). Alternatively, it may be that BLNK is not a prerequisite for PLCγ2 activity and Ca^{2+} mobilization, when negative regulators of BCR signaling are not effectively engaged (Gerlach et al., 2003) as might be the case for SHIP phosphatase here.

The strong decrease in the F-actin density in IRF4KO cells upon BCR-mediated spreading may result from the signaling defect to actin cytoskeleton downstream of Syk and BLNK (Weber et al., 2008). The same study by Weber and colleagues also suggested that engagement of the actin machinery is less dependent of BCAP or PI3K activation (Weber et al., 2008). Unbalanced interconversion of phosphoinosi-

tides may contribute to the observed phenotype as well. Low levels of the negative BCR regulatory protein, SHIP, may inefficiently deplete membrane PI(3,4,5)P_3, supplying conversion into PI(4,5)P_2 by PTEN, and thus providing more substrates for PLCγ activity (Rohrschneider et al., 2000). At the same time, hyperactive PLCγ2 converts PI(4,5)P_2 thereby affecting dynamics of actin cytoskeletal regulatory proteins that bind phospholipids leading to enhanced actin depolymerization and elevated Ca^{2+} signaling (Saarikangas et al., 2010). Increased intracellular Ca^{2+} in turn has also been implicated in F-actin depletion at the immunological synapse in B and T cells, possibly via cofilin activation (Maus et al., 2013; Hartzell et al., 2016). As hypomorphic IRF4 expression was unable to proportionally restore cytoskeletal phenotype, despite diminishing Ca^{2+} flux, it is possible that Ca^{2+} levels are of less importance than other regulatory pathways downstream of Syk, BLNK, phosphoinositides or PLCγ2 (Figure 17).

In contrast to Syk and BLNK, the PI3K pathway is hyperactivated in the absence of IRF4. Strong PI3K activation is associated with the execution of the plasma cell differentiation program (Omori et al., 2006) and will interfere with germinal center initiation. At the same time, it has been established that IRF4-deficient B cells are intrinsically incapable of developing into early GC B cells (Willis et al., 2014) and IRF4 activity seem to drive transcription of *Bcl-6* (Ochiai et al., 2013). Indeed, recent studies confirm that downregulation of *IRF4* expression below naive B cell levels in human tonsils occurs at the stage of germinal center B cells, and is particularly low in DZ GC B cells (King et al., 2020; Holmes et al., 2020). Consistent with the upregulation of *Irf4* downstream of BCR stimulation, *Irf4* is upregulated in activated and preGC B cells (King et al., 2020; Cattoretti et al., 2006; Willis et al., 2014; Sciammas et al., 2006). In this respect, based on IRF4 levels, IRF4KO DT40 cells are closer to DZ GC B cells. However, PI3K activity is the hallmark of LZ rather than DZ GC B cells (Sander et al., 2015) and it is likely that GC B cells are not completely devoid of the IRF4 protein. Hypomorhic IRF4 expression was sufficient to restore pAkt levels, which may suggest that phenotypic effects of IRF4 are indeed highly dependent on its graded expression (Sciammas et al., 2006). Attenuated MAPK1/2 seen in IRF4KO and IRF4KO/IRF4 cells may protect GC B cells from premature differentiation toward plasma cells, as MAPK1/2 signaling is necessary for the Blimp1 upregulation (Yasuda et al., 2011). The diminished responses of Syk, BLNK, MAPK1/2 in IRF4KO and IRF4KO/IRF4 cells upon BCR crosslinking, also noted in GC B cells (Khalil et al., 2012), suggest that complex interplay of transcription factors and the cell cycle stage are likely responsible for dynamic changes in the phenotype of B cells in the germinal center, where IRF4 expression in downmodulated.

We cannot rule out that inability of hypomorphic expression of IRF4 to restore activation of certain molecules downstream of the BCR may also be a characteristic of this particular cell line or clone. This may also suggest that regardless of precise expression level, IRF4 downmodulation results in reduced activation of BLNK,

MAPK1/2 and F-actin accumulation. Given the BCR signaling phenotype of IRF4KO/IRF4 B cells and since it is likely that B cells at any GC stage are not completely devoid of IRF4 expression, IRF4KO/IRF4 clones with hypomorhic IRF4 expression could potentially be used as more physiological model of GC B cells.

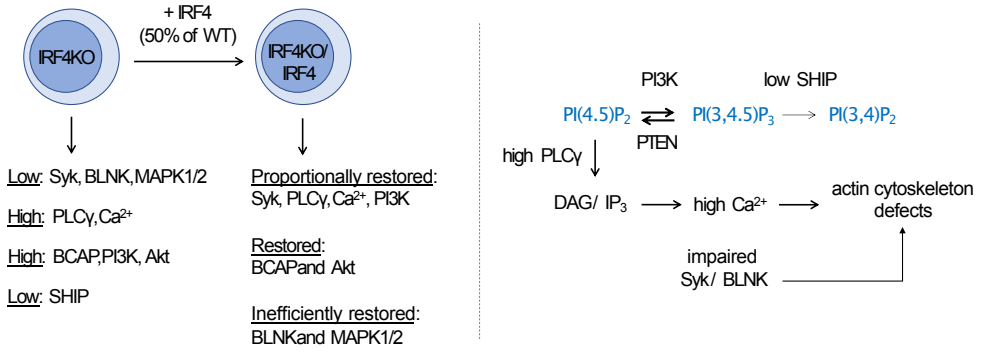

Figure 17. Overview of the BCR signaling defects observed in DT40 chicken B cells lacking IRF4 expression and in cells with hypomorphic expression of IRF4 (on the left). A proposed model, which explains how defects in BCR signaling in IRF4 knockout B cells may result in abnormal actin cytoskeletal responses (on the right).

6 Conclusions

Protective antibody responses require intact functioning of the B cell compartment. It is established that the actin cytoskeleton is critical for B cell development and the normal physiology of B cells. Actin regulation is important for cellular processes where reorganization of cellular membranes takes place, including cell migration, cell division, endo- and exocytosis, which in B cells translates into specific functions of, for instance, tissue surveillance and localization, activation-induced proliferation, antigen presentation and cytokine secretion. Beyond this, there is ample evidence of the intimate connection between actin cytoskeleton and B cell receptor activation and signaling, which are central for antigen-specific B cell-mediated immune responses. The details and molecular partners in this interplay are not completely resolved and likely involve participation of B cell-specific actin regulatory proteins, the role of many of which in B cell-mediated immunity are still poorly characterized. Differentiation stage-specific transcription factors may in turn shape the repertoire of available BCR signaling and actin regulatory proteins and influence the activation response in a way that is optimal for the specific differentiation stage of a B cell.

It is clear that BCR signaling and the actin cytoskeleton are interconnected. One of the actin regulatory proteins, the expression of which is enriched in B cells, is MIM. With multiple proposed functions and at times contradicting results, a better understanding of its physiology seemed necessary. We first resorted to an in silico approach to get new insights into MIM function by applying computational tools and mining publicly available online databases. Our results reveal a high degree of conservation of MIM in vertebrates, suggesting functional importance of its regions subjected to a strong negative selection across species. Careful examination of short functional motifs observed in MIM supports previous findings, which associate MIM with regulation of membrane dynamics, actin cytoskeleton and centrosome biogenesis. Motifs found inside intrinsically disordered regions of MIM may be of particular importance as in our analysis these regions also show a high level of intra-molecular co-dependence and contain a low concentration of ”pathogenic” SNPs, suggesting potential cooperation between these regions and their functional significance. Majority of the identified short functional motifs, however, still remain to be validated experimentally.

MIM has received a great deal of attention due to the initial characterization of its gene transcript as ”missing-in-metastasis”. Our inspection of gene expression databases instead confirms that *Mim* is differentially expressed in various cancers,

where it can be up- or downregulated depending on the cancer type. Evidence for protein expression on the other hand in available studies has to be considered cautiously in the light of the fact that there seem to be no good validated antibodies, which would unambiguously identify endogenous MIM protein in tissue sections. In several publications information on used antibodies is simply missing or incomplete. *Mim* is not listed in the Cancer Gene Census (Sondka et al., 2018) and conditions under which abnormal function of its product may contribute to cancer or severe disarrangement in other suggested cellular functions remain to be established. In particular, lack of MIM has been reported to predispose mice to lymphomagenesis (Yu et al., 2012). Generation of B cell lymphomas and aberrant B cell numbers noted in these mice suggested disturbed functioning of this cell compartment and prompted us to investigate immunological phenotype of MIM KO mice in greater detail.

We found that B cell development in the bone marrow of MIM-deficient mice was intact and that the numbers of B1 and B2 cells in the periphery was largely normal with only a slightly elevated number of marginal zone (MZ) B cells in the spleen. Impaired BCR signaling in response to surface-bound, but not soluble antigen stimulation in $MIM^{-/-}$ cells suggests that MIM may participate in the discrimination of properties of the antigens and antigen-presenting substrates, supporting BCR signaling by stiff and immobilized antigens. This we believe is the reason of reduced IgM responses upon immunization with T cell-independent type 2 model antigen, NP-FICOLL, in which case B cells need to recognize and respond to NP-FICOLL molecules trapped on the surface of other cells. In addition, results from NP-FICOLL immunizations show that, unlike the common belief that TI-2 antigens stimulate only IgM and IgG3 production, in our study NP-FICOLL-immunized animals produced all NP-specific IgG isotypes equally well, thus suggesting that screening of TI-2 responses should not be restricted to only IgM and IgG3 (Perlmutter et al., 1978; García de Vinuesa et al., 1999). Our results also suggest that MIM restricts reprogramming of cellular metabolism toward oxidative phosphorylation downstream of TLR4 and TLR9. It remains to be seen how MIM modulates in vivo antibody responses against antigens associated or delivered together with Toll-like receptor ligands.

B cell development and differentiation into antibody-secreting cells are under a tight transcriptional control. IRF4 is an important transcription factor, critical for the progression of B cells through various developmental checkpoints. Given the importance of BCR signaling in B cell function, we analyzed how IRF4 deficiency affects expression levels of BCR signaling pathway molecules and ultimately BCR signaling in an IRF4-KO DT40 chicken B cell lines. Our data show that IRF4 deficiency results in reduced activation of Syk, BLNK, attenuated MAPK1/2 and defective engagement of actin cytoskeleton as well as upregulation of PI3K, PLCγ and Ca^{2+} signaling upon BCR stimulation. Some phenotypic features of IRF4-KO B cells strikingly resembles that of DZ GC B cells, where IRF4 expression is significantly downregulated (King et al., 2020; Khalil et al., 2012). Together, our results suggest that transcription factors are not only downstream effectors of the BCR signaling but themselves influence

the landscape of the BCR signaling components and ultimately B cell activation via developmental stage-specific expression.

Acknowledgments

The work has been carried out at the University of Turku and I am grateful to all the people of the University, Faculty of Medicine, Institute of Biomedicine, MediCity Research Laboratory, Turku Bioscience Centre of the University of Turku and Åbo Akademi University, and Central Animal Laboratory with whom I had a privilege to work with.

First and foremost I am grateful to my thesis supervisor, Pieta Mattila. Thank you for your help, support, guidance throughout my studies, sleepless nights that I am the only one to blame for, for showing your attitude and enthusiasm in science. One can learn a lot from you just by looking at the way you work and do things. I was also extremely lucky to work with such a nice person who at the same time happened to be my boss. You create a positive atmosphere in the group where everyone can feel comfortable and productive. I wish an excellence to your lab and well to your family.

I am deeply honored and would like to thank Professor Lars Nitschke for accepting the invitation to be the opponent at the thesis defense.

My deepest appreciation to the work of my pre-examiners, Susanna Fagerholm and Tuure Kinnunen who helped me to shape the text of the dissertation in the way others can read.

I am extremely grateful to my thesis committee members, Jeroen Pouwels and Jukka Alinikula, for your comments and invaluable feedback on my work and how to make it better and more efficient throughout all the years of my PhD studies.

This work would not be possible without invaluable contributions of my co-authors. I would like to thank Olli Lassila and his team at the University of Turku: Paulina Budzyńska, Minna Kylaniemi, Kalle-Peka Nera, Sini Junttila, Asta Laiho, and Jukka Alinikula ("IRF4" project). Our collaborators, David Burt (University of Queensland, Australia), Jacqueline Smith and Lel Eöry (University of Edinburgh, UK), Lydia Scarfò and Cristina Scielzo (San Raffaele Scientific Institute, Italy) ("Computational analysis of MIM" project). Our collaborators: Marco Fritzsche and Lena Cords (University of Oxford, UK), Yolanda Carrasco (University of Madrid, Spain), and members of our laboratory: Petar Petrov, Sara Hernández-Pérez, Vid Šuštar, Elina Kuokkanen, Rufus Samuel, and Marika Vainio ("MIM in immune responses" project). I would like to especially thank Paulina Budzyńska and Petar Petrov – driving forces of the "IRF4" and "Computational analysis of MIM" projects, respectively.

I would like to thank Riitta Lahesmaa for the opportunity to start my research work in Finland and sincerely appreciate your efforts in bringing top-level immunol-

ogy researchers to discuss science with us right here in Turku.

I would also like to thank Sirpa Jalkanen, Riitta Lahesmaa, John Eriksson and Jyrki Heino for the flawless work of MediCity Research Laboratories, Turku Bioscience Centre, and BioCity Turku.

I thank Turku Doctoral Programme of Molecular Medicine (TuDMM) for the financial support, curriculum and extra-curriculum activities. I especially thank Nina Widberg, Eeva Valve and Outi Irjala for their help and support.

I wish to thank Centre for International Mobility (CIMO) and organizers of the 14th CIMO Winter School: Hannele Ahti, Tarja Mäkelä, and Leonard Khirug for financial support and opportunity to start my work in Finland. The financial support from University of Turku, Finnish Cultural Foundation, Academy of Finland, Jane and Aatos Erkko Foundation, Sigrid Juselius Foundation, Magnus Ehrnrooth Foundation, and Cancer Society of South-West Finland is greatly appreciated as personal grants as well as our group funding.

I thank Sirkku Grönroos, Riina Plosila, Eeva Hirvensalo, Pasi Viljakainen, Mikael Wasberg, Juha Strandén, Mårten Hedman, Linnea Linko, Ioan Iagar, Antti-Pekka Laine, Satu Alanko, Ulla Karhunen, Maija Lespinasse, Terhi Jokilehto, Anne Lahdenperä, Heli Törmänen, Elina Wiik, and Katri Kulmala for their assistance and excellent administrative and technical support.

I would like to acknowledge the work of people from all TBC Core Facilities and especially Perttu Terho, Ketlin Adel, Jouko Sandholm, Markku Saari, Oso Rissanen, Zsofia Winter, Inna Starskaia, and Markus Peurla for their help with flow cytometers, microscopes and other instruments.

My deep appreciation of the work of people from Central Animal Laboratory: Rafael Frias, Emrah Yatkin, Ville Helle, Iida Reiman, Kristiina Halme, Nina Kulmala, Nina Juoperi, Terhi Hiltula-Maisala, Aila Saari, Paulina Chrusciel, Varpu Laine, Nea Konttinen, Joonas Khabbal. I wish all the researchers knew about your hard work that keep all animal experiments going well.

I would like to acknowledge all my labmates and colleagues that I was lucky to work with over the last years. Does not matter if we worked on the same project, just met at the coffee breaks, spent time over the dinners or beer – I learned something from all of you and I hope I gave you something in return.

I warmly thank all the past and present members of the Riitta Lahesmaa and Harri Lähdesmäki groups for sharing your knowledge and continuous support: Kaur Alasoo, Tarmo Äijö, Kanchan Bala, Santosh Bhosale, Zhi Chen, Sanna Edelman, Laura Elo, Bogata Fezazi, Marjo Hakkarainen, Saara Hämälistö, Sarita Heinonen, Jussi Jalonen, Päivi Junni, Henna Kallionpää, Kartiek Kanduri, Meraj Khan, Moin Khan, Ida Koho, Lingjia Kong, Minna Kyläniemi, Essi Laajala, Kirsti Laurila, Sari Lehtimäki, Niina Lietzén, Tapio Lönnberg, Riikka Lund, Henrik Mannerström, Imran Mohammad, Robert Moulder, Johanna Myllyviita, Elisa Närvä, Elizabeth Ngyen, Lotta Oikari, Viveka Öling, Elina Pietilä, Nelly Rahkonen, Omid Rasool, Maheswara Emani Reddy, Roosa Sahla, Jussi Salmi, Verna Salo, Sunita Singh, Aki Stubb, Sub-

hash Tripathi (for Indian wisdom), Soile Tuomela, Ullah Ubaid, Miro Viitala. I especially thank Sanna and Mahesh for your friendship, mentorship and help. Also greetings to Maple – I shake her strong paws.

I am grateful to people from Pathology Unit: Ilmo Leivo, Olli Carpen, Vanina Heuser, Kaisa Huhtinen, Kowan-Ja Jee, Katja Kaipio, Taina Korpela, Tarja Lamminen, Laura Lehtinen, Song-Ping Li, Emmi Lokka, Paula Merilahti, Minna Peippo, Heikki Peuravuori, Pia Roering, Stina Syrjänen, Tatjana Peskova, Gudrun Wahlström, and Gun West for sharing reagents, space and your spirit with the Mattila Lab. I also thank Pekka Hänninen, Joanna Pylvänäinen, Henok Karvonen, Elena Tcarenkova, and Elnaz Fazeli from Biophysics Lab and Turku Bioimaging for sharing your wisdom at the 5th floor.

I also would like to thank people not mentioned above for work and pub collaborations and good memories, especially: Julia Kulkova (my CIMO buddy), RAS signaling and Epigenetics people and Co: Cristina Valensisi (ice cream only with aceto balsamico), Alessio Ligabue, Arafat Najumudeen (thanks for the shelter), Kalyan Pasumarthy, Num Wistbacka, David Hawkins, Camilo Guzmán, Elina Siljamäki, Sebastian Landor, Maja Šolman, Olga Blaževitš, Jenny Joutsen; Gennady Yegutkin, Karolina Losenkova, Mariachiara Zuccarini, Maksim Skaldin, Akira Takeda, Juan Palacios Ortega, Inês Félix (and Archie).

I would like to thank all current and past members of the Lymphocyte Cytoskeleton Group:
Sara Hernández-Pérez (for your kindness, support and occasional Spanish treats),
Petar Petrov (for your invaluable help and solid Bulgarian spirit),
Luqman Awoniyi (for Nigerian friendship and sport activities),
Diogo Cunha (for Portuguese drive, although Finland will convert you eventually),
Marika Vainio (for Finnish wisdom and because everything is just “cool”),
Vid Šuštar (for Slovenian hospitality and curiosity),
Elina Kuokkanen (for Finnish spirit and care for Nature),
Laura Grönfors (for keeping everything in good shape and Finnish order(s)),
Rufus Vinod (for your help and Pakistani cordiality).

I also thank Citarra Burrows, Sofia Forstén, Hanna-Maria Judin, Elmeri Kiviluoto, Salli Leimu, Vilma Paavola, Katriina Palttila, Johanna Rajala, Katja Stoltzenberg, Eveliina Uski – it was very nice to know and work with you.

I wish to thank Yulia Lopatnikova, Nelly Popova, Nikolai Kolesnikov, Denis Kainov, Alexander Zhovmer, Fedor Kireev for the support and encouragement. I thank Alexander Efremov, Dmitriy No, Sergey Sedykh, Tatyana Sedykh, Vladislav Mileyko, Inna Mileyko, Mikhail Mishchenko, Anna Popova, Heta Holvitie for your friendship, new places that we experienced together or old places we were at, and Irina Rusu for teaching me something new.

I especially would like to thank people who made it to Turku on several occasions, Ekaterina Tretyakova (courageous traveller) and my dear friends, Kirill and Maria Muzalevskiy, for whom I immensely grateful for always being there for me.

My warm thank you, E.A., for the light moments we shared together, and that I will always remember.

And, of course, I thank my family and parents, Marina and Vladimir, for the worries and continuous support. Спасибо моим родителям за ваши переживания и постоянную поддержку. Вы много для меня значите и мою благодарность сложно передать словами. Спасибо за то, что вы у меня есть.

29.01.2022
Alexey Sarapulov

References

Adzhubei, I. A., Schmidt, S., Peshkin, L., Ramensky, V. E., Gerasimova, A., Bork, P., Kondrashov, A. S., and Sunyaev, S. R. (2010). A method and server for predicting damaging missense mutations. *Nature Methods*, 7(4):248–249. ↑72, ↑91

Aiba, Y., Kameyama, M., Yamazaki, T., Tedder, T. F., and Kurosaki, T. (2008). Regulation of B-cell development by BCAP and CD19 through their binding to phosphoinositide 3-kinase. *Blood*, 111(3):1497–503. ↑25

Akkaya, M. and Pierce, S. K. (2019). From zero to sixty and back to zero again: the metabolic life of B cells. *Current Opinion in Immunology*, 57:1–7. ↑52

Akkaya, M., Traba, J., Roesler, A. S., Miozzo, P., Akkaya, B., Theall, B. P., Sohn, H., Pena, M., Smelkinson, M., Kabat, J., Dahlstrom, E., Dorward, D. W., Skinner, J., Sack, M. N., and Pierce, S. K. (2018). Second signals rescue B cells from activation-induced mitochondrial dysfunction and death. *Nature Immunology*, 19(8):871–884. ↑33, ↑52, ↑53, ↑54, ↑100

Alberts, B., Johnson, A., Lewis, J., Raff, M., Roberts, K., and Walter, P. (2015). *Molecular biology of the cell*. Garland Science, New York, 6th ed. edition. ↑37

Alinikula, J., Kohonen, P., Nera, K. P., and Lassila, O. (2010). Concerted action of Helios and Ikaros controls the expression of the inositol 5-phosphatase SHIP. *European Journal of Immunology*, 40(9):2599–2607. ↑86, ↑87

Alinikula, J., Nera, K.-P., Junttila, S., and Lassila, O. (2011). Alternate pathways for Bcl6-mediated regulation of B cell to plasma cell differentiation. *European journal of immunology*, 41(8):2404–2413. ↑86

Allman, D., Lindsley, R. C., DeMuth, W., Rudd, K., Shinton, S. A., and Hardy, R. R. (2001). Resolution of three nonproliferative immature splenic B cell subsets reveals multiple selection points during peripheral B cell maturation. *Journal of immunology (Baltimore, Md. : 1950)*, 167(12):6834–40. ↑22

Andersson, C., Lin, H., Liu, C., Levy, D., Mitchell, G. F., Larson, M. G., and Vasan, R. S. (2019). Integrated Multiomics Approach to Identify Genetic Underpinnings of Heart Failure and Its Echocardiographic Precursors: Framingham Heart Study. *Circulation: Genomic and Precision Medicine*, 12(12):533–542. ↑63

Antón, I. M., Lu, W., Mayer, B. J., Ramesh, N., and Geha, R. S. (1998). The Wiskott-Aldrich syndrome protein-interacting protein (WIP) binds to the adaptor protein Nck. *Journal of Biological Chemistry*, 273(33):20992–20995. ↑45

Antonczyk, A., Krist, B., Sajek, M., Michalska, A., Piaszyk-Borychowska, A., Plens-Galaska, M., Wesoly, J., and Bluyssen, H. A. (2019). Direct inhibition of IRF-dependent transcriptional regulatory mechanisms associated with disease. *Frontiers in Immunology*, 10(MAY):1–23. ↑56

Arakawa, H., Lodygin, D., and Buerstedde, J. M. (2001). Mutant loxP vectors for selectable marker recycle and conditional knock-outs. *BMC biotechnology*, 1:7. ↑85

Arana, E., Vehlow, A., Harwood, N. E., Vigorito, E., Henderson, R., Turner, M., Tybulewicz, V. L. J., and Batista, F. D. (2018). Activation of the small GTPase Rac2 via the B cell receptor regulates B cell adhesion and immunological-synapse formation. *Immunity*, 28(1):88–99. ↑51

Ashkenazy, H., Abadi, S., Martz, E., Chay, O., Mayrose, I., Pupko, T., and Ben-Tal, N. (2016). ConSurf 2016: an improved methodology to estimate and visualize evolutionary conservation in macromolecules. *Nucleic acids research*, 44(W1):W344–50. ↑72, ↑90

Atwood, S. X., Li, M., Lee, A., Tang, J. Y., and Oro, A. E. (2013). GLI activation by atypical protein kinase C ι/λ regulates the growth of basal cell carcinomas. *Nature*, 494(7438):484–8. ↑63, ↑65, ↑92, ↑93

Aung, N., Vargas, J. D., Yang, C., Cabrera, C. P., Warren, H. R., Fung, K., Tzanis, E., Barnes, M. R., Rotter, J. I., Taylor, K. D., Manichaikul, A. W., Lima, J. A., Bluemke, D. A., Piechnik, S. K., Neubauer, S., Munroe, P. B., and Petersen, S. E. (2019). Genome-wide analysis of left ventricular image-derived phenotypes identifies fourteen loci associated with cardiac morphogenesis and heart failure development. *Circulation*, 140(16):1318–1330. ↑63

Avalos, A. M. and Ploegh, H. L. (2014). Early BCR events and antigen capture, processing, and loading on MHC class II on B cells. *Frontiers in Immunology*, 5(MAR):1–5. ↑32

Avila-Herrera, A. and Pollard, K. S. (2015). Coevolutionary analyses require phylogenetically deep alignments and better null models to accurately detect inter-protein contacts within and between species. *BMC Bioinformatics*, 16(1):1–18. ↑68, ↑90

Bachmann, M., Rohrer, U., Kundig, T., Burki, K., Hengartner, H., and Zinkernagel, R. (1993). The influence of antigen organization on B cell responsiveness. *Science*, 262(5138):1448–1451. ↑32

Baeker, T. R., Simons, E. R., and Rothstein, T. L. (1987). Cytochalasin induces an increase in cytosolic free calcium in murine B lymphocytes. *Journal of Immunology*, 138(8):2691–2697. ↑41

Bailey, T. L., Boden, M., Buske, F. A., Frith, M., Grant, C. E., Clementi, L., Ren, J., Li, W. W., and Noble, W. S. (2009). MEME SUITE: tools for motif discovery and searching. *Nucleic acids research*, 37(Web Server issue):W202–8. ↑74

Barr, F. A., Silljé, H. H. W., and Nigg, E. A. (2004). Polo-like kinases and the orchestration of cell division. *Nature reviews. Molecular cell biology*, 5(6):429–40. ↑93

Basso, K., Margolin, A. A., Stolovitzky, G., Klein, U., Dalla-Favera, R., and Califano, A. (2005). Reverse engineering of regulatory networks in human B cells. *Nature genetics*, 37(4):382–90. ↑73

Batista, F. D., Iber, D., and Neuberger, M. S. (2001). B cells acquire antigen from target cells after synapse formation. *Nature*, 411(6836):489–494. ↑34, ↑36, ↑43

Batista, F. D. and Neuberger, M. S. (2000). B cells extract and present immobilized antigen: implications for affinity discrimination. *The EMBO journal*, 19(4):513–20. ↑36, ↑37

Baumgart, F. and Cordey, J. (2001). Stiffness - An unknown world of mechanical science? *Injury*, 32:14–23. ↑35

Baumgarth, N. (2010). The double life of a B-1 cell: self-reactivity selects for protective effector functions. *Nature Reviews Immunology*, 11(1):34–46. ↑23

Baumgarth, N., Herman, O. C., Jager, G. C., Brown, L., Herzenberg, L. A., and Herzenberg, L. A. (1999). Innate and acquired humoral immunities to influenza virus are mediated by distinct arms of the immune system. *Proceedings of the National Academy of Sciences of the United States of America*, 96(5):2250–5. ↑23

Becker-Herman, S., Meyer-Bahlburg, A., Schwartz, M. A., Jackson, S. W., Hudkins, K. L., Liu, C., Sather, B. D., Khim, S., Liggitt, D., Song, W., Silverman, G. J., Alpers, C. E., and Rawlings, D. J. (2011). WASp-deficient B cells play a critical, cell-intrinsic role in triggering autoimmunity. *The Journal of experimental medicine*, 208(10):2033–42. ↑50

Berry, C. T., Liu, X., Myles, A., Nandi, S., Chen, Y. H., Hershberg, U., Brodsky, I. E., Cancro, M. P., Lengner, C. J., May, M. J., and Freedman, B. D. (2020). BCR-Induced Ca(2+) Signals Dynamically Tune Survival, Metabolic Reprogramming, and Proliferation of Naive B Cells. *Cell reports*, 31(2):107474. ↑33, ↑53

Bershteyn, M., Atwood, S. X., Woo, W.-M., Li, M., and Oro, A. E. (2010). MIM and cortactin antagonism regulates ciliogenesis and hedgehog signaling. *Developmental cell*, 19(2):270–83. ↑59, ↑63, ↑64, ↑65, ↑93, ↑101

Bikah, G., Carey, J., Ciallella, J. R., Tarakhovsky, A., and Bondada, S. (1996). CD5-mediated negative regulation of antigen receptor-induced growth signals in B-1 B cells. *Science*, 274(5294):1906–1909. ↑23

Blair, D., Dufort, F. J., and Chiles, T. C. (2012). Protein kinase Cβ is critical for the metabolic switch to glycolysis following B-cell antigen receptor engagement. *Biochemical Journal*, 448(1):165–169. ↑52

Blom, N., Sicheritz-Pontén, T., Gupta, R., Gammeltoft, S., and Brunak, S. (2004). Prediction of post-translational glycosylation and phosphorylation of proteins from the amino acid sequence. *Proteomics*, 4(6):1633–1649. ↑71

Bolger-Munro, M., Choi, K., Scurll, J. M., Abraham, L., Chappell, R. S., Sheen, D., Dang-Lawson, M., Wu, X., Priatel, J. J., Coombs, D., Hammer, J. A., and Gold, M. R. (2019). Arp2/3 complex-driven spatial patterning of the BCR enhances immune synapse formation, BCR signaling and B cell activation. *eLife*, 8. ↑35, ↑43, ↑44, ↑49, ↑95

Bompard, G. (2005). Involvement of Rac in actin cytoskeleton rearrangements induced by MIM-B. *Journal of Cell Science*, 118(22):5393–5403. ↑57, ↑58, ↑59, ↑64

Bone, H. and Williams, N. A. (2001). Antigen-receptor cross-linking and lipopolysaccharide trigger distinct phosphoinositide 3-kinase-dependent pathways to NF-κB activation in primary B cells. *International Immunology*, 13(6):807–816. ↑100

Bonifaz, L. C., Cervantes-Silva, M. P., Ontiveros-Dotor, E., López-Villegas, E. O., and Sánchez-García, F. J. (2015). A role for mitochondria in antigen processing and presentation. *Immunology*, 144(3):461–471. ↑53

Boothby, M. and Rickert, R. C. (2017). Metabolic Regulation of the Immune Humoral Response. *Immunity*, 46(5):743–755. ↑54, ↑98, ↑100

Bourguignon, L. Y. and Bourguignon, G. J. (1984). Capping and the Cytoskeleton. *International Review of Cytology*, 87(C):195–224. ↑41

Brezski, R. J. and Monroe, J. G. (2007). B Cell Antigen Receptor-Induced Rac1 Activation and Rac1-Dependent Spreading Are Impaired in Transitional Immature B Cells Due to Levels of Membrane Cholesterol. *The Journal of Immunology*, 179(7):4464–4472. ↑51

Brooks, S. R., Li, X., Volanakis, E. J., and Carter, R. H. (2000). Systematic analysis of the role of CD19 cytoplasmic tyrosines in enhancement of activation in Daudi human B cells: clustering of phospholipase C and Vav and of Grb2 and Sos with different CD19 tyrosines. *Journal of immunology (Baltimore, Md. : 1950)*, 164(6):3123–31. ↑45

Brown, A. S., Meera, P., Quinones, G., Magri, J., Otis, T. S., Pulst, S. M., and Oro, A. E. (2020). Receptor protein tyrosine phosphatases control Purkinje neuron firing. *Cell Cycle*, 19(2):153–159. ↑63

Brown, B. K. and Song, W. (2001). The actin cytoskeleton is required for the trafficking of the B cell antigen receptor to the late endosomes. *Traffic (Copenhagen, Denmark)*, 2(6):414–27. ↑43

Brunswick, M., Finkelman, F. D., Highet, P. F., Inman, J. K., Dintzis, H. M., and Mond, J. J. (1988). Picogram quantities of anti-Ig antibodies coupled to dextran induce B cell proliferation. *Journal of immunology (Baltimore, Md. : 1950)*, 140(10):3364–3372. ↑33

Buerstedde, J. M. and Takeda, S. (1991). Increased ratio of targeted to random integration after transfection of chicken B cell lines. *Cell*, 67(1):179–188. ↑85

Buhl, A. M., Pleiman, C. M., Rickert, R. C., and Cambier, J. C. (1997). Qualitative regulation of B cell antigen receptor signaling by CD19: Selective requirement for PI3-kinase activation, inositol-1,4,5-trisphosphate production and Ca2+ mobilization. *Journal of Experimental Medicine*, 186(11):1897–1910. ↑35

Burbage, M., Keppler, S. J., Gasparrini, F., Martínez-Martín, N., Gaya, M., Feest, C., Domart, M.-C., Brakebusch, C., Collinson, L., Bruckbauer, A., and Batista, F. D. (2015). Cdc42 is a key regulator of B cell differentiation and is required for antiviral humoral immunity. *The Journal of Experimental Medicine*, 212(1):53–72. ↑51

Callahan, C. A., Ofstad, T., Horng, L., Wang, J. K., Zhen, H. H., Coulombe, P. A., and Oro, A. E. (2004). MIM/BEG4, a Sonic hedgehog-responsive gene that potentiates Gli-dependent transcription. *Genes & development*, 18(22):2724–9. ↑65, ↑93

Campellone, K. G. and Welch, M. D. (2010). A nucleator arms race: cellular control of actin assembly. *Nature Reviews Microbiology*, 11(4):237–251. ↑39, ↑40

Cao, M., Zhan, T., Ji, M., and Zhan, X. (2012). Dimerization is necessary for MIM-mediated membrane deformation and endocytosis. *The Biochemical journal*, 446(3):469–75. ↑59

Caro, P., Kishan, A. U., Norberg, E., Stanley, I. A., Chapuy, B., Ficarro, S. B., Polak, K., Tondera, D., Gounarides, J., Yin, H., Zhou, F., Green, M. R., Chen, L., Monti, S., Marto, J. A., Shipp, M. A., and Danial, N. N. (2012). Metabolic Signatures Uncover Distinct Targets in Molecular Subsets of Diffuse Large B Cell Lymphoma. *Cancer Cell*, 22(4):547–560. ↑101

Caro-Maldonado, A., Wang, R., Nichols, A. G., Kuraoka, M., Milasta, S., Sun, L. D., Gavin, A. L., Abel, E. D., Kelsoe, G., Green, D. R., and Rathmell, J. C. (2014). Metabolic reprogramming is required for antibody production that is suppressed in anergic but exaggerated in chronically BAFF-exposed B cells. *Journal of immunology (Baltimore, Md. : 1950)*, 192(8):3626–36. ↑52, ↑53, ↑100

Carrasco, Y. R. and Batista, F. D. (2007). B cells acquire particulate antigen in a macrophage-rich area at the boundary between the follicle and the subcapsular sinus of the lymph node. *Immunity*, 27(1):160–171. ↑27, ↑30, ↑34, ↑100

Carrasco, Y. R., Fleire, S. J., Cameron, T., Dustin, M. L., and Batista, F. D. (2004). LFA-1/ICAM-1 Interaction Lowers the Threshold of B Cell Activation by Facilitating B Cell Adhesion and Synapse Formation. *Immunity*, 20(5):589–599. ↑80, ↑100

Carter, R. H., Wang, Y., and Brooks, S. (2002). Role of CD19 signal transduction in B cell biology. *Immunologic Research*, 26(1-3):45–54. ↑25

Case, J. B., Bonami, R. H., Nyhoff, L. E., Steinberg, H. E., Sullivan, A. M., and Kendall, P. L. (2015). Bruton's Tyrosine Kinase Synergizes with Notch2 To Govern Marginal Zone B Cells in Nonobese Diabetic Mice. *Journal of immunology (Baltimore, Md. : 1950)*, 195(1):61–70. ↑23

Casellas, R., Tien-An Yang Shih, Kleinewietfeld, M., Rakonjac, J., Nemazee, D., Rajewsky, K., and Nussenzweig, M. C. (2001). Contribution of receptor editing to the antibody repertoire. *Science*, 291(5508):1541–1544. ↑22

Castello, A., Gaya, M., Tucholski, J., Oellerich, T., Lu, K.-H., Tafuri, A., Pawson, T., Wienands, J., Engelke, M., and Batista, F. D. (2013). Nck-mediated recruitment of BCAP to the BCR regulates the PI(3)K-Akt pathway in B cells. *Nature immunology*, 14(9):966–75. ↑25, ↑45

Cattoretti, G., Shaknovich, R., Smith, P. M., Jack, H.-M., Murty, V. V., and Alobeid, B. (2006). Stages of Germinal Center Transit Are Defined by B Cell Transcription Factor Coexpression and Relative Abundance. *The Journal of Immunology*, 177(10):6930–6939. ↑56, ↑105

Cerami, E., Gao, J., Dogrusoz, U., Gross, B. E., Sumer, S. O., Aksoy, B. A., Jacobsen, A., Byrne, C. J., Heuer, M. L., Larsson, E., Antipin, Y., Reva, B., Goldberg, A. P., Sander, C., and Schultz, N. (2012). The cBio Cancer Genomics Portal: An Open Platform for Exploring Multidimensional Cancer Genomics Data. *Cancer Discovery*, 2(5):401 LP – 404. ↑72, ↑91

Chen, Y., Park, Y.-B., Patel, E., and Silverman, G. J. (2009). IgM Antibodies to Apoptosis-Associated Determinants Recruit C1q and Enhance Dendritic Cell Phagocytosis of Apoptotic Cells. *The Journal of Immunology*, 182(10):6031–6043. ↑24

Cherfils, J. and Zeghouf, M. (2013). Regulation of Small GTPases by GEFs, GAPs, and GDIs. *Physiological Reviews*, 93(1):269–309. ↑39, ↑44

Chica, C., Labarga, A., Gould, C. M., López, R., and Gibson, T. J. (2008). A tree-based conservation scoring method for short linear motifs in multiple alignments of protein sequences. *BMC Bioinformatics*, 9(1):229. ↑70

Cho, S. H., Raybuck, A. L., Stengel, K., Wei, M., Beck, T. C., Volanakis, E., Thomas, J. W., Hiebert, S., Haase, V. H., and Boothby, M. R. (2016). Germinal centre hypoxia and regulation of antibody qualities by a hypoxia response system. *Nature*, 537(7619):234–238. ↑54

Choi, S. C. and Morel, L. (2020). Immune metabolism regulation of the germinal center response. *Experimental and Molecular Medicine*, 52(3):348–355. ↑54, ↑55

Choi, Y. S. and Baumgarth, N. (2008). Dual role for B-1a cells in immunity to influenza virus infection. *Journal of Experimental Medicine*, 205(13):3053–3064. ↑23

Choi, Y. S., Dieter, J. A., Rothaeusler, K., Luo, Z., and Baumgarth, N. (2012). B-1 cells in the bone marrow are a significant source of natural IgM. *European Journal of Immunology*, 42(1):120–129. ↑23

Chung, J. B., Sater, R. A., Fields, M. L., Erikson, J., and Monroe, J. G. (2002). CD23 defines two distinct subsets of immature B cells which differ in their responses to T cell help signals. *International Immunology*, 14(2):157–166. ↑22

Chung, J. B., Wells, A. D., Adler, S., Jacob, A., Turka, L. A., and Monroe, J. G. (2003). Incomplete Activation of CD4 T Cells by Antigen-Presenting Transitional Immature B Cells: Implications for Peripheral B and T Cell Responsiveness. *The Journal of Immunology*, 171(4):1758–1767. ↑22

Cinamon, G., Zachariah, M. A., Lam, O. M., Foss, F. W., and Cyster, J. G. (2008). Follicular shuttling of marginal zone B cells facilitates antigen transport. *Nature immunology*, 9(1):54–62. ↑30

Claassen, E., Ott, A., Boersma, W. J., Deen, C., Schellekens, M. M., Dijkstra, C. D., Kors, N., and Van Rooijen, N. (1989). Marginal zone of the murine spleen in autotransplants: functional and histological observations in the response against a thymus-independent type 2 antigen. *Clinical and experimental immunology*, 77(3):445–51. ↑30

Clarke, A. J., Riffelmacher, T., Braas, D., Cornall, R. J., and Simon, A. K. (2018). B1a B cells require autophagy for metabolic homeostasis and self-renewal. *The Journal of Experimental Medicine*, 215(2):399 LP – 413. ↑52

Consortium, T. . G. P., 1000 Genomes Project Consortium, Auton, A., Brooks, L. D., Durbin, R. M., Garrison, E. P., Kang, H. M., Korbel, J. O., Marchini, J. L., McCarthy, S., McVean, G. A., and Abecasis, G. R. (2015). A global reference for human genetic variation. *Nature*, 526(7571):68. ↑72

Cornall, R. J., Cheng, A. M., Pawson, T., and Goodnow, C. C. (2000). Role of Syk in B-cell development and antigen-receptor signaling. *Proceedings of the National Academy of Sciences of the United States of America*, 97(4):1713–1718. ↑24

Coughlin, J. J., Stang, S. L., Dower, N. A., and Stone, J. C. (2005). RasGRP1 and RasGRP3 Regulate B Cell Proliferation by Facilitating B Cell Receptor-Ras Signaling. *The Journal of Immunology*, 175(11):7179 LP – 7184. ↑25, ↑99

Crotty, S. (2015). A brief history of T cell help to B cells. *Nature reviews. Immunology*, 15(3):185–9. ↑27

Crotty, S. (2019). T Follicular Helper Cell Biology: A Decade of Discovery and Diseases. *Immunity*, 50(5):1132–1148. ↑27

CRUMPTON, M. J. (1974). Protein Antigens: The Molecular Bases of Antigenicity and Immunogenicity. In Sela, M., editor, *The Antigens*, pages 1–78. Elsevier. ↑32, ↑33

Dahlberg, C. I. M., Torres, M.-L., Petersen, S. H., Baptista, M. A. P., Keszei, M., Volpi, S., Grasset, E. K., Karlsson, M. C. I., Walter, J. E., Snapper, S. B., Notarangelo, L. D., and Westerberg, L. S. (2015). Deletion of WASp and N-WASp in B cells cripples the germinal center response and results in production of IgM autoantibodies. *Journal of autoimmunity*. ↑50

Davis, C. A., Hitz, B. C., Sloan, C. A., Chan, E. T., Davidson, J. M., Gabdank, I., Hilton, J. A., Jain, K., Baymuradov, U. K., Narayanan, A. K., Onate, K. C., Graham, K., Miyasato, S. R., Dreszer, T. R., Strattan, J. S., Jolanki, O., Tanaka, F. Y., and Cherry, J. M. (2018). The Encyclopedia of DNA elements (ENCODE): data portal update. *Nucleic acids research*, 46(D1):D794–D801. ↑74, ↑92

Dawson, J. C., Timpson, P., Kalna, G., and Machesky, L. M. (2012). Mtss1 regulates epidermal growth factor signaling in head and neck squamous carcinoma cells. *Oncogene*, 31(14):1781–93. ↑62, ↑91

de Groot, C., Wormmeester, J., and Mangnus-Smet, C. (1981). Capping of surface immunoglobulin on rabbit and mouse lymphocytes. II. Cytoskeletal involvement in different subpopulations. *European journal of cell biology*, 25(1):202–211. ↑34, ↑41

De Silva, N. S., Simonetti, G., Heise, N., and Klein, U. (2012). The diverse roles of IRF4 in late germinal center B-cell differentiation. *Immunological reviews*, 247(1):73–92. ↑56

Deenen, G. J. and Kroese, F. G. (1993). Kinetics of peritoneal B-1a cells (CD5 B cells) in young adult mice. *European Journal of Immunology*, 23(1):12–16. ↑23

Delves, P. J., Martin, S. J., Burton, D. R., and Roitt, I. M. (2017). *Roitt's essential immunology*. John Wiley & Sons, Inc., Chichester, West Sussex ; Hoboken, [NJ], 13th edition. ↑16

Depoil, D., Fleire, S., Treanor, B. L., Weber, M., Harwood, N. E., Marchbank, K. L., Tybulewicz, V. L. J., and Batista, F. D. (2008). CD19 is essential for B cell activation by promoting B cell receptor–antigen microcluster formation in response to membrane-bound ligand. *Nature Immunology*, 9(1):63–72. ↑34, ↑35

Dillard, P., Varma, R., Sengupta, K., and Limozin, L. (2014). Ligand-Mediated Friction Determines Morphodynamics of Spreading T Cells. *Biophysical Journal*, 107(11):2629–2638. ↑35, ↑100

Dinkel, H., Van Roey, K., Michael, S., Kumar, M., Uyar, B., Altenberg, B., Milchevskaya, V., Schneider, M., Kühn, H., Behrendt, A., Dahl, S. L., Damerell, V., Diebel, S., Kalman, S., Klein, S., Knudsen, A. C., Mäder, C., Merrill, S., Staudt, A., Thiel, V., Welti, L., Davey, N. E., Diella, F., and Gibson, T. J. (2016). ELM 2016–data update and new functionality of the eukaryotic linear motif resource. *Nucleic acids research*, 44(D1):D294–300. ↑70

Discher, D. E., Janmey, P., and Wang, Y.-l. (2005). Tissue Cells Feel and Respond to the Stiffness of Their Substrate. *Science*, 310(5751):1139 LP – 1143. ↑35

Dominguez, R. and Holmes, K. C. (2011). Actin Structure and Function. *Annual Review of Biophysics*, 40(1):169–186. ↑38

Donahue, A. C. and Fruman, D. A. (2004). PI3K signaling controls cell fate at many points in B lymphocyte development and activation. *Seminars in Cell and Developmental Biology*, 15(2):183–197. ↑25, ↑45

Donahue, A. C. and Fruman, D. A. (2007). Distinct signaling mechanisms activate the target of rapamycin in response to different B-cell stimuli. *European Journal of Immunology*, 37(10):2923–2936. ↑25

Doughty, C. A., Bleiman, B. F., Wagner, D. J., Dufort, F. J., Mataraza, J. M., Roberts, M. F., and Chiles, T. C. (2006). Antigen receptor-mediated changes in glucose metabolism in B lymphocytes: role of phosphatidylinositol 3-kinase signaling in the glycolytic control of growth. *Blood*, 107(11):4458–65. ↑52

Drummond, M. L., Li, M., Tarapore, E., Nguyen, T. T. L., Barouni, B. J., Cruz, S., Tan, K. C., Oro, A. E., and Atwood, S. X. (2018). Actin polymerization controls cilia-mediated signaling. *The Journal of Cell Biology*. ↑63, ↑93, ↑101

Du, P., Wang, S., Tang, X., An, C., Yang, Y., and Jiang, W. G. (2017). Reduced Expression of Metastasis Suppressor-1 (MTSS1) Accelerates Progression of Human Bladder Uroepithelium Cell Carcinoma. *Anticancer research*, 37(8):4499–4505. ↑61

Du, P., Ye, L., Li, H., Yang, Y., and Jiang, W. G. (2012). The tumour suppressive role of metastasis suppressor-1, MTSS1, in human kidney cancer, a possible connection with the SHH pathway. *Journal of experimental therapeutics & oncology*, 10(2):91–9. ↑61

Du, P., Ye, L., Ruge, F., Yang, Y., and Jiang, W. G. (2011). Metastasis suppressor-1, MTSS1, acts as a putative tumour suppressor in human bladder cancer. *Anticancer research*, 31(10):3205–12. ↑61

Dufort, F. J., Bleiman, B. F., Gumina, M. R., Blair, D., Wagner, D. J., Roberts, M. F., Abu-Amer, Y., and Chiles, T. C. (2007). Cutting edge: IL-4-mediated protection of primary B lymphocytes from apoptosis via Stat6-dependent regulation of glycolytic metabolism. *Journal of immunology (Baltimore, Md. : 1950)*, 179(8):4953–7. ↑52

Dufort, F. J., Gumina, M. R., Ta, N. L., Tao, Y., Heyse, S. A., Scott, D. A., Richardson, A. D., Seyfried, T. N., and Chiles, T. C. (2014). Glucose-dependent de novo lipogenesis in B lymphocytes: A requirement for atp-citrate lyase in lipopolysaccharide-induced differentiation. *Journal of Biological Chemistry*, 289(10):7011–7024. ↑55

Dugina, V. B., Shagieva, G. S., and Kopnin, P. B. (2019). Biological Role of Actin Isoforms in Mammalian Cells. *Biochemistry (Moscow)*, 84(6):583–592. ↑37

Duret, L., Gasteiger, E., and Perrière, G. (1996). LALNVIEW: a graphical viewer for pairwise sequence alignments. *Computer applications in the biosciences : CABIOS*, 12(6):507–10. ↑70

Dustin, M. L. and Choudhuri, K. (2016). Signaling and Polarized Communication Across the T Cell Immunological Synapse. *Annual Review of Cell and Developmental Biology*, 32(1):303–325. ↑34

Eitzen, G. (2003). Actin remodeling to facilitate membrane fusion. *Biochimica et biophysica acta*, 1641(2-3):175–81. ↑42

Engelke, M., Oellerich, T., Dittmann, K., Hsiao, H.-H., Urlaub, H., Serve, H., Griesinger, C., and Wienands, J. (2013). Cutting Edge: Feed-Forward Activation of Phospholipase Cγ2 via C2 Domain–Mediated Binding to SLP65. *The Journal of Immunology*, 191(11):5354–5358. ↑104

Erdős, G. and Dosztányi, Z. (2020). Analyzing Protein Disorder with IUPred2A. *Current Protocols in Bioinformatics*, 70(1):e99. ↑89

Erikson, J., Radic, M. Z., Camper, S. A., Hardy, R. R., Carmack, C., and Weigert, M. (1991). Expression of anti-DNA immunoglobulin transgenes in non-autoimmune mice. *Nature*, 349(6307):331–334. ↑22

Ersching, J., Efeyan, A., Mesin, L., Jacobsen, J. T., Pasqual, G., Grabiner, B. C., Dominguez-Sola, D., Sabatini, D. M., and Victora, G. D. (2017). Germinal Center Selection and Affinity Maturation Require Dynamic Regulation of mTORC1 Kinase. *Immunity*, 46(6):1045–1058.e6. ↑54

Esplin, B. L., Welner, R. S., Zhang, Q., Borghesi, L. A., and Kincade, P. W. (2009). A differentiation pathway for B1 cells in adult bone marrow. *Proceedings of the National Academy of Sciences of the United States of America*, 106(14):5773–5778. ↑23

Feldmann, M. and Basten, A. (1971). THE RELATIONSHIP BETWEEN ANTIGENIC STRUCTURE AND THE REQUIREMENT FOR THYMUS-DERIVED CELLS IN THE IMMUNE RESPONSE. *The Journal of Experimental Medicine*, 134(1):103–119. ↑32

Ferguson, A. R., Youd, M. E., and Corley, R. B. (2004). Marginal zone B cells transport and deposit IgM-containing immune complexes onto follicular dendritic cells. *International immunology*, 16(10):1411–22. ↑27, ↑30

Field, M. C., Sali, A., and Rout, M. P. (2011). Evolution: On a bender–BARs, ESCRTs, COPs, and finally getting your coat. *The Journal of cell biology*, 193(6):963–72. ↑94

Fillatreau, S., Sweenie, C. H., McGeachy, M. J., Gray, D., and Anderton, S. M. (2002). B cells regulate autoimmunity by provision of IL-10. *Nature Immunology*, 3(10):944–950. ↑20

Finkin, S., Hartweger, H., Oliveira, T. Y., Kara, E. E., and Nussenzweig, M. C. (2019). Protein Amounts of the MYC Transcription Factor Determine Germinal Center B Cell Division Capacity. *Immunity*, 51(2):324–336.e5. ↑54

Firat-Karalar, E. N. and Welch, M. D. (2011). New mechanisms and functions of actin nucleation. *Current Opinion in Cell Biology*, 23(1):4–13. ↑39

Flanagan, J. and Koch, G. L. (1978). Cross-linked surface Ig attaches to actin. *Nature*, 273(5660):278–281. ↑41

Fleire, S. J., Goldman, J. P., Carrasco, Y. R., Weber, M., Bray, D., and Batista, F. D. (2006). B cell ligand discrimination through a spreading and contraction response. *Science (New York, N.Y.)*, 312(5774):738–41. ↑34, ↑42, ↑43

Fliegauf, M., Benzing, T., and Omran, H. (2007). When cilia go bad: Cilia defects and ciliopathies. *Nature Reviews Molecular Cell Biology*, 8(11):880–893. ↑101

Förster, I. and Rajewsky, K. (1987). Expansion and functional activity of Ly-1+ B cells upon transfer of peritoneal cells into allotype-congenic, newborn mice. *European Journal of Immunology*, 17(4):521–528. ↑23

Freeman, S. A., Lei, V., Dang-Lawson, M., Mizuno, K., Roskelley, C. D., and Gold, M. R. (2011). Cofilin-Mediated F-Actin Severing Is Regulated by the Rap GTPase and Controls the Cytoskeletal Dynamics That Drive Lymphocyte Spreading and BCR Microcluster Formation. *The Journal of Immunology*, 187(11):5887–5900. ↑42, ↑44

Fu, C., Turck, C. W., Kurosaki, T., and Chan, A. C. (1998). BLNK: a Central Linker Protein in B Cell Activation. *Immunity*, 9(1):93–103. ↑25, ↑44

Fujikawa, K., Miletic, A. V., Alt, F. W., Faccio, R., Brown, T., Hoog, J., Fredericks, J., Nishi, S., Mildiner, S., Moores, S. L., Brugge, J., Rosen, F. S., and Swat, W. (2003). Vav1/2/3-null mice

define an essential role for Vav family proteins in lymphocyte development and activation but a differential requirement in MAPK signaling in T and B cells. *The Journal of experimental medicine*, 198(10):1595–608. ↑44, ↑45

Fujimoto, M., Bradney, A. P., Poe, J. C., Steeber, D. A., and Tedder, T. F. (1999). Modulation of B lymphocyte antigen receptor signal transduction by a CD19/CD22 regulatory loop. *Immunity*, 11(2):191–200. ↑35

Fukuda, T., Kitamura, D., Taniuchi, I., Maekawa, Y., Benhamou, L. E., Sarthou, P., and Watanabe, T. (1995). Restoration of surface IgM-mediated apoptosis in an anti-IgM-resistant variant of WEHI-231 lymphoma cells by HS1, a protein-tyrosine kinase substrate. *Proceedings of the National Academy of Sciences*, 92(16):7302–7306. ↑50

GABBIANI, G., CHAPONNIER, C., ZUMBE, A., and VASSALLI, P. (1977). Actin and tubulin co-cap with surface immunoglobulins in mouse B lymphocytes. *Nature*, 269(5630):697–698. ↑41

Gao, J., Aksoy, B. A., Dogrusoz, U., Dresdner, G., Gross, B., Sumer, S. O., Sun, Y., Jacobsen, A., Sinha, R., Larsson, E., Cerami, E., Sander, C., and Schultz, N. (2013). Integrative analysis of complex cancer genomics and clinical profiles using the cBioPortal. *Science signaling*, 6(269):pl1. ↑72, ↑91

García de Vinuesa, C., O'Leary, P., Sze, D. M.-Y., Toellner, K. M., and MacLennan, I. C. (1999). T-independent type 2 antigens induce B cell proliferation in multiple splenic sites, but exponential growth is confined to extrafollicular foci. *European journal of immunology*, 29(4):1314–23. ↑108

Garcia-Manteiga, J. M., Mari, S., Godejohann, M., Spraul, M., Napoli, C., Cenci, S., Musco, G., and Sitia, R. (2011). Metabolomics of B to plasma cell differentiation. *Journal of Proteome Research*, 10(9):4165–4176. ↑55

Gasiorowski, J. Z., Murphy, C. J., and Nealey, P. F. (2013). Biophysical Cues and Cell Behavior: The Big Impact of Little Things. *Annual Review of Biomedical Engineering*, 15(1):155–176. ↑35

Gauld, S. B. and Cambier, J. C. (2004). Src-family kinases in B-cell development and signaling. *Oncogene*, 23(48):8001–8006. ↑24

Gerlach, J., Ghosch, S., Jumaa, H., Reth, M., Wienands, J., Chan, A. C., and Nitschke, L. (2003). B cell defects in SLP65/BLNK-deficient mice can be partially corrected by the absence of CD22, an inhibitory coreceptor for BCR signaling. *European Journal of Immunology*, 33(12):3418–3426. ↑104

Ghosn, E. E. B., Yang, Y., Tung, J., Herzenberg, L. A., and Herzenberg, L. A. (2008). CD11b expression distinguishes sequential stages of peritoneal B-1 development. *Proceedings of the National Academy of Sciences of the United States of America*, 105(13):5195–200. ↑23

Girkontaite, I., Missy, K., Sakk, V., Harenberg, A., Tedford, K., Pötzel, T., Pfeffer, K., and Fischer, K.-D. (2001). Lsc is required for marginal zone B cells, regulation of lymphocyte motility and immune responses. *Nature Immunology*, 2(9):855–862. ↑30, ↑100

Gitlin, A. D., Shulman, Z., and Nussenzweig, M. C. (2014). Clonal selection in the germinal centre by regulated proliferation and hypermutation. *Nature*, 509(7502):637–640. ↑27

Glassmann, A., Molly, S., Surchev, L., Nazwar, T. A., Holst, M., Hartmann, W., Baader, S. L., Oberdick, J., Pietsch, T., and Schilling, K. (2007). Developmental expression and differentiation-related neuron-specific splicing of metastasis suppressor 1 (Mtss1) in normal and transformed cerebellar cells. *BMC developmental biology*, 7(1):111. ↑89

Godin, I. E., Garcia-Porrero, J. A., Coutinho, A., Dieterlen-Lièvre, F., and Marcos, M. A. R. (1993). Para-aortic splanchnopleura from early mouse embryos contains B1a cell progenitors. *Nature*, 364(6432):67–70. ↑23

Goldsby, R. A., Kindt, T. J., Osborne, B. A., and Kuby, J. (2003). *Immunology*. W. H. Freeman, New York, 5th edition. ↑16, ↑19

González, D., Van Der Burg, M., García-Sanz, R., Fenton, J. A., Langerak, A. W., González, M., Van Dongen, J. J., San Miguel, J. F., and Morgan, G. J. (2007). Immunoglobulin gene rearrangements and the pathogenesis of multiple myeloma. *Blood*, 110(9):3112–3121. ↑21

Gonzalez-Quevedo, R., Shoffer, M., Horng, L., and Oro, A. E. (2005). Receptor tyrosine phosphatase-dependent cytoskeletal remodeling by the hedgehog-responsive gene MIM/BEG4. *The Journal of cell biology*, 168(3):453–63. ↑58, ↑59, ↑64

Goode, B. L. and Eck, M. J. (2007). Mechanism and function of formins in the control of actin assembly. *Annual Review of Biochemistry*, 76:593–627. ↑38

Goodnow, C. C., Crosbie, J., Adelstein, S., Lavoie, T. B., Smith-Gill, S. J., Brink, R. A., Pritchard-Briscoe, H., Wotherspoon, J. S., Loblay, R. H., Raphael, K., Trent, R. J., and Basten, A. (1988). Altered immunoglobulin expression and functional silencing of self-reactive B lymphocytes in transgenic mice. *Nature*, 334(6184):676–682. ↑22, ↑32

Grakoui, A., Bromley, S. K., Sumen, C., Davis, M. M., Shaw, A. S., Allen, P. M., and Dustin, M. L. (1999). The immunological synapse: a molecular machine controlling T cell activation. *Science (New York, N.Y.)*, 285(5425):221–227. ↑34, ↑80

Grazi, E. (1997). What is the diameter of the actin filament? *FEBS Letters*, 405(3):249–252. ↑38

Grumont, R. J. and Gerondakis, S. (2000). Rel induces interferon regulatory factor 4 (IRF-4) expression in lymphocytes: Modulation of interferon-regulated gene expression by Rel/nuclear factor κB. *Journal of Experimental Medicine*, 191(8):1281–1291. ↑56

Guinamard, R., Okigaki, M., Schlessinger, J., and Ravetch, J. V. (2000). Absence of marginal zone B cells in Pyk-2–deficient mice defines their role in the humoral response. *Nature Immunology*, 1(1):31–36. ↑23, ↑30, ↑100

Gunning, P. W., Ghoshdastider, U., Whitaker, S., Popp, D., and Robinson, R. C. (2015). The evolution of compositionally and functionally distinct actin filaments. *Journal of Cell Science*, 128(11):2009–2019. ↑38

Guo, B., Su, T. T., and Rawlings, D. J. (2004). Protein kinase C family functions in B-cell activation. *Current Opinion in Immunology*, 16(3):367–373. ↑26

Guo, F., Velu, C. S., Grimes, H. L., and Zheng, Y. (2009). Rho GTPase Cdc42 is essential for B-lymphocyte development and activation. *Blood*, 114(14):2909–2916. ↑51

Gupta, N., Wollscheid, B., Watts, J. D., Scheer, B., Aebersold, R., and DeFranco, A. L. (2006). Quantitative proteomic analysis of B cell lipid rafts reveals that ezrin regulates antigen receptor–mediated lipid raft dynamics. *Nature Immunology*, 7(6):625–633. ↑44

Guthmiller, J. J., Graham, A. C., Zander, R. A., Pope, R. L., and Butler, N. S. (2017). Cutting Edge: IL-10 Is Essential for the Generation of Germinal Center B Cell Responses and Anti- Plasmodium Humoral Immunity. *The Journal of Immunology*, 198(2):617–622. ↑20

Ha, S. A., Tsuji, M., Suzuki, K., Meek, B., Yasuda, N., Kaisho, T., and Fagarasan, S. (2006). Regulation of B1 cell migration by signals through Toll-like receptors. *Journal of Experimental Medicine*, 203(11):2541–2550. ↑23

Haas, K. M. (2011). Programmed Cell Death 1 Suppresses B-1b Cell Expansion and Long-Lived IgG Production in Response to T Cell-Independent Type 2 Antigens. *The Journal of Immunology*, 187(10):5183–5195. ↑30, ↑100

Haas, K. M., Poe, J. C., Steeber, D. A., and Tedder, T. F. (2005). B-1a and B-1b cells exhibit distinct developmental requirements and have unique functional roles in innate and adaptive immunity to S. pneumoniae. *Immunity*, 23(1):7–18. ↑23

Haferlach, T., Kohlmann, A., Wieczorek, L., Basso, G., Kronnie, G. T., Béné, M.-C., De Vos, J., Hernández, J. M., Hofmann, W.-K., Mills, K. I., Gilkes, A., Chiaretti, S., Shurtleff, S. A., Kipps, T. J., Rassenti, L. Z., Yeoh, A. E., Papenhausen, P. R., Liu, W.-M., Williams, P. M., and Foà, R. (2010). Clinical utility of microarray-based gene expression profiling in the diagnosis and subclassification of leukemia: report from the International Microarray Innovations in Leukemia Study Group. *Journal of clinical oncology : official journal of the American Society of Clinical Oncology*, 28(15):2529–37. ↑73

Hagman, J. (2009). Conveying the Message: Identification of Ig-α and Ig-β as Components of the B Cell Receptor Complex. *The Journal of Immunology*, 183(3):1503–1504. ↑24

Hallek, M., Cheson, B. D., Catovsky, D., Caligaris-Cappio, F., Dighiero, G., Döhner, H., Hillmen, P., Keating, M., Montserrat, E., Chiorazzi, N., Stilgenbauer, S., Rai, K. R., Byrd, J. C., Eichhorst, B.,

O'Brien, S., Robak, T., Seymour, J. F., and Kipps, T. J. (2018). iwCLL guidelines for diagnosis, indications for treatment, response assessment, and supportive management of CLL. *Blood*, 131(25):2745–2760. ↑73

Hammad, H., Vanderkerken, M., Pouliot, P., Deswarte, K., Toussaint, W., Vergote, K., Vandersarren, L., Janssens, S., Ramou, I., Savvides, S. N., Haigh, J. J., Hendriks, R., Kopf, M., Craessaerts, K., de Strooper, B., Kearney, J. F., Conrad, D. H., and Lambrecht, B. N. (2017). Transitional B cells commit to marginal zone B cell fate by Taok3-mediated surface expression of ADAM10. *Nature Immunology*, 18(3):313–320. ↑23

Hampton, H. R. and Chtanova, T. (2019). Lymphatic migration of immune cells. *Frontiers in Immunology*, 10(MAY):19–23. ↑27

Hao, J.-J., Liu, Y., Kruhlak, M., Debell, K. E., Rellahan, B. L., and Shaw, S. (2009). Phospholipase C-mediated hydrolysis of PIP2 releases ERM proteins from lymphocyte membrane. *The Journal of cell biology*, 184(3):451–62. ↑44

Hao, S. and August, A. (2005). Actin Depolymerization Transduces the Strength of B-Cell Receptor Stimulation. *Molecular Biology of the Cell*, 16(5):2275–2284. ↑41, ↑42, ↑44

Hardy, R. R., Kincade, P. W., and Dorshkind, K. (2007). The Protean Nature of Cells in the B Lymphocyte Lineage. *Immunity*, 26(6):703–714. ↑21

Hartley, S. B., Crosbie, J., Brink, R., Kantor, A. B., Basten, A., and Goodnow, C. C. (1991). Elimination from peripheral lymphoid tissues of self-reactive B lymphocytes recognizing membrane-bound antigens. *Nature*, 353(6346):765–769. ↑22

Hartzell, C. A., Jankowska, K. I., Burkhardt, J. K., and Lewis, R. S. (2016). Calcium influx through CRAC channels controls actin organization and dynamics at the immune synapse. *eLife*, 5(2016JULY):1–28. ↑44, ↑105

Harwood, N. E. and Batista, F. D. (2011). The Cytoskeleton Coordinates the Early Events of B-cell Activation. *Cold Spring Harbor Perspectives in Biology*, 3(2):a002360–a002360. ↑34

Hayakawa, K., Hardy, R. R., Herzenberg, L. A., and Herzenberg, L. A. (1985). Progenitors for Ly-1 B cells are distinct from progenitors for other B cells. *Journal of Experimental Medicine*, 161(6):1554–1568. ↑23

Heesters, B. A., Chatterjee, P., Kim, Y.-A., Gonzalez, S. F., Kuligowski, M. P., Kirchhausen, T., and Carroll, M. C. (2013). Endocytosis and recycling of immune complexes by follicular dendritic cells enhances B cell antigen binding and activation. *Immunity*, 38(6):1164–75. ↑31, ↑34

Heesters, B. A., van der Poel, C. E., Das, A., and Carroll, M. C. (2016). Antigen Presentation to B Cells. *Trends in Immunology*, 37(12):844–854. ↑30

Heilker, R., Spiess, M., and Crottet, P. (1999). Recognition of sorting signals by clathrin adaptors. *BioEssays*, 21(7):558–567. ↑89

Heintzman, N. D., Stuart, R. K., Hon, G., Fu, Y., Ching, C. W., Hawkins, R. D., Barrera, L. O., Van Calcar, S., Qu, C., Ching, K. A., Wang, W., Weng, Z., Green, R. D., Crawford, G. E., and Ren, B. (2007). Distinct and predictive chromatin signatures of transcriptional promoters and enhancers in the human genome. *Nature genetics*, 39(3):311–8. ↑92

Heldin, C.-H. (1995). Dimerization of cell surface receptors in signal transduction. *Cell*, 80(2):213–223. ↑31

Hendriks, R. W. and Middendorp, S. (2004). The pre-BCR checkpoint as a cell-autonomous proliferation switch. *Trends in Immunology*, 25(5):249–256. ↑21

Henriksen, A., Godal, T., and Landaas, T. O. (1980). Mitogenic effect on human lymphocytes of insolubilized anti-immunoglobulins. I. Specificity of the stimulating agent. *Journal of immunology (Baltimore, Md. : 1950)*, 124(2):921–5. ↑33

Hepler, P. K. (2016). The Cytoskeleton and Its Regulation by Calcium and Protons. *Plant Physiology*, 170(1):3–22. ↑44

Holmes, A. B., Corinaldesi, C., Shen, Q., Kumar, R., Compagno, N., Wang, Z., Nitzan, M., Grunstein, E., Pasqualucci, L., Dalla-Favera, R., and Basso, K. (2020). Single-cell analysis of germinal-center B cells informs on lymphoma cell of origin and outcome. *Journal of Experimental Medicine*, 217(10). ↑105

Holodick, N. E. and Rothstein, T. L. (2013). Atypical response of B-1 cells to BCR ligation: A speculative model. *Frontiers in Immunology*, 4(DEC):1–8. ↑23

Hsu, C.-J., Hsieh, W.-T., Waldman, A., Clarke, F., Huseby, E. S., Burkhardt, J. K., and Baumgart, T. (2012). Ligand Mobility Modulates Immunological Synapse Formation and T Cell Activation. *PLoS ONE*, 7(2):e32398. ↑35

Hsu, M.-C., Toellner, K.-M., Vinuesa, C. G., and Maclennan, I. C. M. (2006). B cell clones that sustain long-term plasmablast growth in T-independent extrafollicular antibody responses. *Proceedings of the National Academy of Sciences of the United States of America*, 103(15):5905–10. ↑30, ↑100

Huber, M. and Lohoff, M. (2014). IRF4 at the crossroads of effector T-cell fate decision. *European Journal of Immunology*, 44(7):1886–1895. ↑56

Imamura, Y., Oda, A., Katahira, T., Bundo, K., Pike, K. A., Ratcliffe, M. J., and Kitamura, D. (2009). BLNK binds active H-Ras to promote B cell receptor-mediated capping and ERK activation. *Journal of Biological Chemistry*, 284(15):9804–9813. ↑104

Inaba, A., Tuong, Z. K., Riding, A. M., Mathews, R. J., Martin, J. L., Saeb-Parsy, K., and Clatworthy, M. R. (2020). B Lymphocyte–Derived CCL7 Augments Neutrophil and Monocyte Recruitment, Exacerbating Acute Kidney Injury. *The Journal of Immunology*, 205(5):1376–1384. ↑20

Ingham, R. J., Krebs, D. L., Barbazuk, S. M., Turck, C. W., Hirai, H., Matsuda, M., and Gold, M. R. (1996). B cell antigen receptor signaling induces the formation of complexes containing the Crk adapter proteins. *Journal of Biological Chemistry*, 271(50):32306–32314. ↑44

Ishiai, M., Kurosaki, M., Pappu, R., Okawa, K., Ronko, I., Fu, C., Shibata, M., Iwamatsu, A., Chan, A. C., and Kurosaki, T. (1999). BLNK required for coupling Syk to PLC gamma 2 and Rac1-JNK in B cells. *Immunity*, 10(1):117–125. ↑85

Italiani, P. and Boraschi, D. (2014). From monocytes to M1/M2 macrophages: Phenotypical vs. functional differentiation. *Frontiers in Immunology*, 5(OCT):1–22. ↑27

Jabara, H. H., McDonald, D. R., Janssen, E., Massaad, M. J., Ramesh, N., Borzutzky, A., Rauter, I., Benson, H., Schneider, L., Baxi, S., Recher, M., Notarangelo, L. D., Wakim, R., Dbaibo, G., Dasouki, M., Al-Herz, W., Barlan, I., Baris, S., Kutukculer, N., Ochs, H. D., Plebani, A., Kanariou, M., Lefranc, G., Reisli, I., Fitzgerald, K. A., Golenbock, D., Manis, J., Keles, S., Ceja, R., Chatila, T. A., and Geha, R. S. (2012). DOCK8 functions as an adaptor that links TLR-MyD88 signaling to B cell activation. *Nature Immunology*, 13(6):612–620. ↑100

Jang, K.-J., Mano, H., Aoki, K., Hayashi, T., Muto, A., Nambu, Y., Takahashi, K., Itoh, K., Taketani, S., Nutt, S. L., Igarashi, K., Shimizu, A., and Sugai, M. (2015). Mitochondrial function provides instructive signals for activation-induced B-cell fates. *Nature communications*, 6(1):6750. ↑53

Jellusova, J. (2018). Cross-talk between signal transduction and metabolism in B cells. *Immunology letters*, 201:1–13. ↑100

Johansen, T. and Lamark, T. (2011). Selective autophagy mediated by autophagic adapter proteins. *Autophagy*, 7(3):279–96. ↑89

Johmura, S., Oh-hora, M., Inabe, K., Nishikawa, Y., Hayashi, K., Vigorito, E., Kitamura, D., Turner, M., Shingu, K., Hikida, M., and Kurosaki, T. (2003). Regulation of Vav localization in membrane rafts by adaptor molecules Grb2 and BLNK. *Immunity*, 18(6):777–787. ↑45

Johnston, R. J., Poholek, A. C., DiToro, D., Yusuf, I., Eto, D., Barnett, B., Dent, A. L., Craft, J., and Crotty, S. (2009). Bcl6 and Blimp-1 Are Reciprocal and Antagonistic Regulators of T Follicular Helper Cell Differentiation. *Science*, 325(5943):1006–1010. ↑27

Jumaa, H., Mitterer, M., Reth, M., and Nielsen, P. J. (2001). The absence of SLP65 and Btk blocks B cell development at the preB cell receptor-positive stage. *European Journal of Immunology*, 31(7):2164–2169. ↑22

Junt, T., Moseman, E. A., Iannacone, M., Massberg, S., Lang, P. A., Boes, M., Fink, K., Henrickson, S. E., Shayakhmetov, D. M., Di Paolo, N. C., Van Rooijen, N., Mempel, T. R., Whelan, S. P., and Von Andrian, U. H. (2007). Subcapsular sinus macrophages in lymph nodes clear lymph-borne viruses and present them to antiviral B cells. *Nature*, 450(7166):110–114. ↑27, ↑30

Kalampokis, I., Yoshizaki, A., and Tedder, T. F. (2013). IL-10-producing regulatory B cells (B10 cells) in autoimmune disease. *Arthritis Research & Therapy*, 15(Suppl 1):S1. ↑20

Kantor, A. B., Merrill, C. E., Herzenberg, L. A., and Hillson, J. L. (1997). An unbiased analysis of V(H)-D-J(H) sequences from B-1a, B-1b, and conventional B cells. *Journal of immunology (Baltimore, Md. : 1950)*, 158(3):1175–86. ↑23

Kawabata Galbraith, K., Fujishima, K., Mizuno, H., Lee, S.-J., Uemura, T., Sakimura, K., Mishina, M., Watanabe, N., and Kengaku, M. (2018). MTSS1 Regulation of Actin-Nucleating Formin DAAM1 in Dendritic Filopodia Determines Final Dendritic Configuration of Purkinje Cells. *Cell reports*, 24(1):95–106.e9. ↑65, ↑99

Kelly, A. E., Kranitz, H., Dötsch, V., and Mullins, R. D. (2006). Actin binding to the central domain of WASP/Scar proteins plays a critical role in the activation of the Arp2/3 complex. *The Journal of biological chemistry*, 281(15):10589–97. ↑92

Ketchum, C., Miller, H., Song, W., and Upadhyaya, A. (2014). Ligand mobility regulates B cell receptor clustering and signaling activation. *Biophysical journal*, 106(1):26–36. ↑35, ↑43, ↑100

Khalil, A. M., Cambier, J. C., and Shlomchik, M. J. (2012). B cell receptor signal transduction in the GC is short-circuited by high phosphatase activity. *Science (New York, N.Y.)*, 336(6085):1178–81. ↑105, ↑108

Khan, A., Fornes, O., Stigliani, A., Gheorghe, M., Castro-Mondragon, J. A., van der Lee, R., Bessy, A., Chèneby, J., Kulkarni, S. R., Tan, G., Baranasic, D., Arenillas, D. J., Sandelin, A., Vandepoele, K., Lenhard, B., Ballester, B., Wasserman, W. W., Parcy, F., and Mathelier, A. (2018). JASPAR 2018: update of the open-access database of transcription factor binding profiles and its web framework. *Nucleic acids research*, 46(D1):D260–D266. ↑74, ↑92

Kim, S., Lee, K., Choi, J.-H., Ringstad, N., and Dynlacht, B. D. (2015). Nek2 activation of Kif24 ensures cilium disassembly during the cell cycle. *Nature communications*, 6:8087. ↑93

Kim, Y. J., Sekiya, F., Poulin, B., Bae, Y. S., and Rhee, S. G. (2004). Mechanism of B-Cell Receptor-Induced Phosphorylation and Activation of Phospholipase C-γ2. *Molecular and Cellular Biology*, 24(22):9986–9999. ↑25

Kim, Y.-M., Pan, J. Y.-J., Korbel, G. A., Peperzak, V., Boes, M., and Ploegh, H. L. (2006). Monovalent ligation of the B cell receptor induces receptor activation but fails to promote antigen presentation. *Proceedings of the National Academy of Sciences of the United States of America*, 103(9):3327–32. ↑32

King, H. W., Orban, N., Riches, J. C., Clear, A. J., Warnes, G., Teichmann, S. A., and James, L. K. (2020). Antibody repertoire and gene expression dynamics of diverse human B cell states during affinity maturation. *bioRxiv*, page 2020.04.28.054775. ↑105, ↑108

Kirkland, T. N., Sieckmann, D. G., Longo, D. L., and Mosier, D. E. (1980). Cellular requirements for antigen presentation in the induction of a thymus-independent antibody response in vitro. *Journal of immunology (Baltimore, Md. : 1950)*, 124(4):1721–6. ↑30

Klein, U., Casola, S., Cattoretti, G., Shen, Q., Lia, M., Mo, T., Ludwig, T., Rajewsky, K., and Dalla-Favera, R. (2006). Transcription factor IRF4 controls plasma cell differentiation and class-switch recombination. *Nature immunology*, 7(7):773–82. ↑56

Kline, G. H., Hartwell, L., Beck-Engeser, G. B., Keyna, U., Zaharevitz, S., Klinman, N. R., and Jäck, H. M. (1998). Pre-B cell receptor-mediated selection of pre-B cells synthesizing functional mu heavy chains. *Journal of immunology (Baltimore, Md. : 1950)*, 161(4):1608–18. ↑22

Koonin, E. V. and Makarova, K. S. (2019). Origins and evolution of CRISPR-Cas systems. *Philosophical transactions of the Royal Society of London. Series B, Biological sciences*, 374(1772):20180087. ↑16

Kosakovsky Pond, S. L. and Frost, S. D. W. (2005). Not so different after all: a comparison of methods for detecting amino acid sites under selection. *Molecular biology and evolution*, 22(5):1208–22. ↑72

Kozono, Y., Duke, R. C., Schleicher, M. S., and Holers, V. M. (1995). Co-ligation of mouse complement receptors 1 and 2 with surface IgM rescues splenic B cells and WEHI-231 cells from anti-surface IgM-induced apoptosis. *European Journal of Immunology*, 25(4):1013–1017. ↑33

Kulakovskiy, I. V., Vorontsov, I. E., Yevshin, I. S., Sharipov, R. N., Fedorova, A. D., Rumynskiy, E. I., Medvedeva, Y. A., Magana-Mora, A., Bajic, V. B., Papatsenko, D. A., Kolpakov, F. A., and Makeev, V. J. (2018). HOCOMOCO: towards a complete collection of transcription factor binding models for human and mouse via large-scale ChIP-Seq analysis. *Nucleic acids research*, 46(D1):D252–D259. ↑74, ↑92

Kumar, M., Gouw, M., Michael, S., Sámano-Sánchez, H., Pancsa, R., Glavina, J., Diakogianni, A., Valverde, J. A., Bukirova, D., Signalyševa, J., Palopoli, N., Davey, N. E., Chemes, L. B., and Gibson, T. J. (2020). ELM-the eukaryotic linear motif resource in 2020. *Nucleic Acids Research*, 48(D1):D296–D306. ↑68

Kumar, S., Stecher, G., Suleski, M., and Hedges, S. B. (2017). TimeTree: A Resource for Timelines, Timetrees, and Divergence Times. *Molecular Biology and Evolution*, 34(7):1812–1819. ↑71

Kuokkanen, E., Šuštar, V., and Mattila, P. K. (2015). Molecular Control of B Cell Activation and Immunological Synapse Formation. *Traffic*, 16(4):311–326. ↑34

Kurosaki, T. (2011). Regulation of BCR signaling. *Molecular Immunology*, 48(11):1287–1291. ↑104

Kwak, K., Quizon, N., Sohn, H., Saniee, A., Manzella-Lapeira, J., Holla, P., Brzostowski, J., Lu, J., Xie, H., Xu, C., Spillane, K. M., Tolar, P., and Pierce, S. K. (2018). Intrinsic properties of human germinal center B cells set antigen affinity thresholds. *Science Immunology*, 3(29):eaau6598. ↑43

Lam, W. Y., Becker, A. M., Kennerly, K. M., Wong, R., Curtis, J. D., Llufrio, E. M., McCommis, K. S., Fahrmann, J., Pizzato, H. A., Nunley, R. M., Lee, J., Wolfgang, M. J., Patti, G. J., Finck, B. N., Pearce, E. L., and Bhattacharya, D. (2016). Mitochondrial Pyruvate Import Promotes Long-Term Survival of Antibody-Secreting Plasma Cells. *Immunity*, 45(1):60–73. ↑55

Lane, P. J., Gray, D., Oldfield, S., and MacLennan, I. C. (1986). Differences in the recruitment of virgin B cells into antibody responses to thymus-dependent and thymus-independent type-2 antigens. *European Journal of Immunology*. ↑30

Lanzavecchia, A. (1985). Antigen-specific interaction between T and B cells. *Nature*, 314(6011):537–9. ↑36

Lee, A. M., Colin-York, H., and Fritzsche, M. (2017). CalQuo 2 : Automated Fourier-space, population-level quantification of global intracellular calcium responses. *Scientific Reports*, 7(1):1–11. ↑81, ↑96

Lee, S. H. and Dominguez, R. (2010). Regulation of actin cytoskeleton dynamics in cells. *Molecules and cells*, 29(4):311–25. ↑39, ↑41

Lee, S. H., Kerff, F., Chereau, D., Ferron, F., Klug, A., and Dominguez, R. (2007). Structural basis for the actin-binding function of missing-in-metastasis. *Structure (London, England : 1993)*, 15(2):145–55. ↑57, ↑58, ↑72, ↑90

Lee, Y.-G., Macoska, J. A., Korenchuk, S., and Pienta, K. J. (2002). MIM, a potential metastasis suppressor gene in bladder cancer. *Neoplasia (New York, N.Y.)*, 4(4):291–4. ↑56, ↑61

Letunic, I. and Bork, P. (2018). 20 years of the SMART protein domain annotation resource. *Nucleic Acids Research*, 46(D1):D493–D496. ↑70, ↑71

Li, J., Yin, W., Jing, Y., Kang, D., Yang, L., Cheng, J., Yu, Z., Peng, Z., Li, X., Wen, Y., Sun, X., Ren, B., and Liu, C. (2019). The Coordination Between B Cell Receptor Signaling and the Actin Cytoskeleton During B Cell Activation. *Frontiers in Immunology*, 9(JAN):1–13. ↑41

Li, L., Baxter, S. S., Gu, N., Ji, M., and Zhan, X. (2017). Missing-in-metastasis protein downregulates CXCR4 by promoting ubiquitylation and interaction with small Rab GTPases. *Journal of cell science*, 130(8):1475–1485. ↑63, ↑66

Lillemeier, B. F., Mörtelmaier, M. A., Forstner, M. B., Huppa, J. B., Groves, J. T., and Davis, M. M. (2010). TCR and Lat are expressed on separate protein islands on T cell membranes and concatenate during activation. *Nature Immunology*, 11(1):90–96. ↑32

Limon, J. J. and Fruman, D. A. (2012). Akt and mTOR in B cell activation and differentiation. *Frontiers in Immunology*, 3(AUG):1–12. ↑25

Lin, J., Liu, J., Wang, Y., Zhu, J., Zhou, K., Smith, N., and Zhan, X. (2005). Differential regulation of cortactin and N-WASP-mediated actin polymerization by missing in metastasis (MIM) protein. *Oncogene*, 24(12):2059–66. ↑58, ↑59, ↑64, ↑93

Liu, C., Bai, X., Wu, J., Sharma, S., Upadhyaya, A., Dahlberg, C. I. M., Westerberg, L. S., Snapper, S. B., Zhao, X., and Song, W. (2013). N-wasp is essential for the negative regulation of B cell receptor signaling. *PLoS biology*, 11(11):e1001704. ↑50

Liu, C., Miller, H., Orlowski, G., Hang, H., Upadhyaya, A., and Song, W. (2012a). Actin reorganization is required for the formation of polarized B cell receptor signalosomes in response to both soluble and membrane-associated antigens. *Journal of immunology (Baltimore, Md. : 1950)*, 188(7):3237–46. ↑34, ↑41, ↑42, ↑99

Liu, C., Miller, H., Sharma, S., Beaven, A., Upadhyaya, A., and Song, W. (2012b). Analyzing actin dynamics during the activation of the B cell receptor in live B cells. *Biochemical and Biophysical Research Communications*, 427(1):202–206. ↑42

Liu, K., Wang, G., Ding, H., Chen, Y., Yu, G., and Wang, J. (2010a). Downregulation of metastasis suppressor 1(MTSS1) is associated with nodal metastasis and poor outcome in Chinese patients with gastric cancer. *BMC cancer*, 10(1):428. ↑61

Liu, W., Chen, E., Zhao, X. W., Wan, Z. P., Gao, Y. R., Davey, A., Huang, E., Zhang, L., Crocetti, J., Sandoval, G., Joyce, M. G., Miceli, C., Lukszo, J., Aravind, L., Swat, W., Brzostowski, J., and Pierce, S. K. (2012c). The scaffolding protein synapse-associated protein 97 is required for enhanced signaling through isotype-switched IgG memory B cell receptors. *Science signaling*, 5(235):ra54. ↑27

Liu, W., Komiya, Y., Mezzacappa, C., Khadka, D. K., Runnels, L., and Habas, R. (2011). MIM regulates vertebrate neural tube closure. *Development (Cambridge, England)*, 138(10):2035–47. ↑65

Liu, W., Meckel, T., Tolar, P., Sohn, H. W., and Pierce, S. K. (2010b). Antigen affinity discrimination is an intrinsic function of the B cell receptor. *The Journal of experimental medicine*, 207(5):1095–111. ↑34

Liu, Y., Beyer, A., and Aebersold, R. (2016). On the Dependency of Cellular Protein Levels on mRNA Abundance. *Cell*, 165(3):535–550. ↑104

Loberg, R. D., Neeley, C. K., Adam-Day, L. L., Fridman, Y., St John, L. N., Nixdorf, S., Jackson, P., Kalikin, L. M., and Pienta, K. J. (2005). Differential expression analysis of MIM (MTSS1) splice variants and a functional role of MIM in prostate cancer cell biology. *International journal of oncology*, 26(6):1699–705. ↑56, ↑61

Londhe, P., Yu, P. Y., Ijiri, Y., Ladner, K. J., Fenger, J. M., London, C., Houghton, P. J., and Guttridge, D. C. (2018). Classical NF-κB metabolically reprograms sarcoma cells through regulation of hexokinase 2. *Frontiers in Oncology*, 8(APR). ↑101

López-Lago, M., Lee, H., Cruz, C., Movilla, N., and Bustelo, X. R. (2000). Tyrosine Phosphorylation Mediates Both Activation and Downmodulation of the Biological Activity of Vav. *Molecular and Cellular Biology*, 20(5):1678–1691. ↑45

Löytynoja, A. (2014). Phylogeny-aware alignment with PRANK. *Methods in molecular biology (Clifton, N.J.)*, 1079:155–70. ↑71

Luxembourg, A. T., Brunmark, A., Kong, Y., Jackson, M. R., Peterson, P. A., Sprent, J., and Cai, Z. (1998). Requirements for Stimulating Naive CD8+ T Cells via Signal 1 Alone. *The Journal of Immunology*, 161(10):5226 LP – 5235. ↑35, ↑100

Ma, S., Guan, X.-Y., Lee, T. K., and Chan, K. W. (2007). Clinicopathological significance of missing in metastasis B expression in hepatocellular carcinoma. *Human pathology*, 38(8):1201–6. ↑62, ↑91

Maas, A. and Hendriks, R. W. (2001). Role of Bruton's tyrosine kinase in B cell development. *Developmental Immunology*, 8(3-4):171–181. ↑29

Machesky, L. M. and Johnston, S. A. (2007). MIM: a multifunctional scaffold protein. *Journal of molecular medicine (Berlin, Germany)*, 85(6):569–76. ↑57, ↑89, ↑92

MacKay, F. and Schneider, P. (2009). Cracking the BAFF code. *Nature Reviews Immunology*, 9(7):491–502. ↑22

Malhotra, S., Kovats, S., Zhang, W., and Coggeshall, K. M. (2009). B cell antigen receptor endocytosis and antigen presentation to T cells require Vav and dynamin. *The Journal of biological chemistry*, 284(36):24088–97. ↑43

Maravillas-Montero, J. L. and Santos-Argumedo, L. (2012). The myosin family: unconventional roles of actin-dependent molecular motors in immune cells. *Journal of Leukocyte Biology*, 91(1):35–46. ↑41

Marshall-Clarke, S., Tasker, L., and Parkhouse, R. M. (2000). Immature B lymphocytes from adult bone marrow exhibit a selective defect in induced hyperexpression of major histocompatibility complex class II and fail to show B7.2 induction. *Immunology*, 100(2):141–151. ↑22

Martin, F. and Kearney, J. F. (2000). Positive selection from newly formed to marginal zone B cells depends on the rate of clonal production, CD19, and btk. *Immunity*, 175(5):70–79. ↑23

Martin, F. and Kearney, J. F. (2002). Marginal-zone B cells. *Nature Reviews Immunology*, 2(5):323–335. ↑22, ↑23, ↑32

Martin, F., Oliver, A. M., and Kearney, J. F. (2001). Marginal Zone and B1 B Cells Unite in the Early Response against T-Independent Blood-Borne Particulate Antigens. *Immunity*, 14(5):617–629. ↑23

Maruyama, S., Kubagawa, H., and Cooper, M. D. (1985). Activation of human B cells and inhibition of their terminal differentiation by monoclonal anti-mu antibodies. *Journal of immunology (Baltimore, Md. : 1950)*, 135(1):192–9. ↑33

Mateu, M. G. (2012). Mechanical properties of viruses analyzed by atomic force microscopy: A virological perspective. *Virus Research*, 168(1-2):1–22. ↑35

Mattila, P. K., Batista, F. D., and Treanor, B. (2016). Dynamics of the actin cytoskeleton mediates receptor cross talk: An emerging concept in tuning receptor signaling. *The Journal of Cell Biology*, 212(3):267–280. ↑41, ↑95

Mattila, P. K., Feest, C., Depoil, D., Treanor, B., Montaner, B., Otipoby, K. L., Carter, R., Justement, L. B., Bruckbauer, A., and Batista, F. D. (2013). The Actin and Tetraspanin Networks Organize Receptor Nanoclusters to Regulate B Cell Receptor-Mediated Signaling. *Immunity*, 38(3):461–474. ↑32, ↑35, ↑42, ↑95

Mattila, P. K., Pykäläinen, A., Saarikangas, J., Paavilainen, V. O., Vihinen, H., Jokitalo, E., and Lappalainen, P. (2007). Missing-in-metastasis and IRSp53 deform PI(4,5)P2-rich membranes by an inverse BAR domain-like mechanism. *The Journal of cell biology*, 176(7):953–64. ↑58, ↑59, ↑64, ↑92

Mattila, P. K., Salminen, M., Yamashiro, T., and Lappalainen, P. (2003). Mouse MIM, a Tissue-specific Regulator of Cytoskeletal Dynamics, Interacts with ATP-Actin Monomers through Its C-terminal WH2 Domain. *Journal of Biological Chemistry*, 278(10):8452–8459. ↑57, ↑58, ↑59, ↑92

Maus, M., Medgyesi, D., Kiss, E., Schneider, A. E., Enyedi, A., Szilágyi, N., Matkó, J., and Sármay, G. (2013). B cell receptor-induced Ca2+ mobilization mediates F-actin rearrangements and is indispensable for adhesion and spreading of B lymphocytes. *Journal of leukocyte biology*, 93(4):537–47. ↑44, ↑105

McLeod, S. J., Ingham, R. J., Bos, J. L., Kurosaki, T., and Gold, M. R. (1998). Activation of the Rap1 GTPase by the B cell antigen receptor. *The Journal of biological chemistry*, 273(44):29218–29223. ↑44

Mérida, I., Carrasco, S., and Avila-Flores, A. (2010). Diacylglycerol Signaling: The C1 Domain, Generation of DAG, and Termination of Signals. In Kazanietz, Marcelo G. (School of Medicine University of Pennsylvania, Philadeliphia, U., editor, *Protein Kinase C in Cancer Signaling and Therapy*, pages 55–78. Humana Press, Totowa, NJ. ↑99

Merrell, K. T., Benschop, R. J., Gauld, S. B., Aviszus, K., Decote-Ricardo, D., Wysocki, L. J., and Cambier, J. C. (2006). Identification of Anergic B Cells within a Wild-Type Repertoire. *Immunity*, 25(6):953–962. ↑32

Mészáros, B., Dosztányi, Z., and Simon, I. (2012). Disordered binding regions and linear motifs–bridging the gap between two models of molecular recognition. *PloS one*, 7(10):e46829. ↑93

Mészáros, B., Erdos, G., and Dosztányi, Z. (2018). IUPred2A: context-dependent prediction of protein disorder as a function of redox state and protein binding. *Nucleic acids research*, 46(W1):W329–W337. ↑71

Michie, K. A., Bermeister, A., Robertson, N. O., Goodchild, S. C., and Curmi, P. M. (2019). Two Sides of the Coin: Ezrin/Radixin/Moesin and Merlin Control Membrane Structure and Contact Inhibition. *International journal of molecular sciences*, 20(8). ↑41, ↑44

Millard, T. H., Bompard, G., Heung, M. Y., Dafforn, T. R., Scott, D. J., Machesky, L. M., and Fütterer, K. (2005). Structural basis of filopodia formation induced by the IRSp53/MIM homology domain of human IRSp53. *The EMBO journal*, 24(2):240–50. ↑57

Miller, J. F. and Mitchell, G. F. (1968). Cell to cell interaction in the immune response. I. Hemolysin-forming cells in neonatally thymectomized mice reconstituted with thymus or thoracic duct lymphocytes. *The Journal of experimental medicine*, 128(4):801–20. ↑27

Minguet, S., Dopfer, E. P., Pollmer, C., Freudenberg, M. A., Galanos, C., Reth, M., Huber, M., and Schamel, W. W. (2008). Enhanced B-cell activation mediated by TLR4 and BCR crosstalk. *European journal of immunology*, 38(9):2475–87. ↑100

Minguet, S., Dopfer, E.-P., and Schamel, W. W. A. (2010). Low-valency, but not monovalent, antigens trigger the B-cell antigen receptor (BCR). *International Immunology*, 22(3):205–212. ↑32

Minkeviciene, R., Hlushchenko, I., Virenque, A., Lahti, L., Khanal, P., Rauramaa, T., Koistinen, A., Leinonen, V., Noe, F. M., and Hotulainen, P. (2019). MIM-Deficient Mice Exhibit Anatomical Changes in Dendritic Spines, Cortex Volume and Brain Ventricles, and Functional Changes in Motor Coordination and Learning. *Frontiers in Molecular Neuroscience*, 12(November):1–20. ↑63

Mitchell, G. F. and Miller, J. F. (1968). Cell to cell interaction in the immune response. II. The source of hemolysin-forming cells in irradiated mice given bone marrow and thymus or thoracic duct lymphocytes. *The Journal of experimental medicine*, 128(4):821–37. ↑27

Mittrücker, H.-W., Matsuyama, T., Grossman, A., Kündig, T. M., Potter, J., Shahinian, A., Wakeham, A., Patterson, B., Ohashi, P. S., and Mak, T. W. (1997). Requirement for the Transcription Factor LSIRF/IRF4 for Mature B and T Lymphocyte Function. *Science*, 275(5299):540 LP – 543. ↑56

Mond, J. J., Finkelman, F. D., Sarma, C., Ohara, J., and Serrate, S. (1985). Recombinant interferon-gamma inhibits the B cell proliferative response stimulated by soluble but not by Sepharose-bound anti-immunoglobulin antibody. *Journal of immunology (Baltimore, Md. : 1950)*, 135(4):2513–2517. ↑33

Mond, J. J., Mongini, P. K., Sieckmann, D., and Paul, W. E. (1980). Role of T lymphocytes in the response to TNP-AECM-Ficoll. *Journal of immunology (Baltimore, Md. : 1950)*, 125(3):1066–70. ↑29

Monroe, J. G. and Cambier, J. C. (1983). B cell activation. I. Anti-immunoglobulin-induced receptor cross-linking results in a decrease in the plasma membrane potential of murine B lymphocytes. *The Journal of experimental medicine*, 157(6):2073–86. ↑31

Monroe, J. G. and Dorshkind, K. (2007). Fate Decisions Regulating Bone Marrow and Peripheral B Lymphocyte Development. *Advances in Immunology*, 95(07):1–50. ↑22

Moore, P. B., Huxley, H. E., and DeRosier, D. J. (1970). Three-dimensional reconstruction of F-actin, thin filaments and decorated thin filaments. *Journal of Molecular Biology*, 50(2):279–296. ↑38

Morbach, H., Schickel, J. N., Cunningham-Rundles, C., Conley, M. E., Reisli, I., Franco, J. L., and Meffre, E. (2016). CD19 controls Toll-like receptor 9 responses in human B cells. *Journal of Allergy and Clinical Immunology*, 137(3):889–898.e6. ↑29, ↑100

Morley, M. P., Wang, X., Hu, R., Brandimarto, J., Tucker, N. R., Felix, J. F., Smith, N. L., van der Harst, P., Ellinor, P. T., Margulies, K. B., Musunuru, K., and Cappola, T. P. (2019). Cardioprotective Effects of MTSS1 Enhancer Variants. *Circulation*, 139(17):2073–2076. ↑63

Morris, D. L. and Rothstein, T. L. (1993). Abnormal transcription factor induction through the surface immunoglobulin M receptor of B-1 lymphocytes. *Journal of Experimental Medicine*, 177(3):857–861. ↑23

Morrison, D. K. (2012). MAP kinase pathways. *Cold Spring Harbor perspectives in biology*, 4(11):a011254–a011254. ↑25

Mosier, D. E. and Subbarao, B. (1982). Thymus-independent antigens: complexity of B-lymphocyte activation revealed. *Immunology today*, 3(8):217–22. ↑29, ↑30

Muri, J., Thut, H., Bornkamm, G. W., and Kopf, M. (2019). B1 and Marginal Zone B Cells but Not Follicular B2 Cells Require Gpx4 to Prevent Lipid Peroxidation and Ferroptosis. *Cell Reports*, 29(9):2731–2744.e4. ↑52

Murrell, B., Moola, S., Mabona, A., Weighill, T., Sheward, D., Kosakovsky Pond, S. L., and Scheffler, K. (2013). FUBAR: a fast, unconstrained bayesian approximation for inferring selection. *Molecular biology and evolution*, 30(5):1196–205. ↑72

Murrell, B., Wertheim, J. O., Moola, S., Weighill, T., Scheffler, K., and Kosakovsky Pond, S. L. (2012). Detecting individual sites subject to episodic diversifying selection. *PLoS genetics*, 8(7):e1002764. ↑72

Murugesan, S., Hong, J., Yi, J., Li, D., Beach, J. R., Shao, L., Meinhardt, J., Madison, G., Wu, X., Betzig, E., and Hammer, J. A. (2016). Formin-generated actomyosin arcs propel T cell receptor microcluster movement at the immune synapse. *Journal of Cell Biology*, 215(3):383–399. ↑43

Natkanski, E., Lee, W.-Y., Mistry, B., Casal, A., Molloy, J. E., and Tolar, P. (2013). B Cells Use Mechanical Energy to Discriminate Antigen Affinities. *Science*, 340(6140):1587–1590. ↑36, ↑37, ↑43

Nemazee, D. (2017). Mechanisms of central tolerance for B cells. *Nature Reviews Immunology*, 17(5):281–294. ↑22

Ng, P. C. and Henikoff, S. (2006). Predicting the effects of amino acid substitutions on protein function. *Annual Review of Genomics and Human Genetics*, 7:61–80. ↑68

Niiro, H. and Clark, E. A. (2002). Regulation of B-cell fate by antigen-receptor signals. *Nature Reviews Immunology*, 2(12):945–956. ↑34

Nolte, M. A., Beliën, J. A., Schadee-Eestermans, I., Jansen, W., Unger, W. W., van Rooijen, N., Kraal, G., and Mebius, R. E. (2003). A Conduit System Distributes Chemokines and Small Blood-borne Molecules through the Splenic White Pulp. *The Journal of Experimental Medicine*, 198(3):505–512. ↑27

Nossal, G. J., Abbot, A., Mitchell, J., and Lummus, Z. (1968). Antigens in immunity. XV. Ultrastructural features of antigen capture in primary and secondary lymphoid follicles. *The Journal of experimental medicine*, 127(2):277–290. ↑34

Nowosad, C. R., Spillane, K. M., and Tolar, P. (2016). Germinal center B cells recognize antigen through a specialized immune synapse architecture. *Nature Immunology*, 17(7):870–877. ↑43

Nurieva, R. I., Chung, Y., Martinez, G. J., Yang, X. O., Tanaka, S., Matskevitch, T. D., Wang, Y.-H., and Dong, C. (2009). Bcl6 Mediates the Development of T Follicular Helper Cells. *Science*, 325(5943):1001–1005. ↑27

Nutt, S. L., Hodgkin, P. D., Tarlinton, D. M., and Corcoran, L. M. (2015). The generation of antibody-secreting plasma cells. *Nature Reviews Immunology*, 15(3):160–171. ↑28

Nutt, S. L. and Kee, B. L. (2007). The transcriptional regulation of B cell lineage commitment. *Immunity*, 26(6):715–25. ↑21

Nyhoff, L. E., Clark, E. S., Barron, B. L., Bonami, R. H., Khan, W. N., and Kendall, P. L. (2018). Bruton's Tyrosine Kinase Is Not Essential for B Cell Survival beyond Early Developmental Stages. *The Journal of Immunology*, 200(7):2352–2361. ↑29

Ochiai, K., Maienschein-Cline, M., Simonetti, G., Chen, J., Rosenthal, R., Brink, R., Chong, A. S., Klein, U., Dinner, A. R., Singh, H., and Sciammas, R. (2013). Transcriptional regulation of germinal center B and plasma cell fates by dynamical control of IRF4. *Immunity*, 38(5):918–29. ↑56, ↑105

Oellerich, T., Bremes, V., Neumann, K., Bohnenberger, H., Dittmann, K., Hsiao, H. H., Engelke, M., Schnyder, T., Batista, F. D., Urlaub, H., and Wienands, J. (2011). The B-cell antigen receptor signals through a preformed transducer module of SLP65 and CIN85. *EMBO Journal*, 30(17):3620–3634. ↑25

Oh-Hora, M., Johmura, S., Hashimoto, A., Hikida, M., and Kurosaki, T. (2003). Requirement for Ras Guanine Nucleotide Releasing Protein 3 in Coupling Phospholipase C-γ2 to Ras in B Cell Receptor Signaling. *Journal of Experimental Medicine*, 198(12):1841–1851. ↑25

Okada, T., Maeda, A., Iwamatsu, A., Gotoh, K., and Kurosaki, T. (2000). BCAP: The tyrosine kinase substrate that connects B cell receptor to phosphoinositide 3-kinase activation. *Immunity*, 13(6):817–827. ↑85

Okrut, J., Prakash, S., Wu, Q., Kelly, M. J. S., and Taunton, J. (2015). Allosteric N-WASP activation by an inter-SH3 domain linker in Nck. *Proceedings of the National Academy of Sciences*, 112(47):E6436 LP – E6445. ↑45, ↑89, ↑92

Oliver, A. M., Martin, F., Gartland, G. L., Carter, R. H., and Kearney, J. F. (1997). Marginal zone B cells exhibit unique activation, proliferative and immunoglobulin secretory responses. *European Journal of Immunology*, 27(9):2366–2374. ↑101

Omori, S. A., Cato, M. H., Anzelon-Mills, A., Puri, K. D., Shapiro-Shelef, M., Calame, K., and Rickert, R. C. (2006). Regulation of Class-Switch Recombination and Plasma Cell Differentiation by Phosphatidylinositol 3-Kinase Signaling. *Immunity*, 25(4):545–557. ↑105

Onabajo, O. O., Seeley, M. K., Kale, A., Qualmann, B., Kessels, M., Han, J., Tan, T.-H., and Song, W. (2008). Actin-Binding Protein 1 Regulates B Cell Receptor-Mediated Antigen Processing and Presentation in Response to B Cell Receptor Activation. *The Journal of Immunology*, 180(10):6685–6695. ↑43

Otipoby, K. L., Waisman, A., Derudder, E., Srinivasan, L., Franklin, A., and Rajewsky, K. (2015). The B-cell antigen receptor integrates adaptive and innate immune signals. *Proceedings of the National Academy of Sciences*, 112(39):12145–12150. ↑29, ↑100

Pal Singh, S., Dammeijer, F., and Hendriks, R. W. (2018). Role of Bruton's tyrosine kinase in B cells and malignancies. *Molecular Cancer*, 17(1):57. ↑25

Pao, L. I., Lam, K. P., Henderson, J. M., Kutok, J. L., Alimzhanov, M., Nitschke, L., Thomas, M. L., Neel, B. G., and Rajewsky, K. (2007). B Cell-Specific Deletion of Protein-Tyrosine Phosphatase Shp1 Promotes B-1a Cell Development and Causes Systemic Autoimmunity. *Immunity*, 27(1):35–48. ↑26

Papa, S., Choy, P. M., and Bubici, C. (2019). The ERK and JNK pathways in the regulation of metabolic reprogramming. *Oncogene*, 38(13):2223–2240. ↑101

Parker, D. C. (1980). Induction and Suppression of Polyclonal Antibody Responses by Anti-Ig Reagents and Antigen-Nonspecific Helper Factors:. A Comparison of the Effects of Anti-Fab, Anti-IgM, and Anti IgD on Murine B Cells. *Immunological Reviews*, 52(1):115–139. ↑29, ↑33

Parr, C. and Jiang, W. G. (2009). Metastasis suppressor 1 (MTSS1) demonstrates prognostic value and anti-metastatic properties in breast cancer. *European journal of cancer (Oxford, England : 1990)*, 45(9):1673–83. ↑61

Parry, S. L., Hasbold, J., Holman, M., and Klaus, G. G. (1994a). Hypercross-linking surface IgM or IgD receptors on mature B cells induces apoptosis that is reversed by costimulation with IL-4 and anti-CD40. *Journal of immunology (Baltimore, Md. : 1950)*, 152(6):2821–9. ↑33

Parry, S. L., Holman, M. J., Hasbold, J., and Klaus, G. G. (1994b). Plastic-immobilized anti-μ or anti-δ antibodies induce apoptosis in mature murine B lymphocytes. *European Journal of Immunology*, 24(4):974–979. ↑33

Paul, W. E., editor (2008). *Fundamental Immunology*. Lippincott Williams & Wilkins, 6th edition. ↑16

Paunola, E., Mattila, P. K., and Lappalainen, P. (2002). WH2 domain: a small, versatile adapter for actin monomers. *FEBS letters*, 513(1):92–7. ↑93

Pengo, N., Scolari, M., Oliva, L., Milan, E., Mainoldi, F., Raimondi, A., Fagioli, C., Merlini, A., Mariani, E., Pasqualetto, E., Orfanelli, U., Ponzoni, M., Sitia, R., Casola, S., and Cenci, S. (2013). Plasma cells require autophagy for sustainable immunoglobulin production. *Nature immunology*, 14(3):298–305. ↑55

Perlmutter, R. M., Hansburg, D., Briles, D. E., Nicolotti, R. A., Davie, J. M., and Smale, S. T. (1978). Subclass restriction of murine anti-carbohydrate antibodies. *Journal of immunology (Baltimore, Md. : 1950)*. ↑108

Petro, J. B., Gerstein, R. M., Lowe, J., Carter, R. S., Shinners, N., and Khan, W. N. (2002). Transitional type 1 and 2 B lymphocyte subsets are differentially responsive to antigen receptor signaling. *Journal of Biological Chemistry*, 277(50):48009–48019. ↑22

Pettersen, E. F., Goddard, T. D., Huang, C. C., Couch, G. S., Greenblatt, D. M., Meng, E. C., and Ferrin, T. E. (2004). UCSF Chimera–a visualization system for exploratory research and analysis. *Journal of computational chemistry*, 25(13):1605–12. ↑72

Phan, T. G., Green, J. A., Gray, E. E., Xu, Y., and Cyster, J. G. (2009). Immune complex relay by subcapsular sinus macrophages and noncognate B cells drives antibody affinity maturation. *Nature immunology*, 10(7):786–93. ↑34

Phan, T. G., Grigorova, I., Okada, T., and Cyster, J. G. (2007). Subcapsular encounter and complement-dependent transport of immune complexes by lymph node B cells. *Nature immunology*, 8(9):992–1000. ↑30

Pillai, S. and Cariappa, A. (2009). The follicular versus marginal zone B lymphocyte cell fate decision. *Nature Reviews Immunology*, 9(11):767–777. ↑23

Pinto, S. M., Manda, S. S., Kim, M.-S., Taylor, K., Selvan, L. D. N., Balakrishnan, L., Subbannayya, T., Yan, F., Prasad, T. S. K., Gowda, H., Lee, C., Hancock, W. S., and Pandey, A. (2014). Functional Annotation of Proteome Encoded by Human Chromosome 22. *Journal of Proteome Research*, 13(6):2749–2760. ↑57

Pollard, T. D. (2007). Regulation of actin filament assembly by Arp2/3 complex and formins. *Annual Review of Biophysics and Biomolecular Structure*, 36:451–477. ↑38

Pond, S. L. K., Frost, S. D. W., and Muse, S. V. (2005). HyPhy: hypothesis testing using phylogenies. *Bioinformatics (Oxford, England)*, 21(5):676–9. ↑71

Pone, E. J., Zhang, J., Mai, T., White, C. A., Li, G., Sakakura, J. K., Patel, P. J., Al-Qahtani, A., Zan, H., Xu, Z., and Casali, P. (2012). BCR-signalling synergizes with TLR-signalling for induction of AID and immunoglobulin class-switching through the non-canonical NF-κB pathway. *Nature communications*, 3:767. ↑54

Porat-Shliom, N., Milberg, O., Masedunskas, A., and Weigert, R. (2013). Multiple roles for the actin cytoskeleton during regulated exocytosis. *Cellular and Molecular Life Sciences*, 70(12):2099–2121. ↑43

Pore, D. and Gupta, N. (2015). The Ezrin-Radixin-Moesin Family of Proteins in the Regulation of B-Cell Immune Response. *Critical Reviews in Immunology*, 35(1):15–31. ↑44

Pozzan, T., Arslan, P., Tsien, R. Y., and Rink, T. J. (1982). Anti-Immunoglobulin, cytoplasmic free calcium, and capping in B lymphocytes. *Journal of Cell Biology*, 94(2):335–340. ↑31

Price, M. J., Patterson, D. G., Scharer, C. D., and Boss, J. M. (2018). Progressive Upregulation of Oxidative Metabolism Facilitates Plasmablast Differentiation to a T-Independent Antigen. *Cell reports*, 23(11):3152–3159. ↑52, ↑53, ↑100

Prior, L., Pierson, S., Woodland, R. T., and Riggs, J. (1994). Rapid restoration of B-cell function in XID mice by intravenous transfer of peritoneal cavity B cells. *Immunology*. ↑30

Pritchard, N. R. and Smith, K. G. C. (2003). B cell inhibitory receptors and autoimmunity. *Immunology*, 108(3):263–73. ↑26

Prohaska, T. A., Que, X., Diehl, C. J., Hendrikx, S., Chang, M. W., Jepsen, K., Glass, C. K., Benner, C., and Witztum, J. L. (2018). Massively Parallel Sequencing of Peritoneal and Splenic B Cell Repertoires Highlights Unique Properties of B-1 Cell Antibodies. *Journal of immunology (Baltimore, Md. : 1950)*, 200(5):1702–1717. ↑23

Puré, E. and Vitetta, E. (1980). Induction of murine B cell proliferation by insolubilized anti-immunoglobulins. *Journal of immunology (Baltimore, Md. : 1950)*, 125(3):1240–2. ↑33

Quách, T. D., Manjarrez-Orduño, N., Adlowitz, D. G., Silver, L., Yang, H., Wei, C., Milner, E. C. B., and Sanz, I. (2011). Anergic Responses Characterize a Large Fraction of Human Autoreactive Naive B Cells Expressing Low Levels of Surface IgM. *The Journal of Immunology*, 186(8):4640–4648. ↑32

Quinones, G. A., Jin, J., and Oro, A. E. (2010). I-BAR protein antagonism of endocytosis mediates directional sensing during guided cell migration. *The Journal of cell biology*, 189(2):353–67. ↑58, ↑64

Racine, R. and Winslow, G. M. (2009). IgM in microbial infections: Taken for granted? *Immunology Letters*, 125(2):79–85. ↑23

Ramensky, V., Bork, P., and Sunyaev, S. (2002). Human non-synonymous SNPs: Server and survey. *Nucleic Acids Research*, 30(17):3894–3900. ↑68

Ramesh, N., Antón, I. M., Hartwig, J. H., and Geha, R. S. (1997). WIP, a protein associated with Wiskott-Aldrich syndrome protein, induces actin polymerization and redistribution in lymphoid cells. *Proceedings of the National Academy of Sciences of the United States of America*, 94(26):14671–14676. ↑45

Rao, Y. and Haucke, V. (2011). Membrane shaping by the Bin/amphiphysin/Rvs (BAR) domain protein superfamily. *Cellular and molecular life sciences : CMLS*, 68(24):3983–93. ↑57, ↑58

Rauch, P. J., Chudnovskiy, A., Robbins, C. S., Weber, G. F., Etzrodt, M., Hilgendorf, I., Tiglao, E., Figueiredo, J. L., Iwamoto, Y., Theurl, I., Gorbatov, R., Waring, M. T., Chicoine, A. T., Mouded, M., Pittet, M. J., Nahrendorf, M., Weissleder, R., and Swirski, F. K. (2012). Innate response activator B cells protect against microbial sepsis. *Science*, 335(6068):597–601. ↑20

Rawlings, D. J., Saffran, D. C., Tsukada, S., Largaespada, D. A., Grimaldi, J. C., Cohen, L., Mohr, R. N., Bazan, J. F., Howard, M., Copeland, N. G., Jenkins, N. A., and Witte, O. N. (1993). Mutation of unique region of Bruton's tyrosine kinase in immunodeficient XID mice. *Science*, 261(5119):358–361. ↑29

Recher, M., Burns, S. O., De La Fuente, M. A., Volpi, S., Dahlberg, C., Walter, J. E., Moffitt, K., Mathew, D., Honke, N., Lang, P. A., Patrizi, L., Falet, H., Keszei, M., Mizui, M., Csizmadia, E., Candotti, F., Nadeau, K., Bouma, G., Delmonte, O. M., Frugoni, F., Ferraz Fomin, A. B., Buchbinder, D., Lundequist, E. M., Massaad, M. J., Tsokos, G. C., Hartwig, J., Manis, J., Terhorst, C., Geha, R. S., Snapper, S., Lang, K. S., Malley, R., Westerberg, L., Thrasher, A. J., and Notarangelo, L. D. (2012). B cell-intrinsic deficiency of the Wiskott-Aldrich syndrome protein (WASp) causes severe abnormalities of the peripheral B-cell compartment in mice. *Blood*, 119(12):2819–2828. ↑50

Rehe, G. T., Katona, I. M., Brunswick, M., Wahl, L. M., June, C. H., and Mond, J. J. (1990). Activation of human B lymphocytes by nanogram concentrations of anti-IgM-dextran conjugates. *European Journal of Immunology*, 20(8):1837–1842. ↑33

Rhodes, D. R., Yu, J., Shanker, K., Deshpande, N., Varambally, R., Ghosh, D., Barrette, T., Pandey, A., and Chinnaiyan, A. M. (2004). ONCOMINE: a cancer microarray database and integrated data-mining platform. *Neoplasia (New York, N.Y.)*, 6(1):1–6. ↑73, ↑91

Ricci, J. E. and Chiche, J. (2018). Metabolic reprogramming of non-Hodgkin's B-cell lymphomas and potential therapeutic strategies. *Frontiers in Oncology*, 8(DEC):1–23. ↑101

Rice, P., Longden, I., and Bleasby, A. (2000). EMBOSS: the European Molecular Biology Open Software Suite. *Trends in genetics : TIG*, 16(6):276–7. ↑72

Rickert, R. C., Rajewsky, K., and Roes, J. (1995). Impairment of T-cell-dependent B-cell responses and B-1 cell development in CD19-deficient mice. *Nature*, 376(6538):352–5. ↑35

Roberts, A. D., Davenport, T. M., Dickey, A. M., Ahn, R., Sochacki, K. A., and Taraska, J. W. (2020). Structurally distinct endocytic pathways for B cell receptors in B lymphocytes. *Molecular Biology of the Cell*, 110(9):mbc.E20–08–0532. ↑36, ↑43

Rohrschneider, L. R., Fuller, J. F., Wolf, I., Liu, Y., and Lucas, D. M. (2000). Structure, function, and biology of SHIP proteins. *Genes & development*, 14(5):505–20. ↑105

Roman-Garcia, S., Merino-Cortes, S. V., Gardeta, S. R., de Bruijn, M. J., Hendriks, R. W., and Carrasco, Y. R. (2018). Distinct roles for Bruton's Tyrosine Kinase in B cell immune synapse formation. *Frontiers in Immunology*, 9(SEP):1–16. ↑43

Roper, S. I., Wasim, L., Malinova, D., Way, M., Cox, S., and Tolar, P. (2019). B cells extract antigens at arp2/3-generated actin foci interspersed with linear filaments. *eLife*, 8:1–24. ↑49

Saarikangas, J., Kourdougli, N., Senju, Y., Chazal, G., Segerstråle, M., Minkeviciene, R., Kuurne, J., Mattila, P. K., Garrett, L., Hölter, S. M., Becker, L., Racz, I., Hans, W., Klopstock, T., Wurst, W., Zimmer, A., Fuchs, H., Gailus-Durner, V., Hrabě de Angelis, M., von Ossowski, L., Taira, T., Lappalainen, P., Rivera, C., and Hotulainen, P. (2015). MIM-Induced Membrane Bending Promotes Dendritic Spine Initiation. *Developmental cell*. ↑63

Saarikangas, J., Mattila, P. K., Varjosalo, M., Bovellan, M., Hakanen, J., Calzada-Wack, J., Tost, M., Jennen, L., Rathkolb, B., Hans, W., Horsch, M., Hyvonen, M. E., Perala, N., Fuchs, H., Gailus-Durner, V., Esposito, I., Wolf, E., de Angelis, M. H., Frilander, M. J., Savilahti, H., Sariola, H., Sainio, K., Lehtonen, S., Taipale, J., Salminen, M., and Lappalainen, P. (2011). Missing-in-metastasis MIM/MTSS1 promotes actin assembly at intercellular junctions and is required for integrity of kidney epithelia. *Journal of Cell Science*, 124(8):1245–1255. ↑63, ↑65, ↑75, ↑94, ↑99, ↑101

Saarikangas, J., Zhao, H., and Lappalainen, P. (2010). Regulation of the actin cytoskeleton-plasma membrane interplay by phosphoinositides. *Physiological reviews*, 90(1):259–89. ↑44, ↑45, ↑105

Saarikangas, J., Zhao, H., Pykäläinen, A., Laurinmäki, P., Mattila, P. K., Kinnunen, P. K., Butcher, S. J., and Lappalainen, P. (2009). Molecular Mechanisms of Membrane Deformation by I-BAR Domain Proteins. *Current Biology*, 19(2):95–107. ↑58

Sabouri, Z., Perotti, S., Spierings, E., Humburg, P., Yabas, M., Bergmann, H., Horikawa, K., Roots, C., Lambe, S., Young, C., Andrews, T. D., Field, M., Enders, A., Reed, J. H., and Goodnow, C. C. (2016). IgD attenuates the IgM-induced anergy response in transitional and mature B cells. *Nature Communications*, 7:1–11. ↑32

Saci, A. and Carpenter, C. L. (2005). RhoA GTPase regulates B cell receptor signaling. *Molecular Cell*, 17(2):205–214. ↑50

Safari, F. and Suetsugu, S. (2012). The BAR Domain Superfamily Proteins from Subcellular Structures to Human Diseases. *Membranes*, 2(1):91–117. ↑57

Safer, D., Sosnick, T. R., and Elzinga, M. (1997). Thymosin beta 4 binds actin in an extended conformation and contacts both the barbed and pointed ends. *Biochemistry*, 36(19):5806–16. ↑93

Saijo, K., Mecklenbräuker, I., Santana, A., Leitger, M., Schmedt, C., and Tarakhovsky, A. (2002). Protein kinase C β controls nuclear factor κB activation in B cells through selective regulation of the IκB kinase α. *Journal of Experimental Medicine*, 195(12):1647–1652. ↑26

Saito, T., Chiba, S., Ichikawa, M., Kunisato, A., Asai, T., Shimizu, K., Yamaguchi, T., Yamamoto, G., Seo, S., Kumano, K., Nakagami-Yamaguchi, E., Hamada, Y., Aizawa, S., and Hirai, H. (2003). Notch2 is preferentially expressed in mature B cells and indispensable for marginal zone B lineage development. *Immunity*, 18(5):675–685. ↑23

Sanchez, M., Misulovin, Z., Burkhardt, A. L., Mahajan, S., Costa, T., Franke, R., Bolen, J. B., and Nussenzweig, M. (1993). Signal transduction by immunoglobulin is mediated through Igα and Igβ. *Journal of Experimental Medicine*, 178(3):1049–1055. ↑24

Sander, S., Chu, V. T., Yasuda, T., Franklin, A., Graf, R., Calado, D. P., Li, S., Imami, K., Selbach, M., Di Virgilio, M., Bullinger, L., and Rajewsky, K. (2015). PI3 Kinase and FOXO1 Transcription Factor Activity Differentially Control B Cells in the Germinal Center Light and Dark Zones. *Immunity*, 43(6):1075–1086. ↑105

Sato, S., Miller, A. S., Howard, M. C., and Tedder, T. F. (1997). Regulation of B lymphocyte development and activation by the CD19/CD21/CD81/Leu 13 complex requires the cytoplasmic domain of CD19. *Journal of immunology (Baltimore, Md. : 1950)*, 159(7):3278–87. ↑25, ↑35

Scharenberg, A. M., Humphries, L. A., and Rawlings, D. J. (2007). Calcium signalling and cell-fate choice in B cells. *Nature Reviews Immunology*, 7(10):778–789. ↑25, ↑104

Schemionek, M., Masouleh, B. K., Klaile, Y., Krug, U., Hebestreit, K., Schubert, C., Dugas, M., Büchner, T., Wörmann, B., Hiddemann, W., Berdel, W. E., Brümmendorf, T. H., Müller-Tidow, C., and Koschmieder, S. (2015). Identification of the adapter molecule MTSS1 as a potential oncogene-specific tumor suppressor in acute myeloid leukemia. *PLoS ONE*, 10(5):1–15. ↑61

Scher, I. (1982). CBA/N immune defective mice; evidence for the failure of a B cell subpopulation to be expressed. *Immunological reviews*, 64:117–36. ↑23, ↑29, ↑32

Scher, I., Steinberg, A. D., Berning, A. K., and Paul, W. E. (1975). X-linked B-lymphocyte immune defect in CBA/N mice. II. Studies of the mechanisms underlying the immune defect. *The Journal of experimental medicine*, 142(3):637–50. ↑29

Schnyder, T., Castello, A., Feest, C., Harwood, N. E., Oellerich, T., Urlaub, H., Engelke, M., Wienands, J., Bruckbauer, A., and Batista, F. D. (2011). B Cell Receptor-Mediated Antigen Gathering

Requires Ubiquitin Ligase Cbl and Adaptors Grb2 and Dok-3 to Recruit Dynein to the Signaling Microcluster. *Immunity*, 34(6):905–918. ↑43, ↑99

Schoenhals, M., Jourdan, M., Bruyer, A., Kassambara, A., Klein, B., and Moreaux, J. (2017). Hypoxia favors the generation of human plasma cells. *Cell Cycle*, 16(11):1104–1117. ↑55

Schreiner, G. F., Fujiwara, K., Pollard, T. D., and Unanue, E. R. (1977). Redistribution of myosin accompanying capping of surface Ig. *Journal of Experimental Medicine*, 145(5):1393–1398. ↑41

Schreiner, G. F. and Unanue, E. R. (1976). Calcium-sensitive modulation of Ig capping: evidence supporting a cytoplasmic control of ligand-receptor complexes. *The Journal of Experimental Medicine*, 143(1):15–31. ↑41

Schreiner, G. F. and Unanue, E. R. (1977). Capping and the lymphocyte: Models for membrane reorganization. *Journal of Immunology*, 119(5):1549–1551. ↑34

Schweighoffer, E., Nys, J., Vanes, L., Smithers, N., and Tybulewicz, V. L. (2017). TLR4 signals in B lymphocytes are transduced via the B cell antigen receptor and SYK. *Journal of Experimental Medicine*, 214(5):1269–1280. ↑100

Schweighoffer, E., Vanes, L., Mathiot, A., Nakamura, T., and Tybulewicz, V. L. (2003). Unexpected requirement for ZAP-70 in pre-B cell development and allelic exclusion. *Immunity*, 18(4):523–533. ↑22

Sciammas, R., Shaffer, A. L., Schatz, J. H., Zhao, H., Staudt, L. M., and Singh, H. (2006). Graded expression of interferon regulatory factor-4 coordinates isotype switching with plasma cell differentiation. *Immunity*, 25(2):225–36. ↑56, ↑105

Setz, C. S., Khadour, A., Renna, V., Iype, J., Gentner, E., He, X., Datta, M., Young, M., Nitschke, L., Wienands, J., Maity, P. C., Reth, M., and Jumaa, H. (2019). Pten controls B-cell responsiveness and germinal center reaction by regulating the expression of IgD BCR. *The EMBO Journal*, 38(11):1–17. ↑32

Shabalina, S. A. and Koonin, E. V. (2008). Origins and evolution of eukaryotic RNA interference. *Trends in Ecology and Evolution*, 23(10):578–587. ↑16

Shaheen, S., Wan, Z., Li, Z., Chau, A., Li, X., Zhang, S., Liu, Y., Yi, J., Zeng, Y., Wang, J., Chen, X., Xu, L., Chen, W., Wang, F., Lu, Y., Zheng, W., Shi, Y., Sun, X., Li, Z., Xiong, C., and Liu, W. (2017). Substrate stiffness governs the initiation of B cell activation by the concerted signaling of PKCβ and focal adhesion kinase. *eLife*, 6:e23060. ↑36, ↑99

Sharma, S., Orlowski, G., and Song, W. (2009). Btk Regulates B Cell Receptor-Mediated Antigen Processing and Presentation by Controlling Actin Cytoskeleton Dynamics in B Cells. *The Journal of Immunology*, 182(1):329–339. ↑45

Shimada, A., Niwa, H., Tsujita, K., Suetsugu, S., Nitta, K., Hanawa-Suetsugu, K., Akasaka, R., Nishino, Y., Toyama, M., Chen, L., Liu, Z. J., Wang, B. C., Yamamoto, M., Terada, T., Miyazawa, A., Tanaka, A., Sugano, S., Shirouzu, M., Nagayama, K., Takenawa, T., and Yokoyama, S. (2007). Curved EFC/F-BAR-Domain Dimers Are Joined End to End into a Filament for Membrane Invagination in Endocytosis. *Cell*, 129(4):761–772. ↑58

Shinohara, H., Yasuda, T., Aiba, Y., Sanjo, H., Hamadate, M., Watarai, H., Sakurai, H., and Kurosaki, T. (2005). PKCβ regulates BCR-mediated IKK activation by facilitating the interaction between TAK1 and CARMA1. *Journal of Experimental Medicine*, 202(10):1423–1431. ↑26

Shukla, V. and Lu, R. (2014). IRF4 and IRF8: Governing the virtues of B lymphocytes. *Frontiers in Biology*, 9(4):269–282. ↑56

Shulman, Z., Gitlin, A. D., Weinstein, J. S., Lainez, B., Esplugues, E., Flavell, R. A., Craft, J. E., and Nussenzweig, M. C. (2014). Dynamic signaling by T follicular helper cells during germinal center B cell selection. *Science*, 345(6200):1058–1062. ↑27

Sieckmann, D. G., Scher, I., Asofsky, R., Mosier, D. E., and Paul, W. E. (1978). Activation of mouse lymphocytes by anti-immunoglobulin. II. A thymus-independent response by a mature subset of B lymphocytes. *The Journal of experimental medicine*, 148(6):1628–43. ↑31, ↑32

Siegrist, C.-A. (2018). Vaccine Immunology. In Plotkin, S. A., Orenstein, W. A., Offit, P. A., and Edwards, K. M. B. T. P. V. S. E., editors, *Plotkin's Vaccines*, pages 16–34.e7. Elsevier. ↑27

Simonetti, F. L., Teppa, E., Chernomoretz, A., Nielsen, M., and Marino Buslje, C. (2013). MISTIC: Mutual information server to infer coevolution. *Nucleic acids research*, 41(Web Server issue):W8–14. ↑72

Simunovic, M., Voth, G. A., Callan-Jones, A., and Bassereau, P. (2015). When Physics Takes Over: BAR Proteins and Membrane Curvature. *Trends in cell biology*, 25(12):780–792. ↑58

Sistig, T., Lang, F., Wrobel, S., Baader, S. L., Schilling, K., and Eiberger, B. (2017). Mtss1 promotes maturation and maintenance of cerebellar neurons via splice variant-specific effects. *Brain structure & function*, 222(6):2787–2805. ↑63

Smith, D. H., Peter, G., Ingram, D. L., Harding, A. L., and Anderson, P. (1973). Responses of children immunized with the capsular polysaccharide of Hemophilus influenzae, type b. *Pediatrics*, 52(5):637–44. ↑23

Smythe, E. and Ayscough, K. R. (2006). Actin regulation in endocytosis. *Journal of cell science*, 119(Pt 22):4589–98. ↑43

Snapper, C. M., Yamada, H., Smoot, D., Sneed, R., Lees, A., and Mond, J. J. (1993). Comparative in vitro analysis of proliferation, Ig secretion, and Ig class switching by murine marginal zone and follicular B cells. *Journal of immunology (Baltimore, Md. : 1950)*, 150(7):2737–45. ↑33, ↑101

Sondka, Z., Bamford, S., Cole, C. G., Ward, S. A., Dunham, I., and Forbes, S. A. (2018). The COSMIC Cancer Gene Census: describing genetic dysfunction across all human cancers. *Nature Reviews Cancer*, 18(11):696–705. ↑108

Spillane, K. M. and Tolar, P. (2017). B cell antigen extraction is regulated by physical properties of antigen-presenting cells. *The Journal of Cell Biology*, 216(1):217–230. ↑36, ↑37, ↑43

Stavnezer, J., Jeroen E.J. Guikema, and Schrader, C. E. (2008). Mechanism and Regulation of Class Switch Recombination. *Annual Review of Immunology*, 26(1):261–292. ↑28

Stein, A., Pache, R. A., Bernadó, P., Pons, M., and Aloy, P. (2009). Dynamic interactions of proteins in complex networks: a more structured view. *The FEBS journal*, 276(19):5390–405. ↑93

Stoddart, A., Jackson, A. P., and Brodsky, F. M. (2005). Plasticity of B cell receptor internalization upon conditional depletion of clathrin. *Molecular biology of the cell*, 16(5):2339–48. ↑36, ↑43

Stork, B., Engelke, M., Frey, J., Horejsí, V., Hamm-Baarke, A., Schraven, B., Kurosaki, T., and Wienands, J. (2004). Grb2 and the non-T cell activation linker NTAL constitute a Ca(2+)-regulating signal circuit in B lymphocytes. *Immunity*, 21(5):681–691. ↑86

Su, T. T., Guo, B., Kawakami, Y., Sommer, K., Chae, K., Humphries, L. A., Kato, R. M., Kang, S., Patrone, L., Wall, R., Teitell, M., Leitges, M., Kawakami, T., and Rawlings, D. J. (2002). PKC-β controls IκB kinase lipid raft recruitment and activation in response to BCR signaling. *Nature Immunology*, 3(8):780–786. ↑22, ↑26, ↑99

Su, Y. W. and Jumaa, H. (2003). LAT links the pre-BCR to calcium signaling. *Immunity*, 19(2):295–305. ↑22

Suthers, A. N. and Sarantopoulos, S. (2017). TLR7/TLR9- and B cell receptor-signaling crosstalk: Promotion of potentially dangerous B Cells. *Frontiers in Immunology*, 8(JUL):1–8. ↑100

Suyama, M., Torrents, D., and Bork, P. (2006). PAL2NAL: robust conversion of protein sequence alignments into the corresponding codon alignments. *Nucleic acids research*, 34(Web Server issue):W609–12. ↑71

Suzuki, K., Grigorova, I., Phan, T. G., Kelly, L. M., and Cyster, J. G. (2009). Visualizing B cell capture of cognate antigen from follicular dendritic cells. *The Journal of experimental medicine*, 206(7):1485–93. ↑31

Szydłowski, M., Jabłońska, E., and Juszczyński, P. (2014). FOXO1 Transcription Factor: A Critical Effector of the PI3K-AKT Axis in B-Cell Development. *International Reviews of Immunology*, 33(2):146–157. ↑25

Takata, M., Sabe, H., Hata, A., Inazu, T., Homma, Y., Nukada, T., Yamamura, H., and Kurosaki, T. (1994). Tyrosine kinases Lyn and Syk regulate B cell receptor-coupled Ca2+ mobilization through distinct pathways. *The EMBO journal*, 13(6):1341–1349. ↑85

Tanaka, S. and Baba, Y. (2020). *B Cell Receptor Signaling*, pages 23–36. Springer Singapore, Singapore. ↑24, ↑26

Tang, Z., Li, C., Kang, B., Gao, G., Li, C., and Zhang, Z. (2017). GEPIA: A web server for cancer and normal gene expression profiling and interactive analyses. *Nucleic Acids Research*. ↑73, ↑91

Taniuchi, I., Kitamura, D., Maekawa, Y., Fukuda, T., Kishi, H., and Watanabe, T. (1995). Antigen-receptor induced clonal expansion and deletion of lymphocytes are impaired in mice lacking HS1 protein, a substrate of the antigen-receptor-coupled tyrosine kinases. *The EMBO journal*, 14(15):3664–78. ↑50

Taylor, C. T. and Colgan, S. P. (2017). Regulation of immunity and inflammation by hypoxia in immunological niches. *Nature Reviews Immunology*, 17(12):774–785. ↑54

Taylor, M. D., Bollt, O., Iyer, S. C., and Robertson, G. P. (2018). Metastasis suppressor 1 (MTSS1) expression is associated with reduced in-vivo metastasis and enhanced patient survival in lung adenocarcinoma. *Clinical and Experimental Metastasis*, 35(1-2):15–23. ↑61

Taylor, R. B., Duffus, W. P., Raff, M. C., and de Petris, S. (1971). Redistribution and pinocytosis of lymphocyte surface immunoglobulin molecules induced by anti-immunoglobulin antibody. *Nature: New biology*, 233(42):225–229. ↑34, ↑36, ↑41

Teti, G., La Via, M. F., Misefari, A., and Venza-Teti, D. (1981). Cytochalasin a inhibits B-lymphocyte capping and activation by antigens. *Immunology Letters*, 3(3):151–154. ↑41

Thomas, J. D., Sideras, P., Smith, C. I., Vořechovský, I., Chapman, V., and Paul, W. E. (1993). Colocalization of X-linked agammaglobulinemia and X-linked immunodeficiency genes. *Science*, 261(5119):355–358. ↑29

Thome, M., Charton, J. E., Pelzer, C., and Hailfinger, S. (2010). Antigen receptor signaling to NF-kappaB via CARMA1, BCL10, and MALT1. *Cold Spring Harbor perspectives in biology*, 2(9):a003004. ↑26

Thurnheer, M. C., Zuercher, A. W., Cebra, J. J., and Bos, N. A. (2014). B1 Cells Contribute to Serum IgM, But Not to Intestinal IgA, Production in Gnotobiotic Ig Allotype Chimeric Mice. *The Journal of Immunology*. ↑23

Tolar, P. (2017). Cytoskeletal control of B cell responses to antigens. *Nature Reviews Immunology*, 17(10):621–634. ↑41

Tony, H. P., Phillips, N. E., and Parker, D. C. (1985). Role of membrane immunoglobulin (Ig) crosslinking in membrane Ig-mediated, major histocompatibility-restricted T cell-B cell cooperation. *The Journal of Experimental Medicine*, 162(5):1695–1708. ↑32

Tordai, A., Franklin, R. A., Patel, H., Gardner, A. M., Johnson, G. L., and Gelfand, E. W. (1994). Cross-linking of surface IgM stimulates the Ras/Raf-1/MEK/MAPK cascade in human B lymphocytes. *Journal of Biological Chemistry*, 269(10):7538–7543. ↑25

Tornberg, U. C. and Holmberg, D. (1995). B-1a, B-1b and B-2 B cells display unique V(H)DJ(H) repertoires formed at different stages of ontogeny and under different selection pressures. *EMBO Journal*, 14(8):1680–1689. ↑23

Treanor, B., Depoil, D., Bruckbauer, A., and Batista, F. D. (2011). Dynamic cortical actin remodeling by ERM proteins controls BCR microcluster organization and integrity. *The Journal of Experimental Medicine*, 208(5):1055–1068. ↑42, ↑44

Treanor, B., Depoil, D., Gonzalez-Granja, A., Barral, P., Weber, M., Dushek, O., Bruckbauer, A., and Batista, F. D. (2010). The Membrane Skeleton Controls Diffusion Dynamics and Signaling through the B Cell Receptor. *Immunity*, 32(2):187–199. ↑41, ↑42, ↑95

Tseng, Y., Kole, T. P., Lee, J. S., Fedorov, E., Almo, S. C., Schafer, B. W., and Wirtz, D. (2005). How actin crosslinking and bundling proteins cooperate to generate an enhanced cell mechanical response. *Biochemical and Biophysical Research Communications*, 334(1):183–192. ↑41

Tsubata, T. (2018). Ligand recognition determines the role of inhibitory B cell co-receptors in the regulation of B cell homeostasis and autoimmunity. *Frontiers in Immunology*, 9(OCT):1–6. ↑26

Tsui, C., Martinez-Martin, N., Gaya, M., Maldonado, P., Llorian, M., Legrave, N. M., Rossi, M., MacRae, J. I., Cameron, A. J., Parker, P. J., Leitges, M., Bruckbauer, A., and Batista, F. D. (2018). Protein Kinase C-beta Dictates B Cell Fate by Regulating Mitochondrial Remodeling, Metabolic Reprogramming, and Heme Biosynthesis. *Immunity*, 48(6):1144–1159.e5. ↑53

Tumanov, A. V., Kuprash, D. V., and Nedospasov, S. A. (2003). The role of lymphotoxin in development and maintenance of secondary lymphoid tissues. *Cytokine & Growth Factor Reviews*, 14(3-4):275–288. ↑20

Tybulewicz, V. L. J. and Henderson, R. B. (2009). Rho family GTPases and their regulators in lymphocytes. *Nature reviews. Immunology*, 9(9):630–44. ↑44

Tyler, J. J., Allwood, E. G., and Ayscough, K. R. (2016). WASP family proteins, more than Arp2/3 activators. *Biochemical Society Transactions*, 44(5):1339–1345. ↑39

Übelhart, R., Hug, E., Bach, M. P., Wossning, T., Dühren-von Minden, M., Horn, A. H. C., Tsiantoulas, D., Kometani, K., Kurosaki, T., Binder, C. J., Sticht, H., Nitschke, L., Reth, M., and Jumaa, H. (2015). Responsiveness of B cells is regulated by the hinge region of IgD. *Nature immunology*, 16(5):534–43. ↑32

Vadakekolathu, J., Al-Juboori, S. I. K., Johnson, C., Schneider, A., Buczek, M. E., Di Biase, A., Pockley, A. G., Ball, G. R., Powe, D. G., and Regad, T. (2018). MTSS1 and SCAMP1 cooperate to prevent invasion in breast cancer. *Cell death & disease*, 9(3):344. ↑67

Van Dyke, R. W. (1993). Acidification of rat liver lysosomes: Quantitation and comparison with endosomes. *American Journal of Physiology - Cell Physiology*, 265(4 34-4). ↑53

Vanshylla, K., Bartsch, C., Hitzing, C., Krümpelmann, L., Wienands, J., and Engels, N. (2018). Grb2 and GRAP connect the B cell antigen receptor to Erk MAP kinase activation in human B cells. *Scientific Reports*, 8(1):1–17. ↑25

Vasu, K. and Nagaraja, V. (2013). Diverse Functions of Restriction-Modification Systems in Addition to Cellular Defense. *Microbiology and Molecular Biology Reviews*, 77(1):53–72. ↑16

Vicente-Manzanares, M., Ma, X., Adelstein, R. S., and Horwitz, A. R. (2009). Non-muscle myosin II takes centre stage in cell adhesion and migration. *Nature Reviews Molecular Cell Biology*, 10(11):778–790. ↑45

Victora, G. D. and Nussenzweig, M. C. (2012). Germinal centers. *Annual review of immunology*, 30:429–57. ↑27

Vinuesa, C. G. and Chang, P.-P. (2013). Innate B cell helpers reveal novel types of antibody responses. *Nature immunology*, 14(2):119–26. ↑28, ↑29

Volkmann, C., Brings, N., Becker, M., Hobeika, E., Yang, J., and Reth, M. (2016). Molecular requirements of the B-cell antigen receptor for sensing monovalent antigens. *The EMBO Journal*, 35(21):2371–2381. ↑32

Volpi, S., Santori, E., Abernethy, K., Mizui, M., Dahlberg, C. I., Recher, M., Capuder, K., Csizmadia, E., Ryan, D., Mathew, D., Tsokos, G. C., Snapper, S., Westerberg, L. S., Thrasher, A. J., Candott, F., and Notarangelo, L. D. (2016). N-WASP is required for B-cell-mediated autoimmunity in Wiskott-Aldrich syndrome. *Blood*, 127(2):216–220. ↑50

Walmsley, M. J., Ooi, S. K. T., Reynolds, L. F., Smith, S. H., Ruf, S., Mathiot, A., Vanes, L., Williams, D. A., Cancro, M. P., and Tybulewicz, V. L. J. (2003). Critical roles for Rac1 and Rac2 GTPases in B cell development and signaling. *Science (New York, N.Y.)*, 302(5644):459–62. ↑51

Wan, Z., Chen, X., Chen, H., Ji, Q., Chen, Y., Wang, J., Cao, Y., Wang, F., Lou, J., Tang, Z., and Liu, W. (2015). The activation of IgM- or isotype-switched IgG- and IgE-BCR exhibits distinct mechanical force sensitivity and threshold. *eLife*, 4. ↑37

Wan, Z., Xu, C., Chen, X., Xie, H., Li, Z., Wang, J., Ji, X., Chen, H., Ji, Q., Shaheen, S., Xu, Y., Wang, F., Tang, Z., Zheng, J.-S., Chen, W., Lou, J., and Liu, W. (2018). PI(4,5)P2 determines the threshold of mechanical force–induced B cell activation. *The Journal of Cell Biology*, 217(7):2565 LP – 2582. ↑37

Wan, Z., Zhang, S., Fan, Y., Liu, K., Du, F., Davey, A. M., Zhang, H., Han, W., Xiong, C., and Liu, W. (2013). B Cell Activation Is Regulated by the Stiffness Properties of the Substrate Presenting the Antigens. *The Journal of Immunology*, 190(9). ↑36, ↑37

Wang, D., Eraslan, B., Wieland, T., Hallström, B., Hopf, T., Zolg, D. P., Zecha, J., Asplund, A., Li, L.-H., Meng, C., Frejno, M., Schmidt, T., Schnatbaum, K., Wilhelm, M., Ponten, F., Uhlen, M., Gagneur, J., Hahne, H., and Kuster, B. (2019). A deep proteome and transcriptome abundance atlas of 29 healthy human tissues. *Molecular Systems Biology*, 15(2):e8503. ↑57

Wang, G., Chen, Q., Zhang, X., Zhang, B., Zhuo, X., Liu, J., Jiang, Q., and Zhang, C. (2013). PCM1 recruits Plk1 to the pericentriolar matrix to promote primary cilia disassembly before mitotic entry. *Journal of Cell Science*, 126(6):1355 LP – 1365. ↑93

Wang, J., Lin, F., Wan, Z., Sun, X., Lu, Y., Huang, J., Wang, F., Zeng, Y., Chen, Y.-H., Shi, Y., Zheng, W., Li, Z., Xiong, C., and Liu, W. (2018). Profiling the origin, dynamics, and function of traction force in B cell activation. *Science Signaling*, 11(542):eaai9192. ↑43

Wang, J. C. and Hammer, J. A. (2020). The role of actin and myosin in antigen extraction by B lymphocytes. *Seminars in Cell & Developmental Biology*, 102(July):90–104. ↑43, ↑46

Wang, J. C., Lee, J. Y.-J., Christian, S., Dang-Lawson, M., Pritchard, C., Freeman, S. A., and Gold, M. R. (2017). The Rap1-cofilin-1 pathway coordinates actin reorganization and MTOC polarization at the B cell immune synapse. *Journal of Cell Science*, 130(6):jcs.191858. ↑43

Wang, Y., Shibasaki, F., and Mizuno, K. (2005). Calcium signal-induced cofilin dephosphorylation is mediated by slingshot via calcineurin. *Journal of Biological Chemistry*, 280(13):12683–12689. ↑44

Wang, Y., Zhou, K., Zeng, X., Lin, J., and Zhan, X. (2007). Tyrosine phosphorylation of missing in metastasis protein is implicated in platelet-derived growth factor-mediated cell shape changes. *The Journal of biological chemistry*, 282(10):7624–31. ↑59, ↑64, ↑71

Watanabe, N., Nomura, T., Takai, T., Chiba, T., Honjo, T., and Tsubata, T. (1998). Antigen receptor cross-linking by anti-immunoglobulin antibodies coupled to cell surface membrane induces rapid apoptosis of normal spleen B cells. *Scandinavian Journal of Immunology*. ↑33

Watanabe-Matsui, M., Muto, A., Matsui, T., Itoh-Nakadai, A., Nakajima, O., Murayama, K., Yamamoto, M., Ikeda-Saito, M., and Igarashi, K. (2011). Heme regulates B-cell differentiation, antibody class switch, and heme oxygenase-1 expression in B cells as a ligand of Bach2. *Blood*, 117(20):5438–5448. ↑53

Waters, L. R., Ahsan, F. M., Wolf, D. M., Shirihai, O., and Teitell, M. A. (2018). Initial B Cell Activation Induces Metabolic Reprogramming and Mitochondrial Remodeling. *iScience*, 5:99–109. ↑52, ↑54

Weber, G. F., Chousterman, B. G., Hilgendorf, I., Robbins, C. S., Theurl, I., Gerhardt, L. M., Iwamoto, Y., Quach, T. D., Ali, M., Chen, J. W., Rothstein, T. L., Nahrendorf, M., Weissleder, R., and Swirski, F. K. (2014). Pleural innate response activator B cells protect against pneumonia via a GM-CSF-IgM axis. *Journal of Experimental Medicine*, 211(6):1243–1256. ↑20, ↑23

Weber, M., Treanor, B., Depoil, D., Shinohara, H., Harwood, N. E., Hikida, M., Kurosaki, T., and Batista, F. D. (2008). Phospholipase C- 2 and Vav cooperate within signaling microclusters to propagate B cell spreading in response to membrane-bound antigen. *Journal of Experimental Medicine*, 205(4):853–868. ↑34, ↑35, ↑44, ↑104

Weisel, F. J., Mullett, S. J., Elsner, R. A., Menk, A. V., Trivedi, N., Luo, W., Wikenheiser, D., Hawse, W. F., Chikina, M., Smita, S., Conter, L. J., Joachim, S. M., Wendell, S. G., Jurczak, M. J., Winkler, T. H., Delgoffe, G. M., and Shlomchik, M. J. (2020). Germinal center B cells selectively oxidize fatty acids for energy while conducting minimal glycolysis. *Nature Immunology*, 21(3):331–342. ↑54

Wennerberg, K., Rossman, K. L., and Der, C. J. (2005). The Ras superfamily at a glance. *Journal of Cell Science*, 118(5):843–846. ↑44

Westerberg, L. S., Dahlberg, C., Baptista, M., Moran, C. J., Detre, C., Keszei, M., Eston, M. A., Alt, F. W., Terhorst, C., Notarangelo, L. D., and Snapper, S. B. (2012). Wiskott-Aldrich syndrome protein (WASP) and N-WASP are critical for peripheral B-cell development and function. *Blood*, 119(17):3966–3974. ↑50

White, M. C. and Quarmby, L. M. (2008). The NIMA-family kinase, Nek1 affects the stability of centrosomes and ciliogenesis. *BMC cell biology*, 9:29. ↑93

Wickramarachchi, D. C., Theofilopoulos, A. N., and Kono, D. H. (2010). Immune pathology associated with altered actin cytoskeleton regulation. *Autoimmunity*, 43(1):64–75. ↑39, ↑41

Wienands, J., Schweikert, J., Wollscheid, B., Jumaa, H., Nielsen, P. J., and Reth, M. (1998). SLP-65: A new signaling component in B lymphocytes which requires expression of the antigen receptor for phosphorylation. *Journal of Experimental Medicine*, 188(4):791–795. ↑45

Wild, P. S., Felix, J. F., Schillert, A., Teumer, A., Chen, M. H., Leening, M. J., Völker, U., Großmann, V., Brody, J. A., Irvin, M. R., Shah, S. J., Pramana, S., Lieb, W., Schmidt, R., Stanton, A. V., Malzahn, D., Smith, A. V., Sundström, J., Minelli, C., Ruggiero, D., Lyytikäinen, L. P., Tiller, D., Smith, J. G., Monnereau, C., Di Tullio, M. R., Musani, S. K., Morrison, A. C., Pers, T. H., Morley, M., Kleber, M. E., Aragam, J., Benjamin, E. J., Bis, J. C., Bisping, E., Broeckel, U., Cheng, S., Deckers, J. W., Del Greco M, F., Edelmann, F., Fornage, M., Franke, L., Friedrich, N., Harris, T. B., Hofer, E., Hofman, A., Huang, J., Hughes, A. D., Kähönen, M., Kruppa, J., Lackner, K. J., Lannfelt, L., Laskowski, R., Launer, L. J., Leosdottir, M., Lin, H., Lindgren, C. M., Loley, C., MacRae, C. A., Mascalzoni, D., Mayet, J., Medenwald, D., Morris, A. P., Müller, C., Müller-Nurasyid, M., Nappo, S., Nilsson, P. M., Nuding, S., Nutile, T., Peters, A., Pfeufer, A., Pietzner, D., Pramstaller, P. P., Raitakari, O. T., Rice, K. M., Rivadeneira, F., Rotter, J. I., Ruohonen, S. T., Sacco, R. L., Samdarshi, T. E., Schmidt, H., Sharp, A. S., Shields, D. C., Sorice, R., Sotoodehnia, N., Stricker, B. H., Surendran, P., Thom, S., Töglhofer, A. M., Uitterlinden, A. G., Wachter, R., Völzke, H., Ziegler, A., Münzel, T., März, W., Cappola, T. P., Hirschhorn, J. N., Mitchell, G. F., Smith, N. L., Fox, E. R., Dueker, N. D., Jaddoe, V. W., Melander, O., Russ, M., Lehtimäki, T., Ciullo, M., Hicks, A. A., Lind, L., Gudnason, V., Pieske, B., Barron, A. J., Zweiker, R., Schunkert, H., Ingelsson, E., Liu, K., Arnett, D. K., Psaty, B. M., Blankenberg, S., Larson, M. G., Felix, S. B., Franco, O. H., Zeller, T., Vasan, R. S., and Dörr, M. (2017). Large-scale genome-wide analysis identifies genetic variants associated with cardiac structure and function. *Journal of Clinical Investigation*, 127(5):1798–1812. ↑63

Willis, S. N., Good-Jacobson, K. L., Curtis, J., Light, A., Tellier, J., Shi, W., Smyth, G. K., Tarlinton, D. M., Belz, G. T., Corcoran, L. M., Kallies, A., and Nutt, S. L. (2014). Transcription factor IRF4 regulates germinal center cell formation through a B cell-intrinsic mechanism. *Journal of immunology (Baltimore, Md. : 1950)*, 192(7):3200–6. ↑56, ↑105

Woodings, J. A., Sharp, S. J., and Machesky, L. M. (2003). MIM-B, a putative metastasis suppressor protein, binds to actin and to protein tyrosine phosphatase delta. *The Biochemical journal*, 371(Pt 2):463–71. ↑58, ↑59, ↑64, ↑92, ↑93

Woodruff, M. F. A., Reid, B., and James, K. (1967). Effect of Antilymphocytic Antibody and Antibody Fragments on Human Lymphocytes in vitro. *Nature*, 215(5101):591–594. ↑31

Xia, S., Li, X., Johnson, T., Seidel, C., Wallace, D. P., and Li, R. (2010). Polycystin-dependent fluid flow sensing targets histone deacetylase 5 to prevent the development of renal cysts. *Development*, 137(7):1075–1084. ↑57, ↑63, ↑99, ↑101

Xu, J., Foy, T. M., Laman, J. D., Elliott, E. A., Dunn, J. J., Waldschmidt, T. J., Elsemore, J., Noelle, R. J., and Flavell, R. A. (1994). Mice deficient for the CD40 ligand. *Immunity*, 1(5):423–31. ↑54

Xu, Y., Harder, K. W., Huntington, N. D., Hibbs, M. L., and Tarlinton, D. M. (2005). Lyn tyrosine kinase: Accentuating the positive and the negative. *Immunity*, 22(1):9–18. ↑26

Yamagishi, A., Masuda, M., Ohki, T., Onishi, H., and Mochizuki, N. (2004). A novel actin bundling/filopodium-forming domain conserved in insulin receptor tyrosine kinase substrate p53 and missing in metastasis protein. *The Journal of biological chemistry*, 279(15):14929–36. ↑57, ↑58, ↑59

Yamanashi, Y., Fukuda, T., Nishizumi, H., Inazu, T., Higashi, K. I., Kitamura, D., Ishida, T., Yamamura, H., Watanabe, T., and Yamamoto, T. (1997). Role of tyrosine phosphorylation of HS1 in B cell antigen receptor-mediated apoptosis. *Journal of Experimental Medicine*, 185(7):1387–1392. ↑50

Yamazaki, T., Takeda, K., Gotoh, K., Takeshima, H., Akira, S., and Kurosaki, T. (2002). Essential immunoregulatory role for BCAP in B cell development and function. *Journal of Experimental Medicine*, 195(5):535–545. ↑104

Yang, Y., Wang, C., Yang, Q., Kantor, A. B., Chu, H., Ghosn, E. E., Qin, G., Mazmanian, S. K., Han, J., and Herzenberg, L. A. (2015). Distinct mechanisms define murine B cell lineage immunoglobulin heavy chain (IgH) repertoires. *eLife*, 4(September 2015):1–31. ↑23

Yang, Z. (2007). PAML 4: phylogenetic analysis by maximum likelihood. *Molecular biology and evolution*, 24(8):1586–91. ↑23, ↑71

Yasuda, T., Kometani, K., Takahashi, N., Imai, Y., Aiba, Y., and Kurosaki, T. (2011). ERKs induce expression of the transcriptional repressor Blimp-1 and subsequent plasma cell differentiation. *Science signaling*, 4(169):ra25. ↑105

Yoder, M. C. (2002). Embryonic hematopoiesis in mice and humans. *Acta Paediatrica, International Journal of Paediatrics, Supplement*, 91(438):5–8. ↑21

You, Y., Myers, R. C., Freeberg, L., Foote, J., Kearney, J. F., Justement, L. B., and Carter, R. H. (2011). Marginal zone B cells regulate antigen capture by marginal zone macrophages. *Journal of immunology (Baltimore, Md. : 1950)*, 186(4):2172–81. ↑27, ↑30

Youd, M. E., Ferguson, A. R., and Corley, R. B. (2002). Synergistic roles of IgM and complement in antigen trapping and follicular localization. *European journal of immunology*, 32(8):2328–37. ↑30

Young, R. M. and Staudt, L. M. (2013). Targeting pathological B cell receptor signalling in lymphoid malignancies. *Nature reviews. Drug discovery*, 12(3):229–43. ↑101

Yu, D., Zhan, X. H., Niu, S., Mikhailenko, I., Strickland, D. K., Zhu, J., Cao, M., and Zhan, X. (2011). Murine missing in metastasis (MIM) mediates cell polarity and regulates the motility response to growth factors. *PloS one*, 6(6):e20845. ↑99

Yu, D., Zhan, X. H., Zhao, X. F., Williams, M. S., Carey, G. B., Smith, E., Scott, D., Zhu, J., Guo, Y., Cherukuri, S., Civin, C. I., and Zhan, X. (2012). Mice deficient in MIM expression are predisposed to lymphomagenesis. *Oncogene*, 31(30):3561–8. ↑61, ↑67, ↑94, ↑99, ↑100, ↑101, ↑108

Yuseff, M.-I., Reversat, A., Lankar, D., Diaz, J., Fanget, I., Pierobon, P., Randrian, V., Larochette, N., Vascotto, F., Desdouets, C., Jauffred, B., Bellaiche, Y., Gasman, S., Darchen, F., Desnos, C., and Lennon-Duménil, A.-M. (2011). Polarized secretion of lysosomes at the B cell synapse couples antigen extraction to processing and presentation. *Immunity*, 35(3):361–74. ↑36, ↑43

Zamorano, J., Rivas, D., Gayo, A., Mozo, L., and Gutiérrez, C. (1995). Soluble, but not immobilized, anti-IgM antibody inhibits post-activation events leading to T-cell-dependent B-cell differentiation. *Immunology*, 85(2):241–7. ↑33

Zeleniak, A. E., Huang, W., Brinkman, M. K., Fishel, M. L., and Hill, R. (2017). Loss of MTSS1 results in increased metastatic potential in pancreatic cancer. *Oncotarget*, 8(10):16473–16487. ↑61, ↑66

Zeleniak, A. E., Huang, W., Fishel, M. L., and Hill, R. (2018). PTEN-Dependent Stabilization of MTSS1 Inhibits Metastatic Phenotype in Pancreatic Ductal Adenocarcinoma. *Neoplasia (New York, N.Y.)*, 20(1):12–24. ↑66, ↑93

Zeng, Y., Yi, J., Wan, Z., Liu, K., Song, P., Chau, A., Wang, F., Chang, Z., Han, W., Zheng, W., Chen, Y.-H., Xiong, C., and Liu, W. (2015). Substrate stiffness regulates B-cell activation, proliferation, class switch, and T-cell-independent antibody responses in vivo. *European Journal of Immunology*, 45(6):1621–1634. ↑36

Zhan, T., Cao, C., Li, L., Gu, N., Civin, C. I., and Zhan, X. (2016). MIM regulates the trafficking of bone marrow cells via modulating surface expression of CXCR4. *Leukemia*, 30(6):1327–1334. ↑63, ↑67, ↑99

Zhang, M., Alicot, E. M., Chiu, I., Li, J., Verna, N., Vorup-Jensen, T., Kessler, B., Shimaoka, M., Chan, R., Friend, D., Mahmood, U., Weissleder, R., Moore, F. D., and Carroll, M. C. (2006). Identification of the target self-antigens in reperfusion injury. *Journal of Experimental Medicine*, 203(1):141–152. ↑24

Zhao, P., Chen, B., Li, L., Wu, H., Li, Y., Shaneen, B., Zhan, X., and Gu, N. (2019). Missing-in-metastasis protein promotes internalization of magnetic nanoparticles via association with clathrin light chain and Rab7. *Biochimica et Biophysica Acta - General Subjects*, 1863(2):502–510. ↑67

Zhong, J., Shaik, S., Wan, L., Tron, A. E., Wang, Z., Sun, L., Inuzuka, H., and Wei, W. (2013). SCF β-TRCP targets MTSS1 for ubiquitination-mediated destruction to regulate cancer cell proliferation and migration. *Oncotarget*, 4(12):2339–53. ↑66, ↑93

Zhu, J. W., Brdicka, T., Katsumoto, T. R., Lin, J., and Weiss, A. (2008). Structurally Distinct Phosphatases CD45 and CD148 Both Regulate B Cell and Macrophage Immunoreceptor Signaling. *Immunity*, 28(2):183–196. ↑24

Zikherman, J., Parameswaran, R., and Weiss, A. (2012). Endogenous antigen tunes the responsiveness of naive B cells but not T cells. *Nature*, 489(7414):160–4. ↑32

Zouggari, Y., Ait-Oufella, H., Bonnin, P., Simon, T., Sage, A. P., Guérin, C., Vilar, J., Caligiuri, G., Tsiantoulas, D., Laurans, L., Dumeau, E., Kotti, S., Bruneval, P., Charo, I. F., Binder, C. J., Danchin, N., Tedgui, A., Tedder, T. F., Silvestre, J.-S., and Mallat, Z. (2013). B lymphocytes trigger monocyte mobilization and impair heart function after acute myocardial infarction. *Nature medicine*, 19(10):1273–1280. ↑20

TURUN
YLIOPISTO
UNIVERSITY
OF TURKU

Painosalama, Turku, Finland 2022

ISBN 978-951-29-8789-4 (PRINT)
ISBN 978-951-29-8790-0 (PDF)
ISSN 0355-9483 (PRINT)
ISSN 2343-3213 (ONLINE)